ZERO DISCHARGE OF PHARMACEUTICAL WASTEWATER USING ACTIVATED SLUDGE: PROCESS OPTIMIZATION AND SCALE - UP OF A NOVEL BIOREACTOR

Thesis submitted by

Rajib Kumar Das

Doctor of Philosophy (Engineering)

Department of Chemical Engineering

Faculty Council of Engineering & Technology

Jadavpur University

Kolkata, India

May 2023

JADAVPUR UNIVERSITY

KOLKATA – 700032

INDEX NO. 258/16/E

1. **Title of Thesis:** ZERO DISCHARGE OF PHARMACEUTICAL WASTEWATER USING ACTIVATED SLUDGE: PROCESS OPTIMIZATION AND SCALE-UP OF A NOVEL BIOREACTOR.

2. **Name, Designation and Institution of Supervisor:**

Prof. Ujjaini Sarkar
Department of Chemical Engineering
Jadavpur University
Kolkata-700032,
India

3. **List of Publication:**

Efficacy of convective-diffusion models to study the transient behaviour of a sewage-sludge-filled packed column for aqueous phase adsorption of fluoroquinolones: Consideration of pseudo-kinetics driven depletion of species, **Rajib Kumar Das,** Debamita Pal, Ujjaini Sarkar, **Journal of Environmental Chemical Engineering, 11 (2023) 109896. https://doi.org/10.1016/j.jece.2023.109896**

4. List of Patents: None

5. List of Presentation in Conference:

R. K. Das, "Characterization of sewage sludge as a potential adsorbent for removal of fluoroquinolones from wastewater". "National Conference on EMERGING DIMENSIONS IN CHEMICAL SCIENCES (EDCS-23)", Organized by Department of Chemistry, University of Kalyani & Chemical Research Society of India, Kolkata Chapter, March 28-29, 2023. (Poster)

Statement of Originality

I, Rajib Kumar Das, registered on 11/05/2016, do hereby declare that this thesis entitled "ZERO DISCHARGE OF PHARMACEUTICAL WASTEWATER USING ACTIVATED SLUDGE: PROCESS OPTIMIZATION AND SCALE - UP OF A NOVEL BIOREACTOR" contains literature survey and original research work done by the undersigned candidate as part of Doctoral studies.

All information in this thesis have been obtained and presented in accordance with existing academic rules and ethical conduct. I declare that, as required by these rules and conduct, I have fully cited and referred all materials and results that are not original to this work.

I also declare that I have checked this thesis as per the "Policy on Anti Plagiarism, Jadavpur University, 2019", and the level of similarity as checked by iThenticate software is 1 *%.*

Rajib Kumar Das

Signature of the Candidate:

Date: 10/05/2023

Professor
CHEMICAL ENGINEERING DEPARTMENT
JADAVPUR UNIVERSITY
Kolkata-700 032

Signature of the Supervisor:

Date: 10.05.2023

Certificate from the Supervisor

This is to certify that the thesis entitled **"Zero discharge of Pharmaceutical wastewater using activated sludge: Process optimization and scale-up of a novel bioreactor"** *submitted by* **Mr. Rajib Kumar Das,** *who got his name registered on* **11.05.2016** *for the award of Ph.D. (Engineering) degree of Jadavpur University is absolutely based upon his own work under the supervision of* **Prof. Ujjaini Sarkar** *and that neither his thesis nor any part of the thesis has been submitted for any degree/diploma or any other academic award anywhere before.*

Professor
CHEMICAL ENGINEERING DEPARTMENT
JADAVPUR UNIVERSITY
Kolkata-700 032

Ujjaini Sarkar 10.05.2023

.....

Signature of the Supervisor and
date with office seal

Dedicated

To

My Mother

Acknowledgement

I would like to express my sincere thanks to all those who contributed in many ways towards the success of this piece of research work and made it an unforgettable experience for me.

First and foremost, I would like to express my deepest sense of gratitude to my mentor and supervisor Prof Ujjaini Sarkar for her excellent supervision and valuable advice throughout the course of my research work. Without her encouragement, enthusiasm, motivation and continuous guidance, I could not have finished this work. She was always there to meet and talk about my queries and ideas, to provide worthful suggestions for thinking through my problems (whether philosophical, analytical or computational). She also made the laboratory a wonderful workplace with the different valuable and necessary equipment for this kind of research work.

I would like to convey my sincere thanks to Prof. Rajat Chakraborty, Prof Kajari Kargupta, Dr. Ratna Dutta, Dr. Sudeshna Saha, Smt Sujata Sardar of the Department of Chemical Engineering, Jadavpur University. They indeed provided me with many fruitful suggestions.

I am also grateful to Mr. Ashim Bhattacharya and Mr. Debu Ari, Process Dynamics & Control Laboratory, Chemical Engineering Department, Jadavpur University, Kolkata 700032 for their kind cooperation on several occasions.

I am grateful to the staff of the Baranagar-Kamarhati sewage treatment plant, Kolkata Municipal Development Authority (KMDA), West Bengal, India, for their kind cooperation during the collection of sewage sludge which was one of the most important part of my research study.

I am grateful to Prof (Dr.) Asim Bhaumik [School of Materials Sciences] and Dr. Subhadeep Datta [School of Physical Sciences], Indian Association for the Cultivation of Science, 2A and 2B, Raja S. C. Mullick Road, Kolkata 700032, for extending help in carrying out XPS and FT-IR based analyses.

I am grateful to Shri Swachchha Majumdar, Chief Scientist and Head, Membrane and Separation Technology Division, CSIR-Central Glass & Ceramic Research Institute, 196, Raja S.C. Mullick Road, Kolkata 700 032, West Bengal, India, for extending help in carrying out contact angle-based analysis.

I am thankful to Mr. Jatish Das, Bioprocess Laboratory, Chemical Engineering Department, Jadavpur University, Kolkata 700032, for extending help during elemental analysis for C, H, N, and S.

I also acknowledge the Metallurgy & Material Engineering Department, Jadavpur University, Kolkata 700032, for helping in carrying out morphological characterization using FE-SEM.

I would also acknowledge invaluable support and immense help received from my colleagues and would like to express my earnest thanks to Dr. Shyamal Jana, Dr. Pabitra Kumar Baidya, Dr. Sibasis Baksi, Mr Rohit Bhagat Kalwar, and Ms Debamita Pal for their kind co-operation during the course of my research work.

I am also thankful to Mr Rakesh Dey for extending his help in many ways during my experimental work.

Lastly, I am indebted to the eternal blessings offered by my parents (Late Gopal Chandra Das and Late Shukla Das) and my family for providing me strength and support in every moment of my life. I would like to thank God for his kindness and love from the beginning of my journey.

Rajib Kumar Das

Abstract

Ciprofloxacin and ofloxacin are two important fluoroquinolone-based antibiotics that are heavily prescribed and consumed in Asian continent, specifically during the post-Covid 19 scenarios. Useful microbial consortiums meant for the biodegradation of sewage sludge get depleted in the presence of these antibiotics. Additionally, the treated sewage wastewater, used in agricultural fields, municipal parks for gardening etc. still contains a large quantity of antibiotics. A specific scheme of in-situ batch equilibrium adsorption of these antibiotics using raw sewage sludge has is assessed.

Modified competitive Langmuir-like model and the LeVan-Vermeulen model are developed using fundamental principles of statistical thermodynamics. These models are further applied and validated for modelling the adsorption of ciprofloxacin and ofloxacin using raw sewage sludge. Parameters from each of these models are evaluated using MATLAB and the fsolve MATLAB Library. The sludge and the post-treated sludge are characterized physically and chemically. A satisfactory fit to the Langmuir adsorption isotherm, for each of the pure components, implies the applicability of the multicomponent adsorption isotherm models. Pseudo-kinetics, intra-particle, and film diffusion models are also examined.

Film diffusion is the rate-controlling step for the adsorption of both ciprofloxacin and ofloxacin. 2^{nd}-order pseudo-kinetics also support chemisorption. At a working pH of 7.8, zwitterionic forms of ciprofloxacin and ofloxacin do not help in the adsorption process through electrostatic interaction as the sludge surface remains negative. Semi-dried raw sewage sludge still exhibits a high adsorption capacity towards ciprofloxacin and ofloxacin in weakly alkaline medium (pH at ~ 7.8) due to the negative charge assisted hydrogen bonding since the carboxylic acid groups of both FQs are hydrogen bonded to the basal oxygen atoms of the sludge layers.

Scale-up of a dynamic adsorption system consisting of a randomly packed column is studied. Raw sewage sludge is used as the primary adsorbent. The Yoon-Nelson model, with a simplified semi-empirical approach, is used to study the adsorption process for an effective scale-up of the continuous removal protocol for the fluoroquinolones. Additionally, the impact of varying bed depths, inlet concentrations, and flow rates is studied for the optimal design of the packed bed.

Two transient convective-diffusion models are developed and validated including pseudo-1^{st} and 2^{nd}-order kinetics driven depletion terms. The data collected under various dynamic conditions are used to optimize the models for analysing the packed bed performance with respect to varying bed height, flow rate and initial concentration of the FQs. Damköhler numbers of the FQs are calculated to predict the breakthrough times of both the FQs. The ratios of Damköhler numbers of ciprofloxacin and ofloxacin do not change much with flow rate. In all the experiments, $D_a s << 1$ for both the FQs, indicating the diffusion process is faster than the rate of pseudo-reaction and diffusion reaches equilibrium before the reaction reaches pseudo-chemical equilibrium. Ratios of the Damköhler numbers, that represent the 1^{st}-order and 2^{nd}-order convective-diffusion models for ciprofloxacin to ofloxacin is < 1.

TABLE OF CONTENTS

Chapter 5: –

Batch equilibrium analysis: Development and validation of competitive multicomponent adsorption models

Chapter 6: –

Transient behaviour of a packed column: Development and validation of convective diffusion models with due considerations for pseudo-kinetics driven depletion of species

Chapter 7: –

Transient behaviour of a packed column: Scale-Up using Semi-Empirical Approach

List of Figures

Chapter 5

Chapter 6

Chapter 7

Chapter 8

Annex II

Supplementary Material A

List of Tables

Chapter 6

Chapter 7

Annex II

Supplementary Material A

Supplementary Material C

Nomenclature

Symbol	Description	Unit
q	Amount adsorbed	g/100ml/g
C	Equilibrium concentration	g/100ml
q_{max}	Maximum amount adsorbed	g/100ml/g
k	Langmuir isotherm constant	-
n	heterogeneity factor	-
K	Halsey isotherm constant	-
q_s	Theoretical isotherm saturation capacity	mg/g
K_{ad}	Dubinin–Radushkevich isotherm constant	mol^2/kJ^2
ε	Dubinin – Radushkevich isotherm constant	-
R	Molar gas constant	8.314J/mol K
T	absolute temperature	K
C_e	Adsorbate equilibrium concentration	g/100ml
K_E	Elovich equilibrium constant	-
q_m	Elovich maximum adsorption capacity	g/100ml/g
X_1	Amount of solute 1 adsorbed per unit weight of adsorbent	g/100ml/g
X_2	Amount of solute 2 adsorbed per unit weight of adsorbent	g/100ml/g
C_{eq1}	Equilibrium concentration of solute 1	g/100ml

Symbol	Description	Unit
C_{eq2}	Equilibrium concentration of solute 1	g/100ml
$X_{m,1}$	maximum amount adsorbed for component 1	g/100ml/g
$X_{m,2}$	maximum amount adsorbed for component 2	g/100ml/g
X_i	Amount adsorbed for the i^{th} species	g/100ml/g
C_{eqi}	Equilibrium concentrations for the i^{th} species	g/100ml
q_e	Amount of adsorbate adsorbed at equilibrium	g/100ml/g
q_t	amount of adsorbate adsorbed at time t	g/100ml/g
k_1	Pseudo first-order rate constant	day^{-1}
k_2	pseudo second-order rate constant	g/100ml/g. day
k_i	Intra-particle diffusional rate constant	g/100ml/g. $day^{1/2}$
C	Constant that indicates the boundary-layer thickness	g/100ml/g
F	Fractional achievement of equilibrium, at different times	-
B_t	Mathematical function of F	-
C_0	Initial concentration of the solute in influent	mg/L
C_t	Solute concentration in effluent at any time	mg/L
K	Adsorption rate constant or BDST model constant	L/mg h
Z	Bed height or depth	cm

Symbol	Description	Unit
N_0	Adsorption capacity	mg/L
v	Linear flow velocity	cm/h
t	Service time	h
k_{Th}	Thomas rate constant	ml/min/g
Q	Flow rate	ml/min
q_0	Maximum adsorption capacity of the adsorbent bed	mg/g
M	Mass of the adsorbent	g
V_{eff}	Volume of the effluent	ml
k_{YN}	Yoon-Nelson rate coefficient	-
τ	time required for 50% breakthrough	min
ε_b	Bed porosity	-
t	Service time	min
ρ_b	Bulk density	g/cc

Chapter 1

Introduction

1.1 Background

With the ever-increasing population all over the world, the demands of daily commodities, food products, medicines, etc. have been augmented manifolds which in turn leads to rapid industrialisation in the current century. The amount of wastewater generation along with the growth of industrialisation has become a significant issue for environmentalists and scientists. The release of effluent from different types of industries containing lethal chemicals, and pharmaceutical wastes into the environmental matrices, contribute a major role in the area of hazardous waste. During the last three decades, the usage of pharmaceuticals has surged by more than 2.5 times globally and as a consequence, the amount of wastewater released to the environment causes a potential threat to the ecosystem if discharged without proper treatment.

Pharmaceuticals are considered to be the major outcome of global scientific and technological advancement which have amplified the normal life span, cured millions of people from fatal diseases, and boosted the standard of living (Marcelo et al., 2021).

Pharmaceuticals are now emerging as fast-escalating complex environmental pollutants because of their prominence. Pharmaceuticals have been found to be contaminating nearly all ecological matrices across the world during the last three decades (Caban and Stepnowski, 2021). The problem of pharmaceutical contaminations in the environmental matrices has become complex because of the usage of a huge number of therapeutic agents and the diversification of their origin (Madhura et al., 2019). The existence of the biotic kingdom of the environment becomes vulnerable as the concentrations of pharmaceuticals in the environmental matrices are ever-rising beyond the sustainable limit. The pharmaceutical residues and the parent chemicals from various sources usually go to the sewage treatment plant (STP) as most urban households, hospitals, and animal husbandry are connected to the public sewage system.

Pharmaceuticals are considered to be the most important class of environmental contaminants which draw the major attention of environmentalists. Due to their strong hydrophilicity and feeble biodegradability, these compounds are tough to remove from wastewater using conventional water treatment processes (Bello and Raman, 2019). Therefore, disposal of such contaminants using wastewater treatment facilities are a more challenging task.

Pharmaceuticals differ significantly in terms of biodegradation, solubility, stability, and absorbability and they can remain biologically active at extremely low concentrations (Ufnalska and Lichtfouse, 2021). Risk assessments indicate that pharmaceuticals at extremely low concentrations in drinking water would offer any health risk to human beings. However, long-term exposure to a particular pharmaceutical compound or mixture of pharmaceuticals would be associated with high-risk factor, and assessment of such risks to human health are required to be

developed. The evaluation of risk assessment to plants and aquatic biosystem for some pharmaceuticals are also required to be established.

1.2 Wastewater: Sewage wastewater particular

Wastewater is defined as the water generated after the use of freshwater, raw water, drinking water, or saline water in a variety of thoughtful applications or processes (Wastewater Engineering). In another way, wastewater is defined as the used water generated from any combination of domestic, industrial, commercial, or agricultural activities, surface runoff or stormwater, and sewer inflow or sewer infiltration (Tilley et al., 2014). In terms of daily usage, wastewater is commonly synonymous with sewage (also called sewerage, domestic wastewater, or municipal wastewater), which is wastewater that is produced by human beings. Sewage wastewater consists of waste in solution or suspension that is meant to be removed from a community. The composition of wastewater is 99.9% water and the remaining 0.1% is what is removed. The other 0.1% is what is cause for concern (UNL Water). That 0.1% includes:

- Nutrients: Phosphorous and Nitrogen
- Fats, oils, grease: cooking oils, body lotions
- Pathogens: disease-causing bacteria and viruses
- BOD-biochemical oxygen demand. BOD is a measure of oxygen needed by aerobic bacteria to break down organic matter. A higher BOD means there is more organic matter that needs to be broken down.
- Other solids

The classification of sewage water includes sanitary, commercial, industrial, agricultural and surface runoff. The spent water from residences, washing water, food preparation wastes, laundry wastes and other waste products of normal living are categorised as 'domestic' or 'sanitary' sewage. Wastewater from premises used mainly for the purpose of a trade or business or for the purpose of sport, recreation, education or entertainment is called 'commercial sewage'. Wastewater originating from industrial premises during the use of water in manufacturing process or cleaning activities is recognised as 'industrial waste water'. Surface runoff, also known as overland flow, is the flow of water occurring on the ground surface when excess rain water, storm water or other sources can no longer infiltrate sufficiently into the soil. All categories of sewage contain '*pathogenic organisms'* that can spread water borne diseases to human beings and other animals. Direct contact with these pathogens or pollution of the water supply can cause infections as a result.

1.3 Pharmaceuticals in sewage wastewater: Antibiotics in particular

The uncontrolled removal of partially treated or untreated wastewater is considered to be the prime sources of pharmaceuticals in the environmental matrices. Though some of the pharmaceuticals are highly degradable in nature, the frequent impositions may lead to pseudo persistence actions (Vulliet et al., 2011). Pharmaceutical manufactories including animal husbandry and aquaculture establishments are the prime producers of pharmaceuticals and subsequently are familiar to be the direct sources of such compounds to the water bodies and the local environment. The different ways for the pharmaceuticals entering into the environment is illustrated in the following Fig. 1.1.

Along with the presence of pharmaceuticals in ground water, these compounds are now being observed in the coastal sea water due to permeation of such compounds in

the ground water (Petrie and Camacho-Mu˜noz, 2021). The presence of pharmaceuticals in water not only degrade the quality of water but also causes a negative effect on the aquatic biota. After the first finding of the water pollutants in the year 1980, several pharmaceuticals gad been noticed in water thereafter (Vieira et al., 2020). The common therapeutic compound that are frequently being detected in water matrices are (i) anticonvulsants (phenytoin, phenobarbital etc.), (ii) non-steroidal anti-inflammatory drugs (acetaminophen, ibuprofen, diclofenac etc.), (iii) hormones (estriol, estrone etc.), (iv) antibiotics (ofloxacin ampicillin, ciprofloxacin, trimethoprim, erythromycin etc.), (v) antihypertensive (losartan, atenolol, furosemide etc.) and antidepressants (meprobamate, diazepam, etizolam etc.).

The discarded pharmaceuticals in residential trash either in metabolised or unmetabolized state, end up in land fillings. When the dumping materials are not maintained properly, they develop groundwater leachates. A major portion of the non-polar drugs are adsorbed onto the sediments and solids of wastewater treatment plant and are then removed with sludge (Rathi et al., 2021). Sludges that are used as fertilisers for agricultural purposes also leach pharmaceuticals in surface and ground water bodies. Animal wastes used as biofertilizers also contain antibiotics and hormones (Li et al., 2020). Human excretions (urine and faeces), piling of unused drugs and pharmaceutical containing substances applied directly on the agricultural

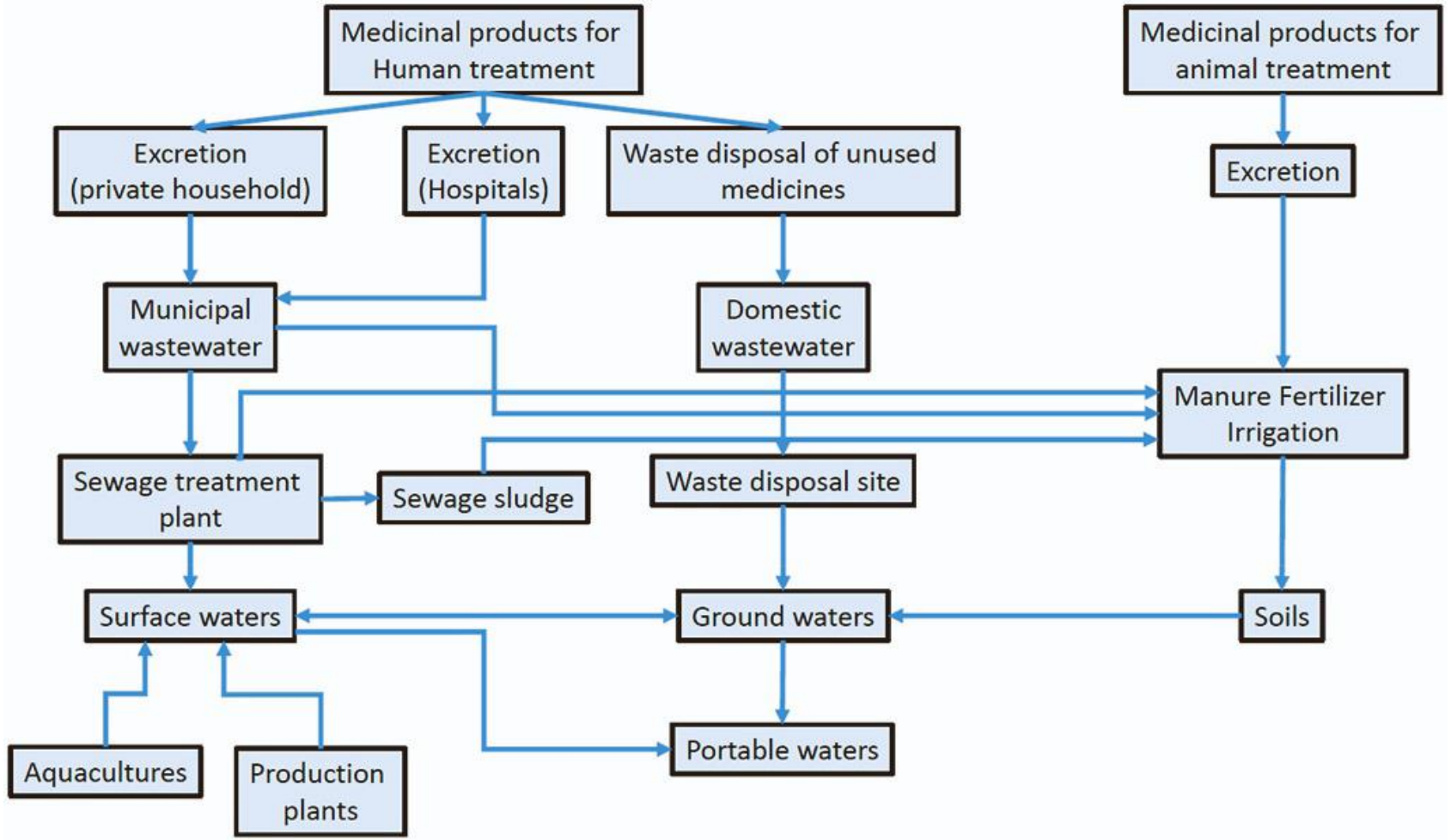

Fig. 1.1 Different routes of pharmaceuticals entering into the environment.

grounds and their subsequent permeation leading the entries of pharmaceuticals into the water bodies. Household effluents are the most common source of environmental pollution caused by pharmaceuticals (Akhil et al., 2021a, b). The second greatest source of pollutants is effluents from hospitals which contain combinations of various medicaments in high concentrations. The third most important source of pharmaceuticals in water is due to the excretion of medicines or their metabolites by animals (Abhinaya et al., 2021). Various pharmaceutical manufactories, aquaculture and agricultural wastewater irrigation are also supposed to be the significant sources for pharmaceuticals in wastewater.

1.3.1 Antibiotics in wastewater

The word "antibiotic" in the modern medicine, generally refers to compounds which have biological activity against living organisms. In other way it refers to substances having antibacterial, antifungal or antiparasitic activity. One of the possible modern definitions considers antibiotics as chemotherapeutic agents as they inhibit or eliminate the growth of microorganisms, such as bacteria, fungi, or protozoa (K. Kümmerer, 2009). The different routes through which antibiotics are taking their entries into the environment are considered to be classified into two categories: uses of antibiotics for human health and antibiotics for veterinary purposes. Humans consume antibiotics and excrete them and the accumulated excretions go to the Wastewater Treatment Plants (WWTP). After their treatment, the generated biosolids and discharged effluents cause pollution of the soil and aquatic matrices of the environment. In veterinary medicines, antibiotics are administered to livestock, which in terms are found in their excretory products as unabsorbed parent antibiotics or metabolites. Excretions used as manures also cause antibiotic contamination of soil and aquatic system of the environment. Antibiotics used in aquaculture also causes

antibiotic contamination to the aquatic environment (I.T. Carvalho et al. 2016). The other unconventional routes of antibiotic contamination of environment is the lack of availability of techniques for recycling of active medicaments from expired drugs. Proper recycling techniques of expired drugs can resist their entries into the environment. The main pathways of antibiotic residues into the environmental matrices are excretions after consumption of antibiotics, poor disposal of unused medicines and the waste generated after their manufactures. All these entry routes lead the antibiotics to the WWTP (C. Afonso-Olivares et al. 2012).

1.4 Ecotoxicology of Ciprofloxacin and Ofloxacin

Because of their limited biodegradability, antibiotics have become a major concern to the environmentalists. Fluoroquinolones, a class of synthetic antibiotics, have been found to be resistant to biodegradation (Sarangapani et al., 2019; Van Doorslaer et al., 2014). The widespread antibiotic-resistant microorganisms have become a potential threat to human health (Amarasiri et al., 2020). In addition to that antibiotics also create problems to the ecosystem, mainly to eukaryotes including phytoplankton and zooplankton in the aquatic environment (Aderemi et al., 2018; Gorokhova et al., 2015**;** Lu et al., 2019**;** Motiei et al., 2020). Antibiotics also have direct impact on the bacterial community of aquatic system (Eckert et al., 2019). Therefore, pollution due to the presence of antibiotics has become a big concern to human health and environment (Polianciuc et al., 2020). Fluoroquinolones such as ciprofloxacin (Fig. 1.2) and ofloxacin (Fig. 1.3) have a prolonged life span in aquatic environments due to their low biodegradability (Janecko et al., 2016).

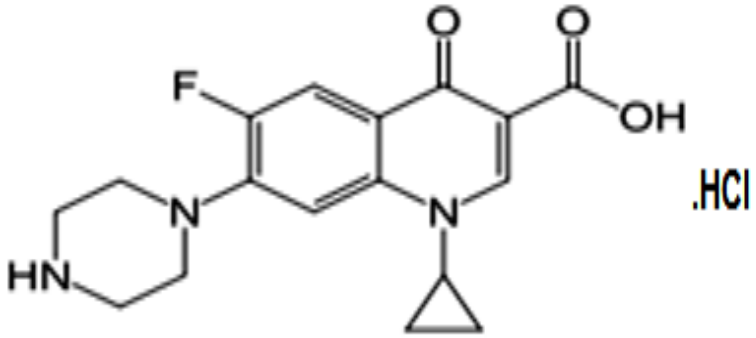

Fig. 1.2 Molecular structure of Ciprofloxacin.

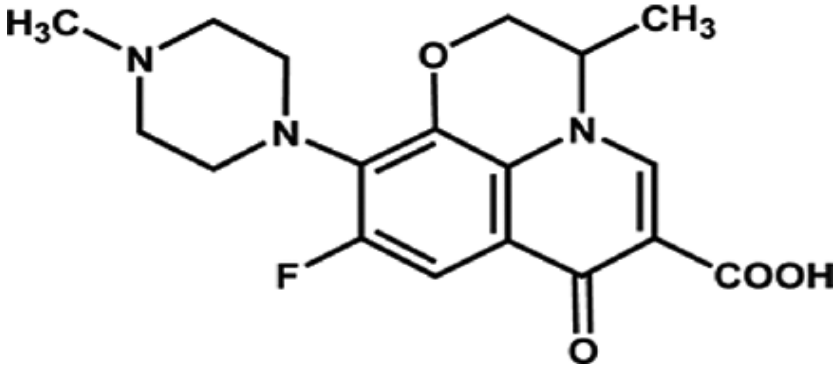

Fig. 1.3 Molecular structure of Ofloxacin.

The concentration of ciprofloxacin in the effluent of the pharmaceutical wastewater treatment plant (WWTP) was found to be around 31000 µg / L (Larsson et al., 2007). As well, around 5000 µg / L of ciprofloxacin was also detected in the effluent of municipal and pharmaceutical wastewater treatment plant and the surrounding river (Gothwal and Shashidhar, 2017**;** Hussain et al., 2016). On the other hand, the effluent of the pharmaceutical wastewater treatment plant was found to contain ofloxacin at a higher concentration than 3000 µg / L (Hussain et al., 2016). Amongst the various fluoroquinolones, ciprofloxacin and ofloxacin have been found to be consumed at a higher rate across the world (Bortone et al., 2021; Hsia et al., 2019) and as a

consequence of that pollution caused by ciprofloxacin and ofloxacin are also tremendous and imparting hazards to aquatic environment. Both ciprofloxacin and ofloxacin are toxic towards aquatic organisms (Table 1.1).

Table 1.1 Toxicity levels of ciprofloxacin and ofloxacin.

Compound	*Toxicity*	*Reference*
Ciprofloxacin	EC_{50} for the cyanobacteria *Microsystis aeruginosa* = 15-51 nmol/L	Halling-Sørensen et al., 2000.
	EC_{50} for the bacteria *Pseudomonas putida* = 241 nmol/L	Kümmerer et al., 2000
	EC_{50} for the detrivorous microbial communities present in the stream = 301.8 nmol/L	Maul et al., 2006
Ofloxacin	EC_{50} [1] value for *Microcystis aeruginosa* (Blue-Green Algae) = 18-24 μg/L	Robinson et al., 2005
	EC_{50} value for (Green Algae) *Pseudokirchneriella subcapitata* = 10400-13700 μg/L	Robinson et al., 2005
	EC_{50} value for the Species: Lemna minor (Duckweed) = 52-201 μg/L	Robinson et al., 2005

1.5 Standard Methods of Sewage Wastewater Treatment

The well-known fact regarding water usage is that the amount of water supplied for various purposes actually ends up as wastewater. This makes the treatment of wastewater extremely important. Wastewater treatment is the schematic methodology that removes most of the contaminants found in wastewater to ensure a healthy and sound environment. Therefore, wastewater management deals with handling of

[1] *EC_{50} stands for the half maximal effective concentration that refers to the concentration of a drug, antibody or toxicant which induces a response halfway between the baseline and maximum after some specified exposure time. It is used as a measure of a drug's potency.*

wastewater in order to protect the environment to ensure wellness of social, economic and public health (Metcalf and Eddy, 1991). Wastewater treatment has become more vital for the following purposes:

- ✓ *Reduction of biodegradable organic substances* which are either released or remains in solution, needs to be broken down by oxidation into gases during the process of water treatment.
- ✓ *Reduction of nutrient concentration in the environment* which along with wastewater enters in the environment and enrich the water bodies that leads to the growth of algae and other aquatic plants. These plants deplete oxygen in water bodies and this hampers aquatic life.
- ✓ *Elimination of pathogens that* are excreted in large quantities in the feces of infected animals and humans (Awuah and Amankwaa-Kuffuor, 2002).
- ✓ *Recycling and Reuse of water* is crucial for sustainability. Wastewater treatment method is broadly classified into three categories i.e. primary, secondary and tertiary. Sometimes, preliminary treatment is done prior to primary treatment.

Preliminary treatment

This treatment method mainly removes coarse suspended materials from the sewer before entering into the primary treatment clarifiers. The devices which are mainly used in this process are screens, grit chambers, and pre-aeration tanks respectively. Preliminary treatment increases the efficiency of operation and maintenance of subsequent treatment units.

Primary treatment

This treatment includes the removal of organic and inorganic solids that can be settled by the physical process of sedimentation. The floating materials (scum) are separated by skimming. BODs up to 50%, 70% of suspended solids and 65% of grease and oil can be eliminated at this stage. Constituents which remain in colloidal or dissolved state are however not removed at this stage. The effluent from primary sedimentation units is referred to as primary effluent (FAO, 2006).

Secondary treatment

In this treatment method, the primary effluent is further treated to remove residual organics and suspended solids. Biodegradable dissolved and colloidal organic substances are removed using aerobic biological treatment methods. The mechanical devices used in the treatment are categorised as follows:

1. Trickling filters along with settling tanks.
2. Activated sludge methods rotating biological contactors (RBC).

The non-mechanical methods used in this treatment process are anaerobic treatment, oxidation ditches, stabilization ponds, etc.

Tertiary treatment

This is the advanced treatment process applied when specific wastewater constituents even cannot be removed by the secondary treatment method. Tertiary treatment enables the removal of significant amounts of nitrogen, phosphorus, heavy metals, biodegradable organics, bacteria and viruses. Two methods are in use to filter secondary effluent effectively. These are traditional sand filter and the newer

membrane filters. Using improved filters and membranes removal of pathogenic helminths has become possible. The latest treatment method includes disk filtration which utilizes large disks of cloth media attached to rotating drums for filtration purpose (FAO, 2006). Disinfection of treated water at this stage is often done by the injection of Chlorine, Ozone and Ultra Violet (UV) irradiation. The outlet water meets the criteria of current international standards for agricultural and urban re-use.

1.6 Assessment of pharmaceuticals in mixture

The assessment of pharmaceuticals in wastewater includes various analytical techniques which have been developed for their rapid and accurate determination. Table 1.2 represents the evolution of different analytical techniques that have been followed during the last 50 years. Various chromatographic techniques have been implemented for the determination and quantification of pharmaceuticals in different water samples. The well-known chromatographic techniques currently in practice are High-Performance Liquid Chromatography with Ultraviolet detector (HPLC-UV) (D.C. da Silva et al. 2018), High Performance Liquid Chromatography with Diode Array Detection (HPLC-DAD) (T. Vieira et al., 2010), Liquid Chromatography coupled with Mass Spectrometry (LC-MS), Liquid Chromatography - Mass Spectrometry / Mass Spectrometry (LC-MS/MS) (C. Ort et al., 2010) and Gas Chromatography-Mass Spectrometry (GC–MS) (M. Farr´e et al., 2007).

The most common chromatographic method used for separation, identification and quantification of most of the non-volatile pharmaceutical compounds is based on High performance liquid chromatography (HPLC) (R. Salgado et al., 2010). As the concentrations of pharmaceuticals present in the environmental water are very low,

therefore a sample preparation and pre-concentration step are necessary before analysis (D.M. Pavlovi´c et al., 2007).

Table 1.2 Evolution of analytical techniques. *Source: (Y. Talero-P´erez al., 2014).*

Time period	*Analytical technique*	*Abbreviature*
Before 1970	Thin-Layer Chromatography	TLC
1970–1980	Gas Chromatography - Electron Capture Detector High Performance Liquid Chromatography	GC-ECD HPLC
1980–1990	Gas Chromatography - Mass Spectrometry (Selected Ion Monitoring) High-performance Liquid Chromatography (Diode Array Detection - Ultraviolet)	GC–MS (SIM) HPLC (DAD-UV)
1990–2000	Gas Chromatography - Mass Spectrometry (Electron Capture Detector.) Liquid Chromatography - Mass Spectrometry Liquid Chromatography - Mass Spectrometry (Quadrupole-quadrupole-Quadrupole) Liquid Chromatography - Mass Spectrometry (Quadrupole-quadrupole-Linear Ion Trap)	GC–MS (ECD) LC-MS LC-MS (QqQ) LC-MS (QqLIT)
2000–2010	Ultra-Performance Liquid Chromatography Ultra-Performance Liquid Chromatography - Time of Flight	UPLC UPLC-TOF
2010 - Present	Ultra-Performance Liquid Chromatography - OROBITRAP Ultra-High-Performance Liquid Chromatography - Electro-Spray Ionization - Mass Spectrometry	UPLC-ORBITRAP UHPLC-ESI-MS

1.7 Specific Methods for Removal of Pharmaceutical Compounds

Contamination of wastewater by pharmaceuticals has become a global problem. Several methods have been applied but still there is an immediate need for development of robust methods and techniques for the complete removal of pharmaceuticals from wastewater. The efficiency of removal of pharmaceuticdependspend on wastewater treatment techniques. The different

techniques vary from one another in terms of long-term viability, effectiveness, cost and their merits and demerits.

1.7.1 Biological Treatment

Biological treatment method is considered to be the most traditional treatment method for pharmaceuticals in wastewater. It is categorized as aerobic and anaerobic processes. Aerobic process includes activation sludge process, membrane bio-reactor (MBR) and sequential batch reactor. The anaerobic process involves anaerobic filter, up-flow anaerobic sludge blanket.

Conventional activated sludge (CAS) is a low-cost treatment process as compared to other advanced treatment methodologies. Biodegradation of pharmaceuticals by microorganism is the key factor in this process. The efficacy of this method depends on hydraulic retention time (HRT) and sludge retention time (SRT). Longer HRT enhances removal efficiencies for most pharmaceuticals (Verlicchi et al., 2010). However, because of the low biodegradability of many pharmaceuticals, CAS does not perform well for all types pharmaceuticals like carbamazepine (Oulton et al., 2010).

Membrane Bio Reactor (MBR) is a combination of conventional biological treatment and membrane separation in a single unit (Tay et al., 2007). An MBR system works more efficiently by controlling the sludge retention time (SRT) and increase removal rate of pharmaceuticals. Oulton et al. 2010, suggested MBR to be more effective as compared to CAS. From the work of Weiss and Reemtsma 2008, it is evident that MBR system is much effective for removal of pharmaceutical compounds which are easily biodegradable in nature. The shortfall of the method is exactly similar to that of CAS. This process is also unable to remove recalcitrant contaminants.

1.7.2 Sewage Sludge as potential adsorbent of pharmaceuticals

Sewage sludge which is a waste material, been investigated as a potential adsorbent. This is a by-product generated after the digestion of biomass from the sewage treatment plant and consists of organic and inorganic (such as sand and metal oxides) components (G. Xu et al. 2015). Sludge contains organic components and thus it can be converted into an adsorbent material. It also aids a waste accumulation issue. Though the relatively low surface area of sewage sludge and sewage sludge-based materials (as compared to commercial carbon adsorbents) are relatively low, but it has demonstrated adsorption capacities comparable to those of commercial carbons (A. Bagreev et al., 2001; A. Ros et al., 2006). Sewage sludge as an adsorbent has been used in preceding studies to remove pollutants such as H2S (A. Bagreev et al., 2001), dyes (F. Rozada et al., 2003; Z. Aksu et al., 2001; L. Leng et al., 2015), phenol (W. Zhu et al., 2014), carbon tetrachloride (X. Chen et al. 2002), pesticides [R. Rojas et al., 2014] and heavy metals (Y. Su et al., 2015) effectively. All these studies indicate a growing interest in the repurposing of sewage sludge for the use in adsorption of pollutants including pharmaceuticals.

1.7.3 Advance Treatment Methods

Due to the shortfall of conventional methods for removal of various types of pharmaceuticals from wastewater effectively, advance methods that introduces adsorption, oxidation and membrane separation have been developed.

Activated carbon both in granular (Granular Activated Carbon; GAC) and powdered (Powdered Activated Carbon; PAC) form is one of the most common adsorbents used in the adsorption process. However, being cost-effective powdered activated carbon is the most preferred choice of adsorbent (Grassi et al., 2013; Gupta et al., 2009).

Although it is being used in the tertiary treatment of wastewater, activated carbon proves as a potential adsorbent for pharmaceuticals removal (Wang and Wang, 2016).

Carbon nanotubes (CNTs) are also used as potential adsorbent for removal of pharmaceuticals from wastewater but unlike conventional adsorbents they have been relatively less explored. The adsorption behaviour of CNTs depends on their surface morphology and chemistry.

Membrane filtration techniques that include nanofiltration (NF) and ultrafiltration (UF) have been implemented as advanced treatment methods in wastewater treatment plants for the removal of natural organic substances and pesticides (Yoon et al., 2007). With regard to the removal of the pharmaceuticals, membrane processes including nanofiltration, ultrafiltration and reverse osmosis (RO) have been reported to be an efficient treatment method. NF also known as low-pressure RO, has pores in nanoscale and was so designed to fill the technical gaps of RO and UF (Yang et al., 2014). The removal efficiency of either of the filtration techniques is affected by the physicochemical properties of the pharmaceuticals like hydrophobicity, charge and molecular weight (Van Der Bruggen et al., 1999; Comerton et al., 2007; Yoon et al., 2007) of the molecules and it has been observed a linear relationship between the retention of pharmaceuticals on the membranes and their respective log K_{ow} values.

Advanced Oxidation Processes (AOPs) which generally occur at ambient conditions of temperature and pressure, involve the generation of highly reactive radicals (especially hydroxyl and sulphate radicals) which have potential effects for water purification (Glaze et al., 1987). AOP treatment processes require chemicals like hydrogen peroxide, ozone, persulphate, transition metals, metal oxides and UV irradiation. This treatment converts or degrades the organic pollutants into carbon di

oxide, water, nitrogen and other smaller molecules that are easily biodegradable. This treatment process is found to be extremely promising for the remediation of contaminated ground, surface, and wastewaters containing organic pollutants such as pesticides, aromatics, etc. which are non-biodegradable in nature (Andreozzi et al., 1999). Due to the high cost of chemicals and energy sources, the implementation of AOP treatment is not feasible in terms of cost.

1.8 Statement of the problem

Ciprofloxacin and ofloxacin belong to a class of antibiotics called Fluoroquinolones (FQs), which have a wide anti-bacterial activity against Gram-positive and Gram-negative bacteria. Since the recent Covid-19 pandemic witnessed a magnanimous rise in the use of antibiotics to prevent secondary bacterial infections, it led to vast production and use of such antibiotics. Ultimately the antibiotics get discharged into the municipal sewer pipes, thereby killing the useful microbial colony. In order to prevent environmental degradation a commercial scale-up of the adsorption of these antibiotics using raw sewage sludge is an absolute necessity.

Batch adsorption experiments are conducted using Raw Sewage Sludge (RSS) as the adsorbent for removing a pair of fluoroquinolones, namely, ciprofloxacin and ofloxacin. Well-known multicomponent adsorption models are parameterized and validated. As wastewater from pharmaceutical industries deals with a large amount of water, continuous treatment is required. Packed columns containing RSS are designed for the continuous adsorption of pharmaceutical wastewater. The transient behavior of various composite fixed beds is analyzed with respect to the removal of ciprofloxacin and ofloxacin. Two dynamic models (1^{st} -order and 2^{nd} -order pseudo kinetic

convective diffusion models) are also developed, on the basis of conservation of species, to simulate the continuous removal process.

1.9 Specific Objectives

i. Treatment of pharmaceutical wastewater containing ciprofloxacin and ofloxacin by adsorption using raw sewage sludge (RSS) as an adsorbent.

ii. Physical and chemical characterization of the raw sewage sludge (RSS).

iii. Design of experiments for batch equilibrium analysis of wastewaters containing ciprofloxacin and ofloxacin.

iv. Development, parameterization, application, and validation of some reputed multicomponent competitive adsorption models using batch equilibrium isotherm data.

v. Evaluation and validation of the pseudo-kinetics, pore, and film diffusions using various models.

vi. Development and validation of two transient forms of a convective-diffusion model, which include depletion terms (in liquid-phase), being represented by the first and second-order pseudo-kinetics with due considerations for the convective and diffusive terms of liquid phase mass transfer along with film diffusion, intra-pellet mass transfer, and depletion of species governed by pseudo-kinetics of competitive adsorption under various dynamic conditions.

vii. Estimation of parameters of the 1^{st} and 2^{nd}-order pseudo-kinetic equations using experimental data collected under dynamic conditions.

viii. Application of each of these convective-diffusion models to carry out a thorough breakthrough analysis under varying dynamic conditions for both ciprofloxacin and ofloxacin.

ix. Checking on the performance of the packed bed with respect to the effects of changes in bed height, flow rate, and initial concentration of both fluoroquinolones (ciprofloxacin and ofloxacin), in combination, using first-order and second-order convective diffusion models and estimated Damköhler numbers.

x. Evaluation of the packed column in terms of its breakthrough performance using the Yoon-Nelson approach. Effects of varying bed heights, concentrations, and flow rates of influent wastewater are specifically examined to obtain the theoretical breakthrough curves for the adsorption column.

1.10 Outline of the thesis

The literatures have been reviewed in connection to various innovative methods applied in this research work in **Chapter 2**. In order to estimate the adsorption capacity, precursor RSS is characterized physically as well as chemically in **Chapter 3**. **Chapter 4** deals with the batch equilibrium adsorption of pure component ciprofloxacin and ofloxacin using RSS. Evaluation of various model isotherms for pure component ciprofloxacin and ofloxacin is carried out in this chapter. **Chapter 5** discusses the multicomponent adsorption of ciprofloxacin and ofloxacin using RSS. Development of two competitive adsorption models, specifically meant for batch equilibrium analysis of the multi-component system, is undertaken with the help of fundamental principles of statistical thermodynamics. Further, estimation and validation of the parameters of these multicomponent models are depicted in this

chapter. The kinetic study explains the suitability in the applications of pseudo kinetics, pore diffusion and film diffusion. The mechanism of macro and micro transport during adsorption of the two compounds by different adsorbents is also analyzed in this chapter. **Chapter 6** emphasizes the transient behavior of the packed bed for continuous adsorption of ciprofloxacin and ofloxacin using RSS. Effects of change in bed height, flow rate and concentration of the feed solution, on the breakthrough curve generated from the continuous study, are portrayed here. Two simple one-dimensional convective diffusion models, including pseudo-kinetics driven depletion terms, are also developed along with the validation of the models for specific cases with no axial dispersion, for variations in flow rate and bed height. **Chapter 7** describes the appropriateness, application and validation of a semi-empirical model. **Chapter 8** highlights various novelty elements in the entire span of research work carried out. Concluding remarks are enumerated along with recommendations for some new dimensions in the future work after discussing the limitations of this research work. The main chapters are followed by two annexures. **Annex-I** describes the parameter estimation technique using MATLAB and the *fsolve* library function. **Annex-II** details the characterization of the post-treated sewage sludge.

Chapter 2

Review of Literature

Foreword

Various work performed by many researchers on the topic related to treatment of pharmaceutical wastewater are hereby reviewed in this context.

- Consideration of hazards associated with wastewater bearing pharmaceuticals and subsequent treatment methodologies of pharmaceutical wastewater.
- Potential hazards with respect to ciprofloxacin and ofloxacin.
- Characterization including both physical and chemical of the natural adsorbent.
- Batch equilibrium analysis, kinetics study and diffusion models including film and pore diffusion.
- Study of transient behaviour of packed bed column applying semi empirical models.

2.1 Pharmaceutical wastewater and its treatment: *Concerns for hazards*

One of the important features of the current environmental research is water pollution caused by emerging pharmaceutical compounds which have been considered as potential hazardous organic pollutants due to their widespread use and prolonged effect on aquatic environment (Ashfaq et al. 2016). Pharmaceutical contaminants have been prevailing in nearly all ecological matrices including influents and effluents from ground water, surface water and sludge, over the last few decades (Caban and Stepnowski, 2021). Nearly 713 pharmaceuticals out of those 11,926 pharmaceutically active compounds have been spotted in wastewater (Femina Carolin et al., 2021). Natural water and wastewater contain these pharmaceutical contaminants in the range of ng / L to µg / L (Kolpin et al. 2002; Daughton et al. 1999), µg / kg to mg / kg in soils and sludge (Walter et al. 2010). Even at such low concentration these organic contaminants show pseudo persistence in the environment and affect adversely the ecosystem and human health (Hernando et al. 2006; Rivera et al. 2013; Sharma et al. 2016).The municipal sewage treatment plants (STP) are considered to be the major point source for these organic pollutants (Onesios et al. 2009; Ericson et al. 2010), because pharmaceuticals in household and hospital sewage is mainly discharged into sewage treatment plants (Gobel et al. 2007; Xu et al. 2007). It has been reported by various researchers that the discharge of effluent from sewage treatment plants is the main source of pharmaceutical contaminations in nearby surface waters (Wuersch et al. 2005; Gulkowska et al. 2008).

Conventional wastewater treatment processes and subsequent clarification are not effective for the complete removal of pharmaceuticals from wastewater (Westerhoff et al. 2005). Many researchers found that advanced treatment processes involving ozonation, chlorination, ultraviolet (UV) irradiation, nanofiltration (NF), reverse

osmosis (RO) and activated car bon adsorption can remove antibiotics from wastewater effectively (Le-Minh et al. 2010). Radjenovic et al., (2009) explained that ozonation is effective in removal of antibiotics from wastewater only with the limitation that the transformed products are also biologically active and further resistant to ozonation. Recent studies suggest that membrane technology may be a very effective tool for the removal of pharmaceuticals from wastewater (Drewes et al. 2002). Currently, effective sewage treatment processes for removal of pharmaceuticals from wastewater involve the use of sewage sludge, advanced oxidation, activated carbon adsorption, membrane separation technology and membrane bioreactor technology are extremely traditional (Jiao et al., 2012; Zhao et al., 2010). Hu et al., (2014) mentioned that biological treatments have been used widely to treat wastewater because of their high removal efficiency, low cost involvement and utilizing the microbial community to convert the contaminants into simpler non-toxic materials. Sewage sludge is used extensively in wastewater treatment process and exhibits as potential remover of carbonaceous pharmaceuticals from wastewater (Kreuzinger et al., 2004; Clara et al., 2005). Various researchers showed that a combination of sewage sludge and trickling filter are widely used as biological wastewater treatment method and can remove pharmaceuticals and other contaminants to varying amounts (Clara et al., 2005; Joss et al., 2005; Kasprzyk-Hordern et al., 2009; Radjenovic et al., 2009; Petrie et al., 2013a). Another investigation revealed that the average removal efficiencies of pharmaceuticals from wastewater in WWTPs using sewage sludge treatment varies from 20% to 99% (Bueno et al., 2012). Pérez et al., (2005) investigated the fate of three sulphonamides at low concentration level in sewage sludge process and observed a removal ranging from 50 – 93% through biodegradation pathway in sewage sludge. Kim et al., (2005)

demonstrated the study of removal of tetracycline antibiotic using sewage sludge process and the subsequent results suggested the removal of tetracycline occurred mainly via adsorption onto the sewage sludge.

2.2 Studies on ciprofloxacin and ofloxacin *(refer to Fig. 1.2 and Fig. 1.3)*

Van Doorslaer et al., (2014) suggested that Ciprofloxacin and Ofloxacin are the antibiotics belonging to the Fluoroquinolones (FQs) family and these antibiotics are broadly used in medical and veterinary purposes. They exhibit antibacterial activities by intercepting the transcription and replication of bacterial DNA by cutting bacterial DNA in the gyrase DNA and type IV topoisomerase enzymatic complexes (Derayea et al., 2021; Yıldırım et al., 2020). These two antibiotics show excellent bioavailability because of rapid absorption following oral administration and exhibit a broad spectrum of activity against both gram-positive and gram-negative bacterial species (Derayea et al., 2021; Guan et al., 2020). Environmental hazards related to the use of antibiotics is the result of antibiotic resistance due to the origination of antibiotic-resistant bacteria which is considered as one of the most emerging health associated problems in recent days (Guan et al., 2020, Wang et al., 2019). Various researchers developed new, sensitive, precise and selective analytical methods for the determination of ciprofloxacin and ofloxacin and their residues in food and the environment (Tian et al., 2020; Yu L et al., 2020). Numerous HPLC-UV methods have been developed for the ascertainment of these compounds in various matrices, like urine and human plasma (Yıldırım et al., 2020, Cairoli et l., 2020). Maia et al., (2020) carried out methods based on HPLC-MS for the determination such antibiotics along with other fluoroquinolones in wastewater.

2.3 Use of sustainable adsorbents for the removal of pharmaceuticals

Adsorption is the process in which the atoms of fluid phase stick to atoms of solid state and the different steps involved in the process of adsorption are (i) transportation of solute from the bulk fluid phase (ii) film diffusion (iii) pore diffusion and (iv) adsorption to the solid surface by weak van der Waals attractions (Vignesh et al., 2022). Various researchers conducted adsorption experiments with powdered activated carbon and elimination rate was up to 99.7% for 29 antibiotics found in surface water. Sotelo et al. (2012) used activated carbon in fixed bed adsorption study and observed the elimination rates of diclofenac and caffeine up to 96% and 99% respectively. Activated carbon has been used in a broad range for the elimination of medicaments present in different water bodies (Nguyen et al., 2020). The major drawback for using activated carbon as adsorbent is the requirement of huge amount of water for cleansing purposes (Vishnu et al., 2021).

Though agricultural wastes are used for the preparation of activated carbon and bio-chars but these materials can be used directly for adsorption of the pharmaceuticals (Baccar et al., 2012). Portinho et al. (2017) studied with grape stalk (Vitis vinifera) for the adsorption of caffeine substrates. Modification of grape stalk was done using phosphoric acid, and the discussion was made between adsorption capacities between the modified and unmodified material and illustrated that the modified grape stalk showed better adsorption capacities than the unmodified material. Villaescusa et al. (2011) examined various adsorbents like waste from wine production (grape stalk), yohimbe extraction (yohimbine bark) and cork bark for the adsorption of paracetamol and observed that Grape stalk was more effective in the adsorption of paracetamol following pseudo second order kinetics.

Tan et al., (2015) utilized biochars produced from pyrolyzing the pine wood at 425^0C for the removal of salicylic acid and ibuprofen effectively by means of adsorption. Yao et al., (2013) used biochars, prepared from sludges from effluent treatment plants for the effective adsorption of gatifloxacin and other pharmaceuticals. Mondal et al., (2016) examined activated biochar produced from mung bean husks for the adsorption of ranitidine hydrochloride in the fixed bed columns. Xie et al., (2016) prepared biochar from pine wood under different thermochemical conditions and investigated the adsorption behaviour of sulfamethoxazole and sulfapyridine.

Another promising natural adsorbent material is clay that exhibits enhanced adsorption for its stable nature, mechanical strength, high specific area, high ion exchange capacity and chemical structure (Srinivasan, 2011). Dordio et al. (2017) carried out experiments using lightweight expanded clay aggregates for the elimination of gemfibrozil, mefenamic acid, and naproxen and found better absolute removals; while using vermiculite obtained high adsorption capacities.

Alkhamis et al. (2008) used chitosan particles for the adsorption of ketotifen fumarate and observed that its adsorption capacity is greater at pH 7 than at 10 and it may had adsorbed both into the bulk structure of the substance and onto its surface in accordance to adsorption mechanisms.

2.4 Sewage sludge as potential adsorbent for the removal of pharmaceuticals

Sewage sludge that has been examined as a potential adsorbent by itself or as a precursor, is a by-product from the sewage treatment process and consists of organic and inorganic components (G. Xu et al., 2015). Various researchers used sewage sludge as an adsorbent in different studies to remove efficiently pollutants such as dyes [Z. Aksu et al., 2001], phenol [W. Zhu et al., 2014] and pesticides [R. Rojas et al.,

2014]. Some researchers have shown that sewage sludge in combination with fish wastes may react synergistically for the removal of carbamazepine from an aqueous solution [D. Bendz et al., 2005]. Rui Ding et al., (2012) carried out experiments with sewage sludge and waste oil sludge-derived materials as adsorbents and obtained an excellent result in removal of oxytetracycline, enrofloxacin and erythromycin from wastewater. Lu Wang et al., (2017) conducted batch experiments with five fluoroquinolones including ciprofloxacin, ofloxacin, norfloxacin, enrofloxacin and lomefloxacin using sewage sludge and investigated the detailed adsorption and biodegradation behavior of the five fluoroquinolones during the batch experiments. The results indicated that adsorption onto the sludge surface is the primary removal pathway of the treatment process using sewage sludge.

2.5 Batch equilibrium study: *Experimental design and parameter estimation*

Adsorption is widely considered to be the most cost-effective and efficient removal technique of micropollutants among the various conventional wastewater treatment processes [Dural et al. 2011]. Adsorption, using sewage sludge is a cost-effective and effective process for the treatment of various emerging organic contaminants (EOCs), and the same is used in wastewater treatment plants [Mishra, 2016]. The following steps that mainly govern the adsorption process are:

I adsorbate transport to the adsorbent from the bulk of the liquid surrounding the

II adsorbent.

III film diffusion: diffusion of the adsorbate across the liquid film surrounding the adsorbent particle.

IV pore diffusion: diffusion of adsorbate within the porous surface of adsorbent particle.

V adsorption to the solid surface by weak van der Waals attraction, electrostatic attractions, sometimes strong chemical bonds and hydrogen bonding.

Removal of micropollutants through adsorption depends on the properties of both the adsorbates and adsorbents. Porosity, surface area, pore volume, as well as the surface functional groups of the adsorbent and the characteristics of the adsorbate i.e. shape, charge, size and hydrophobicity, have impact on the adsorption efficiency [Michael et al. 2013]. The removal pathways of organic micropollutants in sewage sludge system involves adsorption, hydrolysis, biodegradation as well as volatilisation [Kim et al., 2005]. Bing et al., (2010) examined the adsorption of eleven antibiotics including ciprofloxacin and ofloxacin which are the active medicaments of various pharmaceutical formulations, by adsorption with activated sludge. To determine the maximum adsorption capacity five different isotherm models were utilized in this study to find out the best fitted one.

Multicomponent adsorption study implies the competitive adsorption mechanism between more than one component and it is exactly important as industrial effluents usually contain more than one component [Erto et al., 2012]. Estimation of multicomponent adsorption utilizing information obtained from single component isotherm models, is the most complicated problem in the field of adsorption study [Wurster et al. 2000]. Treatment of wastewater containing organic micropollutants using activated sludge is carried out by many researchers [Rogers, 1996; Kim et al., 2005; Li and Zhang, 2010; Ding et al., 2012; Xiancai et al., 2017]. Adsorptive properties of a binary mixture in batch adsorption analysis was carried out by Tang et al. (2012). Modified competitive Langmuir-like model was developed to calculate the

experimental data for binary system was used by many researchers [Banerjee et al., 2020; Banerjee et al., 2014]. The kinetic study of adsorption process for single and binary system were conducted using pseudo-first order and pseudo-second order model by many researchers [Mahmoud et al. 2012; Dural et al. 2011]. Different researchers studied the adsorption mechanism by applying the intra-particle diffusion and film diffusion model respectively [Tang et al. 2012; El-Khaiary and Malash, 2011]. Hill, 1986; Tien, 1994 predicted multicomponent adsorption data from multicomponent models including competitive Langmuir-like model and Le Van-Vermeulen model using parameters from single component system. Various researchers analyzed Ideal Adsorbed Solution model (IAS) to explain multicomponent adsorption [Yun et al. 1996; Erto et al. 2012].

2.6 Transient behavior of packed column: *Development and application of convective diffusion models*

Determination of the breakthrough curve for adsorption in packed bed is a very important concern because it provides the basic but very important information in the design of a packed column. The experimental method is usually a time consuming and un-economical process, particularly for the trace contaminants with long residence times [Xu et al. 2013].

In order to overcome the stringent assumptions of these semi-empirical models, both in their primary and linearized forms, in this piece of research, a robust and novel convective-diffusion model is proposed with generation or depletion terms being governed by pseudo kinetics of adsorption under dynamic condition. A pore and solid diffusion model has been developed for a fixed bed column considering irreversible adsorption isotherms and neglecting outside film resistance [Weber and Chakravorti

1974]. Lapidus and Amundson applied a convective-diffusion model to analyse the transport mechanism of solute in an unsteady one-dimensional saturated flow, neglecting intra-pellet mass transfer [Lapidus and Amundson 1952]. Similarly, a number of research groups analysed packed-bed adsorption using the convective-diffusion model with due consideration for inter-pellet diffusion [Singha et al. 2012; Saha et al. 2012; Thirupathi et al. 2007].

2.7 Transient behavior of packed column: *Scale-Ups using semi-empirical models*

In industry, the wastewater is generated in huge volumes and hence a convenient method to handle such a great volume of water is required to treat the same prior to discharge. Batch adsorption processes are not practically feasible to carry out the treatment method for the industrial scale to deal with huge flow of wastewater [Karunarathne et al. 2013]. The reliable design for the packed bed adsorbent requires the foundation of acceptable modelling framework for establishing the shape of the breakthrough curve [Lee et al. 2000]. Various parameters like bed depth or bed height, inlet and outlet flow rates and influent concentrations are required to be evaluated to study the behaviour of the breakthrough curve corresponding to a fixed bed column [Suyadal et al. 2000]. The dynamics of the fixed bed column depend on several features involving strong non-linearities between the adsorption equilibrium isotherms, competition of solutes of more than one kind for adsorbent sites resulting strong interference effects, mass transfer resistance between the fluid phase and the solid phase, fluid dynamics dispersion phenomenon and making the modelling of the dynamics of the fixed bed adsorption systems more challenging [Sotelo et al. 2012]. Most of the reported studies reveal that adsorption-based separation depend on equilibrium and kinetics of adsorption [Alhamed 2009; Lua and Jia 2009].

Batch equilibrium analysis followed by dynamic study can ascribe the mass transfer mechanism, adsorption capacities of the adsorbents, suitability of the isotherm representing the equilibrium and the effects of different parameters governing the dynamics of the adsorptive systems [Manjare and Ghoshal 2005]. Teeba M et al. (2017) conducted the adsorption study of ciprofloxacin and norfloxacin in a fixed bed column and investigated the various parameters related to the dynamic study in a fixed bed system, including bed height, influent concentration and flow rates respectively.

Sizirici et al. (2020), conducted experiment for removal of organic matter in terms of chemical oxygen demand (COD) from synthetic wastewater using immobilised activated sludge in fixed bed column. The effects of parameters including column bed height and influent COD concentrations on removal efficiencies were analysed using breakthrough curves. It was found that the removal efficiency increased with increase in fixed bed height and with a reduction in influent COD concentration.

Semi empirical models are simplified models used to investigate the scale of the laboratory column in order to make an effective design for pilot scale columns [Sarin et al. 2006]. In 1920, Adams and Bohart first proposed the idea of bed depth service time model, and it is being considered to be the simplest semi-empirical model in the packed bed study that permits the most rapid determination of the adsorbent bed performance [McKay and Bino 1990]. Working principle of this model is based on theory of surface reaction rate, i.e. the adsorption rate is proportional to the fraction of remaining adsorption capacity of the adsorbent bed [Lehmann et al. 2001]. This model also illustrates the correlation between the bed height or depth of the packed bed column and the service time [Kratochvil et al. 2000]. The model is validated based on the assumption that external mass transfer resistance and intra-particle diffusion both are negligible and the adsorption kinetics is mainly controlled by the surface chemical

interaction between the solute and the adsorbent, rare in real systems [Ayoob et al. 2007]. Inherent assumption of the BDST model is the symmetry of the breakthrough curves and the same is not practically possible to achieve and here lies the major limitation of this model [Zulfadhly et al. 2001]. Although the BDST model suffers from certain limitations, it is practiced worldwide. The model is favourable only in describing the initial part of the breakthrough curve i.e. up to the breakthrough point or saturation points (up to 10-50% approximately). BDST model is not suitable for analysing systems receiving longer period of time to reach equilibrium, as the solid-phase loading of the column bed does not bear a certain relationship with time at various bed heights of the column [Ko et al. 2003]. In order to eliminate such limitation a constant bed capacity of the column throughout the operation is considered for the original BDST model. This proposition may not be true in certain instances [Ayoob et al. 2007].

Apart from BDST model, dynamics and performance of an adsorption column is also described by the Thomas model [Thomas 1944]. This model has been derived from the second-order reaction kinetics (the rate determining step) and is followed in any adsorption process [Suksabye 2008]. This model assumes Langmuir's pseudo-kinetics of adsorption-desorption ignoring resistances from both intra-particle mass transfer and external fluid film and also assumes that there is no axial dispersion in the fixed bed [Franco 2017]. Primary disadvantage of this model is that it has been derived from second-order reversible reaction kinetics where physical adsorption does not follow chemical interactions always, rather controlled mainly by the inter phase mass transfer [Rao et al. 2002]. Experimental values can be fitted to the Thomas Model to find the maximum adsorption capacity of the packed bed column and the kinetic rate constant [Fu et al. 2004; Malkoc et al. 2006].

Another semi-empirical model, that is well used in the dynamic study of fixed bed adsorption is known as Yoon-Nelson model proposed by Yoon and Nelson [Yoon and Nelson 1984] assumes that the probability of solute adsorption and breakthrough is proportional to the decreasing rate of the adsorption probability within the fixed bed. This model is brief and independent of the adsorbate and adsorbent characteristics as well as geometric parameters of the fixed-bed column [Ahmed et al. 2018].

In most of the semi-empirical models, including Thomas model and BDST model, cross sections of the functional adsorbent bed are considered homogeneous, thereby neglecting the radial movements. This causes significant error in the analysis because these models are developed on the basis of a strictly plug flow behavior. Thomas model assumes Langmuir equilibrium relationship to hold good for the specific adsorbent, but are mostly used extensively disregarding the sorbate-adsorbent adsorption equilibrium. Also, the original Thomas model was found computationally complex as it uses first order Bessel function (Thomas 1944). The simplified Bohart-Adams model is generally unable to accurately predict the nature of the breakthrough curve beyond the breakthrough concentration of 30% (Aksu 2007). Even though the semi-empirical models are derived independently, a critical analysis performed by Khim Hoong Chu (Chu 2020) shows the mathematical equivalence of simplified Bohart-Adams, simplified Thomas, and Yoon-Nelson models.

Chapter 3:-

Physical and chemical characterization of raw sewage sludge

Adsorption is a simple, widely-adopted, and eco-friendly method, for its ease of operation, low investment, and relatively higher capability in removing contaminants while generating fewer hazardous by-products as compared to other available treatment methods. Among various commercial adsorbents, raw sewage sludge [RSS] is a widely used adsorbent with a proven ability to remove various micropollutants from wastewater. It is a matrix composed of carbonaceous matter along with other chemical and biological constituents. RSS is an effective adsorbent due to the presence of a high degree of porosity and internal surface area. Adsorption of CIP and OFLX on RSS depends on several factors like hydrophobicity, specific surface area, surface charge, and surface functional groups of the RSS.

3.1 Physical and Chemical Characterization

The raw sewage sludge is perfectly dried at around 35^{o}C in an air oven for 5-6 days. The dried mass is then pulverized using a mortar and pestle and is then sieved through a screen (BS 60 mesh). The mass obtained after sieving is kept in a desiccator at normal temperature and further characterized physically and chemically.

3.1.1 Analysis of Scanning Electron Micrography (SEM) based images

The surface topography of adsorbent material is examined by a Field Emission Scanning Electron Micrograph (FE-SEM) with x6000 magnification. A Field Emission Scanning Electron Microscope (FE-SEM) [Make: HITACHI, Japan; Model: SU3800] is used in this analysis. FE-SEM study for both raw and post-treated sludge is carried out in order to examine the change in the surface texture and actual loading capacity of raw sludge before and after adsorption.

The Scanning Electron Micrograph (SEM) image of raw sludge obtained from the analysis is shown in Fig. 3.1. Fig. 3.1 represents the SEM image of the raw sludge surface and reveals the particle morphology and surface structure of the raw sludge.

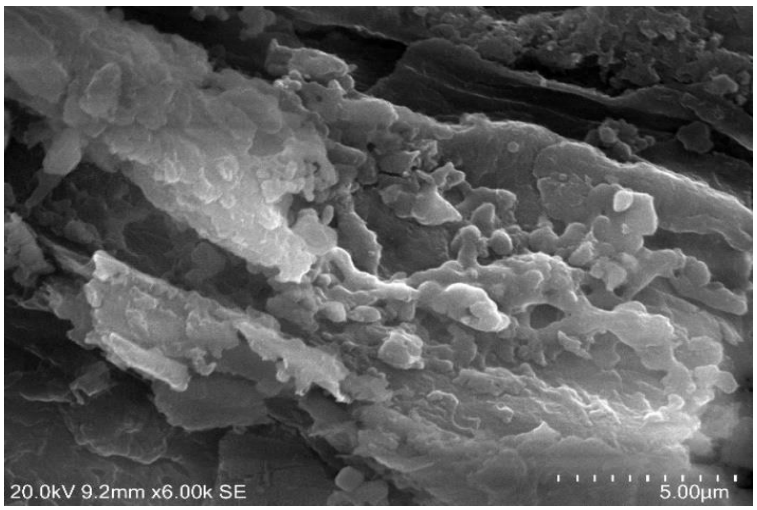

Fig. 3.1 Scanning electron micrograph (SEM) image of Raw Sewage Sludge at ×6000 magnification.

The surface morphology of the sample is extremely rich and heterogeneous in nature. Some cavities are seen and different forms like fluffy sponges, balls, and simply small formless particles are observed. These structures could benefit in the water permeation and thus make the adsorbate molecules accessible.

3.1.2 Fourier Transform Infrared Spectroscopy (FTIR) based analysis

Characterization of the surface functional groups retained on the surface of the raw sewage sludge is investigated by transmission infrared spectrum obtained using Fourier Transform Infrared Spectroscopy (FT-IR). An FT-IR spectrophotometer (Make: PerkinElmer; Model: FT-IR C120947) is used for this purpose. The entire IR spectrum is taken in the transmission range of 4000 cm^{-1} - 400 cm^{-1}. The FT-IR spectrum is received at a resolution of 1 cm^{-1}. The spectrum of KBr, set as a background in the spectrometer, is subtracted from the spectrum of the raw sewage sludge sample each time. The FTIR spectroscopy output is represented by the % transmittance vs wavenumber in cm^{-1}.

The spectral analysis of raw sewage sludge represented in Fig. 3.2 indicates a significant peak at 3412 cm^{-1}, probably due to broad H bonded O-H stretching of alcohols [J. Coates, 2006]. The bands at 2923 cm^{-1} and 2852 cm^{-1} correspond to methylene C-H asymmetric or symmetric stretchings of alkanes [Reveille et al., 2003]. No characteristic functional group is found corresponding to the band at 2343 cm^{-1}. The bands at 2028 cm^{-1} and 1875 cm^{-1} indicate carbonyl compounds. The band at 1639 cm^{-1} is due to the alkenyl -C=C- stretching or -N-H bending of primary amine [EI-Hendawy, 2003]. The band at 1548 cm^{-1} corresponds to mild >N-H bending of a secondary amine. The band at 1426 cm^{-1} is assigned to organic sulfates or carbonates [Sheen et al., 2008]. The bands at 1384 cm^{-1} and 1033 cm^{-1} [Smidt et al., 2002] are

attributed to methyl C-H asymmetric stretch and primary alcohol C-O and P-O-C stretching of aliphatic phosphate respectively. The peak at 796 cm^{-1} is due to the mild =C-H bending of alkenes. The bands at 779 cm^{-1}, 759 cm^{-1}, and 730 cm^{-1} correspond to mild C-Cl stretch of aliphatic chloro-compounds.

The band at 730 cm^{-1} is due to the presence of weak $–(CH_2)_n$ bend of alkanes and alkyls. The bands at 694 cm^{-1} and 643 cm^{-1} are attributed to C-Br stretch of aliphatic bromo-compounds, C-H stretch of thiols and alkyne C-H bend respectively. The band at 533 cm^{-1} is attributed to C-I stretch corresponding to aliphatic iodo-compounds. The band at 467 cm^{-1} may be due to S-S polysulphides.

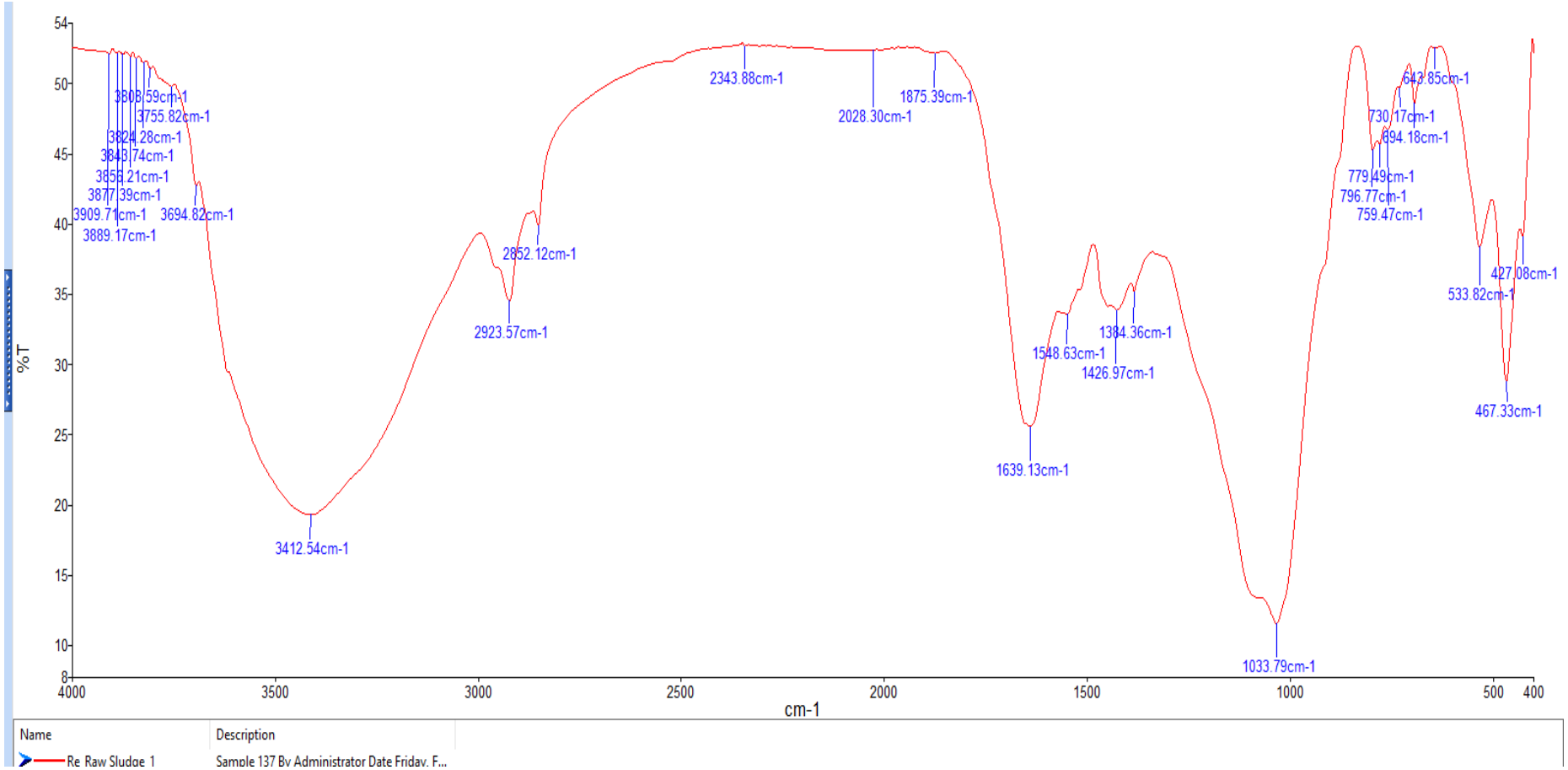

Fig. 3.2 FT-IR spectra of untreated sludge before adsorption.

3.1.3 Elemental analysis of raw sewage sludge:

The elemental analysis of the raw and post-treated sludge is carried out for estimating Carbon (C), Hydrogen (H), Nitrogen (N), and Sulphur (S) present in the samples. The same is carried out using a CHNS Analyzer (Make: ELEMENTAR, Germany; Model: VARIO MICRO CUBE). Temperatures of the combustion tube and the reduction tube are set at 1150^{o}C and 850^{o}C respectively. The pressure of the helium gas (carrier) is maintained at 1100 – 1200 millibar. The results are given in Table 3.1.

Table 3.1 Elemental analysis of raw sewage sludge obtained from CHNS analyzer.

Sample	C % (wt % daf)	H% (wt % daf)	N% (wt % daf)	S% (wt % daf)
Raw Sludge	19.97	2.847	2.03	0.455

The carbon, hydrogen and nitrogen load of raw sewage sludge is estimated as 19.97 wt % daf, 2.847 wt % daf, and 2.03 wt % daf respectively. The sulphur content is found to be much less as compared to the other three elements.

3.1.4 Point of Zero Charge

The nature of the surface charge of the raw sewage sludge is determined by successive measurements of the zeta potential range using a zeta sizer [Make: Malvern Inc., USA; Series: Nano-Z; Model No: ZEN 2600]. The sludge solutions of varying pH are adjusted to approximately 1.0, 3.0, 5.0, 7.0, 8.0, 10.0, and 12.0 by adding 0.1 (M) HCl and 0.1 (M) NaOH to the primary raw sludge sample (as much required) at 25^{o}C. The average zeta potential for each of the pH-adjusted samples is measured using a zeta-sizer. By plotting the measured values of zeta potential against the values of pH, a

curve is regressed using the pH-zeta potential scattered dataset. Afterward, the nature of the surface charge is ascertained effectively at a particular value of the working pH. It is explicit that solution pH affects the surface charge of raw sewage sludge. At a working solution pH of 7.8, maintained constant for all the experiments of batch adsorption, the surface of sewage sludge remains negative all along [refer Fig. 3.3].

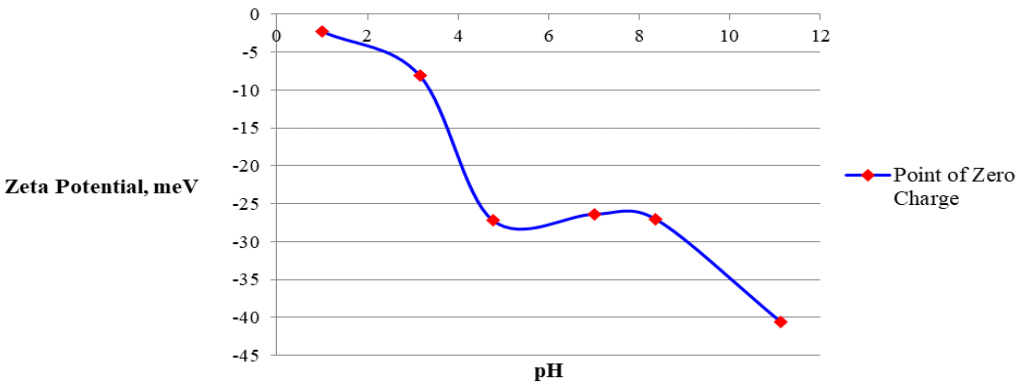

Fig. 3.3 Zeta potential versus pH of untreated sewage sludge.

3.1.5 Measurement of Hydrophobicity of Raw Sewage Sludge (RSS)

Measurement of contact angles using a wettability analyzer [Make: KRÜSS Scientific, Germany; Model: DSA4; Drop shape: Sessile] is important in order to elucidate the hydrophobicity of raw sewage sludge surface before adsorption of ciprofloxacin and ofloxacin. In this case, 1 µL of millipore ultra-pure water is dropped over the solid surface, and the contact angle is measured with the help of a goniometer.

The contact angle (θ) and hence the degree of wettability changes when solid and liquid surfaces interact with each other [Mobin et al., 2022; Aslam et al., 2021]. Quantification of contact angle allows assessment of hydrophobicity of a liquid film on solid surface. According to the theory of wetting, a solid surface, in contact with water is considered to be hydrophobic in nature, distinctively, if the contact angle of

the surface area of the material with water (θ_{H2O}) > 90°. On the other hand, if θ_{H2O}< 90°, the surface is considered susceptible to wetting [Vazirinasab et al., 2018].

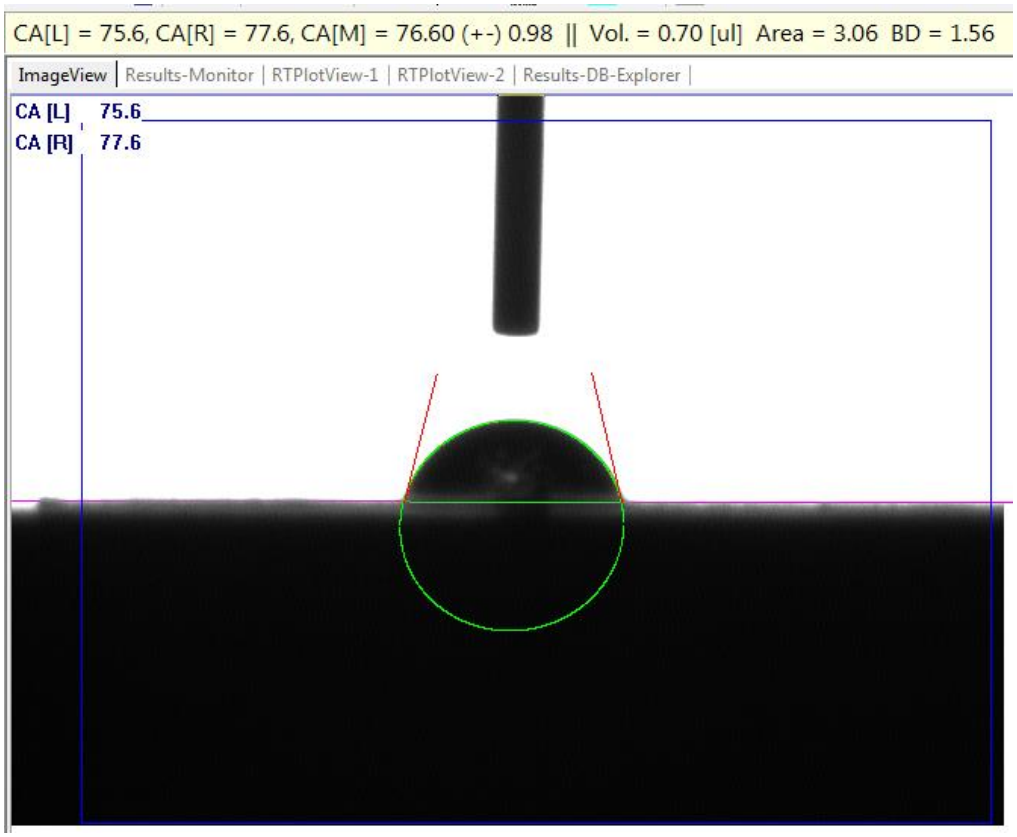

Fig. 3.4 Contact angle measurement of Raw Sewage Sludge (RSS).

It is observed that the average θ_{H_2O} for raw sewage sludge surface is 76.6° (± 0.98°) [see Fig. 3.4] indicating the surface is hydrophilic in nature.

3.1.6 X-ray photoelectron spectroscopy (XPS) based analysis

The X-ray photoelectron spectroscopy (XPS) based analysis, primarily meant for surface analysis is conducted using an advanced electron spectroscopy system [Make: Omicron Nano Technology GmbH, United Kingdom; Model: EIS-Sphera]. A monochromatized Al Kα source [Model: XM 500; $h\nu$ = 1486.7 eV] is used for high-resolution X-rays. XPS spectra for different elements are obtained by plotting intensity against binding energy. XPS-based analysis ascertains the elemental composition and

chemical states of the raw sludge [Zhang et al., 2022]. The full-scan XPS spectrum of raw sludge is represented in Fig. 3.5. High-resolution spectra reveal the presence of various elements assigned to O 1s (532.2 eV), N 1s (399.7 eV) and C 1s (284.5 eV), Ca 2p (347.4 eV), Si 2p (102.8 eV) etc. in raw sludge (see Fig. 3.5).

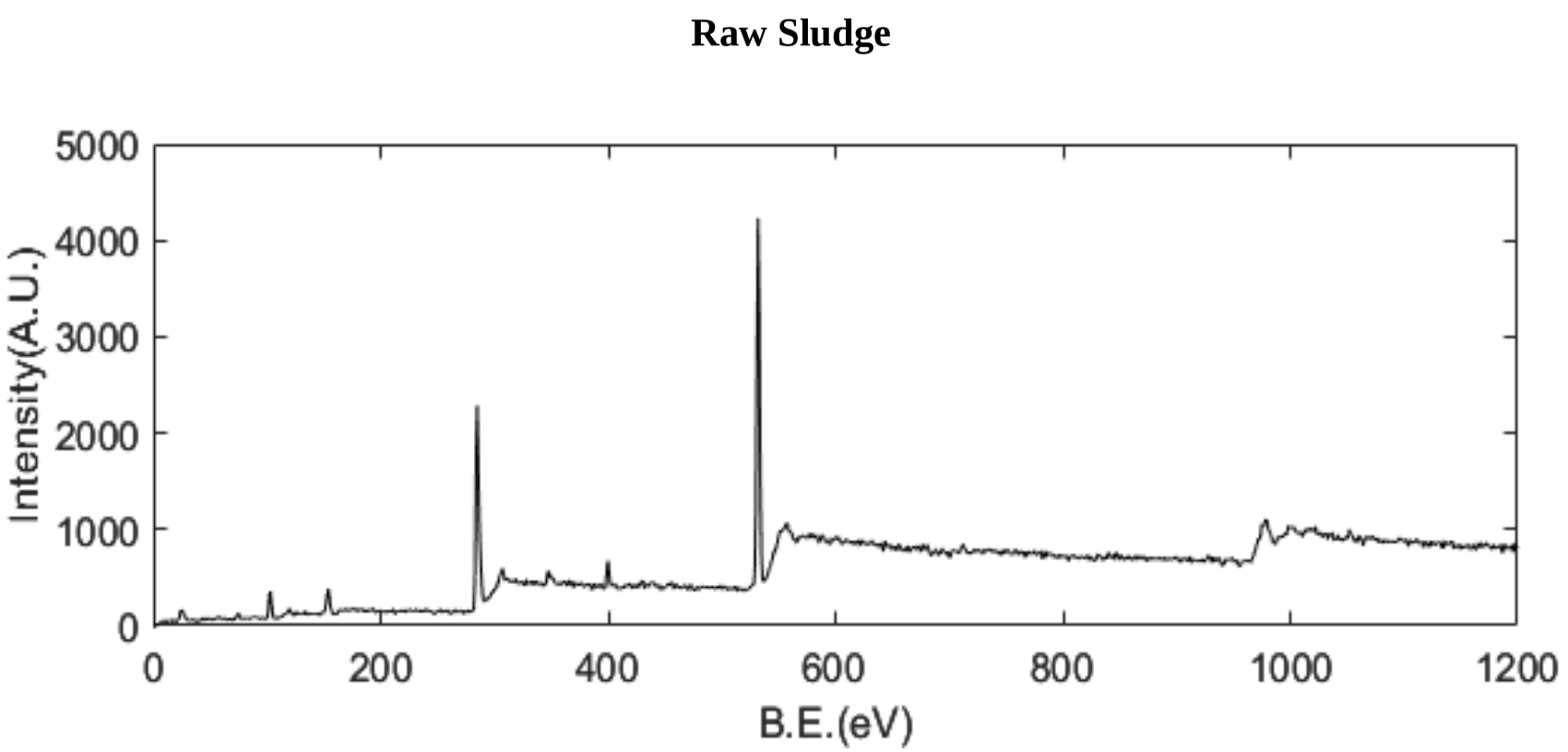
Raw Sludge
Intensity(A.U.)
5000
4000
3000
2000
1000
0
0
200
400
600
800
1000
1200
B.E.(eV)

(A)

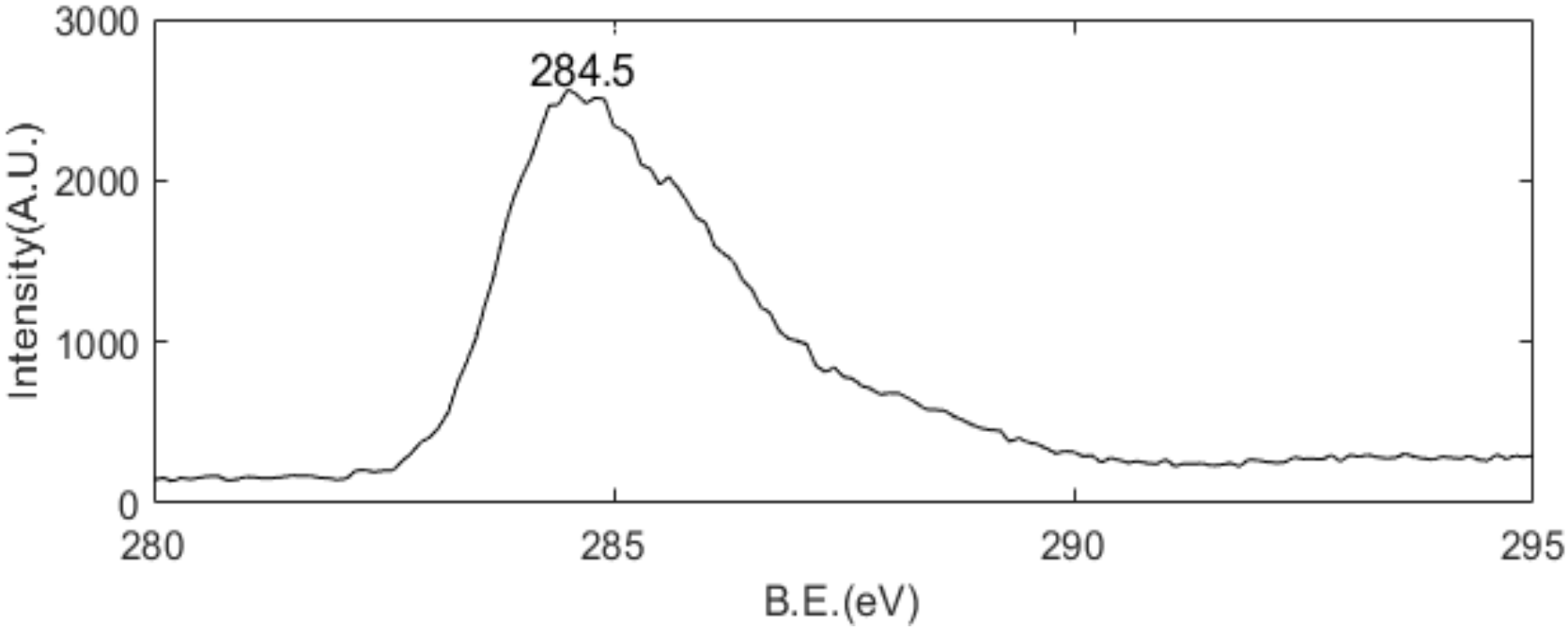

(A: C 1s)

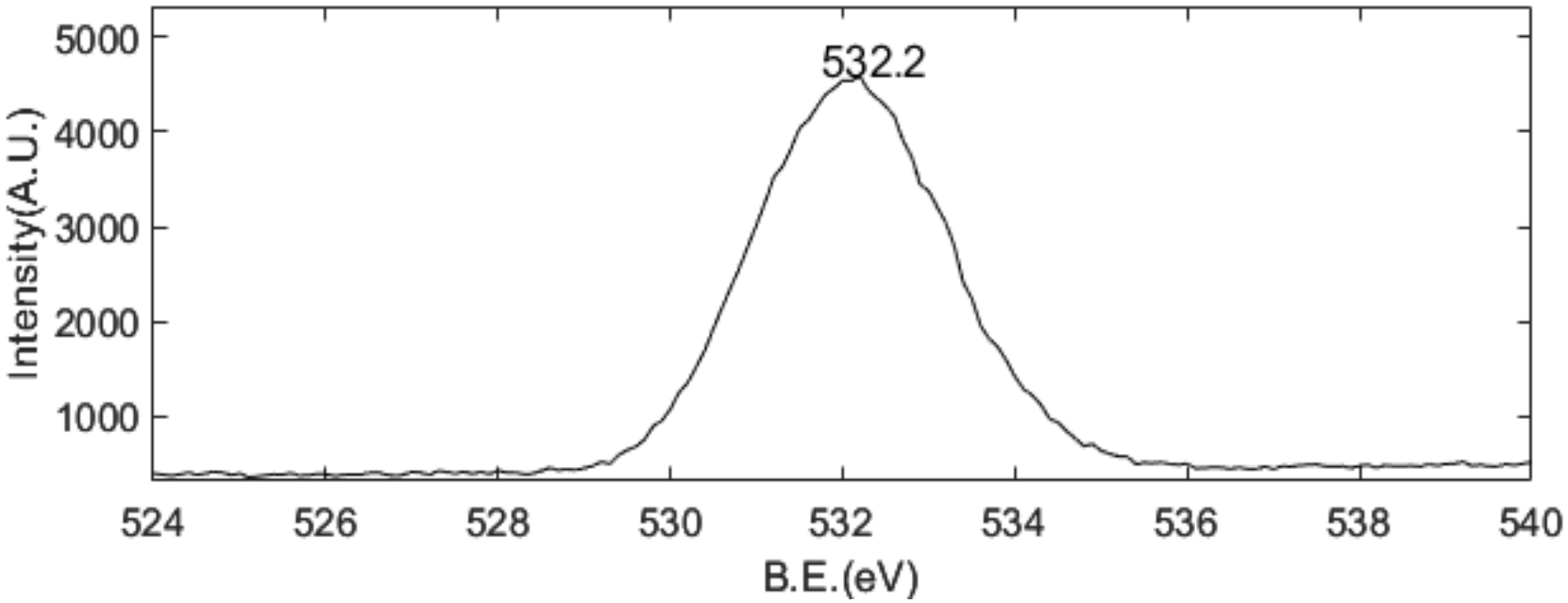
532.2
Intensity(A.U.)
5000
4000
3000
2000
1000
524
526
528
530
532
534
536
538
540
B.E.(eV)

(A: O 1s)

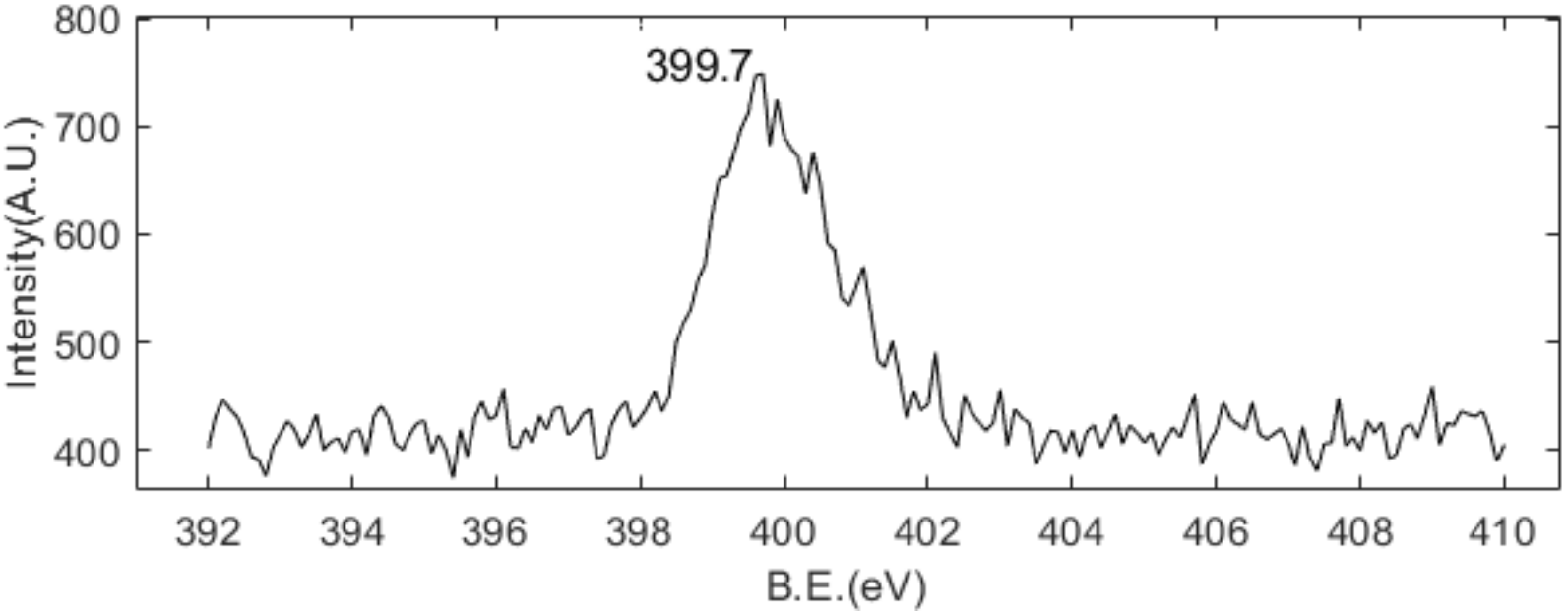
399.7
Intensity(A.U.)
800
700
600
500
400
392
394
396
398
400
402
404
406
408
410
B.E.(eV)

(A: N 1s)

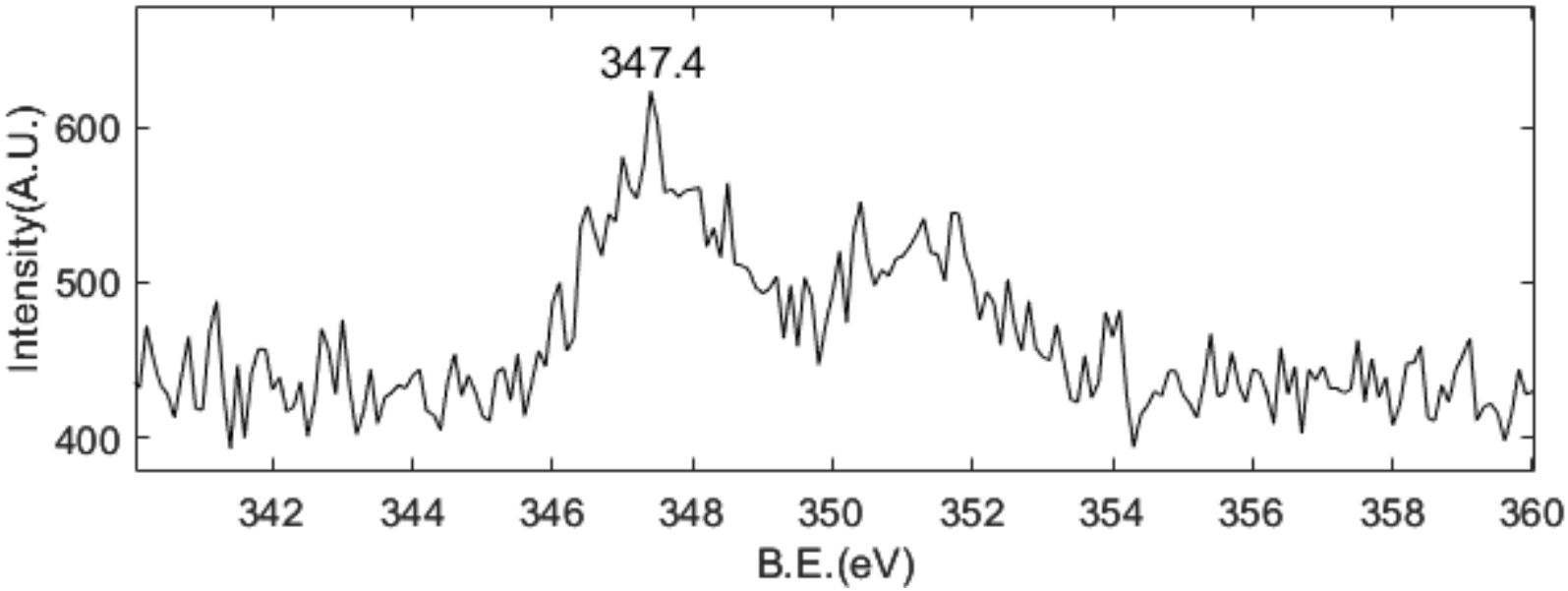
347.4
Intensity(A.U.)
600
500
400
342
344
346
348
350
352
354
356
358
360
B.E.(eV)

(A: Ca 2p)

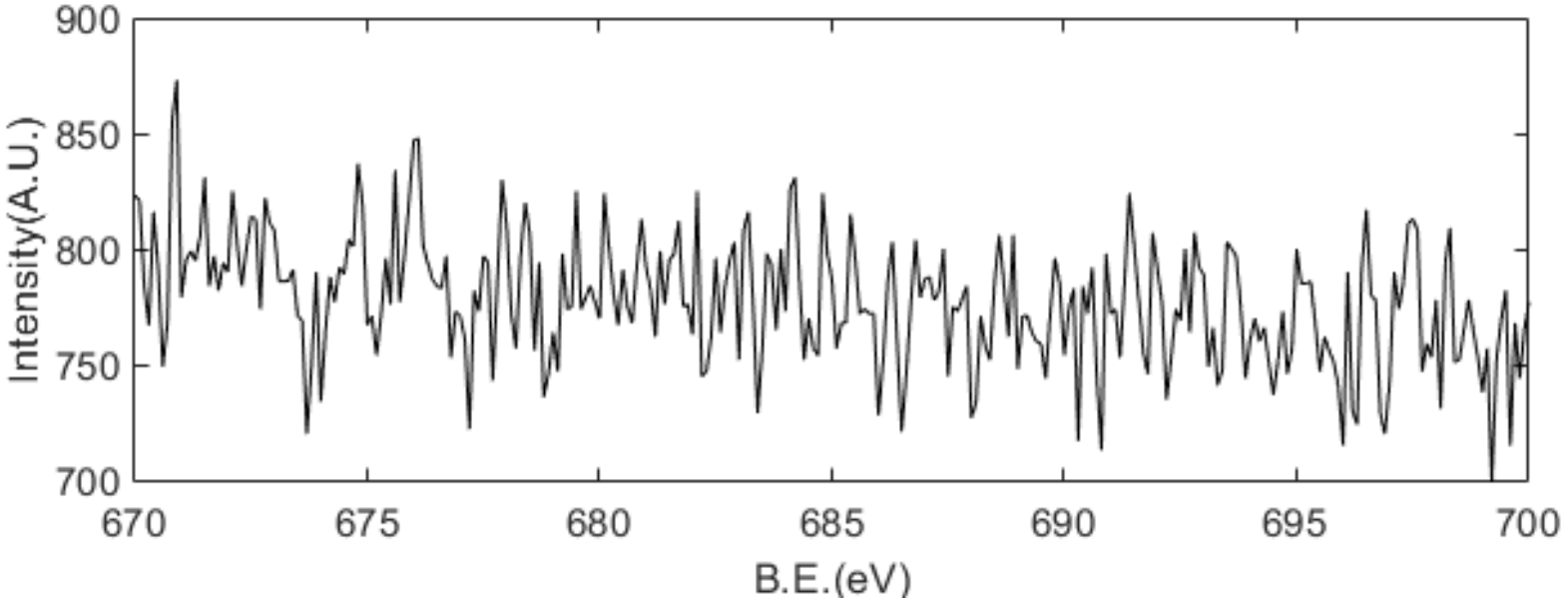
900
850
800
750
700
Intensity(A.U.)
670
675
680
685
690
695
700
B.E.(eV)

(A: F 1s)

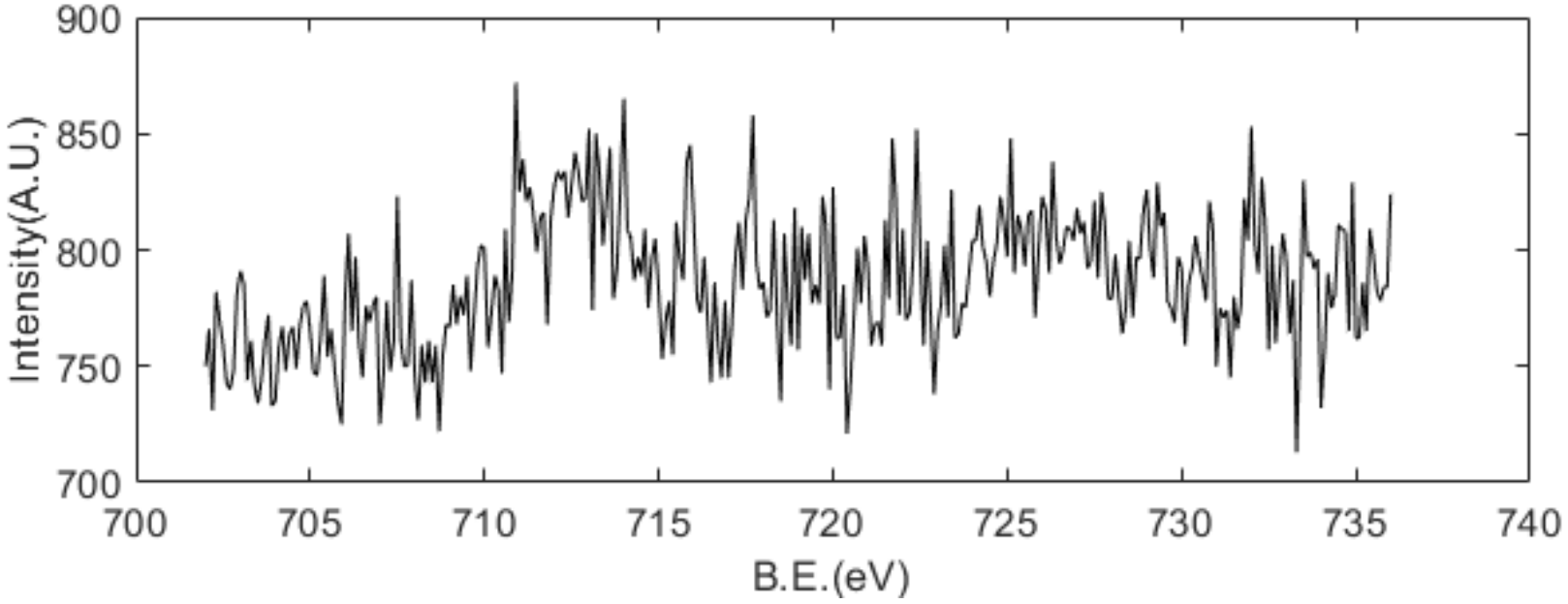
900
850
800
750
700
Intensity(A.U.)
700
705
710
715
720
725
730
735
740
B.E.(eV)

(A: Fe 2p)

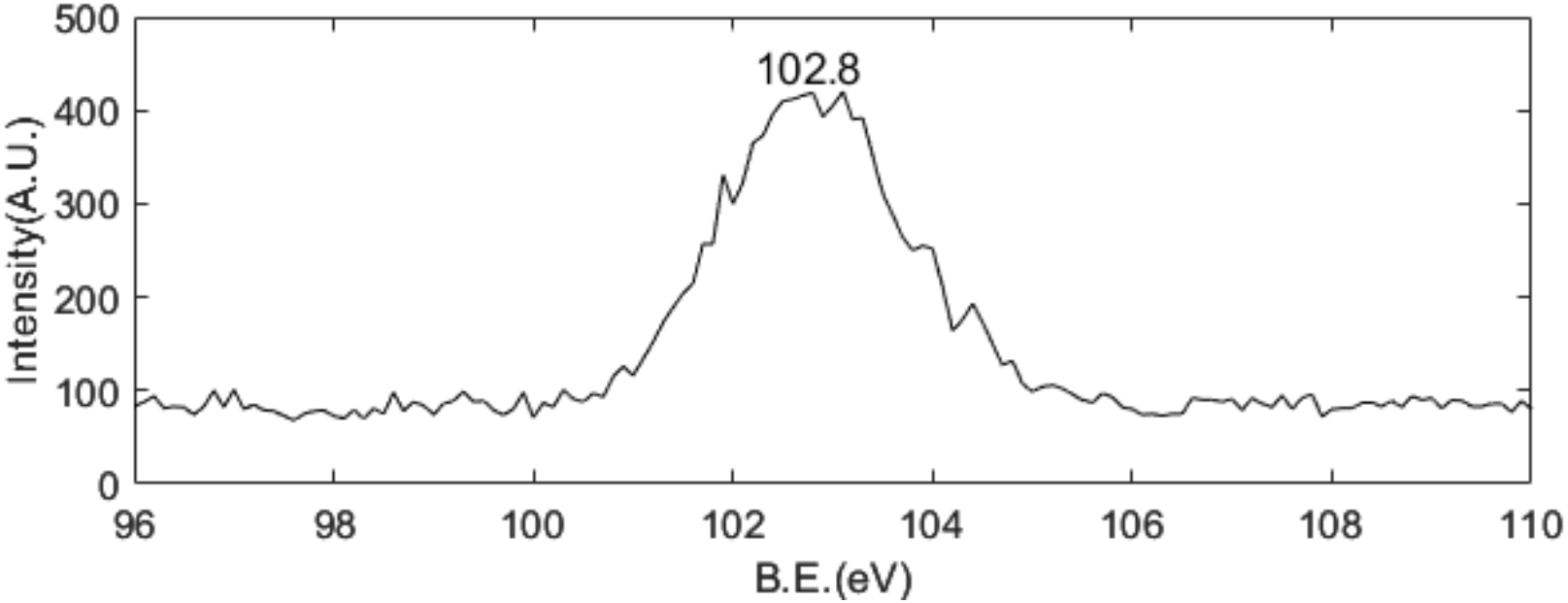
500
400
300
200
100
0
Intensity(A.U.)
102.8
96
98
100
102
104
106
108
110
B.E.(eV)

(A: Si 2p)

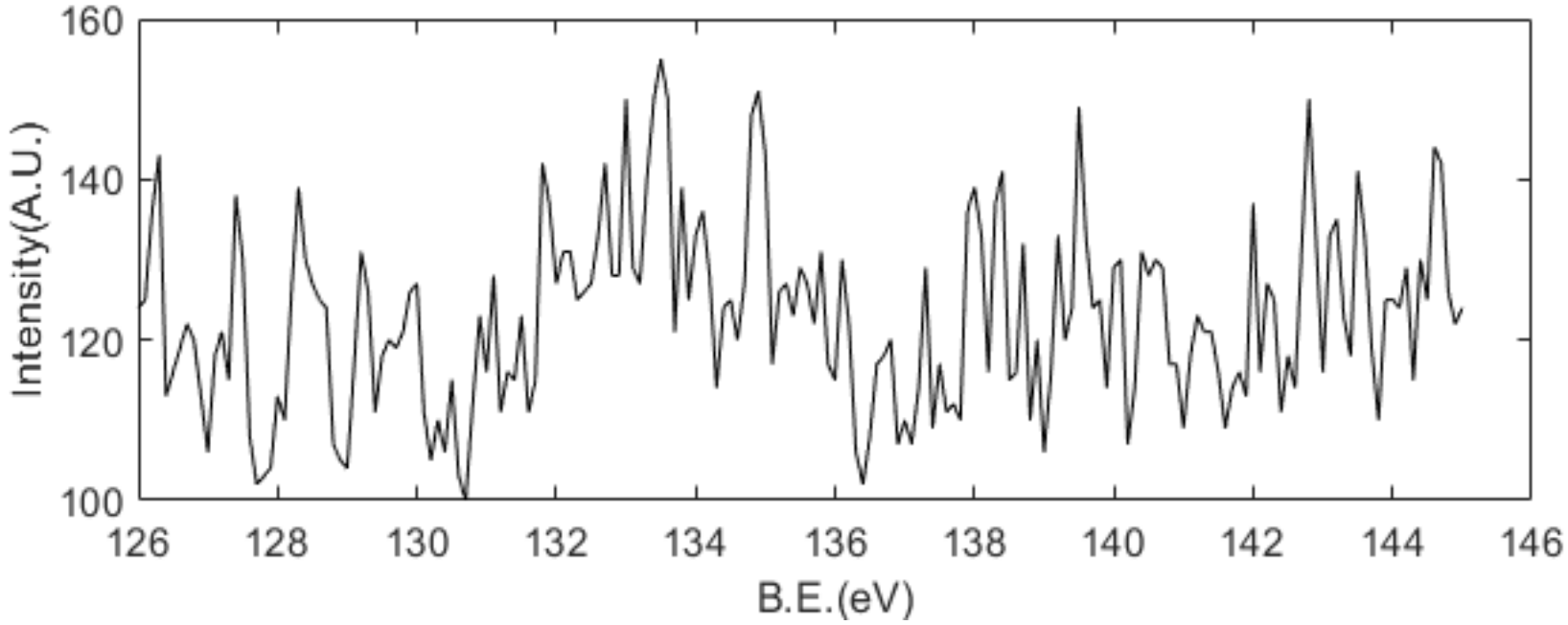
160
140
120
100
Intensity(A.U.)
126
128
130
132
134
136
138
140
142
144
146
B.E.(eV)

(A: P 2p)

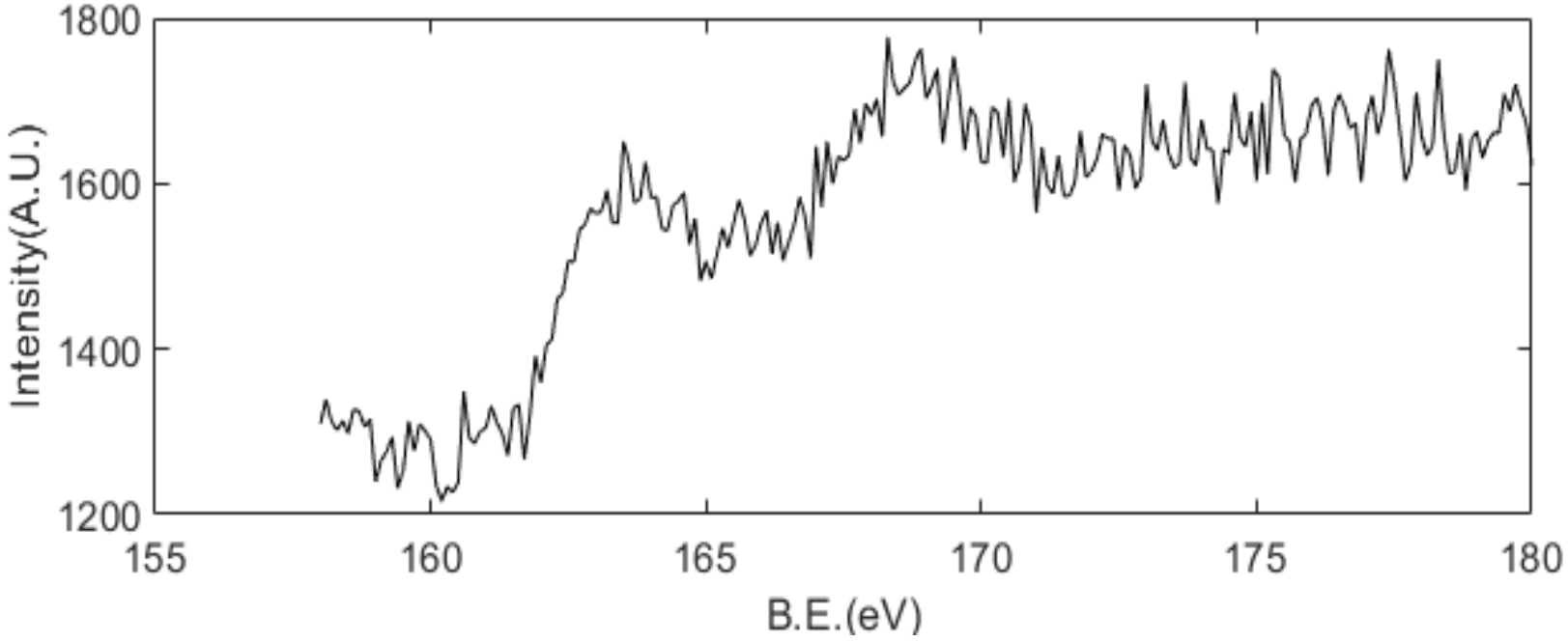

(A: S 2p)

Fig. 3.5 XPS spectrum of (A) raw sludge.

Chapter 4:-

Batch adsorption equilibrium analysis: *Pure component analysis*

In the field of environmental engineering, adsorption has become extremely significant as it eliminates a large amount of organic and inorganic chemicals while producing barely a few hazardous by-products as compared to other conventional treatment processes. Numerous attempts have been made to model single-component behaviour from a theoretical perspective. This study includes several experiments for batch equilibrium analysis of each of the pure components, namely ciprofloxacin, and ofloxacin.

From a practical point of view, since industrial or municipal effluents contain more than one contaminant, it is necessary to establish multicomponent adsorption where competitive adsorption of more than one component is the key factor. Adsorption systems with a single component as the adsorbate are represented by simplified models. Experiments carried out to analyse batch equilibrium ultimately establish the

validity of a specific adsorption isotherm. In contrast, models representing multicomponent adsorption involve inherent difficulties owing to competition between the adsorbates for the common adsorption sites of the adsorbent and mutual interactions between the adsorbing molecules. Treatment of wastewater containing organic micropollutants using activated sludge is carried out by many researchers [Rogers, 1996; Kim *et al*., 2005; Zhang *et al*., 2011; Liu *et al*., 2012; Xiancai *et al*., 2017]. The primary objective of this specific study, as described in this Chapter, is to develop specific models like the modified competitive Langmuir-like model and the LeVan-Vermeulen model, describing the multicomponent adsorption process using fundamental hypotheses of statistical thermodynamics and application of these models for the adsorption of ciprofloxacin and ofloxacin in combination.

4.1 Experimental

4.1.1 Collection and Processing of Sludge

Raw Sewage Sludge [RSS] is collected from the Municipal wastewater treatment plant [Kamarhati Municipality, North 24 Parganas, West Bengal, India]. The sludge is allowed to get naturally air-dried for a period of 5-6 days. The same is thus converted into a semi-solid mass. With this dried semi-solid sludge, the batch equilibrium analysis is carried out.

4.1.2 Chemicals

Adsorption of a single component is carried out using the pure ciprofloxacin [Make: Sigma–Aldrich, India; CAS No: 86483-48-9; Grade: Analytical] and pure ofloxacin [Make: Sigma–Aldrich, India; CAS No: 82419-36-1; Grade: Analytical]. CIFRAN-500 (Make: Ranbaxy Laboratories Ltd., India) and OFLOMAC-200 (Make: Macleods Pharmaceuticals Ltd., India) are used as the representative sources for CIP and OFLX

respectively for the batch adsorption study. The mobile phase consists of acetonitrile [Make: Sigma–Aldrich, India; CAS No.: 75-05-8; Grade: HPLC grade], ultra-pure water [Make: Sigma–Aldrich, India; CAS No.: 7732-18-5; Grade: HPLC grade], Tri-ethylamine [Make: Sigma–Aldrich, India; CAS No.: 121-44-8; Grade: HPLC grade] and phosphoric acid [Make: Sigma–Aldrich, India; CAS No.: 7664-38-2; Grade: HPLC grade].

4.1.3 Batch equilibrium analysis: *Design of experiments*

In this study, raw sludge, collected from Kamarhati Municipality Waste Water Treatment Plant [WWTP] (South 24 Parganas, West Bengal, India), is used. Solutions of pure component ciprofloxacin and ofloxacin of various concentrations in the range of 5 ppm to 100 ppm are prepared separately for the analysis of single component adsorption. 0.5 g of RSS is added to the solutions of both the components and equilibrium is achieved just on 7 days for both the components. Batch equilibrium analysis of a multicomponent system is conducted using feed solutions containing a combination of ciprofloxacin and ofloxacin of different concentrations (*Range:* 5 ppm – 100 ppm), prepared with de-mineralized water. CIFRAN-500 (Make: Ranbaxy Laboratories Limited, India) and OFLOMAC-200 (Make: Macleods Pharmaceuticals Ltd., India) are used as primary sources of the active components of ciprofloxacin and ofloxacin respectively. 100 ml of each of the feed solutions of a certain concentration is taken in a 250 ml conical flask where 0.5 gm of raw sludge is added. Each solution is kept under isothermal conditions with occasional stirring, for 7 days till equilibrium is attained. Sample solutions are then filtered through Whatman No. 1 (diameter: 125 mm) filter paper to remove the raw sludge (adsorbent) and subsequently filtered through 0.45 µm filter kit prior to analysis of the specific analytes using HPLC. These solutions are further analysed using HPLC (refer to *section 5.2.3* of Chapter 5) in

triplicate after batch equilibrium was attained (Ref. Supplementary Material C) to estimate specific concentrations of each of ciprofloxacin and ofloxacin present before and after equilibrium adsorption.

The equilibrium concentration is determined by

$$q_e = \frac{(C_0 - C_e)V}{m} \tag{4.1}$$

Where q_e= adsorbate concentration at equilibrium in mg adsorbate/g. adsorbent, C_0 = initial concentration of adsorbate in mg/L, C_e = equilibrium concentration of the adsorbate in mg/L, V = volume of the solution, and m = weight of the adsorbent in g.

4.1.4 Analytical technique

Analysis of ciprofloxacin and ofloxacin (in solution) is performed using a High-Performance Liquid Chromatography (HPLC) based system (Make: Waters, Germany; Model: 515) equipped with a 190-400 nm wavelength UV detector, a quaternary gradient system pump with a pressure range 0-4000 psi and a column oven with an operating temperature range in between 25^{o}C and 100^{o}C. Temperature of the column is maintained at 25^{o}C. Identification of compounds is carried out with a UV detector (Make: Waters, Germany; Model: 2489), and the wavelength is set at 300 nm. In order to ensure simultaneous detection of ciprofloxacin and ofloxacin, in solution, a reverse phase column (Make: Waters, Germany; Model: Sunfire C18) having dimensions 150 mm x 4.6 mm and a particle size limitation of 5µm is employed. pH of the mobile phase, passing through the column, is so maintained that the same modulates within a range of 2-7. The mobile phase is a combination of HPLC grade acetonitrile (Make: Sigma-Aldrich, India; CAS No.: 75-05-8) and a buffer solution in the ratio of 20:80 (v/v). The buffer solution is prepared by adding 2ml tri-ethylamine

(Make: Sigma-Aldrich, India; CAS No.: 121-44-8) in 200 ml HPLC grade ultrapure water (Make: Sigma-Aldrich, India; CAS No.: 7732-18-5). Following this, the pH is adjusted to 6 by adding ortho-phosphoric acid (Make: Sigma-Aldrich, India; CAS No.: 7664-38-2) dropwise, and the volume is made up to 250 ml. The buffer solution is then filtered through a cellulose acetate membrane filter (Pore size: 0.2 μm). The flow rate of the mobile phase is maintained at 1.0 ml/min. Peak areas are plotted against concentrations of known amounts (very accurately measured) of ciprofloxacin and ofloxacin in order to generate the standard curves of respective antibiotics. Standard curves, thus prepared, are further used to obtain the unknown concentrations of each of the antibiotics, present in solutions, generated before and after the adsorption of these antibiotics. Standard curves of each of the pure component CIP and OFLX and the same in combination, are provided in the Fig. 4.1 (A) and (B).

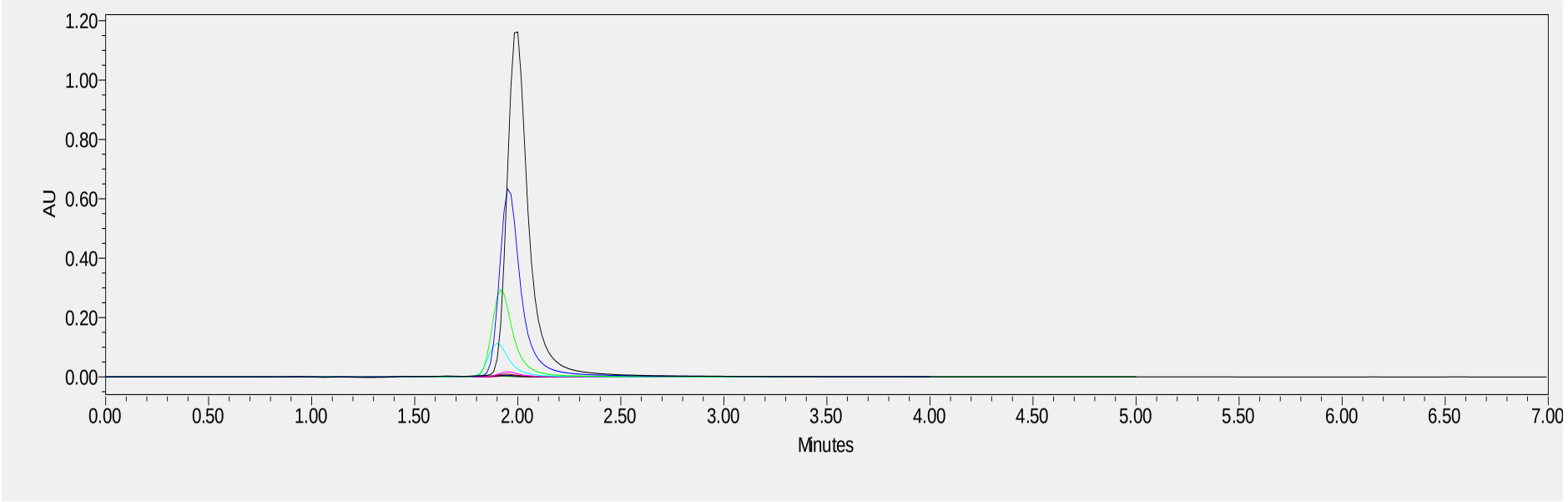

Fig. 4.1 (A) Chromatograms generated from High Performance Liquid Chromatograph [HPLC] for pure component Ciprofloxacin.

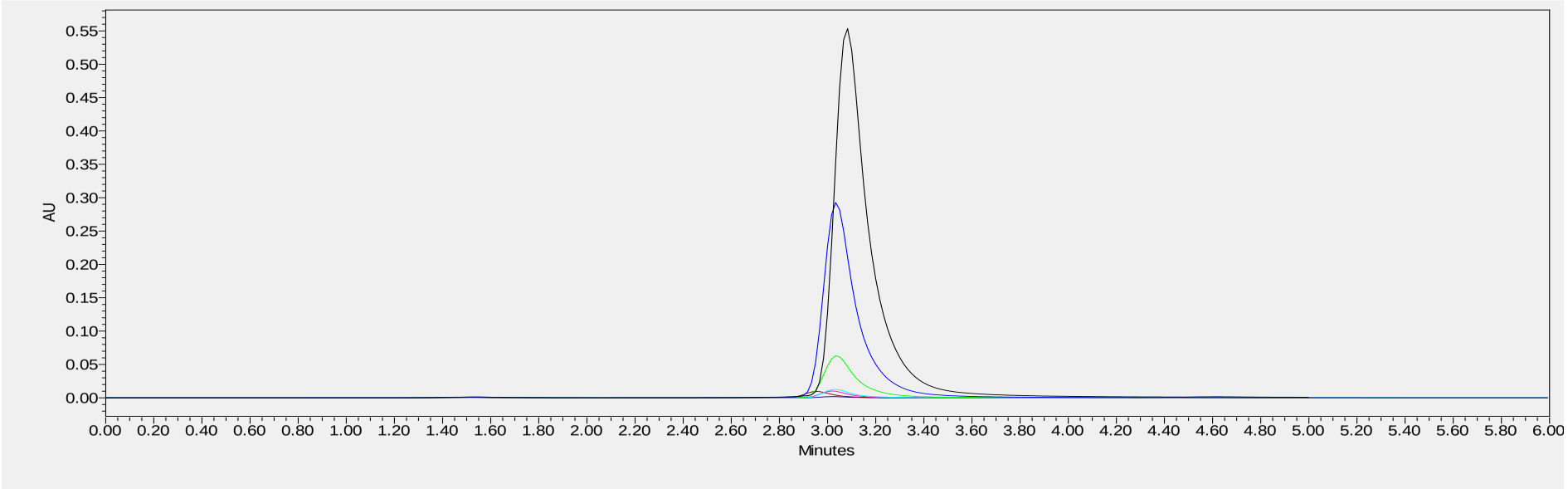

Fig. 4.1 (B) Chromatograms generated from High Performance Liquid Chromatograph [HPLC] for pure component Ofloxacin.

4.2 Isotherm Models for adsorption of single components

4.2.1 Langmuir adsorption isotherm model

Langmuir adsorption isotherm is widely used and accepted, even though several adsorption isotherms are used for the adsorption of single-component. Langmuir isotherm assumes homogeneous adsorption where each molecule holds constant activation energy and enthalpies of adsorption and all the adsorption sites have an equal attraction towards the adsorbates (Foo and Hameed, 2010). Langmuir isotherm model is expressed as follows:

$$q = q_{max}\frac{kC}{1+kC} \tag{4.2}$$

Here q and C represent the amount adsorbed in gram per 100ml solution per gram of adsorbent and its equilibrium concentration in gram per 100ml solution respectively. q_{max} is the maximum amount adsorbed in gram per 100ml solution per gram of adsorbent and k is the Langmuir isotherm constant.

4.2.2 Freundlich adsorption isotherm model

The Freundlich adsorption isotherm describes the reversible and non-ideal adsorption. It is not only restricted to monolayer adsorption like Langmuir isotherm. The Freundlich adsorption isotherm is used to define multilayer adsorption with non-uniformity in the distribution of adsorption heat and affinities towards the heterogeneous surface [Adamson and Gast 1997] and it is represented by the following equation:

$$q = k.C^{1/n} \tag{4.3}$$

where, n and k in Eq. (4.3) describe the heterogeneity factor and the Freundlich isotherm constant respectively.

4.2.3 Halsey adsorption isotherm model

The Halsey adsorption isotherm narrates the process of adsorption as multilayer adsorption and claims the adsorbent to be hetero-porous in nature [Moradi *et al.* 2013]. The Halsey adsorption isotherm is given as:

$$\ln q_e = \left[\left(\frac{1}{n}\right)(\ln K)\right] - \left[\left(\frac{1}{n}\right)(\ln C_e)\right] \tag{4.4}$$

where *n* and *K* indicate the exponent and Halsey isotherm constant respectively.

4.2.4 Dubinin-Radushkevich adsorption isotherm model

The Dubinin–Radushkevich model is generally applied to describe the adsorption mechanism with a gaussian energy distribution onto a heterogeneous surface [Dabrowski 2001]. The model can often be successfully fitted for the intermediate range of concentrations with high solute activities. But the model has unsatisfactory asymptotic properties and does not predict the Henry's law at low pressure [Altin *et al*. 1998]. The Dubinin –Radushkevich adsorption isotherm model is represented as follows:

$$q_e = (q_s)e^{-K_{ad}\varepsilon^2} \tag{4.5}$$

where, q_e = amount of adsorbate in the adsorbent at equilibrium (mg/g), q_s = theoretical saturation capacity (mg/g), K_{ad}= Dubinin–Radushkevich isotherm constant (mol^2/kJ^2) and ε = Dubinin–Radushkevich isotherm constant. The parameter ε can be expressed by the following equation:

$$\varepsilon = RT \ln\left[1 + \frac{1}{C_e}\right] \tag{4.5a}$$

where R, T and C_e represent the universal gas constant (8.314 *J/mol K*), absolute temperature (*K*) and adsorbate equilibrium concentration (gram per 100ml solution) respectively.

4.2.5 Elovich adsorption isotherm model

The equation describing Elovich model [Hamdaouia and Naffrechoux, 2007] assumes that the adsorption sites increase exponentially along with the adsorption process, which depicts a multilayer adsorption. It is expressed by the following equation:

$$\frac{q_e}{q_m} = (K_E C_e) exp\left(\frac{q_e}{q_m}\right) \tag{4.6}$$

where K_E is the Elovich equilibrium constant and q_m is the Elovich maximum adsorption capacity. Elovich maximum adsorption capacity and Elovich constant both can be calculated from the slope and the intercept of the plot $ln(q_e/C_e)$ versus q_e. If the adsorption obeys Elovich equation, the fit will be good , as tested with the R^2 value.

4.3 Batch equilibrium analysis of pure component ciprofloxacin and ofloxacin

Amounts of pure component ciprofloxacin and ofloxacin adsorbed (g/100ml/g adsorbent) are plotted against its corresponding equilibrium concentration (g/100ml solution). Further, the data are fitted to adsorption isotherms namely, Langmuir, Freundlich, Halsey, Dubinin–Radushkevich and Elovich models as described in Equations (4.2) to (4.6) respectively.

Estimated parameters obtained from the linearized regression fits of the Langmuir, Freundlich, Halsey, Dubinin–Radushkevich and Elovich isotherm models along with the correlation coefficient (R^2) for each of the pure components namely ciprofloxacin and ofloxacin are given in Table 4.1 and Table 4.2 respectively. The observed and predicted values of amount adsorbed per amount of adsorbate (g/100ml/g adsorbent) are plotted against equilibrium concentrations (g/100ml) [refer Figs. 4.2 (a_{11}⇒Langmuir isotherm; b_{11}⇒ Freundlich isotherm; c_{11}⇒ Halsey isotherm; d_{11}⇒ Dubinin–Radushkevich isotherm; e_{11}⇒ Elovich isotherm) and Figs. 4.3 (a_{11}⇒Langmuir isotherm; b_{11}⇒ Freundlich isotherm; c_{11}⇒ Halsey isotherm; d_{11}⇒

Dubinin–Radushkevich isotherm; $e_{11}\Rightarrow$ Elovich isotherm) for ciprofloxacin and ofloxacin respectively]. From the numerical values of correlation coefficient (R^2), it is evident that there is a good harmony between the experimental data and fitted lines for Freundlich, Halsey, Dubinin–Radushkevich isotherm models corresponding to ciprofloxacin and ofloxacin respectively. The relative errors (%) between the observed and predicted values [{(Observed – Predicted)/Observed}x 100] are plotted against equilibrium concentrations (g/100ml) [refer Figs. 4.2 ($a_{12}\Rightarrow$Langmuir isotherm; $b_{12}\Rightarrow$ Freundlich isotherm; $c_{12}\Rightarrow$ Halsey isotherm; $d_{12}\Rightarrow$ Dubinin–Radushkevich isotherm; $e_{12}\Rightarrow$ Elovich isotherm) and Figs. 4.3 ($a_{12}\Rightarrow$Langmuir isotherm; $b_{12}\Rightarrow$ Freundlich isotherm; $c_{12}\Rightarrow$ Halsey isotherm; $d_{12}\Rightarrow$ Dubinin–Radushkevich isotherm; $e_{12}\Rightarrow$ Elovich isotherm) for ciprofloxacin and ofloxacin respectively].

The Langmuir adsorption isotherm fits best for the adsorption for ciprofloxacin and ofloxacin in comparison to all other isotherms. Other researchers also obtained similar results during the adsorptive removal of fluoroquinolones [Gopal *et al*. 2022; Bing et al. 2010]. The maximum amount of ciprofloxacin and ofloxacin adsorbed (q_{max}) from Langmuir isotherm model are found to be 0.057 g/100ml/g of adsorbent and 0.017 g/100ml/g of adsorbent respectively. Goodness of fits is evaluated with respect to correlation coefficient (R^2). The same indicated the following order with regard to the fits to various isotherms: R^2 (Langmuir) > R^2 (Dubinin-Radushkevich) > R^2 (Freundlich), R^2 (Halsey) > R^2 (Elovich) for the adsorption of both ciprofloxacin and ofloxacin respectively onto the sewage sludge.

A conformation to the adsorption isotherm models, namely, Langmuir, Freundlich, Halsey, Dubinin-Radushkevich and Elovich designate that RSS may own both homo and heterogeneous surface energy distribution that describes the existence of mono- and heterolayer solute coverage on the surface.

Table 4.1 Langmuir, Freundlich, Halsey, Dubinin-Radushkevich and Elovich isotherm constants, and correlation coefficients for the adsorption of ciprofloxacin onto Raw Sewage Sludge (RSS).

Isotherm	Adsorbent	Parameters		R^2
		q_{max}	k	
Langmuir	RSS	0.0405	492.076	0.9697
		k_f	n	
Freundlich	RSS	0.696	1.645	0.88
		k	n	
Halsey	RSS	0.55	1.6453	0.88
		k_{ad}	q_s	
Dubinin-Radushkevich	RSS	0.0627	0.0151	0.997
		k_e	q_m	
Elovich	RSS	2308.72	0.012	0.595

Table 4.2 Langmuir, Freundlich, Halsey, Dubinin-Radushkevich and Elovich isotherm constants, and correlation coefficients for the adsorption of ofloxacin onto Raw Sewage Sludge (RSS).

Isotherm	Adsorbent	Parameters		R^2
		q_{max}	k	
Langmuir	RSS	0.0156	584.5	0.99
		k_f	n	
Freundlich	RSS	0.2763	1.721	0.9397
		k	n	
Halsey	RSS	0.11	1.721	0.94
		k_{ad}	q_s	
Dubinin-Radushkevich	RSS	0.0071	0.0393	0.961
		k_e	q_m	
Elovich	RSS	1.0266	125	0.823

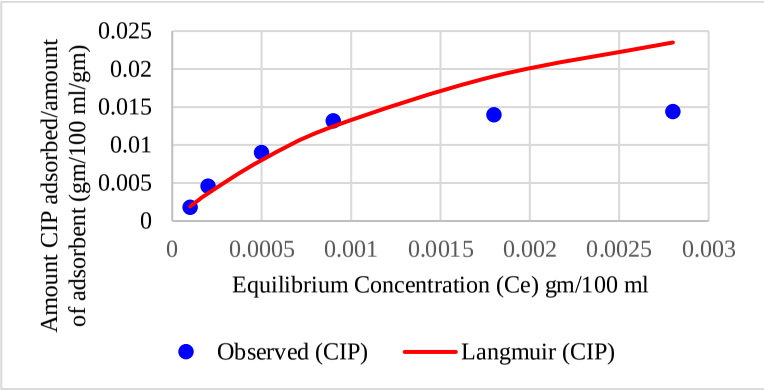

(a_{11})

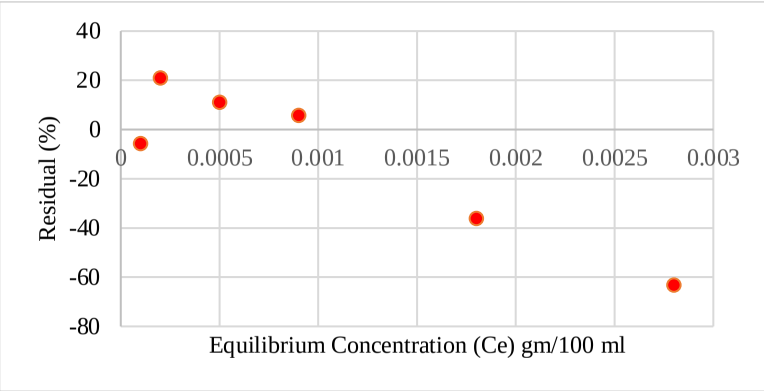

(a_{12})

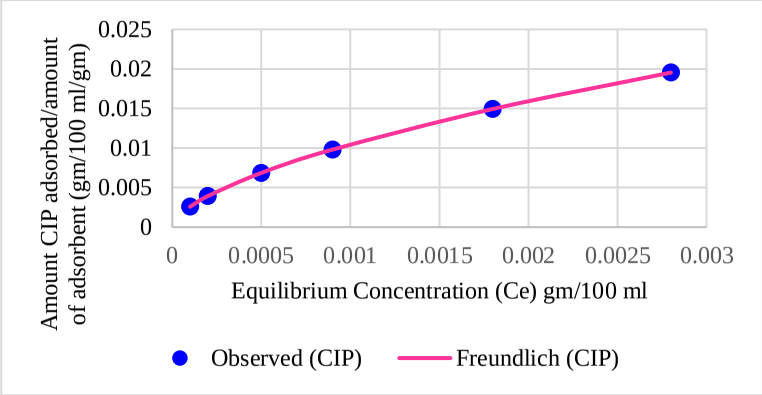

(b_{11})

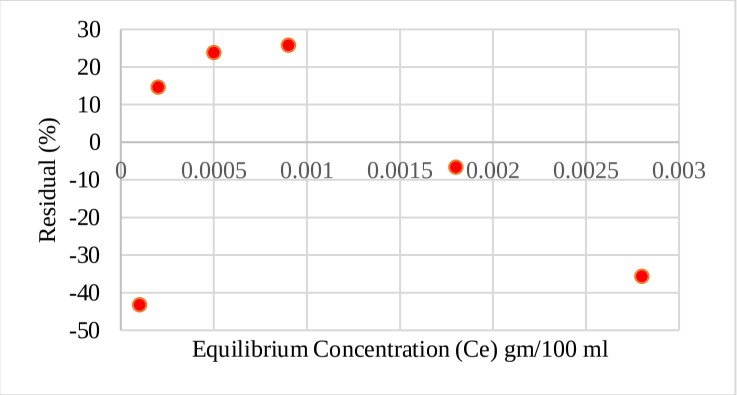

(b_{12})

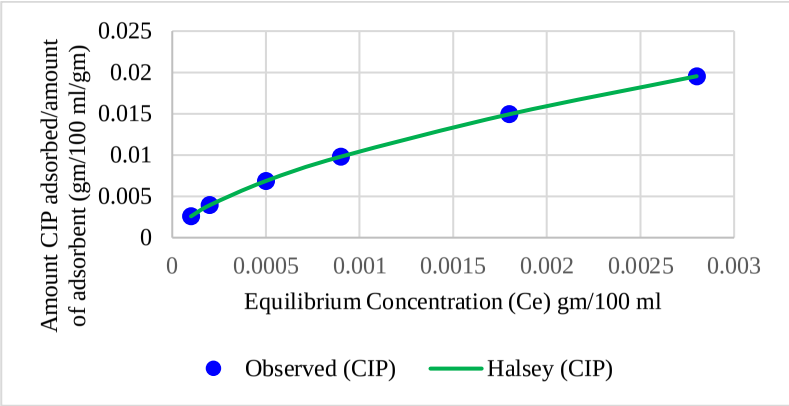

(c_{11})

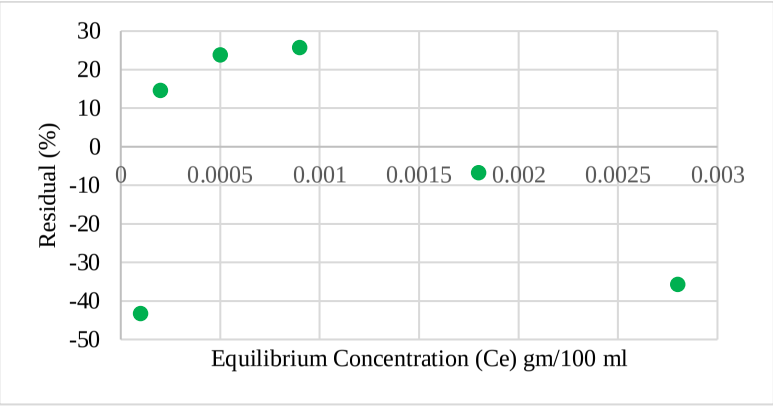

(c_{12})

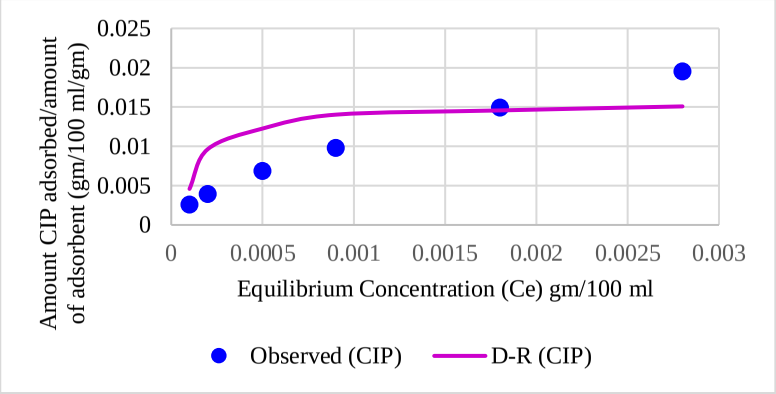

(d_{11})

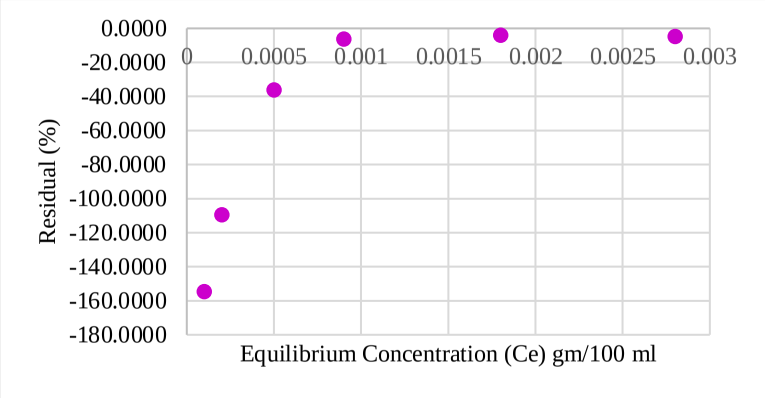

(d_{12})

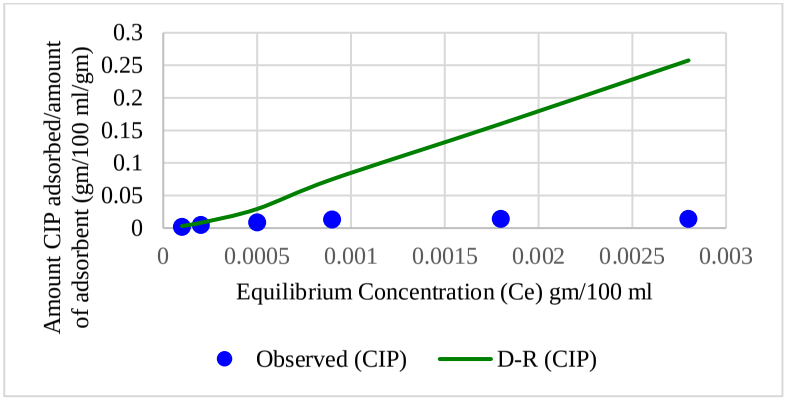

(e_{11})

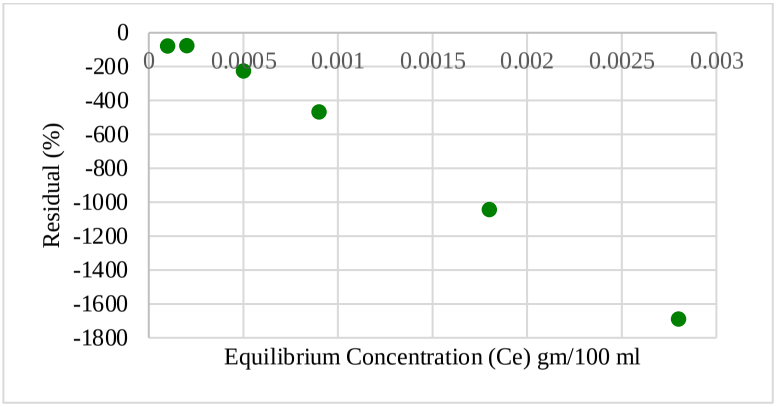

(e_{12})

Fig. 4.2 Predicted ciprofloxacin concentrations using various isotherms (a_{12}⇒Langmuir isotherm; b_{12}⇒ Freundlich isotherm; c_{12}⇒ Halsey isotherm; d_{12}⇒ Dubinin–Radushkevich isotherm; e_{12}⇒ Elovich isotherm) along with residuals[1](a_{12}⇒Langmuir isotherm; b_{12}⇒ Freundlich isotherm; c_{12}⇒ Halsey isotherm; d_{12}⇒ Dubinin–Radushkevich isotherm; e_{12}⇒ Elovich isotherm).

[1] *Residuals [CIP] = [{(observed CIP Concentration-predicted CIP Concentration)/observed CIP Concentration} x 100]*

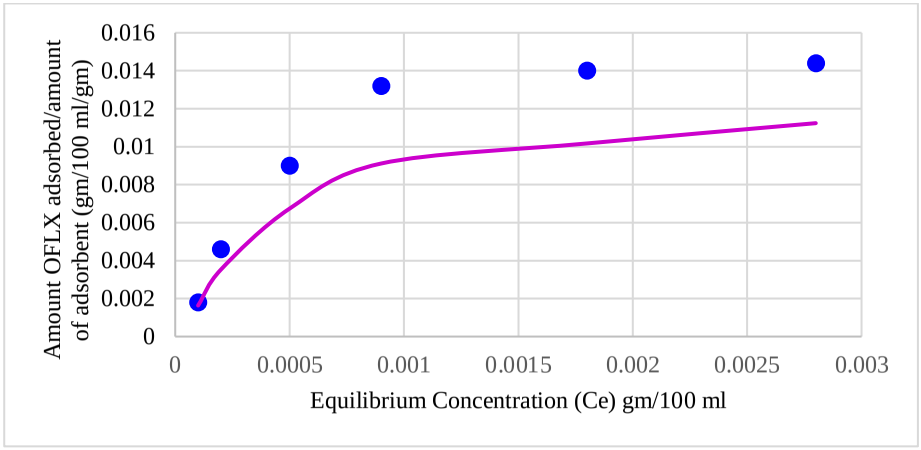

(a_{11})

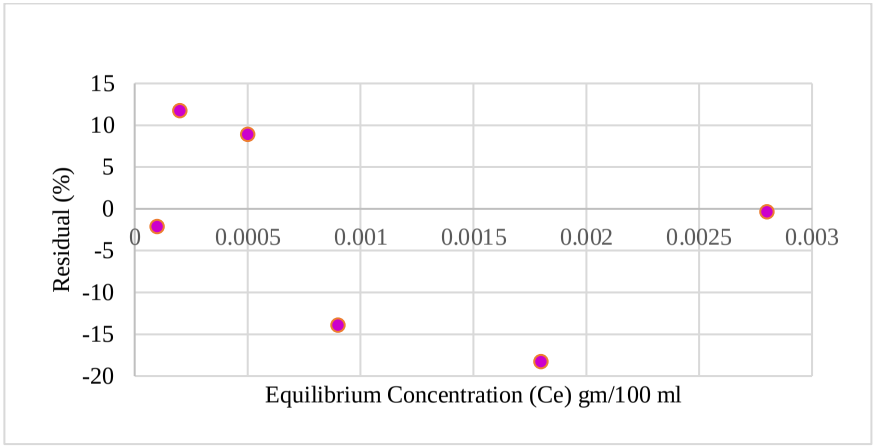

(a_{12})

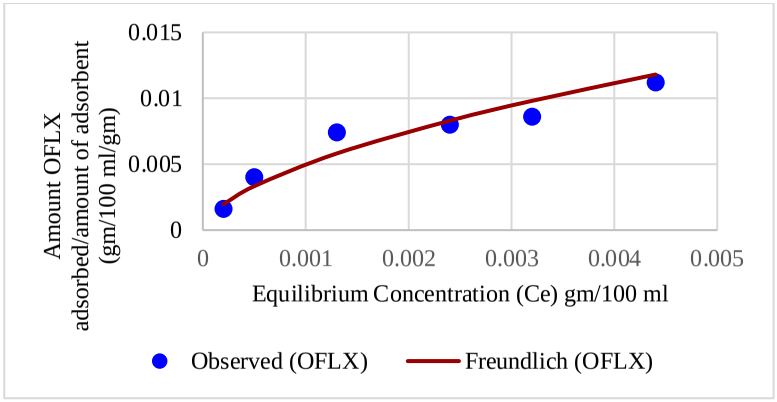

(b_{11})

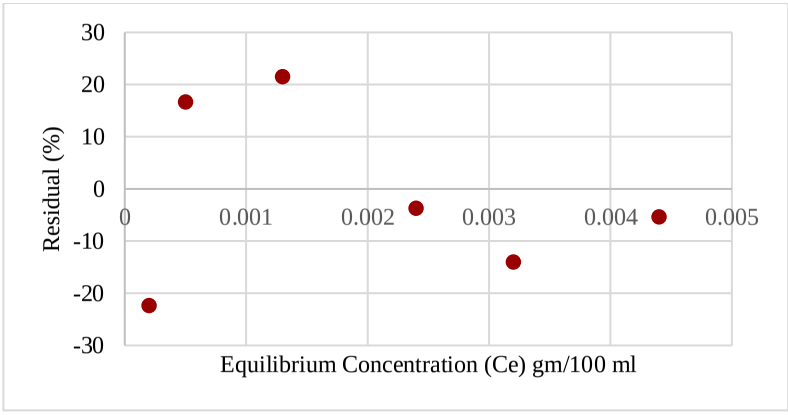

(b_{12})

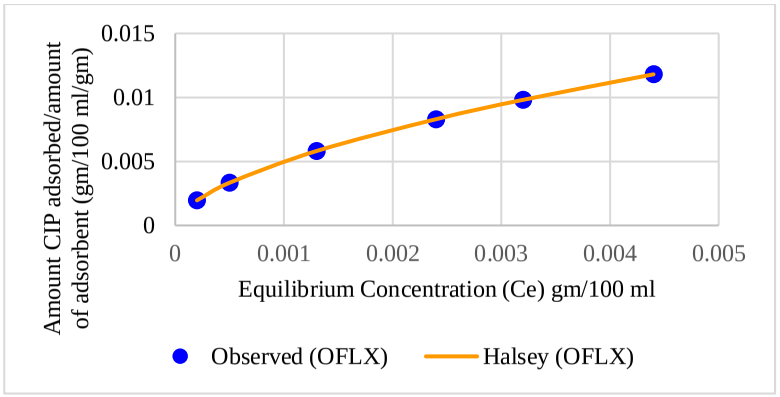

(c_{11})

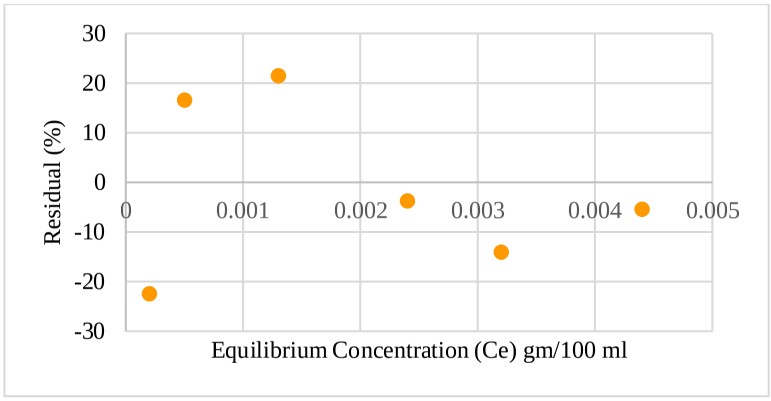

(c_{12})

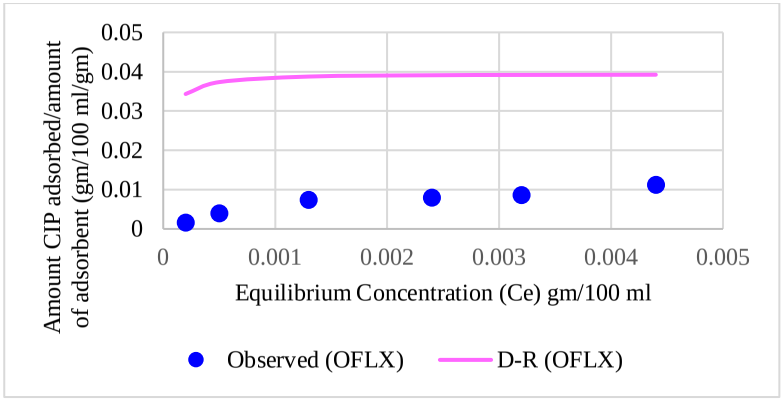

(d_{11})

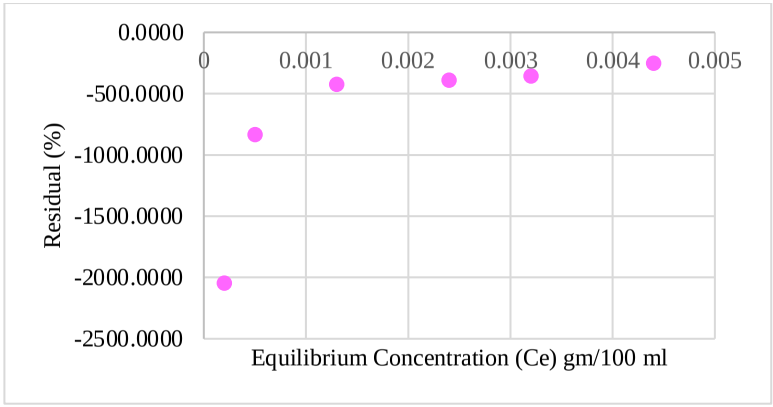

(d_{12})

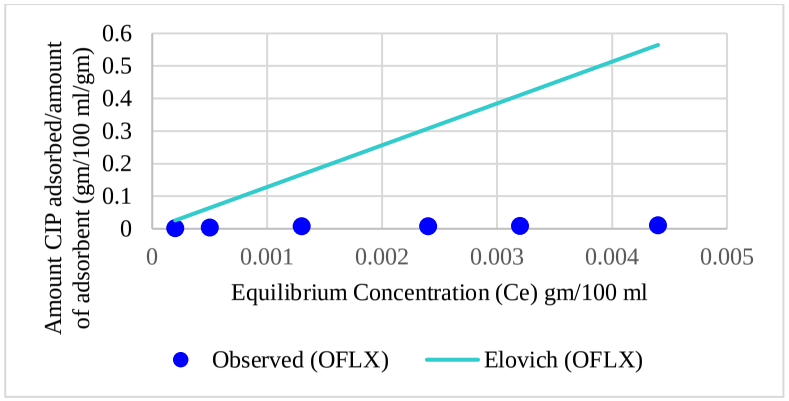

(e_{11})

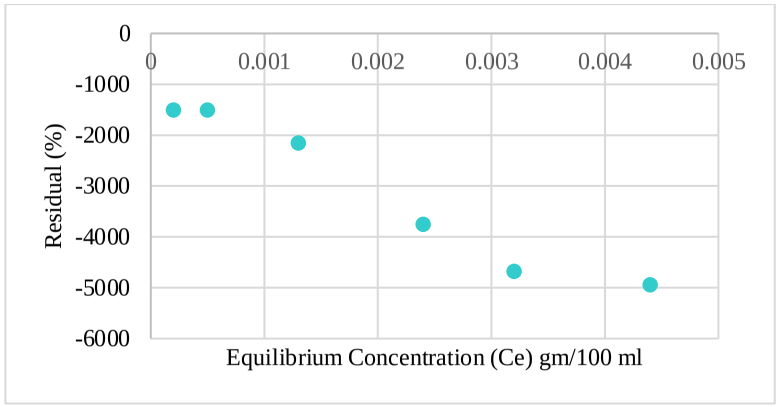

(e_{12})

Fig. 4.3 Predicted ofloxacin concentrations using various isotherms (a_{12}⇒Langmuir isotherm; b_{12}⇒ Freundlich isotherm; c_{12}⇒ Halsey isotherm; d_{12}⇒ Dubinin–Radushkevich isotherm; e_{12}⇒ Elovich isotherm) along with residuals[2](a_{12}⇒Langmuir isotherm; b_{12}⇒ Freundlich isotherm; c_{12}⇒ Halsey isotherm; d_{12}⇒ Dubinin–Radushkevich isotherm; e_{12}⇒ Elovich isotherm).

[2] *Residuals [OFLX] = [{(observed OFLX Concentration-predicted OFLX Concentration)/observed OFLX Concentration} x 100]*

Chapter 5:-

Batch equilibrium analysis: *Development and validation of competitive multicomponent adsorption models*

5.1 Background

Ciprofloxacin and Ofloxacin belong to a class of antibiotics known as Fluoroquinolones (FQs). Individually or in combination with other drugs these two specific drugs constitute the formulations of various pharmaceuticals in the forms of tablets, oral suspensions, intravenous infusions, etc. which are used to treat a number of bacterial infections. These include infections in bones and joints, and within the abdomen, including a certain type of infectious diarrhea, respiratory tract infections, etc. Ciprofloxacin (CIP) and Ofloxacin (OFLX) are broad-spectrum antibiotics with a large use in treating human beings and in animal husbandry. Generally, antibiotics used in human beings and livestock are poorly absorbed by the human body and thus

50% – 90% of the applied antibiotics are finally excreted as metabolites or as precursor chemicals (Schlüsener and Bester, 2006).

Municipal solid wastes and wastewater, generated from within the residential areas under various municipal zones, pharmaceutical manufacturing units, hospitals, livestock farming units, agriculture and aquaculture facilities etc. primarily constitute the most prominent sources of FQs contamination (Sukul and Spiteller, 2007). FQs are mostly brought into the environment through waste disposal, wastewater disposal, and transport across a range of environmental media through various interactions, like run-off, partitioning, percolation, and bioaccumulation (Van Doorslaer et al., 2014). The FQs, including primary and secondary precursors, and corresponding transformation products, are often discharged into the environment, during production and through the routes of consumption or disposal of drugs, both used and unused (Daughton and Ternes, 1999). Residual FQs are thus generally detected in inland surface water, groundwater, samples of soils, and sediments (Gothwal and Shashidhar, 2015). Potential adverse effects of FQs on various organisms present in the environment are of major concern. Bacteria develop drug-resistant genes due to long-term contact or through gene transfer (Gao et al., 2012a; Gao et al., 2012b). Consequently, a shortfall of antibiotics in medication is observed (Séveno et al., 2002). Health risk due to the resistance towards Ciprofloxacin and Ofloxacin is of major research interest.

Toxicity of Ciprofloxacin towards prokaryotes needs to be noted with chronic EC_{50} (half maximal Effect Concentration) values: 15-51 nmol/L for the cyanobacteria *Microsystis aeruginosa* (Halling-Sørensen et al., 2000); 241 nmol/L for the bacteria *Pseudomonas putida* (Kümmerer et al., 2000); 301.8 nmol/L for the detritivorous microbial communities present in the waste stream (Maul et al., 2006). Ofloxacin is

toxic towards *Microcystis aeruginosa* (Blue-Green Algae) with chronic EC_{50} values between 18-24 μg/L (Robinson et al., 2005), for *Pseudokirchneriella subcapitata* (Green Algae) being 10400-13700 μg/L (Robinson et al., 2005), followed by 52-201 μg/L for the Species: Lemna minor (Duckweed) (Robinson et al., 2005). Considering these eco-toxicological effects, it is recommended that pharmaceutical wastewater containing ciprofloxacin and ofloxacin needs to be treated prior to discharge into the inland surface water bodies.

Adsorption, using activated sludge is a cost-effective process for the treatment of various emerging organic contaminants (EOCs), and the same is used in wastewater treatment plants (Mishra, 2016), where waste-reuse is efficiently demonstrated.

Treatment of wastewater containing organic micropollutants using activated sludge is carried out by many researchers (Rogers, 1996; Göbel et al., 2005; Kim et al., 2005; Li and Zhang, 2010; Zhang et al., 2011; Ding et al., 2012; Liu et al., 2012; Xiancai et al., 2017). Adsorption of CIP and OFLX on RSS depends on several factors like hydrophobicity, specific surface area, surface charge, and surface functional groups of RSS. The specific purpose of this piece of research work is to analyze the batch equilibrium adsorption of CIP and OFLX in combination, using raw sewage sludge (RSS) with the help of competitive multicomponent adsorption models.

5.2 Experimental

5.2.1 Collection and Processing of sludge

Raw sewage sludge [RSS] is collected from the Municipal wastewater treatment plant [Kamarhati Municipality, North 24 Parganas, West Bengal, India]. The sludge is allowed to get naturally air-dried for a period of 5-6 days. The same is thus converted

into a semi-solid mass. With this dried semi-solid sludge, the batch equilibrium analysis is carried out.

5.2.2 Chemicals

CIFRAN-500 (Make: Ranbaxy Laboratories Ltd., India) and OFLOMAC-200 (Make: Macleods Pharmaceuticals Ltd., India) are used as the representative sources for CIP and OFLX respectively for the batch adsorption study. Adsorption of a single component is carried out using the pure component Ciprofloxacin [Make: Sigma–Aldrich, India ; CAS No: 86483-48-9; Grade: Analytical] and pure component Ofloxacin [Make: Sigma–Aldrich, India ; CAS No: 82419-36-1; Grade: Analytical]. The mobile phase consists of Acetonitrile [Make: Sigma–Aldrich, India; CAS No.: 75-05-8; Grade: HPLC grade], ultra-pure water [Make: Sigma–Aldrich, India; CAS No.: 7732-18-5; Grade: HPLC grade], Tri-ethylamine [Make: Sigma–Aldrich, India; CAS No.: 121-44-8; Grade: HPLC grade] and phosphoric acid [Make: Sigma–Aldrich, India; CAS No.: 7664-38-2; Grade: HPLC grade].

5.2.3 Analytical technique

Analysis of Ciprofloxacin and Ofloxacin (in solution) is performed using a High-Performance Liquid Chromatography (HPLC) based system (Make: Waters, Germany; Model: 515) equipped with a 190-400 nm wavelength UV detector, a quaternary gradient system pump with a pressure range 0-4000 psi and a column oven with an operating temperature range in between 25^{o}C to 100^{o}C. The protocol is described in detail in Chapter 4 (*section 4.1.4*). Standard curves of CIP and OFLX in combination, along with relevant chromatograms, are provided within *Supplementary Material A* [*refer* Fig. SI, Table SI, Fig. SII, and Fig. SIII]. The LC calibration report

of the standard curves, as generated using Empower 3 Software, a chromatography data system (CDS) [Make: Waters, Germany] is shown in *Supplementary Material B.*

5.2.4 Experiments in batch mode: Analysis

Solutions of pure component ciprofloxacin and ofloxacin of various concentrations in the range of 5 ppm to 100 ppm are prepared separately for analysis of single component adsorption. In this study, raw sludge, collected from Kamarhati Municipality Waste Water Treatment Plant [WWTP] (South 24 Pgs., West Bengal, India), is used. Feed solutions containing a combination of ciprofloxacin and ofloxacin of different concentrations (*Range:* 5 ppm – 100 ppm) are prepared with de-mineralized water. CIFRAN-500 (Make: Ranbaxy Laboratories Limited, India) and OFLOMAC-200 (Make: Macleods Pharmaceuticals Ltd., India) are used as primary sources of the active components of ciprofloxacin and ofloxacin respectively. 100 ml of each of the feed solutions of a certain concentration is taken in a 250 ml conical flask where 0.5 gm of raw sludge is added. Each solution is kept under isothermal conditions with occasional stirring, for 7 days till equilibrium is attained. Sample solutions are then filtered through Whatman No. 1 (diameter: 125 mm) filter paper in order to remove the raw sludge and subsequently filtered through 0.45 µm filter kit prior to analysis of the specific analytes using HPLC. These solutions are then analysed using HPLC (refer to *section 5.2.3*) in triplicate after batch equilibrium was attained (Ref. Supplementary Material C) to estimate specific concentrations of each of ciprofloxacin and ofloxacin present before and after equilibrium adsorption.

The equilibrium concentration is determined by

$$q_{e=}\frac{(C_{0-}C_e)V}{m}$$

Where q_e= adsorbate concentration at equilibrium in terms of mg adsorbate/g. adsorbent, C_0 = initial concentration of adsorbate in mg/L, C_e = equilibrium concentration of the adsorbate in mg/L, V = volume of the solution, and m = weight of the adsorbent in g.

5.3 Theory and Calculations

A number of studies have carried out single-component adsorption of specific adsorbates and their outcomes are fitted to various isotherms namely, Langmuir, Freundlich, BET, Toth, and Temkin isotherms (Sadhukhan et al., 2009).

5.3.1 Adsorption of single components: Choice of model as the basis of competitive models for multicomponent adsorption

Langmuir adsorption isotherm is widely used and accepted, even though several adsorption isotherms are used for the adsorption of single-component. Langmuir isotherm assumes homogeneous adsorption where each molecule holds constant adsorption activation energy and enthalpies and all the adsorption sites have an equal attraction towards the adsorbates (Foo and Hameed, 2010). Langmuir isotherm model is expressed as follows:

$$q = q_{max}\frac{kC}{1+kC} \tag{5.1}$$

Here q and C represent the amount adsorbed in gram per 100ml solution per gram of adsorbent and its equilibrium concentration in gram per 100ml solution respectively. q_{max} is the maximum amount adsorbed in gram per 100ml solution per gram of adsorbent and k is the Langmuir isotherm constant.

5.3.2 Development of models for multicomponent adsorption (Hill, 1986; Tien, 1994)

Modified Competitive Langmuir-like model and LeVan-Vermeulen model [based on the ideal adsorbed solution (IAS) theory] are developed and further applied in this study for the adsorption of ciprofloxacin and ofloxacin. The development of these models is based on the elementary theories of statistical thermodynamics.

5.3.2.1 Modified competitive Langmuir-like model (Model 1): Development

In this specific developmental approach, one ignores interaction in between adsorbed molecules in the adsorbent. This leads to the competitive Langmuir equations where the presence of the second type of adsorbate leads to competition between molecules, depending on the strength of the interaction with the adsorbent surface.

Here, we consider only three components with one of the components present in large quantities, i.e. the solvent. The grand canonical partition function, for a system of non-interacting molecules adsorbed on a homogenous adsorbent can be written as:

$$\Xi = \sum_{\substack{N_1=0 \\ N_1+N_2+N_3 \le M}}^{M} \sum_{N_2=0}^{M} \sum_{N_3=0}^{M} \frac{M!\left(q_1(T)\lambda_1\right)^{N_1}\left(q_2(T)\lambda_2\right)^{N_2}\left(q_3(T)\lambda_3\right)^{N_3}}{N_1!N_2!N_3!(M-N_1-N_2-N_3)!} \tag{5.2}$$

Equation (5.2) represents the grand canonical partition function as a function of temperature through dependence on the single solute partition function $q_i(T)$ (i=1, 2, 3) on temperature. The λ_i s are related to the chemical potentials via the relation,

$$\lambda_1 = \exp(\beta\mu_i) \tag{5.3}$$

where μ_i is the chemical potential of the i^{th} adsorbent. Equation (5.2) can be re-written as

$$\Xi = [1+q_1(T)\lambda_1 + q_2(T)\lambda_2 + q_3(T)\lambda_3]^M \tag{5.4}$$

Using concepts in statistical mechanics, we can relate the derivative of the logarithm of the grand-canonical partition function with respect to the chemical potential to the average of the number of particles present in the grand-canonical system and hence to the number of moles of adsorbate adsorbed. On differentiation, we get

$$\overline{N}_i = \frac{Mq_i(T)\lambda_i}{[1+q_1(T)\lambda_1+q_2(T)\lambda_2+q_3(T)\lambda_3]} \tag{5.5}$$

Since the system is at equilibrium with the bulk solution, the chemical potentials of the components are the same in the bulk as in the solution, where the chemical potential is a function of temperature and concentration. The chemical potential may be written as,

$$\mu_i = \mu_i^p(T,P) + kT\ln\gamma_i x_i \tag{5.6}$$

Therefore, the λ's may be written as,

$$\lambda_i = K_i(T,P)\gamma_i x_i \tag{5.7}$$

Hence the average number of adsorbed molecules is given by,

$$\overline{N}_i = \frac{Mq_i(T)K_i(T,P)\gamma_i x_i}{[1+q_1(T)K_1(T,P)\gamma_1 x_1+q_2(T)K_2(T,P)\gamma_2 x_2+q_3(T)K_3(T,P)\gamma_3 x_3]} \tag{5.8}$$

The x_i's may be written as,

$$x_i = \frac{c_i / M_i}{\sum_i c_i / M_i} \tag{5.9}$$

The c_i's are the mass concentrations of the respective components. Joining all the terms expect concentration into a term $B_i(T,P,c_j)$ for each component we get,

$$\bar{N}_i = \frac{MB_i(T,P,c_j)c_i}{[1+B_1(T,P,c_j)c_1+B_2(T,P,c_j)c_2+B_3(T,P,c_j)c_3]} \tag{5.10}$$

We take component 1 to be the solvent and components 2 and 3 to represent the solutes which are present in trace amounts. For components 2 and 3 we take,

$$A_i(T,P,c_j) = \frac{B_i(T,P,c_j)}{1+B_1(T,P,c_j)c_1} \tag{5.11}$$

Then, for components 2 and 3, equation (5.10) reduces to,

$$\bar{N}_i = \frac{MA_i(T,P,c_j)c_i}{[1+A_2(T,P,c_j)c_2+A_3(T,P,c_j)c_3]} \tag{5.12}$$

For trace amounts of components 2 and 3, the coefficients for the different concentrations become independent of the concentrations and since the solvent is a liquid, it becomes practically independent of pressure. The above equation is the competitive Langmuir model.

$$\bar{N}_i = \frac{MA_ic_i}{(1+A_2c_2+A_3c_3)} \tag{5.13}$$

This specific competitive model is derived using the fact that there are two types of sites, one in which only one of the two components is adsorbed and the other where both components are adsorbed competitively. The grand canonical partition function can thus be written as,

$$\Xi = [1+q_1(T)\lambda_1+q_2(T)\lambda_2+q_3(T)\lambda_3]^{M_1}[1+q_1'(T)\lambda_1+q_2'(T)\lambda_2+q_3'(T)\lambda_3]^{M_2} \tag{5.14}$$

The average number of molecules adsorbed can be deduced in a similar manner as the case of the competitive Langmuir model to get,

$$\bar{N}_i = \frac{M_1 A_i c_i}{\left(1 + A_2 c_2 + A_3 c_3\right)} + \frac{M_2 A_i' c_i}{\left(1 + A_2' c_2 + A_3' c_3\right)} \tag{5.15}$$

Let the total number of sites be,

$$M = M_1 + M_2 \tag{5.16}$$

Depending on the maximum amount adsorbed during single component adsorption, relationships are derived between the two sets of coefficients. Let the maximum amount adsorbed in single component adsorption be greater for component 2. We further assume that, though all sites on the adsorbent are available for adsorption of component 2, only a fraction of them are available for adsorption of component 3. Let M_1 be the sites where only component 2 is adsorbed. Then the following relationships are in synchronization with the above assumptions.

$$\begin{aligned} A_3 &= 0 \\ A_2 &= A_2' = B \\ A_3' &= C \end{aligned} \tag{5.17}$$

Then equation (5.15) becomes,

$$\bar{N}_2 = \frac{(M - M_2) B c_2}{\left(1 + B c_2\right)} + \frac{M_2 B c_2}{\left(1 + B c_2 + C c_3\right)} \tag{5.18}$$

$$\bar{N}_3 = \frac{M_2 C c_3}{\left(1 + B c_2 + C c_3\right)} \tag{5.19}$$

Equations (5.18) and (5.19) give the modified competitive Langmuir model.

The modified competitive Langmuir like model that was modified by Jain and Snoeyink (Jain and Snoeyink, 1973) is used by many researchers (Banerjee et al., 2020; Banerjee et al., 2014; Banerjee et al., 2013) in order to describe antiseptic based

multicomponent systems. This model is based on the assumption that the adsorption capacities of the specific adsorbent with respect to the two competitive adsorbates are not same.

$$X_1 = \frac{(X_{m.1} - X_{m.2})AC_{eq1}}{1+AC_{eq1}} + \frac{X_{m.2}\ AC_{eq1}}{1 + AC_{eq1} + BC_{eq2}} \tag{5.20}$$

$$X_2 = \frac{X_{m.2}\ BC_{eq2}}{1 + AC_{eq1} + BC_{eq2}} \tag{5.21}$$

Here X_1 and X_2 are the amounts of solutes 1 and 2 adsorbed per unit weight of adsorbent at equilibrium concentrations C_{eq1} and C_{eq2} respectively and $X_{m,1}$ and $X_{m,2}$ represent the maximum amount adsorbed for components 1 and 2 respectively, where $X_{m,1} > X_{m,2}$. The constants A and B are affinity constants for components 1 and 2 respectively.

5.3.2.2 Ideal Adsorbed Solution (IAS) model

IAS model assumes that the components comprising the adsorption system constitute an ideal solution in the adsorbed phase. IAS is such that the chemical potential of each of its components, assuming the adsorbed phase to be of negligible volume fraction, can be written as:

$$\mu_i(T, \Pi) = \mu_i^0(T, \Pi) + RT \ln x_i^{ad} \tag{5.22}$$

This is in line with the definition of a bulk ideal solution, with bulk pressure being replaced by the spreading pressure. The thermodynamic equation for the adsorbed phase can be written as,

$$-SdT + Ad\Pi - \sum_n n_i d\mu_i = 0 \tag{5.23}$$

For a single component system at constant temperature, this reduces to,

$$Ad\Pi - n_i^0 d\mu_i^0 = 0 \tag{5.24}$$

We get the equation for calculating spreading pressure by equating the chemical potentials in the adsorbed and bulk phases respectively. Final form of the equation [5.22] is,

$$\frac{\Pi A}{RT} = \int_0^{C_i^0} q_i^0 d(\ln c_i^0) \tag{5.25}$$

where C_i^0 is the bulk concentration of single component system, giving the same spreading pressure as that of the multicomponent system and q_i^0 is related to c_i^0 by the adsorption isotherm. The mole fraction of adsorbent in the adsorbed phase is found by the following relation,

$$C_i = C_i^0 x_i \tag{5.26}$$

Since the adsorbed phase is an ideal solution, the specific adsorption area of a particular solute at a specific spreading pressure is the same in the multicomponent case as it is in the single component case. The total surface area of the adsorbed multicomponent mixture is inversely proportional to the total amount adsorbed, so the total amount adsorbed is given by,

$$q_t = \left(\sum_{i=1}^{N} \frac{x_i}{q_i^0} \right)^{-1} \tag{5.27}$$

The total amount of adsorbed adsorbate per gram of adsorbent is given by,

$$q_i = q_t x_i \tag{5.28}$$

Solving equations (5.25) - (5.28), we get the adsorption isotherm of the multicomponent system. In these equations interactions between molecules of the

same species is taken care of by the pure component adsorption isotherm while the interactions between different species is taken care of by the ideal adsorbed solution theory.

IAS model, established by Myers and Prausnitz for the first time, is considered for adsorption of gaseous mixtures and later it was extended to liquid solutions. The difference in interfacial tension between pure solvent and the solid interface and the solution and the solid interface is known as the spreading pressure of a solute ($\prod_i$). Mathematically, the spreading pressure of a solute is given by the equation:

$$\prod_i = \frac{RT}{S} \int_0^{C^*_{eqi}} \frac{X_i}{C_{eqi}} d\, C_{eqi} \tag{5.29}$$

Here X_i and C_{eqi} are the amount adsorbed and equilibrium concentrations for the i^{th} species in the multicomponent system respectively. C^*_{eqi} is the equilibrium concentration of the i^{th} species in a single component system. S is the surface area of adsorbent, R is the molar gas constant and T is the absolute temperature.

5.3.2.3 LeVan – Vermeulen model (Model 2)

Based on the thermodynamic discrepancy of the competitive Langmuir-like model (LeVan and Vermeulen, 1981), LeVan and Vermeulen modified the same on account of the Ideal Adsorbed Solution Theory (IAS). The third order Taylor series is used for the estimation of the LeVan-Vermeulen model for component 1 and is given by the following equation:

$$X_1 = \frac{\overline{X_m} A C_{eq1}}{1 + A C_{eq1} + B C_{eq2}} + \Delta_{L2.} (1 + \Delta_{L3}) \tag{5.30}$$

Here $\overline{X_m}$, which is the maximum amount adsorbed, can be estimated from the Eq. (5.31)

$$\overline{X_m} = \frac{X_{m,1} A\, C_{eq1} + X_{m,2} BC_{eq2}}{AC_{eq1} + BC_{eq2}} + 2\,\frac{(X_{m,1} - X_{m,2})^2}{(X_{m,1} + X_{m,2})}\,\frac{(AC_{eq1} BC_{eq2})}{(AC_{eq1} + BC_{eq2})^2}$$

$$\times \left[\left(\frac{1}{AC_{eq1} + BC_{eq2}} + \frac{1}{2}\right) \ln(1 + \mathrm{A}C_{eq1} + BC_{eq2}) - 1\right] \quad (5.31)$$

Where $X_{m,1}$ and $X_{m,2}$ represent the maximum amounts adsorbed for the components 1 and 2 respectively. The same is derived from single solute systems. Δ_{L2} and Δ_{L3} are given by the following equations:

$$\Delta_{L2} = (\mathrm{X_{m,1}} - \mathrm{X_{m,2}})\,\frac{(AC_{eq1} BC_{eq2})}{(AC_{eq1} + BC_{eq2})^2}\, ln(1 + AC_{eq1} + BC_{eq2}) \quad (5.32)$$

$$\Delta_{L3} = \frac{(X_{m,1} - X_{m,2})}{(X_{m,1} + X_{m,2})}\,\frac{1}{(AC_{eq1} + BC_{eq2})} \times \left[\frac{(BC_{eq2})^2 + (2BC_{eq2}) - (4AC_{eq1}) - (AC_{eq1})^2}{(AC_{eq1} + BC_{eq2})} \ln\left(1 + AC_{eq1} + BC_{eq2}\right) + \frac{3(AC_{eq1})^2 + 4AC_{eq1} + AC_{eq1} BC_{eq2} - 2BC_{eq2} - 2\,(BC_{eq2})^2}{(1 + AC_{eq1} + BC_{eq2})}\right] \quad (5.33)$$

Isotherm expression for component 2 can be obtained by changing the subscripts of the components of Eqs. (5.30), (5.32) and (5.33).

5.4 Pseudo-kinetics, intraparticle and film diffusion: Insights of adsorption mechanism

Lagergren (Lagergren, 1898) proposed the pseudo-first order kinetic model, given by:

$$\frac{dq_t}{dt} = k_1\,(q_e - q_t) \quad (5.34a)$$

Where, q_e is the amount of adsorbate adsorbed at equilibrium (g. adsorbate/100ml/g of adsorbent), q_t is the amount of adsorbate adsorbed at time t (g. adsorbate/100ml/g of adsorbent) and k_1 (day^{-1}) is the pseudo first-order rate constant. Integrating Eq. (5.34a) for the initial conditions $q_t = 0$ at $t = 0$, we get the linearized form of the model as given below:

$$log(q_e - q_t) = log\,(q_e) - \frac{k_1 . t}{2.3} \quad (5.34b)$$

Plotting $log(q_e - q_t)$ versus t, the values of k_1 and q_e are determined from the slope and the intercept respectively.

The second-order kinetic model is expressed as:

$$\frac{dq_t}{dt} = k_2\ (q_e - q_t)^2 \tag{5.35a}$$

Where k_2 (g. adsorbate/100ml/g. adsorbent min) is the pseudo second-order rate constant. Integrating the Eq. (35a) for the initial conditions at $t = 0$ and $q_t = 0$ we get the linear form:

$$\frac{t}{q_t} = \frac{t}{q_e} + \frac{1}{k_2\, q_e^2} \tag{5.35b}$$

Numerical values of q_e and k_2 are found out from the intercept and slope of the plot of (t/q_t) against t, respectively.

The *intra-particle diffusion model* (Weber Jr and Morris, 1963), represented in equation 36, is applied to find out the mechanism involved in the adsorption process.

$$q_t = k_i t^{1/2} + C \tag{5.36}$$

Where k_i is the intra-particle diffusional rate constant (g. adsorbate/100ml/g. adsorbent $min^{1/2}$) and C (g. adsorbate/100ml/g. adsorbent) is a constant which indicates the boundary-layer thickness. More the numerical values of C, more effective boundary layer is expected for mass transfer. When intra-particle diffusion process becomes the rate controlling step, plot of q_t against $t^{1/2}$ produces a straight line passing through the origin.

Boyd's film diffusion model is based on the assumption that boundary layer around the adsorbent particle imparts the primary resistance to diffusion. The extent of film

resistance during the adsorption process is evaluated using this model. Film diffusion model is given by:

$$F = 1 - \left(\frac{6}{\Pi^2}\right) \sum_{n=1}^{\alpha} \left(\frac{1}{n^2}\right) e^{(-n^2 Bt)} \quad (5.37)$$

Here, F is the fractional achievement of equilibrium, at different times, t (in days) and B_t is a function of F, represented by:

$$F = \frac{q_t}{q_e} \quad (5.38)$$

Where q_t and q_e are the amounts of ciprofloxacin or ofloxacin adsorbed at time t and at equilibrium, respectively. On applying Fourier transform, Reichenberg (Reichenberg, 1953) approximated equations (5.39a) and (5.39b), on integrating Eq.(5.37) under specific bounds of F.

For $F > 0.85$: $B_t = 0.4977 - \ln(1-F)$ (5.39a)

With $F < 0.85$: $B_t = \left(\sqrt{\pi} - \sqrt{\pi - \left(\frac{\pi^2}{3} F\right)}\right)^2$ (5.39b)

Adsorption process is primarily governed by intra-particle diffusion mechanism, if the plot of B_t against time t produces a straight line that passes through origin. If the plot, either linear or nonlinear, does not pass through the origin, it can be concluded that film-diffusion or chemical interaction is the major rate controlling factor during the adsorption process (El-Khaiary and Malash, 2011). The sludge is physically and chemically characterized, as described in Chapter 3.

5.5 Parameter Estimation

The parameters of Eqs. (5.20), (5.21) and (5.30) i.e. A and B are evaluated using the software MATLAB and the *fsolve* MATLAB Library [refer *Annex I*]. The *fsolve* command from the library is devised to minimize a nonlinear sum of squares (SSQ) function, subject to some limitations.

Evaluation of the two models

Evaluation of the following statistical parameters is required to infer on the estimated parameters:

1. The square of errors between model data and experimental data is minimized to get the values of two parameters A and B. The two least square errors functions are solved using *fsolve* command in order to get the values of A and B corresponding to the least error.
2. The uncertainties associated with the estimate of each parameter are termed as the *standard error,* σ. These are the square root of the error term covariance matrix C_{ij} of the fit. The closer this value is to zero, the better is the fit.
3. The higher the percentage of correlation coefficient (R^2) the better is the fit.

5.6 Results and Discussions

5.6.1 Batch equilibrium analysis

Maximum amount of adsorption of pure component ciprofloxacin and ofloxacin is analysed, once equilibrium is reached, using raw sewage sludge as the adsorbent. The observed data sets are plotted and fitted to the Langmuir adsorption isotherm [refer equation (5.1)]. The parameters of Langmuir adsorption isotherm are obtained by plotting *1/q* against *1/c*. From the slope and intercept, maximum amount adsorbed

(q_{max}) and Langmuir constant (k) are calculated respectively. Values of the parameters q_{max}, k and the correlation coefficient (R^2) are tabulated, as given in Table 5.1 below.

Table 5.1

Parameter estimation outputs of Langmuir adsorption isotherm for pure components.

Component	Parameters		R^2
	q_{max} (g. / 100 ml sol. /g.)	k (100 ml / g.)	
Ciprofloxacin hydrochloride	0.0544	359.73	0.9729
Ofloxacin	0.01468	626.10	0.9914

It is evident from Table 4.1 and Table 4.2 that Langmuir isotherm fits well for ciprofloxacin [refer Fig. 4.2(a_{11})] and ofloxacin [refer Fig. 4.3(a_{11})] respectively. This is the main reason for using both the Langmuir-like model [referred as Model 1] and the LeVan-Vermeulen model [referred as Model 2] in this study. The values of equilibrium concentration (g./100 ml) and maximum amount adsorbed (g./100 ml/g. adsorbent), obtained from the batch experiments for the multicomponent systems, are then applied in these two models. The parameters of Eqs. (5.20), (5.21), and (5.30), namely A and B are estimated using MATLAB with the help of *fsolve* MATLAB library [refer *Annex I*]. Optimized values of the model parameters (A and B) and the final objective values for each of these models are given in Table 5.2. Observed amounts of ciprofloxacin and ofloxacin are plotted against equilibrium concentrations of the two components respectively. Predicted concentrations of ciprofloxacin and ofloxacin are estimated using the best-fit [based on the minimum values of the objective function: Sum of the Squares (SSQ) of the residuals] model parameters of both Model 1 and Model 2 [refer eqs. (5.20), (5.21) and (5.30) respectively]. The same are plotted for ciprofloxacin [see Fig. 5.1 (a) and Fig. 5.2 (a)] and ofloxacin [see Fig. 5.1 (b) and Fig. 5.2 (b)] separately. It is evident from these plots that there is a good

convergence of data with the predicted and observed values for both ciprofloxacin than ofloxacin for Langmuir-like model exhibiting competitive adsorption mechanism between ciprofloxacin and ofloxacin involved in the adsorption process.

Table 5.2

Competitive Langmuir like adsorption isotherm (Model 1) and LeVan-Vermeulen model (Model 2) parameters for ciprofloxacin and ofloxacin obtained from *fsolve* library based MATLAB programme.

Model	Parameter		Final objective value
	A	B	
Model 1	3.738	325.18	$8.22*10^{-4}$
Model 2	1141	1164	$4.21*10^{-3}$

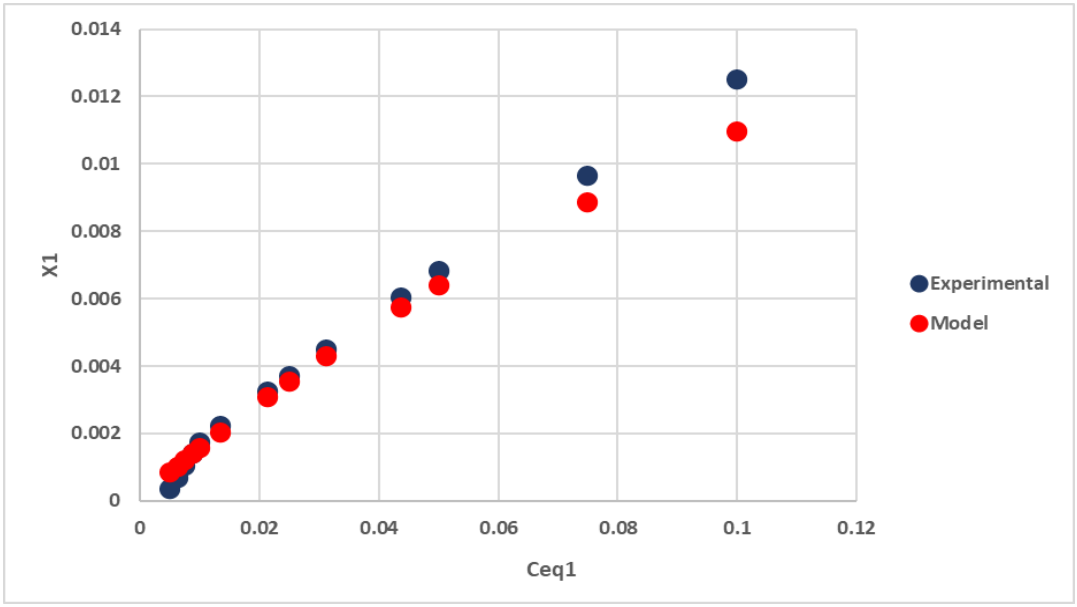

(a)

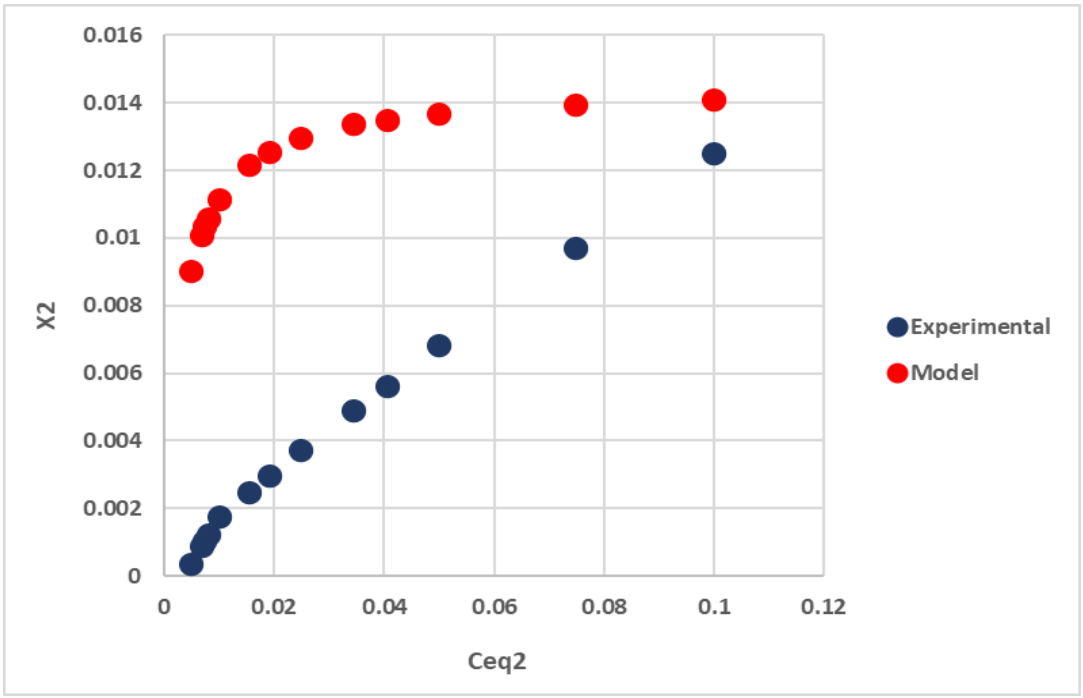

(b)

Fig. 5.1 Multicomponent adsorption isotherms following *Modified Langmuir-like* model (Model-1) for (a) ciprofloxacin; (b) ofloxacin.

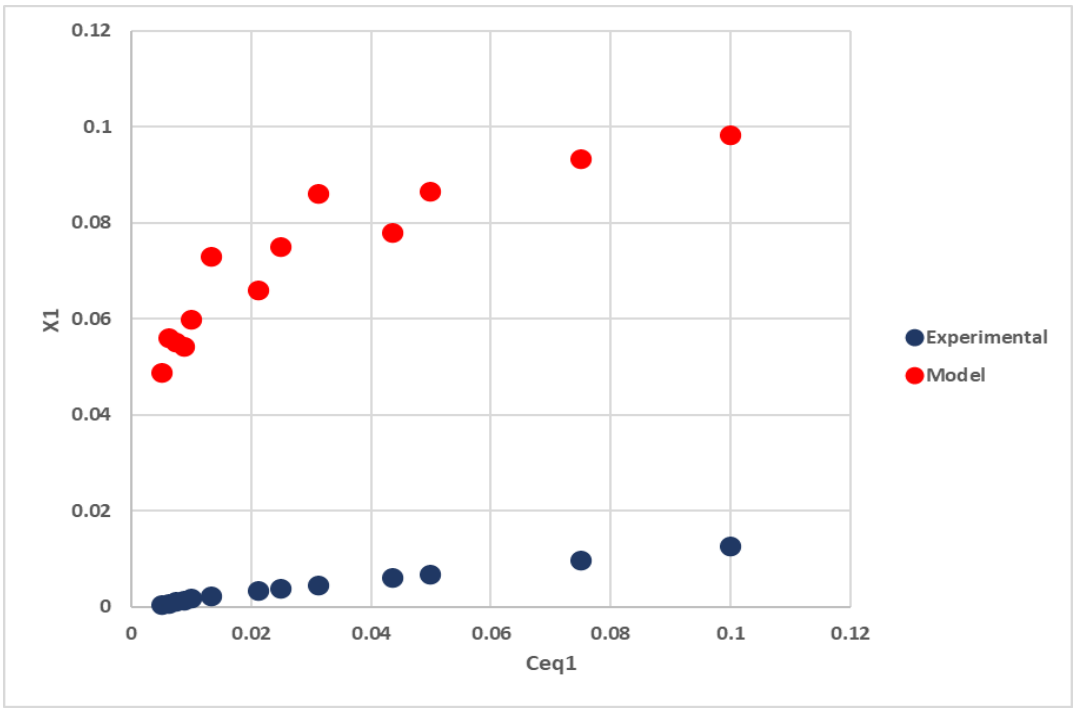

(a)

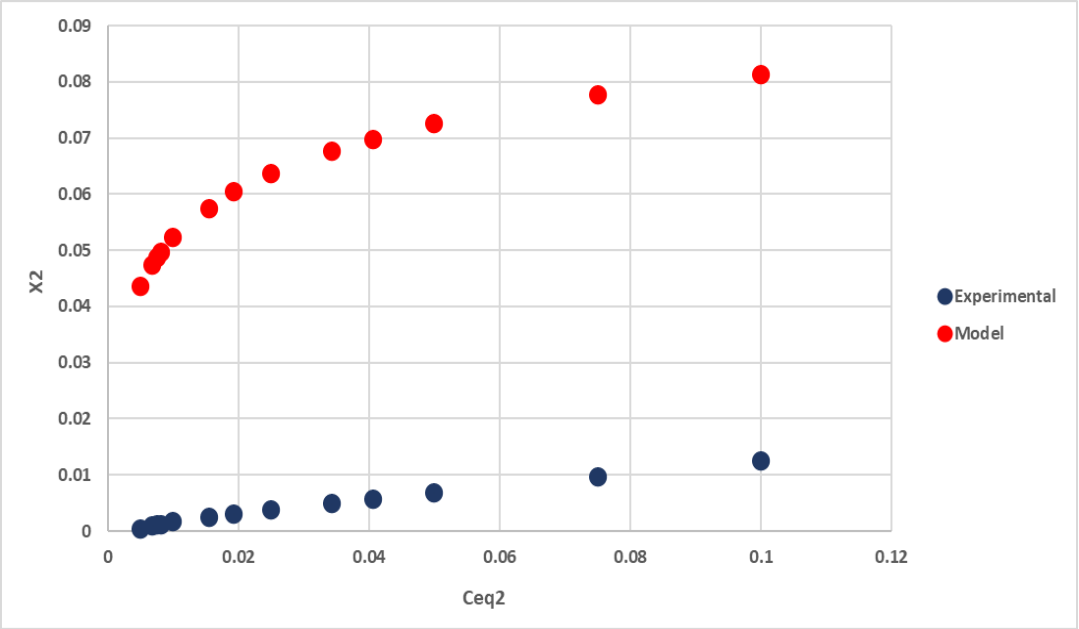

(b)

Fig. 5.2 Multicomponent adsorption isotherms following *LeVan-Vermeulen* model (Model 2) for (a) ciprofloxacin; (b) ofloxacin.

5.6.2 Kinetic Study

Effect of residence time on the adsorption of ciprofloxacin and ofloxacin by raw sewage sludge is examined using the pseudo-kinetic equations related to both physisorption and chemisorption. Amounts of adsorbed ciprofloxacin and ofloxacin increase with time and reach an optimum equilibrium in approximately 14 days. Parameters of the kinetic models, specifically pseudo-first order (eq. 5.34a) and pseudo-second order (eq. 5.35a) are then computed and the subsequent plots are represented in Fig. 5.3 [pseudo 1st order: (i) and (ii); pseudo 2nd order: (iii) and (iv) for ciprofloxacin and ofloxacin respectively]. The values of rate constants k_1, k_2 and q_e are determined from the slopes and intercepts of the linearized plots (see Table 5.3) of *log* $(q_e - q_t)$ *vs. t* (refer eq. 5.34b) for pseudo-first order and (t/q_t) *vs. t* (refer eq. 5.35b) for pseudo-second order kinetic models respectively.

It is evident from Table 5.3 that adsorption of both ciprofloxacin and ofloxacin using raw sewage sludge, follows a pseudo 2nd order kinetic model as the same provides a better fit with R^2 values for ciprofloxacin and ofloxacin being 0.999 and 0.995 respectively, while compared with the 1st order pseudo kinetic model. Predicted values of q_e calculated from pseudo 2nd order kinetic model match well with the experimental values of maximum amounts of adsorption for both the components. The same model also authenticates the process of chemisorption of ciprofloxacin and ofloxacin using raw sewage sludge as the adsorbent. The same has been applied to adsorption of pollutants from aqueous solutions in recent years (Miao *et* al., 2004, Banerjee *et* al., 2013).

Table 5.3 Parameters of the pseudo 1st order and pseudo 2nd order kinetic models for the adsorption of ciprofloxacin and ofloxacin by raw sewage sludge.

Component	$q_{e,exp}$(g. / 100ml/g. of adsorbent)	Pseudo-first order			Pseudo-second order		
		q_e (g./100 ml / g. adsorbent)	k_1 (1/day)	R^2	q_e(g./100 ml / g. adsorbent)	k_2(g./100ml day)	R^2
Ciprofloxacin	0.0138	0.0036	0.2921	0.984	0.0139	226.806	0.999
Ofloxacin	0.0088	0.0515	0.736	0.845	0.009	118.82	0.995

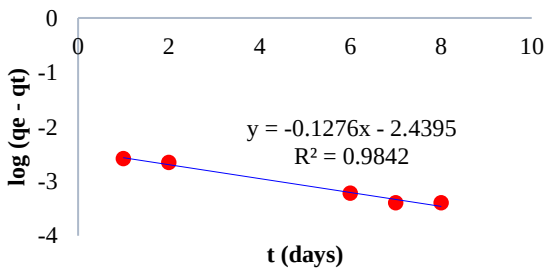

(i)

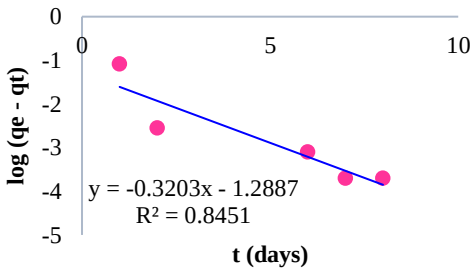

(ii)

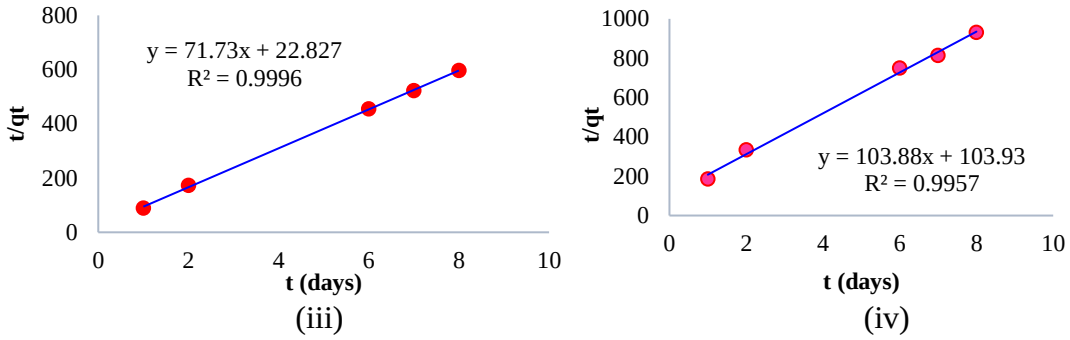

(iii) (iv)

Fig. 5.3 Pseudo first order plots for (i) ciprofloxacin and (ii) ofloxacin; Pseudo second order plots for (iii) ciprofloxacin and (iv) ofloxacin respectively.

5.6.3 Intra-particle diffusion model

The process of adsorption occurs through three consecutive stages, i.e. (i) film diffusion through concentration boundary-layer, (ii) intra-particle diffusion and (iii) adsorption of the molecules of adsorbate(s) on to the interior surface of the pores of the adsorbent (Low, 1960). Intra-particle diffusion model is validated by plotting the experimental data of concentrations of ciprofloxacin and ofloxacin adsorbed onto the raw sewage sludge against time (refer Fig. 5.4). The constant parameter (C) obtained from the intercepts of the linear plots [refer eqn. 5.36] are given in Table 5.4. If the fitted plot passes through origin, intra-particle diffusion would be considered as the rate determining step for the mechanism of adsorption. Experimental data fits well for both the components with high correlation coefficient, $R^2_{ciprofloxacin}$ = 0.986 and $R^2_{ofloxacin}$ = 0.991. All the values of C [for both ciprofloxacin and ofloxacin], are found to be very close to zero. Intra-particle diffusion, thus, is the controlling mechanism for initial mass transfer for the adsorption of both ciprofloxacin and ofloxacin.

Table 5.4 Parameters for intra-particle diffusion model for the adsorption of ciprofloxacin and ofloxacin by raw sewage sludge.

Component	k_i (g./L.g. adsorbent $min^{1/2}$)	C (g/g.adsorbent)	R^2
Ciprofloxacin	0.001	0.009	0.986
Ofloxacin	0.001	0.003	0.991

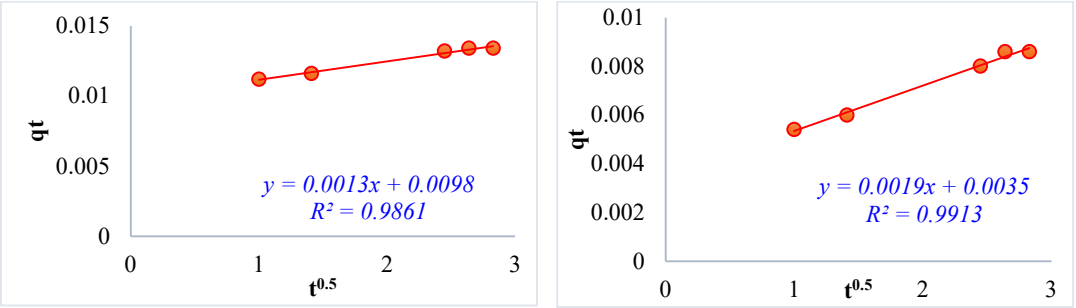

(i) (ii)

Fig. 5.4 Intra-particle diffusion plots for (i) ciprofloxacin and (ii) ofloxacin.

5.6.4 Boyd's Film Diffusion

Boyd's plots are obtained [shown in Fig. 5.5 (i) and Fig. 5.5 (ii) for ciprofloxacin and ofloxacin respectively] by computing B_t from equations (5.37-5.39b) against time (t). It is evident that the plots do not pass through origin. It is observed that intercepts of the plots [refer parameters given in Table 5.5] are largely non-zero. Values of intercepts, in case of adsorption of ciprofloxacin and ofloxacin, are 0.840 and 0.071 respectively. Values of R^2 for ciprofloxacin and ofloxacin are found to be 0.984 and 0.930 respectively.

Table 5.5 Parameters of Boyd's film diffusion model for the adsorption of ciprofloxacin and ofloxacin by raw sewage sludge.

Component	Intercept	R^2
Ciprofloxacin hydrochloride	0.840	0.984
Ofloxacin	0.071	0.930

Film diffusion, thus, controls the adsorption mechanism for both ciprofloxacin and ofloxacin. Specifically, 0.84 is the numerical value of the intercept for ciprofloxacin and the same shows that adsorption of ciprofloxacin is strongly dependent on film diffusion mode. Also, it is observed that ciprofloxacin gets the priority over ofloxacin in the competitive adsorption process on the sludge surface. The quantity of ofloxacin left in solution gets attached to the raw sludge based adsorbent surface by surface coordination through hydrogen bonding. The same is also validated by the pseudo second order kinetic model. Intra-particle diffusion has not been observed as the sole rate controlling factor. Chemisorption is thus the rate controlling factor in this particular study. Considering the values of R^2 [$R^2_{ciprofloxacin}$=0.984 and $R^2_{ofloxacin}$=0.930] Boyd's Film diffusion model represents adsorption of ciprofloxacin better as compared to the adsorption of ofloxacin.

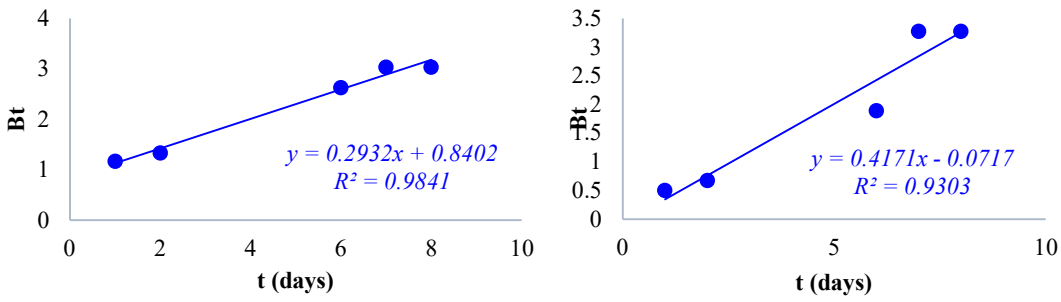

(i) (ii)

Fig. 5.5 Boyd's film diffusion plots for (i) ciprofloxacin and (ii) ofloxacin.

5.7 Probable mechanism of adsorption of ciprofloxacin and ofloxacin onto the raw sewage sludge *[refer Annex II]* (Coates 2006; Vazirinasab *et al.* 2018; Aslam *et al.* 2021a; Aslam *et al.* 2021b; Mobin *et al.* 2022; Zhang *et al.* 2022)

Generally, organic adsorbents containing various oxygenated functional groups and phenolic groups make interactions with FQs through electrostatic attraction, hydrogen bonding, π–π interaction, and hydrophobic interactions. These interactions are possible because of the presence of functional groups like -COOH, $-NH_2$, and -OH in ciprofloxacin and ofloxacin and a variety of functional groups present on the sludge surface (refer to Annex II: Fig. II.2). The possibility of π–π interaction between the semi-dried raw sewage sludge and the adsorbates [CIP and OFLX] leading to the observed adsorption of ciprofloxacin and ofloxacin is much less as abundant ionic groups are present in the sludge surface, as substantiated by the FTIR spectrum of the raw sludge [see Fig. 3.2] and point of zero charge of the adsorbent that refers the surface to be negatively charged at a working pH of ~7.8 [refer Fig. 3.3] (Aslam et al. 2021b, a; Mobin et al. 2022).

In an acidic solution with pH below 6.1, CIP and OFLX molecules exist in a cationic form mainly due to the protonation of the amine group in the piperazine moiety [refer to Fig. 5.6]. When its pH is higher than 8.7, it exists as an anion due to the loss of a proton from the carboxylic group. With 6.1<pH<8.7, CIP exists in a zwitterionic form. In the working pH of 7.8, CIP and OFLX exist primarily in zwitterionic or neutral forms. Also, the semi-dried sludge surface is negative at pH=7.8 [refer to Fig. 3.3]. FT-IR results further suggested that the protonated amine group of ciprofloxacin and ofloxacin, in its zwitterionic form, was not electrostatically attracted to a large extent to the negatively charged sites of the sludge surfaces. Thus, the net ionic attraction between zwitterionic CIP and negative sludge surface is not appreciably effective.

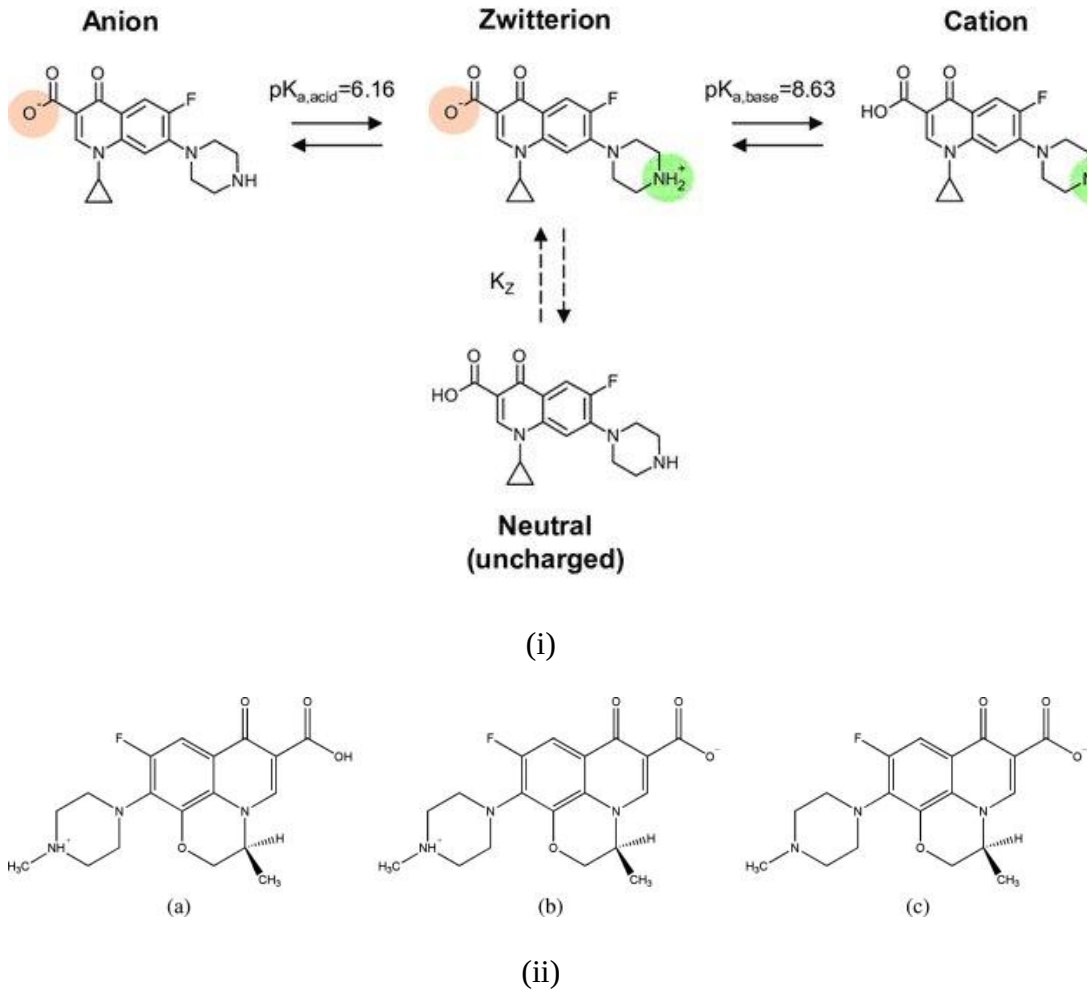

Fig. 5.6 Different ionic states of (i) Ciprofloxacin in different ranges of pH and (ii) Ofloxacin existing at various ranges of pH; (a) Cationic (at pH ~ 4), (b) Neutral or Zwitterionic (at pH ~ 7) and (c) Anionic (at pH ~ 9).

The hydrophobic interaction is also negligible because both the adsorbent and adsorbates are hydrophilic in nature as substantiated by a contact angle measurement study that indicates the contact angles of both the raw sludge [refer to Fig. 3.4] and the treated sludge [refer to Fig. II.3] are less than 90^o. Apart from these theoretical speculations, a modified competitive Langmuir-like model fitted well for ciprofloxacin. The modified competitive Langmuir-like model mainly follows the monolayer adsorption (Luna et al. 2010) of adsorbates onto the semi-dried sludge

surface. The weak hydrophobic interactions, that results from multilayer adsorptions, have very little contribution to the process.

The sewage sludge still exhibits a relatively high adsorption capacity towards ciprofloxacin and ofloxacin in weakly alkaline medium (pH at ~ 7.8) due to the negative charge assisted hydrogen bonding, on the basis of the following equations [see equations 5.40, 5.41, 5.42a, 5.42b or 5.43]. Carboxylic acid groups of both CIP and OFLX are hydrogen bonded to the basal oxygen atoms of the sludge layers.

$$CIP\text{-}COO^- + H_2O \longrightarrow CIP\text{-}COOH + OH^- \quad (5.40)$$

$$OFLX\text{-}COO^- + H_2O \longrightarrow OFLX\text{-}COOH + OH^- \quad (5.41)$$

$$RSS\text{-}O^- + HOOC\text{-}FQs \longrightarrow RSS - [\, O\ldots..H - OOC\,]^- - FQs \quad (5.42a)$$

Or

$$RSS\text{-}COOO^{2-} + HOOC\text{-}FQs \longrightarrow RSS - [\, COOO\ldots..H - OOC\,]^{--}FQs \quad (5.42b)$$

Or

$$(RSS\text{-}O)_3\text{–}P{=}O + HOOC\text{-}FQs \longrightarrow (RSS\text{-}O)_3 - [P{=}O\ldots H\text{-}OOC]\text{-}FQs \quad (5.43)$$

The neutral forms of the two FQs probably react with the raw sewage sludge [RSS] as shown in equations (5.40), (5.41) and (5.42a). The XPS study [refer Fig. II.4 (A O 1s) and (B O 1s)] indicates a shift in the binding energy of O 1s from 532.2 eV to 531.8 eV substantiating the existence of H-bonding between the negatively charged surface of raw sewage sludge and specific functional groups on the surface of two FQs resulting due to lesser electron density on base O element after the formation of H bonds with the FQs.

Outcomes of both pseudo-second-order kinetic model and Boyd's film diffusion model supplement the probable surface-complex interactions of CIP and OFLX with the sludge surface. The same supports that the interactions are chemical in nature and chemisorption is taking place on the surface of the sludge.

A significant change in the sludge surface, after the adsorption of ciprofloxacin and ofloxacin, is observed in the FTIR spectrum of post-treated sludge [refer to Fig. II.2 of *Annex II*]. Certain new bands in the region 1527 cm^{-1} – 1548 cm^{-1} indicate the presence of aromatic ring systems along with amine and carboxylic acid groups. This indicates that both of the FQ molecules interact with the functional groups of the sludge, primarily due to hydrogen bonding. The adsorption process is also evaluated in terms of the XPS study [refer Fig. II.4 (B F 1s)] which indicates that presence of an F atom in the treated sludge originates after the adsorption of the two FQs onto the raw sludge surface.

Chapter 6:-

Transient behavior of a packed column: *Development and validation of convective diffusion models with due considerations for pseudo-kinetics driven depletion of species*

6.1 Background

Large-scale use of the FQs during and after Covid-19 pandemic has increased the quantum of FQs being discharged into inland surface waterbodies with an enhancement of risks (Comber et al. 2020). The FQs exist in the range of ng/L to µg/L in aqueous matrices and ng/Kg to mg/Kg in solid matrices resulting in acute and chronic toxicity as well as the emergence of antibiotic-resistant bacteria (van Doorslaer et al. 2014). Ciprofloxacin (CIP) and ofloxacin (OFLX) are broad spectrum antibiotics belonging to this class. The amount of ciprofloxacin (CIP) and ofloxacin (OFLX) found in aqueous matrices are approximately 44.0 µg/L and 35.5 µg/L respectively (Schlüsener and Bester 2006; Prieto et al. 2011; González-Pleiter et al. 2013).

A huge quantity of pharmaceutical wastewater containing CIP and OFLX can be treated using a packed column with suitable adsorbent. Activated sludge is a widely used environment-friendly adsorbent for its proven ability to remove various micropollutants from wastewater (Clara et al. 2005; Radjenović et al. 2009; Koh et al. 2009; McAdam et al. 2010; Petrie et al. 2013; Wan Ismail et al. 2022). Activated sludge, composed of carbonaceous matter along with other chemical and biological constituents, is an effective adsorbent due to the presence of a high degree of porosity and internal surface area (Rio et al. 2005). The efficiency of the adsorber depends on a proper design, which in turn requires the prediction of effluent concentration-time profile. Effects of several parameters i.e. height and diameter of packing, influent concentration, and flow rate are examined in order to find out the breakthrough curves for a fixed bed column.

Determination of the breakthrough curve for adsorption in a packed bed is a very important concern because it provides basic but very important information in the design of a packed column. The experimental method is usually a time-consuming and un-economical process, particularly for trace contaminants with long residence times (Xu et al. 2013). In order to overcome the stringent assumptions of these semi-empirical models, both in their primary and linearized forms, in this piece of research, a robust and novel convective-diffusion model is proposed with generation/depletion terms being governed by pseudo kinetics of adsorption under dynamic condition. A pore and solid diffusion model is developed for a fixed bed column considering irreversible adsorption isotherms and neglecting outside film resistance (Weber and Chakravorti 1974). Lapidus and Amundson applied a convective-diffusion model to analyze the transport mechanism of solute in an unsteady one-dimensional saturated flow, neglecting intra-pellet mass transfer (Lapidus and Amundson 1952). Similarly,

a number of research groups analysed packed-bed adsorption using the convective-diffusion model with due consideration for inter-pellet diffusion (Thirupathi et al. 2007; Selvaraju and Pushpavanam 2009; Saha et al. 2012; Singha et al. 2012). A fixed bed packed with sewage sludge (adsorbent) and inert granular glass materials (packing material) is used in this study.

6.2 Materials and Methods

6.2.1 Sampling and processing of raw sewage sludge

Raw sewage sludge [RSS] is collected from the Sewage Treatment Plant (STP), managed by Kamarhati Municipality, North 24 Parganas, West Bengal, India. The sludge is dried in ambient air under natural convective mode for a duration of 5-6 days. The dried semi-solid sludge is then used as the adsorbent to serve as the primary component of packing for the fixed bed used during the dynamic study afterward. A list of chemicals used for the study is given in *section 5.2.2* of Chapter 5. The analytical protocol which is followed to analyse ciprofloxacin and ofloxacin in combination is elaborated in Chapter 5 (see *section 5.2.3*).

6.2.2 Operational Conditions

Various factors considered during the breakthrough analysis are bed depths (3, 5, and 7 cm), influent concentrations (50, 100, and 200 ppm), and flow rates (0.67, 0.90, and 2.14 ml/min). The wastewater is fed and treated till the ratio C_t/C_0 becomes equal to 0.85. The experiments are conducted at different bed heights, flow rates, and feed concentrations without changing the pattern of packing of the column with the adsorbent and inert glass beads. Treated wastewater emerging out of the bottom of the column [refer Fig. 6.1] is collected at specific intervals of time and then the same is analyzed in HPLC (refer to *section 5.2.3* of Chapter 5) in triplicate for the unknown

concentrations of ciprofloxacin and ofloxacin simultaneously using respective standard curves.

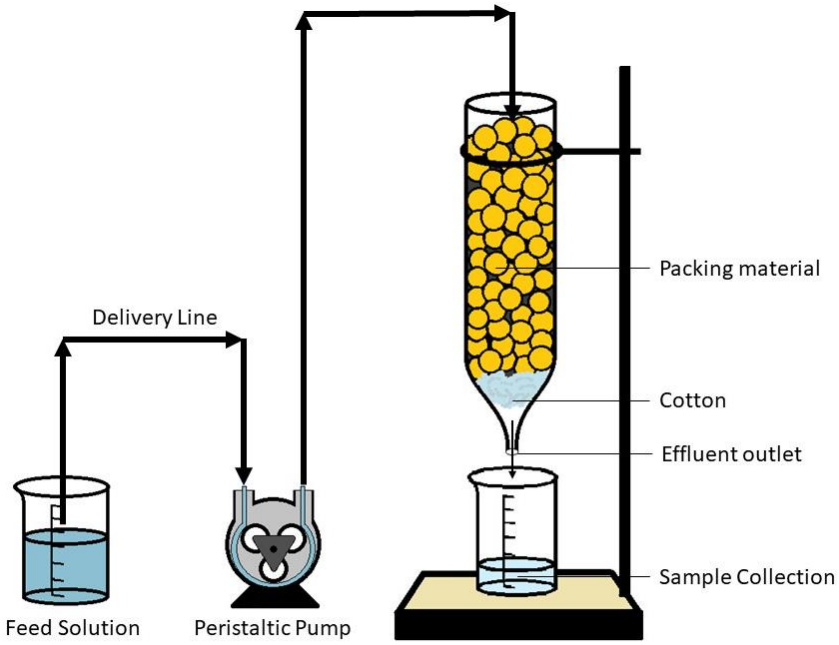

Fig. 6.1 Experimental setup consisting of a packed bed column made by a combination of sewage sludge and glass beads in a ratio of 1:2 for the removal of ciprofloxacin and ofloxacin.

6.3 Theory

In order to model a solid-liquid column adsorption system, it is necessary to describe the adsorption process into four basic steps (refer Fig. 6.2a) (Worch 2012):

(1) liquid phase mass transfer includes convective mass transfer and molecular diffusion.

(2) film diffusion is defined as the interfacial diffusion between the liquid phase and the exterior surface of the adsorbent.

(3) intra-pellet mass transfer concerning pore diffusion and surface diffusion and

(4) the adsorption-desorption reaction governed by 1st and 2nd order pseudo-kinetics (Crittenden and Weber 1978; Crittenden et al. 1986; Friedrich G. Helfferich 1995).

6.3.1 Liquid phase mass transfer

Specific pharmaceutical species (in the forms of molecules and ions) present in the column, can transport both in the axial and radial directions under convective as well as diffusive modes. In order to simplify the model, it is usually assumed that all cross-sections are homogeneous and the radial transports (both convective and diffusive) are neglected (Xu et al. 2013). Considering the axial dispersion to be present, a mass conservation equation is developed, on a macroscopic scale, to relate different process variables in the column, like concentration of the adsorbed adsorbate (*q*), the concentration of the bulk solution (*c*), distance to the inlet (*z*), superficial velocity (u_s) and axial dispersion coefficient (D_z). Starting with a differential control volume [refer Fig. 2b] within the packed column (Costa and Rodrigues 1985; Tien 1994; Fournel et al. 2010), a convective-diffusion based species transport equation is developed [equation (6.1)] considering a depletion term, consisting of the removal of primary species [adsorbate] by virtue of adsorption.

$$\varepsilon_b \frac{\partial C}{\partial t} + u_s \frac{\partial C}{\partial z} + (1 - \varepsilon_b)\rho_a \frac{\partial q}{\partial t} = D_z \frac{\partial^2 C}{\partial z^2} \tag{6.1}$$

where, the initial and boundary conditions are:

$t = 0 \quad \rightarrow \quad C(z,t) = 0,$

$t = 0 \quad \rightarrow \quad q(z,t) = 0,$

$z = 0 \quad \rightarrow \quad C(0, t = 0) = 0,$

$C(0, t > 0) = C_0,$

$z = L \quad \rightarrow \quad \frac{\partial C}{\partial z} = 0$

When the axial dispersion is neglected, equation (6.1) becomes

$$\varepsilon_b \frac{\partial C}{\partial t} + u_s \frac{\partial C}{\partial z} + (1 - \varepsilon_b)\rho_a \frac{\partial q}{\partial t} = 0 \qquad (6.2)$$

The initial and boundary conditions also change to the following:

$t = 0 \quad \rightarrow \quad C\,(z, t) = 0$

$t = 0$, for $z \geq 0 \quad \rightarrow \quad C = 0, q = 0$

$z = 0 \quad \rightarrow \quad C = C_0$ for t > 0

$z = H \quad \rightarrow \quad \frac{\partial C}{\partial z} = 0$

where, ε_b is the bed porosity, t is the time, ρ_a is the adsorbent density, C_{in} is the initial concentration of the influent, and H is the bed height.

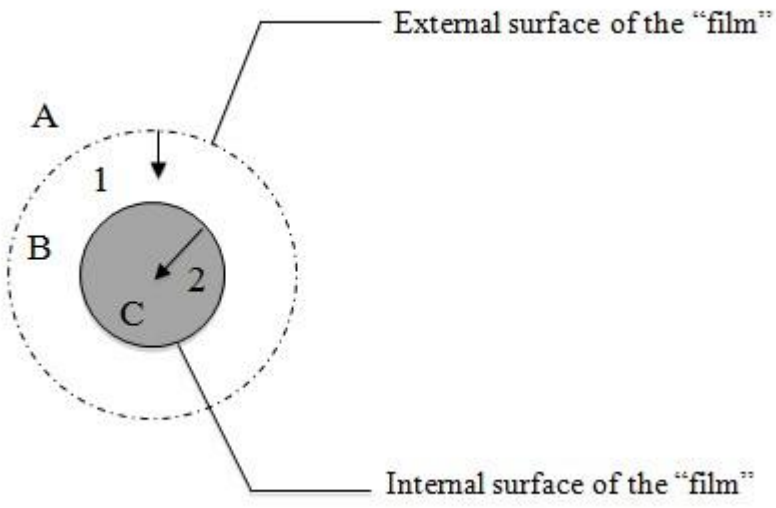

Fig. 6.2a Adsorption process of an adsorbent pellet, represented on a macroscopic scale

In Fig. 6.2a, A= bulk fluid, B = interface region, C = adsorbent pellet, 1 ≡ film diffusion 2 ≡ intra-pellet diffusion

In Fig. 6.2b, 1 = convective mass transfer, 2 = axial dispersion, 3 = adsorbed by adsorbent, 4 = accumulation of adsorbate. In Fig. 6.2b

(1+) - (1-) $\rightarrow$ $-u_s \frac{\partial C}{\partial z}$

(2+) - (2-) $\rightarrow$ $-D_z \frac{\partial^2 C}{\partial z^2}$

(3-) $\rightarrow$ $(1-\varepsilon_b)\rho_a \frac{\partial q}{\partial t}$

(4) $\rightarrow$ $\varepsilon_b \frac{\partial C}{\partial t}$

Equations (1) and (2) are based on the following assumptions (Xu et al. 2013):

(1) the entire process is isothermal;

(2) no chemical reaction occurs in the column;

(3) the packed bed is made of porous spherical adsorbent particles, uniform in size;

(4) the bed is homogeneous and the concentration gradient in the radial direction of the bed is negligible;

(5) the flow rate is constant and invariant with the column position (Petrus and Warchoł 2003); and,

(6) the activity coefficient of each species is unity.

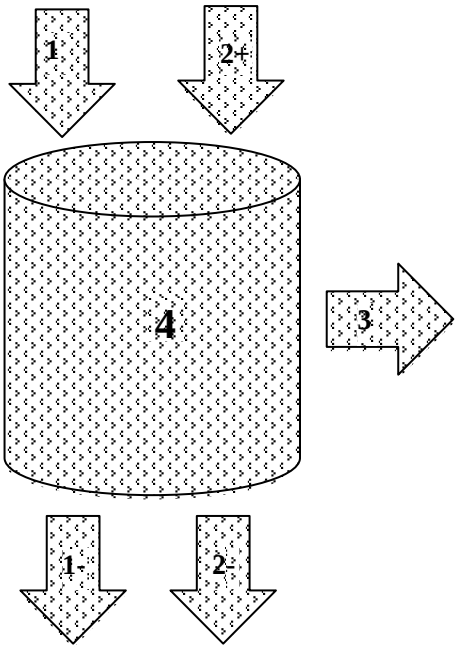

Fig. 6.2b Schematic diagram of the species conservation around a differential control volume.

Now, we can write the bulk density of the bed as: $\rho_b = (1 - \varepsilon_b)\rho_a$

So, equation (6.2) can be written as,

$$\varepsilon_b \frac{\partial C}{\partial t} + u_s \frac{\partial C}{\partial z} + \rho_b \frac{\partial q}{\partial t} = 0 \tag{6.3}$$

Integrating equation (6.3) over the bed from $z = 0$ (where $C = C_0$) to $Z = H$ (where, $C = C_t$), and noting that $\rho_b q \gg \varepsilon_b C$, we obtain

$$\frac{C_t}{C_0} = 1 - \frac{\rho_b H}{u_s C_0} \frac{d\bar{q}}{dt} \tag{6.4}$$

where, $\bar{q}$ is the average solid-phase adsorbate concentration in the bed, given by

$$\bar{q} = \frac{1}{H} \int_0^H q dx \tag{6.5}$$

However, $\bar{q}$ is also a function of time t, since the mass transfer zone shifts from the beginning of the bed to the end with time, thus increasing the adsorbent uptake of the bed with time.

$$\bar{q}_t = \frac{Total\ mass\ of\ adsorbate\ adsorbed\ in\ the\ bed\ upto\ time\ t}{Mass\ of\ adsorbate\ in\ the\ bed} = \frac{m_t^a}{m_A} \tag{6.6}$$

m_A attributes to the weight of sludge taken in the bed. Mass adsorbed by the differential control element of the bed $dm(t)$, at any time is given by the difference of inlet concentration and the outlet concentration at that time i.e.

$$dm(t) = (C_0 - C_t)Qdt \tag{6.7}$$

Where Q = volumetric flow rate of the solution through the bed.

$$\therefore m_t^a = \int_{t=0}^{t} dm(t) = \int_{t=0}^{t} (C_0 - C_t)Qdt \tag{6.8}$$

Thus,

$$\bar{q}_t = \frac{\int_{t=0}^{t} (C_0 - C_t)Qdt}{m_A} \tag{6.9}$$

Also, q_{eq} signifying the maximum amount of adsorbate that can be adsorbed by the bed, that is, the adsorbent loading at time $t = t_{eq}$ (a time when the entire bed is saturated), is given by:

$$q_{eq} = \frac{\int_{t=0}^{t=t_{eq}} (C_0 - C_t)Qdt}{m_A} \tag{6.10}$$

6.3.2 First order model

The pseudo first-order kinetic model is given by the equation

$$\frac{d\bar{q}}{dt} = k_1(q_e - \bar{q}) \tag{6.11}$$

The solution of equation (6.11), subject to the initial condition $\bar{q}$ = 0 at t = 0, is

$$\bar{q} = q_e[1 - exp(-k_1 t)] \tag{6.12}$$

Using equation (6.12) in equation (6.4), we find

$$\frac{C_t}{C_0} = 1 - \frac{\rho_b H k_1 q_e}{u_s C_0} \exp(-k_1 t) \tag{6.13}$$

Let n be the number of bed volumes of fluid that have passed through the bed since t = 0, that is,

$$n = \frac{u_s(t - \frac{H\varepsilon_b}{u_s})}{H} = \frac{Qt}{V_{bed}} - \varepsilon_b \approx \frac{Qt}{V_{bed}} \tag{6.14}$$

Where, Q and V_{bed} are the volumetric flow rate of the fluid though the adsorbent bed and the volume of the bed respectively. The expression for the breakthrough curve, given by equation (6.13), can be written as:

$$\frac{C_t}{C_0} = 1 - D_{a_1} n_{stoic} exp\left(-nD_{a_1}\right) \tag{6.15a}$$

Or,

$$\frac{C_t}{C_0} = 1 - exp\left[-D_{a_1}(n - n_{BT})\right] \tag{6.15b}$$

Where, n_{BT} is the number of bed volumes at breakthrough (i.e. when $C_t \cong 0$). The dimensionless parameters D_{a_1} and n_{stoic} are given by

$$D_{a_1} = \frac{k_1 H}{u_s} = \frac{k_1 V_{bed}}{Q} \tag{6.16}$$

$$n_{stoic} = \frac{\rho_b q_e}{C_0} \tag{6.17}$$

Thus, the two parameters governing the breakthrough curve equation are D_{a_1} and n_{stoic} [from equation (6.15a)], or D_{a_1} and n_{BT} [from equation (6.15b)]. Equating equations (6.15a) and (6.15b), one can obtain,

$$n_{BT} = \frac{ln(D_{a_1} n_{stoic})}{D_{a_1}} \tag{6.18}$$

Assuming n_{stoic} to be constant, differentiating equation (6.18) with respect to D_{a_1} and setting the derivative equal to zero, the maximum number of bed volumes at breakthrough is obtained, as given below,

$$n_{BT,max} = \frac{n_{stoic}}{e} = 0.368 n_{stoic} = 0.368 \frac{\rho_b q_{eq}}{C_0} \tag{6.19}$$

6.3.3 Second-order model

The second-order kinetic model (Ho and McKay 1999), is given by

$$\frac{d\bar{q}}{dt} = k_2 (q_e - \bar{q})^2 \tag{6.20}$$

Integrating equation (6.20), subject to the initial condition: $\bar{q}$ = 0 at t = 0, is given by

$$\bar{q} = \frac{q_e^2 k_2 t}{1 + q_e k_2 t} \tag{6.21}$$

Using equation (6.21) in equation (6.4), gives

$$\frac{C_t}{C_0} = 1 - \frac{\rho_b H k_2 q_e^2}{u_s C_0 (1 + k_2 q_e t)^2} \tag{6.22}$$

Equation (6.22) can also be expressed equivalently as

$$\frac{C_t}{C_0} = 1 - \frac{n_{stoic} D_{a_2}}{\left(1 + n D_{a_2}\right)^2} \tag{6.23a}$$

Or

$$\frac{C_t}{C_0} = 1 - \left(\frac{1+n_{BT}D_{a_2}}{1+nD_{a_2}}\right)^2 \tag{6.23b}$$

where,

$$D_{a_2} = \frac{q_e k_2 H}{u_s} = \frac{q_e k_2 V_{bed}}{Q} \tag{6.24}$$

Thus, from the pseudo second-order kinetic reaction, the two parameters governing breakthrough are D_{a_2} and n_{stoic} [from equation (6.23a)], or D_{a_2} and n_{BT} [from equation (6.23b)]. Equating equations (6.23a) and (6.23b), we obtain

$$n_{BT} = \frac{\sqrt{n_{stoic}D_{a_2}}-1}{D_{a_2}} \tag{6.25}$$

Differentiating equation (6.25) with respect to D_{a_2} and equating to zero, $n_{BT,max}$ is obtained as:

$$n_{BT,max} = \frac{n_{stoic}}{4} = 0.25 n_{stoic} = 0.25\,\frac{\rho_b q_e}{C_0} \tag{6.26}$$

6.4 Method of Solution

The equation of the breakthrough curve given by pseudo 1st order model [equation(6.15a)] and pseudo 2nd order model [equation(6.24a)] have two unknown constants, D_{a_1} and n_{stoic_1} and D_{a_2} and n_{stoic_2} respectively. Once estimated, these can help predict the outlet concentration at any time *t* for $t<t_{eq}$.

From equation (6.17) n_{stoic} can be calculated directly when q_e is known. In order to calculate q_{eq} from equation (6.10), it is necessary to know the outlet concentration C_t as a function of time, which is exactly what we are trying to find out by modelling.

So, the experimental values of outlet concentration C_t versus time t along with the inlet concentration (C_0), for every run, are used to form the model dataset C_t/C_0 vs t.

This data set and the model equations are fed into the *lsqcurvefit* function on **Matlab R2018a** in order to optimize the model parameters to find the best fit curve of input dataset for every run for both FQs for pseudo-first and pseudo-second-order models using a *non-linear least square method*. The model parameters for each of the experiments, are estimated by minimizing the SSQ values (Sum of Squares of Residuals),

$$SSQ = \sum_{i=1}^{n} \frac{(Predicted - Observed)^2}{N-k-1} \tag{6.27}$$

The parameters, so estimated, are finally used to formulate the model equations. Corresponding SSQ values indicate the accuracy of prediction. For sufficiently low SSQ values, it can be concluded that the fit is a 'good fit'. Hence the rate constants (k_1 and q_{eq}) and (k_2 and q_{eq}) can be calculated from the model parameters of both the models using equations (6.16), (6.17) and (6.24). Estimated parameters of the first-order and second-order models are given in Table 6.1. A flowchart representing the sequential methods of solution is given in Fig. 6.3.

Considering pseudo-kinetics to be valid, D_{a1} and D_{a2} can be considered as equivalent Damköhler numbers *(Da)*[1]. Damköhler number (D_a) is a useful ratio for determining whether diffusion rates or reaction rates are 'important' on a relative scale, for defining a steady-state distribution of a chemically reactive species over the length and time scales of interest. For $D_a >> 1$ the reaction rate is much greater than the diffusion rate. Corresponding concentration distribution is said to be diffusion limited (diffusion is slower, so diffusion characteristics dominate and the reaction is assumed to be

[1] ***Damköhler numbers (Da)*** *are, in general, are dimensionless numbers used in chemical engineering to relate the chemical reaction timescale (reaction rate) to the transport phenomena rate occurring in a system. It is named after German chemist* ***Gerhard Damköhler****. In its most commonly used form, the Damköhler number relates the reaction timescale to the convection times scale, flow rate, though the packed bed reactor for a continuous processes:* $\mathrm{Da} = \frac{\text{reaction rate}}{\text{convective mass transport rate}}$

instantaneously in equilibrium). For D_a <<1 diffusion occurs much faster than the reaction, thus diffusion reaches an 'equilibrium' well before the reaction achieves equilibrium.

6.5 Results and discussion

6.5.1 Effect of bed height

For both first-order and second-order models, the effective maximum breakthrough times, for both FQs increase with an increase in bed depth [refer to Table 6.2 and Fig. 6.4] while maintaining flow rate and inlet concentration constant. The experimental breakthroughs come much earlier for ofloxacin as compared to the same for ciprofloxacin. This outcome is in line with the fact that OFLX occupies the pores much faster than CIP. The existing functional groups of the sewage sludge start playing a major role as both the FQs interact with the functional groups of the sludge, primarily due to hydrogen bonding [refer to *section 5.7* of Chapter 5]. In case of ofloxacin, it is observed that the experimental breakthroughs come later than the predicted ones, while the same for ciprofloxacin is not always so. Pseudo-kinetics is not taking care of the complex surface-coordination pathways. This is the probable reason for the mismatch. The first-order and second-order Damköhler numbers initially decreases with an increase in bed height but increases afterward for both the antibiotics, under constant flow rate and inlet concentration, probably due to the competitive adsorption of CIP and OFLX onto the functionalized surface sites.

6.5.2 Effect of flow rate

When bed height and concentration are kept constant, the values of $n_{BT,max}$ for both ciprofloxacin and ofloxacin are seen to increase almost uniformly while D_{a_1} and D_{a_2}

decrease with a decrease in flow rate from 2.14ml/min to 0.67ml/min for both first and second- order models [refer to Table 6.2 and Fig. 6.5].

6.5.3 Effect of inlet concentration

With a constant bed height and flow rate, $n_{BT,max}$ decreases with an increase in the inlet concentration. The rate of increase of$n_{BT,max}$ is found to be much more with inlet concentration varying from 100ppm to 200ppm as compared to the rate of increase of $n_{BT,max}$ with variation of inlet concentration in between 50ppm to 100ppm [refer to Table 6.2 and Fig. 6.6]. At very high concentrations, there is so much of adsorbate available that the rate of adsorption is very high causing faster saturation of bed and this explains much less value of $n_{BT,max}$.

Also, for both the compounds, values of D_{a_1} and D_{a_2} increase subtly when inlet concentration is changed from 50ppm to 100ppm while the corresponding values increase significantly when the inlet concentration increases from 100ppm to 200ppm, keeping the bed height and flow rate constant. The increase in values of Damköhler number also validates the increase in reaction rate with increase in inlet concentration. With the values of Damköhler numbers being << 1, adsorption remains the rate determining step.

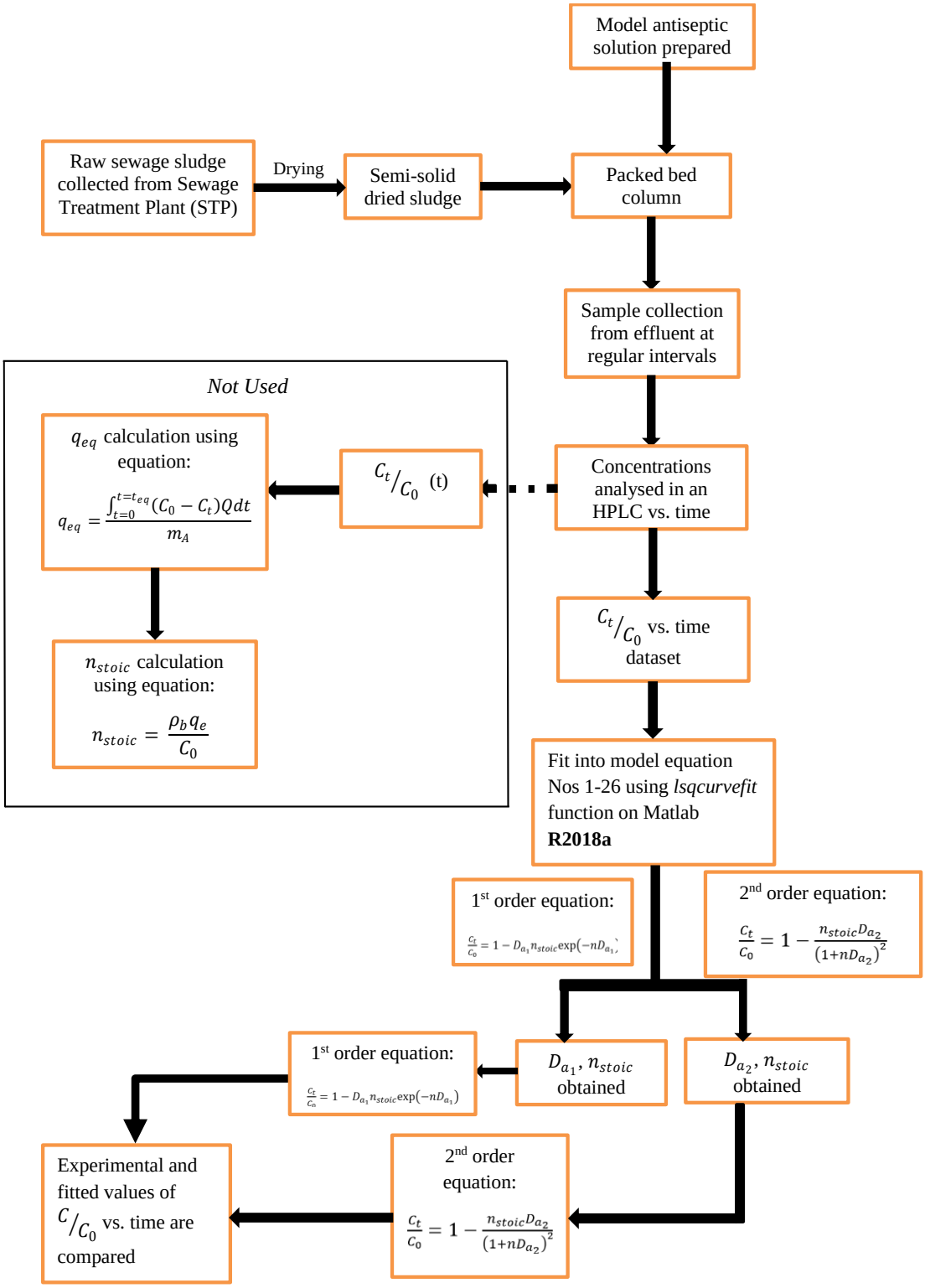

Fig. 6.3 Flowchart representing the sequence of solution.

The accuracy of curve-fitting using non-linear regression analysis is effectively quantified by the SSQ values calculated for both the models with every dataset. From

Table 6.1, it is observed that the SSQ values are predominantly less than 0.02 and even less than 0.01 in quite a number of cases, ensuring a very good fit of the data. Overall, the second order model gives a better fit for ciprofloxacin in 5 out of 7 cases and for ofloxacin in 6 out of 7 cases. So, it can be concluded that both the FQs are chemisorbed onto the sludge. The same is substantiated through a probable mechanism of adsorption of CIP and OFLX, described in *section 5.7* of Chapter 5 (refer to Chapter 3 and Annex II for specific figures that supplement the mechanism). The values of q_e are estimated for both CIP and OFLX for each of the models (see Table 6.1). It is observed that the estimated values of q_e are close to one another for both models for a particular bed height, flow rate and initial concentration. Minor differences are attributed to the differences in the rates of depletion for 1st and 2nd order pseudo-kinetics.

Table 6.1 Estimated parameters of pseudo-first order and pseudo-second order kinetic models for the adsorption of ciprofloxacin and ofloxacin in raw sewage sludge.

Fixed Parameter	Variable Parameter	First-order model						Second-order model					
		n_{stoic}	q_e (g/ml/g)	$n_{BT,max}$	D_{a_1}	k_1 (min^{-1})	SSQ	n_{stoic}	q_e (g/ml/g)	$n_{BT,max}$	D_{a_2}	k_2	SSQ
Ciprofloxacin													
Q=0.9ml/min C_{in}=100ppm	Z=3cm	14.226	0.008	5.235	0.070	0.0043	0.0024	21.803	0.0128	5.4508	0.048	2.2671×10^{-7}	0.002
	Z=5cm	17.782	0.011	6.544	0.057	0.0021	0.0017	28.79	0.0177	7.1975	0.036	7.5013×10^{-8}	0.0034
	Z=7cm	9.999	0.006	3.68	0.069	0.0018	0.0157	14.267	0.0082	3.5677	0.052	1.6697×10^{-7}	0.0133
Z=5cm C_{in}=100ppm	Q=2.14ml/min	13.18	0.0081	4.85	0.07	0.0061	0.0045	20.115	0.0123	5.0287	0.048	3.3566×10^{-7}	0.0046
	Q=0.9ml/min	17.782	0.011	6.544	0.057	0.0021	0.0017	28.79	0.0177	7.1975	0.036	7.5013×10^{-8}	0.0034
	Q=0.67ml/min	21.88	0.013	8.052	0.044	0.0012	0.0047	35.672	0.022	8.9181	0.028	3.4879×10^{-8}	0.0035
Q=0.9ml/min Z=5cm	c_{in}=200ppm	5.872	0.007	2.161	0.152	0.0056	0.0079	7.937	0.0097	1.9843	0.123	4.6213×10^{-7}	0.0025
	c_{in}=100ppm	17.782	0.011	6.544	0.057	0.0021	0.0017	28.7899	0.0177	7.1975	0.036	7.5013×10^{-8}	0.0034
	c_{in}=50ppm	18.483	0.006	6.802	0.038	0.0014	0.0107	28.835	0.0089	7.209	0.026	1.0603×10^{-7}	0.0101
Ofloxacin													
Q=0.9ml/min c_{in}=100ppm	Z=3cm	5.88	0.0035	2.163	0.175	0.011	0.0024	8.161	0.0048	2.0403	0.1307	1.6621×10^{-6}	0.0038
	Z=5cm	8.123	0.005	2.99	0.121	0.004	0.0016	11.769	0.0072	2.9422	0.0885	4.4961×10^{-7}	0.0014
	Z=7cm	5.44	0.003	2.002	0.129	0.0034	0.0184	6.329	0.0036	1.5822	0.1334	9.6368×10^{-7}	0.0119
Z=5cm c_{in}=100ppm	Q=2.14ml/min	4.216	0.0026	1.552	0.214	0.019	0.0074	5.9287	0.0036	1.4822	0.163	3.9086×10^{-6}	0.0023
	Q=0.9ml/min	8.123	0.005	2.99	0.121	0.004	0.0016	11.769	0.0072	2.9422	0.0885	4.4961×10^{-7}	0.0014
	Q=0.67ml/min	9.879	0.006	3.635	0.114	0.003	0.0062	14.57	0.0089	3.6425	0.0793	2.4213×10^{-7}	0.0129
Q=0.9ml/min Z=5cm	c_{in}=200ppm	4.004	0.0049	1.473	0.24	0.008	0.0049	5.721	0.007	1.4302	0.1755	9.1670×10^{-7}	0.0013
	c_{in}=100ppm	8.1234	0.005	2.989	0.1209	0.0044	0.0016	11.769	0.0072	2.9422	0.0885	4.4961×10^{-7}	0.0014
	c_{in}=50ppm	16.7667	0.0051	6.1701	0.0467	0.0017	0.0075	25.766	0.0079	6.4414	0.0317	1.4697×10^{-7}	0.0074

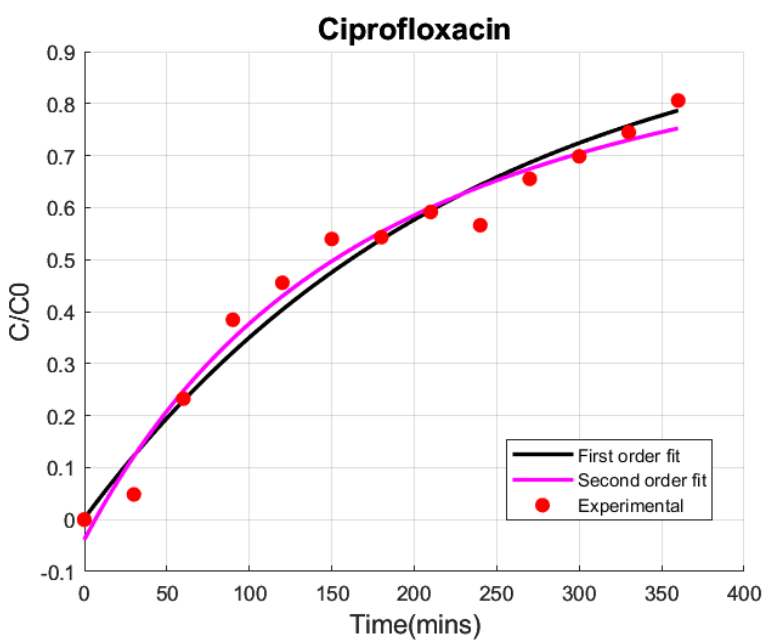

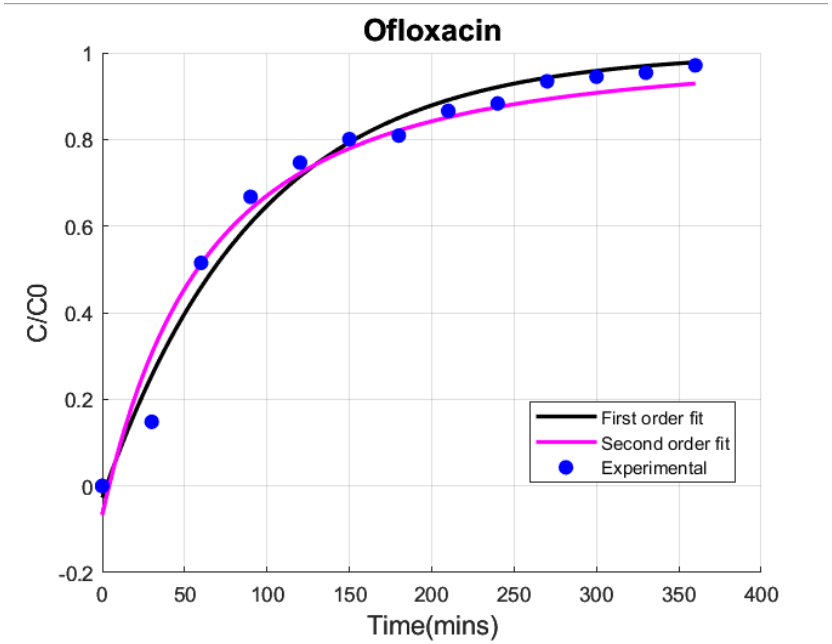

	D_a	n_{stoic}	B.T. Time
1st order	0.0701	14.2259	323
2nd order	0.0476	21.8030	357

3 cm

	D_a	n_{stoic}	B.T. Time
1st order	0.1748	5.8781	132
2nd order	0.1307	8.1611	133

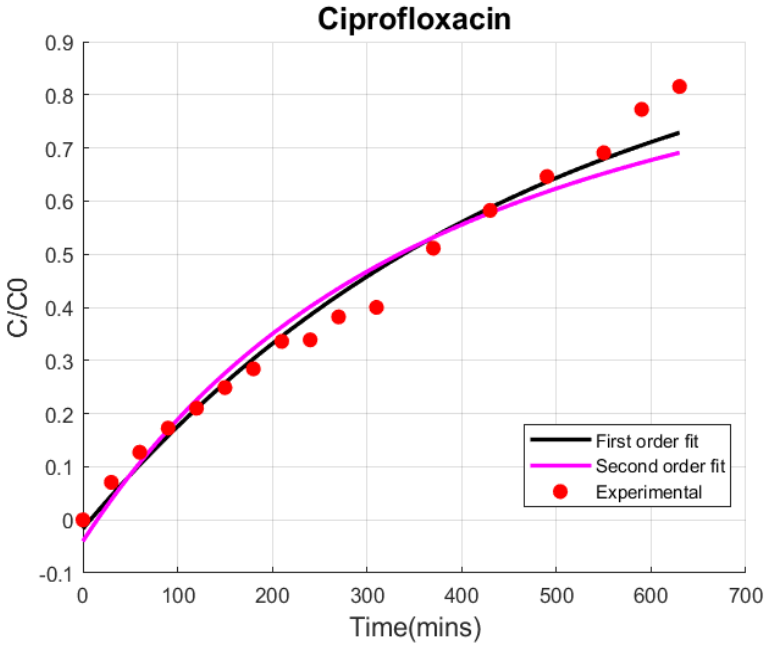

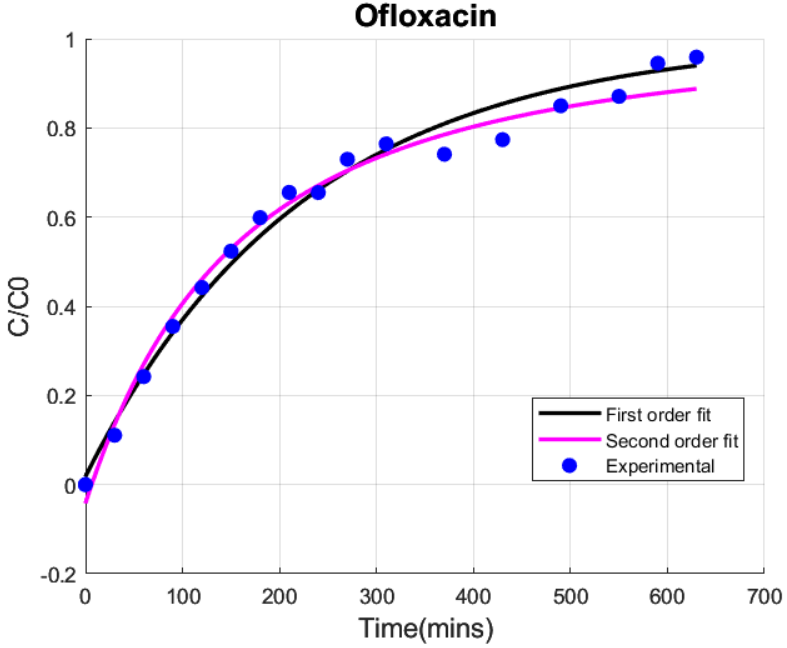

	D_a	n_{stoic}	B.T. Time
1st order	0.057	17.7816	669
2nd order	0.036	28.7899	785

	D_a	n_{stoic}	B.T. Time
1st order	0.1209	8.1234	309
2nd order	0.0885	11.7689	321

5 cm

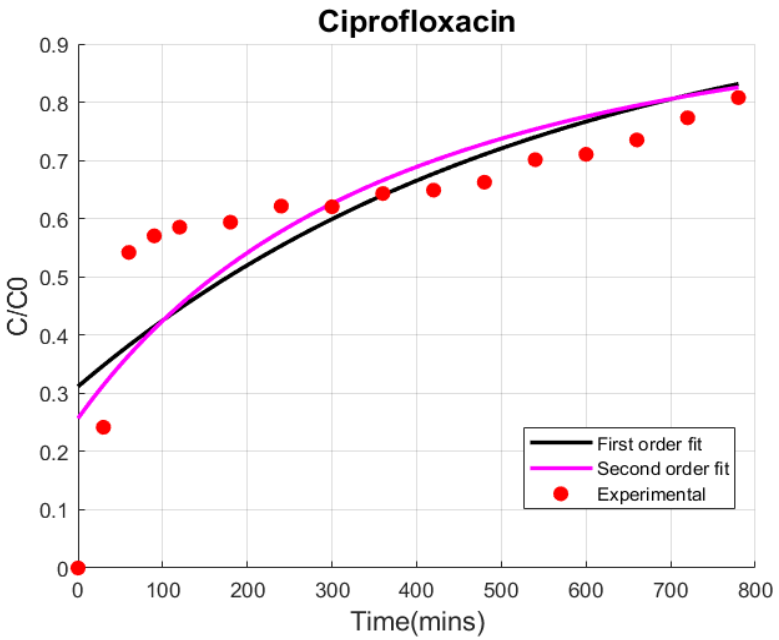

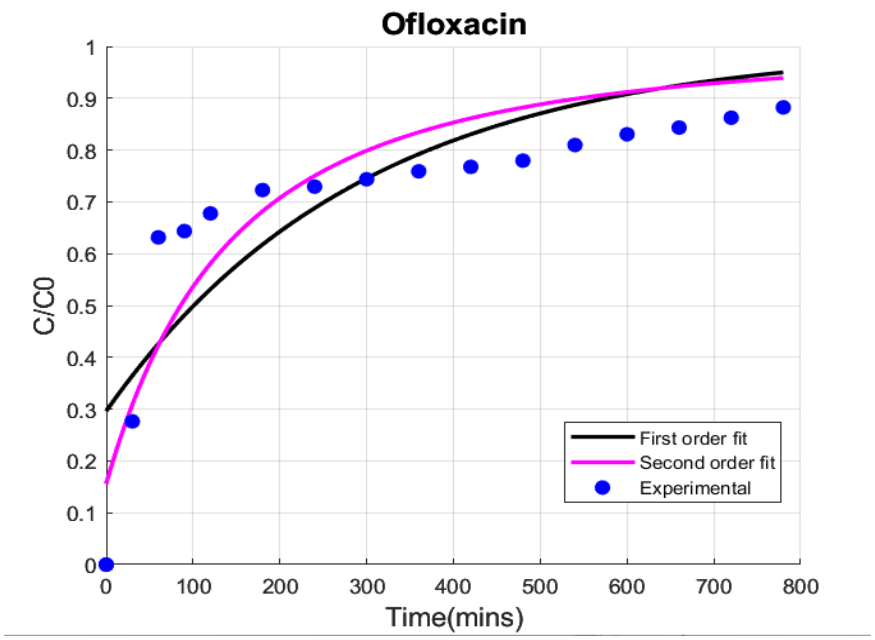

	D_a	n_{stoic}	B.T. Time
1st order	0.069	9.999	845
2nd order	0.052	14.267	898

	D_a	n_{stoic}	B.T. Time
1st order	0.129	5.44	456
2nd order	0.133	6.329	393

7 cm

Fig. 6.4 Predicted breakthrough curves using first-order and second-order kinetic models with respect to experimental data collected for increasing bed heights [a) 3 cm, b) 5 cm, c) 7 cm] at an inflow rate =0.9ml/min and inlet concentration =100ppm.

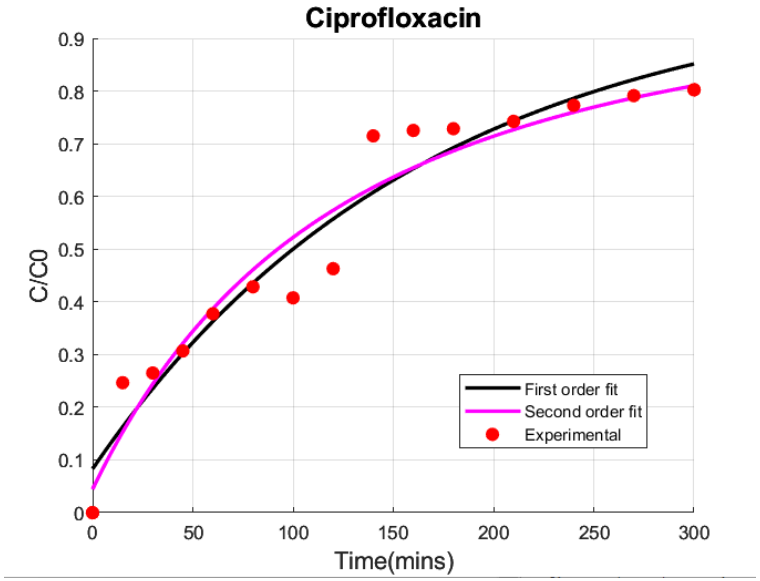

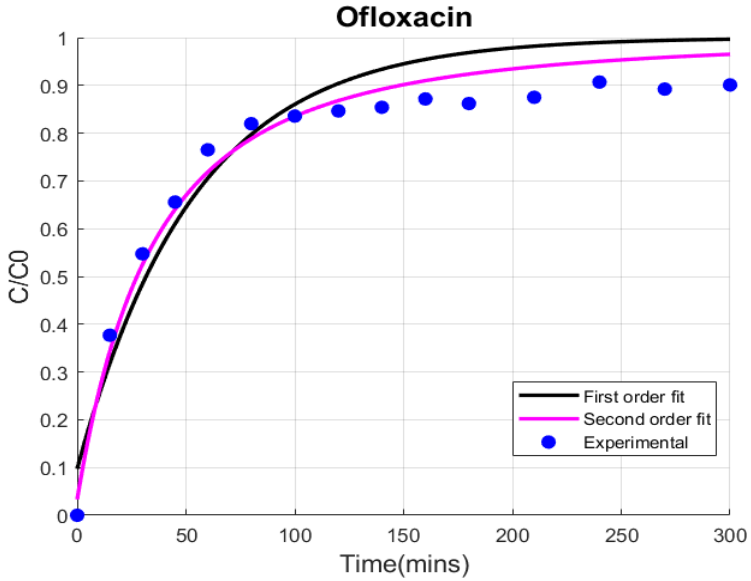

	D_a	n_{stoic}	B.T. Time
1st order	0.069	13.18	251
2nd order	0.048	20.115	286

	D_a	n_{stoic}	B.T. Time
1st order	0.214	4.217	81
2nd order	0.163	5.929	84

2.14 ml/min

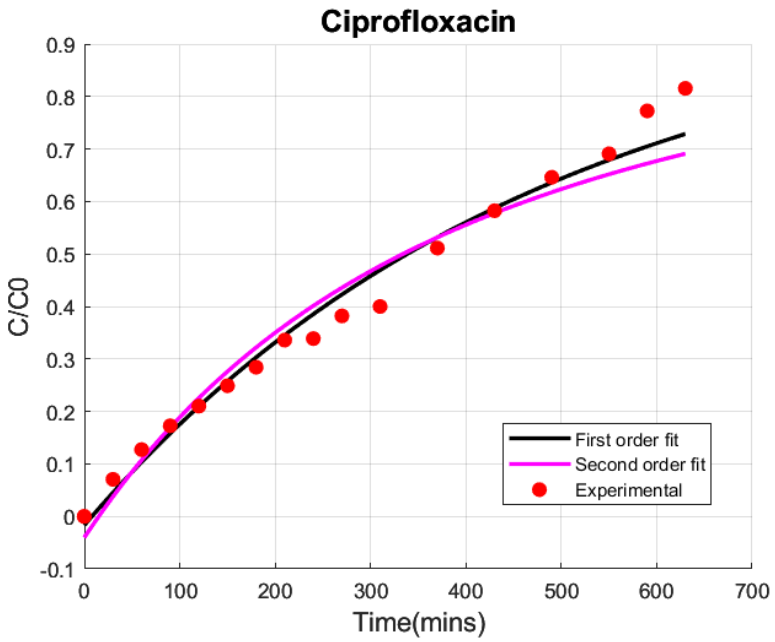

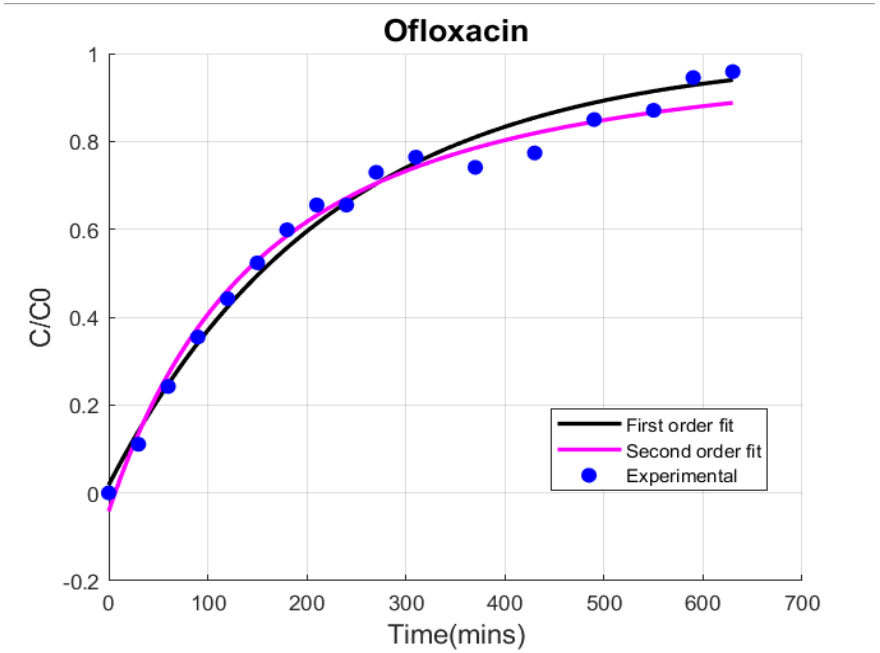

	D_a	n_{stoic}	B.T. Time
1st order	0.057	17.782	669
2nd order	0.036	28.79	785

	D_a	n_{stoic}	B.T. Time
1st order	0.121	8.123	309
2nd order	0.089	11.769	321

0.9 ml/min

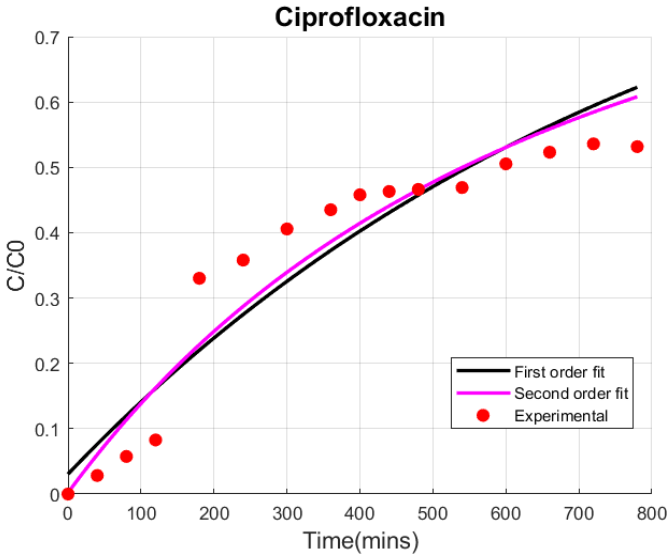

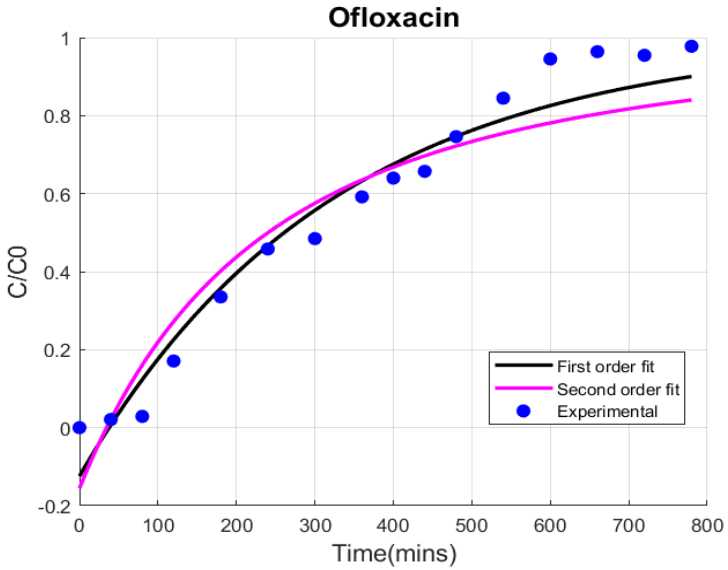

	D_a	n_{stoic}	B.T. Time
1st order	0.057	17.782	669
2nd order	0.036	28.79	785

	D_a	n_{stoic}	B.T. Time
1st order	0.114	9.879	556
2nd order	0.079	14.57	648

0.67 ml/min

Fig. 6.5 Predicted breakthrough curves using first-order and second-order kinetic models with respect to experimental data collected with decreasing flow rates [(a) 2.14ml/min, (b) 0.90ml/min, (c) 0.67ml/min] using a bed height =5cm and inlet concentration =100ppm.

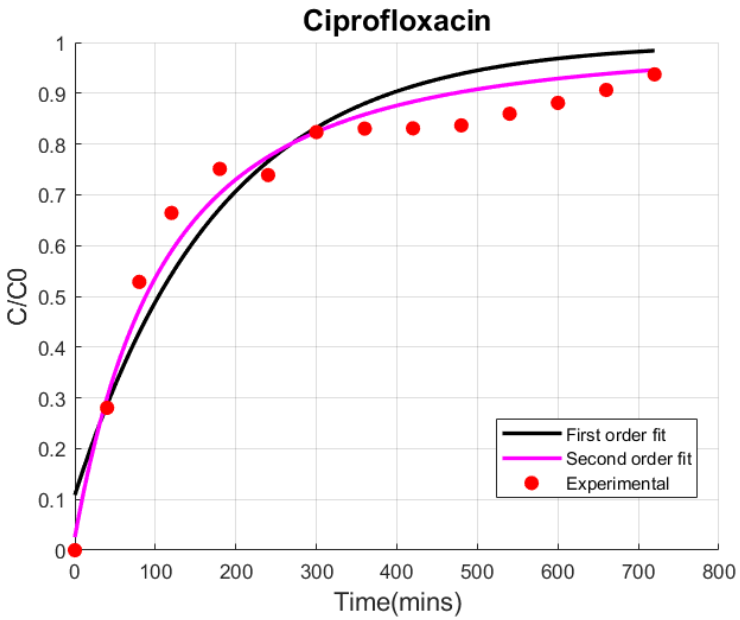

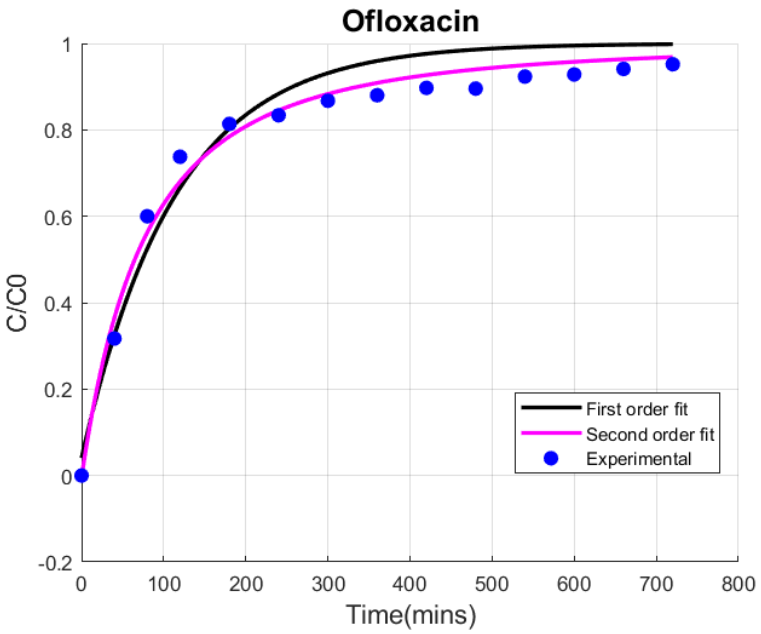

	D_a	n_{stoic}	B.T. Time
1st order	0.152	5.87	269
2nd order	0.123	7.937	268

	D_a	n_{stoic}	B.T. Time
1st order	0.24	4.004	178
2nd order	0.175	5.721	193

200 ppm

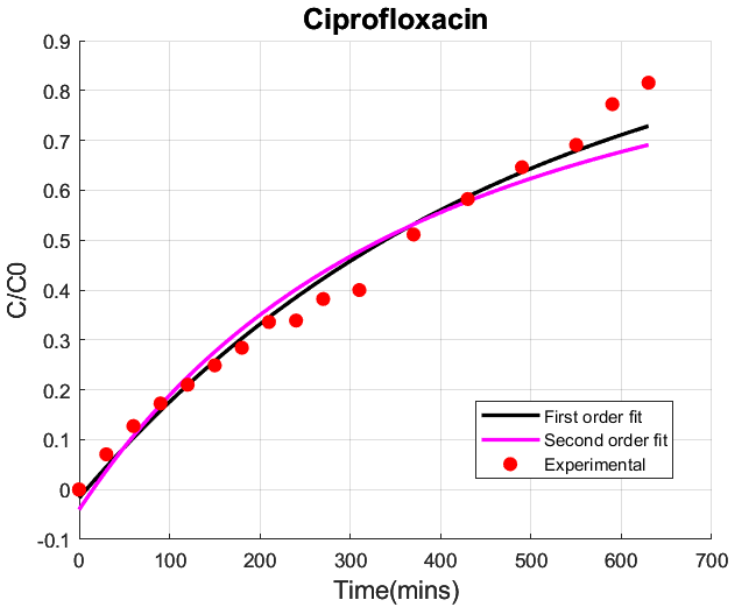

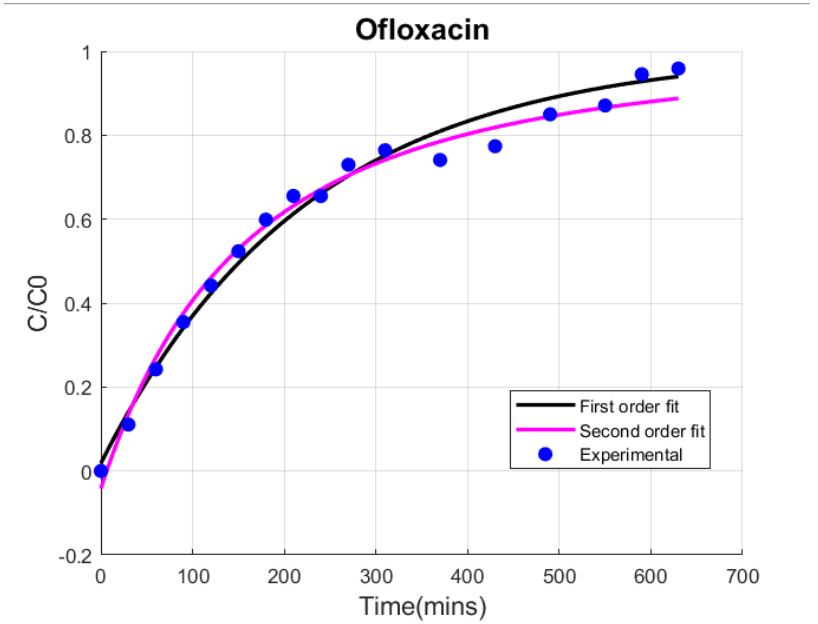

	D_a	n_{stoic}	B.T. Time
1st order	0.057	17.782	669
2nd order	0.036	28.79	785

	D_a	n_{stoic}	B.T. Time
1st order	0.121	8.123	309
2nd order	0.089	11.769	321

100 ppm

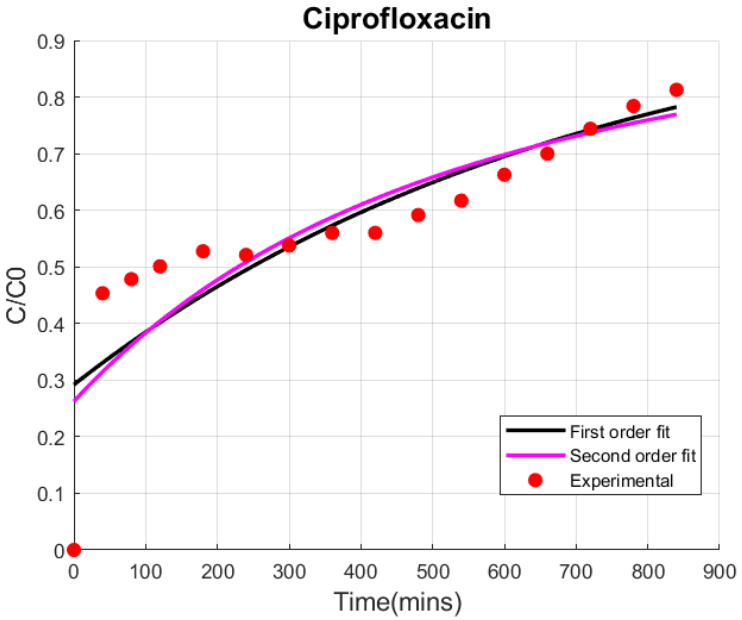

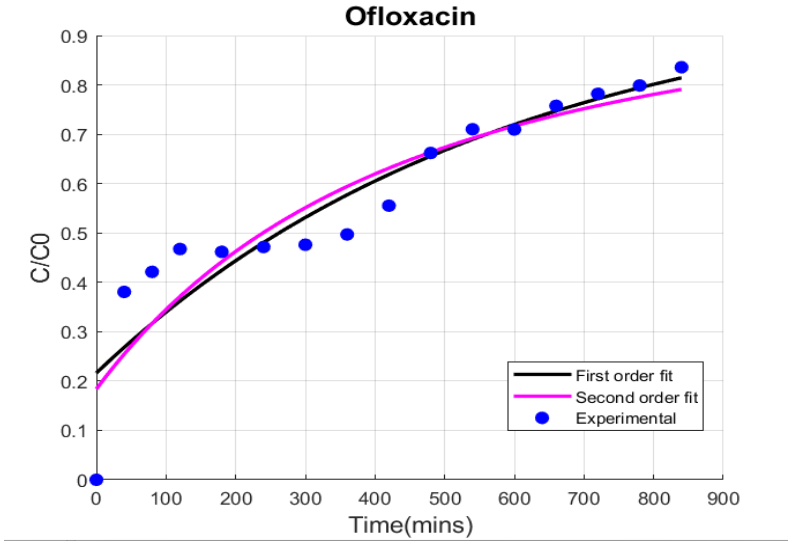

	D_a	n_{stoic}	B.T. Time
1st order	0.0383	18.483	900
2nd order	0.026	28.835	981

	D_a	n_{stoic}	B.T. Time
1st order	0.047	16.767	797
2nd order	0.0327	25.766	878

50 ppm

Fig. 6.6 Predicted breakthrough curves using first-order and second-order kinetic models with respect to experimental data collected with decreasing inlet concentrations: (a) 200ppm, (b) 100ppm, (c) 50ppm at a bed height =5cm and inflow rate =0.90ml/min.

Table 6.2 Breakthrough times in minutes, for the dynamic study of removal of (a) ciprofloxacin and (b) ofloxacin by raw sewage sludge at various flow rates, bed height and initial concentrations.

Parameters	Ciprofloxacin			Ofloxacin		
	Experimental datapoint closest to breakthrough	1st order model prediction	2nd order model prediction	Experimental datapoint closest to breakthrough	1st order model prediction	2nd order model prediction
Bed Height↓						
7 cm	780	845	898	540	456	393
5 cm	630	669	785	430	309	321
3 cm	360	323	357	150	132	133
Flow Rate↓						
2.14 ml/min	300	251	286	80	81	84
0.90 ml/min	630	669	785	430	309	321
0.67 ml/min	Didn't reach breakthrough	1305	1616	540	556	648
Initial Concentration↓						
200ppm	300	269	268	180	178	193
100ppm	630	669	785	430	309	321
50ppm	840	900	981	780	797	878

In general, the breakthrough time (BT) increases with an increase in bed height, a decrease in flow rate and a decrease in inlet concentration. Also, the breakthrough time for ciprofloxacin is higher than the same for ofloxacin indicating a slower adsorption of ciprofloxacin as compared to adsorption of ofloxacin. On a competitive time-scale, ofloxacin occupies the pores faster and ciprofloxacin largely forms surface complexes through hydrogen bonding. In most of the cases the predicted breakthrough times using first-order and second-order convective-diffusion models are quite close to the observed breakthrough times (refer Table 6.2), thereby validating the effectiveness of the adopted method. Minor differences are primarily due to the differences in the rates of depletion for 1st and 2nd order pseudo-kinetics.

In cases, where there is insufficiency of data points, that is, in cases where data is recorded to time lesser than or just up to the breakthrough time, there are deviations from the actual experimental breakthrough times (observed). Best predictions are

achieved when there are a few more datapoints recorded even after the bed has achieved breakthrough. Additionally, the models are still capable of predicting breakthrough times even if the bed did not actually reach breakthrough during the total span of experimentation.

Table 6.3 Variations in the ratio of first-order and second-order Damköhler numbers of ciprofloxacin to ofloxacin with changes in flow rate and inlet concentration.

Parameter	$D_{a_{1_{Cipro}}} : D_{a_{1_{Oflox}}}$	$D_{a_{2_{Cipro}}} : D_{a_{2_{Oflox}}}$
Flow Rate↓		
2.14	1:3.076	1:3.434
0.9	1:2.114	1:2.452
0.67	1:2.569	1:2.511
Initial Concentration↓		
200	1:1.578	1:1.429
100	1:2.114	1:2.452
50	1:1.219	1:1.238

In all the experiments, $D_a s << 1$ for both CIP and OFLX. It indicates a faster diffusion process with respect to the rate of pseudo-reaction. Diffusion thus reaches an 'equilibrium' well before the reaction achieves pseudo chemical equilibrium. Ratios of the Damköhler numbers, meant to represent the first-order and second-order convective-diffusion models for ciprofloxacin to ofloxacin is < 1 (refer to Table 6.3). It indicates a faster rate of pseudo-reaction for ofloxacin as compared to ciprofloxacin. Additionally, the values of pseudo rate constants for ofloxacin are observed to be greater than the same for ciprofloxacin in case of both the models (see Table 6.1).

Chapter 7:-

Transient behavior of a packed column: *Scale-Up using Semi-Empirical Approach*

7.1 Background

Fluoroquinolones (FQs) belong to a class of synthetic antibiotics considered to have broad-spectrum anti-bacterial effects against Gram-positive as well as Gram-negative bacteria (Rusu et al. 2014). These have been tested in vitro against SARS-CoV-2 and molecular docking studies prescribed ciprofloxacin, enoxacin, and moxifloxacin as effective inhibitors of SARS-CoV-2 (Alaaeldin *et al.* 2022). Specific fluoroquinolones have been tested for their potential capacity to bind to the protease of SARS-CoV-2, thereby blocking subsequent replication (Karampela and Dalamaga 2020). Ofloxacin is very potent in the treatment of gastrointestinal disorders, which originate as a less frequent symptom in patients suffering from Covid-19.

Large-scale use of the FQs during Covid-19 pandemic has increased the quantity of FQs being discharged into inland surface waterbodies (Comber *et al.* 2020).

A packed column with suitable adsorbent can be exercised in a continuous process for elimination of the FQs from large quantities of wastewater at the industrial as well as municipal levels. An effective design of a packed column requires prediction of the concentration-time profile for each of the adsorbates, FQs in this case, present in the effluent. The maximum adsorption capacity of a specific adsorbent (with the packed column being operated under continuous mode), needs to be evaluated adequately for developing an effective scale-up correlation (Malkoc and Nuhoglu 2006).

Semi empirical models are simplified models used to investigate the scale of the laboratory column in order to make an effective design for pilot scale columns (Sharma and Forster 1996; Sarin *et al.* 2006). The procedure is carried out by evaluating some of the design parameters, which can capably describe the performance and receptivity of the adsorbent in a dynamic process. The parameters of the representative breakthrough curves (theoretical) are estimated using linear/non-linear least square techniques. Afterwards, the predicted breakthrough curves, so obtained, are compared with the experimental breakthrough curves. The design of a packed column, operated under various flow rates, influent concentrations and bed heights, requires a comparison between the service times obtained experimentally with theoretically predicted values obtained from the parameterised semi-empirical models. Various semi-empirical mathematical models are well known for the design and scale-up of a packed adsorption column. Most familiar models amidst them are BDST, Thomas and Yoon-Nelson models. These models are assessed using experimental data for certain parameters representative of the dynamics of the packed bed, like breakthrough and bed exhaustion time, influent concentration at time t_0 (C_0), effluent concentration at time t (C_t), linear flow rate, bed height, service time etc.

The specific objective of this particular study is the evaluation of a packed column by modelling its breakthrough performance using Yoon-Nelson approach. Effects of varying bed heights, concentrations and flow rates of influent wastewater are specifically examined to obtain the theoretical breakthrough curves for the adsorption column.

7.2 Materials and Methods

7.2.1 Materials

Synthetic wastewaters are prepared by dissolving ciprofloxacin and ofloxacin in ultrapure water for conducting the experiments. CIFRAN-500 (Make: Ranbaxy Laboratories Ltd., India) and OFLOMAC-200 (Make: Macleods Pharmaceuticals Ltd., India) are used as the representative sources for CIP and OFLX respectively for the dynamic study. In order to generate the standard curves for pure component CIP and OFLX, standard analytical grade Ciprofloxacin [Make: Sigma–Aldrich, India ; CAS No: 86483-48-9; Grade: Analytical] and standard analytical grade Ofloxacin [Make: Sigma–Aldrich, India ; CAS No: 82419-36-1; Grade: Analytical] are used respectively. The mobile phase used during HPLC-based analysis consists of Acetonitrile [Make: Sigma–Aldrich, India; CAS No.: 75-05-8; Grade: HPLC grade], ultra-pure water [Make: Sigma–Aldrich, India; CAS No.: 7732-18-5; Grade: HPLC grade], Tri-ethylamine [Make: Sigma–Aldrich, India; CAS No.: 121-44-8; Grade: HPLC grade] and phosphoric acid [Make: Sigma–Aldrich, India; CAS No.: 7664-38-2; Grade: HPLC grade].

7.2.2 Sampling and Processing of raw sewage sludge

Raw sewage sludge [RSS] is collected from the Sewage Treatment Plant (STP), managed by Kamarhati Municipality, North 24 Parganas, West Bengal, India. The

protocol for drying and preparing the RSS to be used in a packed bed column is described in detail in *section 6.2.1* (Chapter 6). A list of chemicals used for the study is given in *section 5.2.2* of Chapter 5. The analytical protocol which is followed to analyse ciprofloxacin and ofloxacin in combination is elaborated in Chapter 5 (see *section 5.2.3*).

7.2.3 Operational Conditions

Various operating parameters for the breakthrough curve analysis are bed depths (3, 5 and 7 cm), influent concentrations (50, 100 and 200 ppm) and flow rates (0.67, 0.90 and 2.14 ml/min). The wastewater is fed and treated till the ratio C_t/C_0 becomes equal to 0.85. The experiments are conducted at different bed heights, flow rates and feed concentrations without changing the random arrangement of packing of the column. The treated wastewater is collected at the outlet at definite intervals of time and then the same is analysed for ciprofloxacin and ofloxacin concentrations, using a standardised analytical technique. Changes in concentrations of ciprofloxacin and ofloxacin at a definite interval of time are analysed by High-Performance Liquid Chromatographic (HPLC) based method (refer to *section 5.2.3* of Chapter 5).

7.2.4 Experimental Design: Breakthrough curve and breakthrough point

In order to carry out the experiments for simultaneous adsorption of ciprofloxacin and ofloxacin continuously from artificially synthesized waste water, a glass column (internal diameter: 25 mm and length: 15 cm) is used. The other accessories of the treatment process are a 1000 ml capacity borosilicate glass beaker used as a storage tank, a pumping system including a peristaltic pump and a distribution arrangement (refer to Fig. 6.1). The column is packed with a known quantity of raw sewage sludge and glass beads (internal diameter range: 0.6 – 0.8 mm) in a ratio of 1:5 in order to get

the desired bed depth of the column and to enhance the porosity of the packed bed. At the bottom portion of the column, a globule of glass wool is provided in order to support the packing of the fixed bed. On the uppermost surface of the packed material, a thin layer of cotton is placed in order to maintain a uniform distribution of influent wastewater throughout the packed bed of the column. The inlet of the column is so equipped that entry effect is minimized to ensure a sustained uniform flow across the cross section of the packed bed. The glass wool at the bottom of the packed column resists the washout of adsorbent material from being eliminated along with the outgoing stream of treated wastewater. Synthetic wastewater containing ciprofloxacin and ofloxacin, is allowed to pass through the fixed bed column in a down-flow mode. Before the experiment the bed is rinsed with di-mineralized water and left overnight for having a closely packed arrangement. A peristaltic pump (Make: Watson Marlow; Model: 101U/R) is used to control the inflow rate of the wastewater.

7.3 Theory

7.3.1 BDST Model

In 1920, Adams and Bohart (Bohart and Adams 1920) first proposed the idea of bed depth service time model, and it is being considered to be the simplest semi-empirical model in the packed bed study that permits the most rapid determination of the adsorbent bed performance (McKay and Bino 1990). Working principle of this model is based on theory of surface reaction rate, i.e. the adsorption rate is proportional to the fraction of remaining adsorption capacity of the adsorbent bed (Muraleedharan et al. 1994; Lehmann et al. 2001). This model also illustrates the correlation between the bed height or depth of the packed bed column and the service time (Kratochvil and Volesky 2000; Vijayaraghavan and Prabu 2006). The model is validated based on the

assumption that external mass transfer resistance and intra-particle diffusion both are negligible and the adsorption kinetics is mainly controlled by the surface chemical interaction between the solute and the adsorbent, rare in real systems (Ayoob et al. 2007). The inherent assumption of the BDST model is the symmetry of the breakthrough curves and the same is not practically possible to achieve. Here lies the major limitation of this model (Zulfadhly et al. 2001). Although the BDST model suffers from certain limitations, it is practised worldwide. The model is favourable only in describing the initial part of the breakthrough curve i.e. up to the breakthrough point or saturation points (up to 10-50% approximately). BDST model is not suitable for analysing systems receiving longer periods of time to reach equilibrium, as the solid-phase loading of the column bed does not bear a certain relationship with time at various bed heights of the column (Ko et al. 2003). In order to eliminate such limitation a constant bed capacity of the column throughout the operation is considered for the original BDST model. This proposition may not be true in certain instances.

The original expression of BDST model is as follows:

$$ln\left(\frac{C_0}{C_t} - 1\right) = ln[exp^{KZN_0/v} - 1] - KC_0t \quad (7.1)$$

where,

C_0 = Initial concentration of the solute in influent (mg/L)

C_t = Solute concentration in effluent at any time (mg/L)

K = Adsorption rate constant or BDST model constant (L/mg h)

Z = Bed height or depth (cm)

N_0 = Adsorption capacity (mg/L)

v = Linear flow velocity (cm/h)

t = Service time (h)

Using the BDST model certain characteristic parameters including adsorption rate constant (K), and adsorption capacity (N_0) of the column bed, can be estimated. Rearranging Eq. (7.1) into a linear form that produces an expression of service time (t), proposed by Hutchins (Hutchins RA. 1973) as:

$$t = \frac{ZN_0}{C_0 v} - \frac{1}{KC_0} ln\left(\frac{C_0}{C_t} - 1\right) \tag{7.2}$$

When, $\exp^{KN_0 Z/v} >> 1$, this model is applicable for both the breakthrough point[1] and exhausted point[2] of the breakthrough curve. If the service time is t_b and exhausted time is t_x at the breakthrough point with the corresponding effluent concentrations being C_b and C_x respectively, then the equation (7.2) may be written as:

$$t_b = \frac{ZN_0}{C_0 v} - \frac{1}{KC_0} ln\left(\frac{C_0}{C_b} - 1\right) \tag{7.3}$$

$$t_x = \frac{ZN_0}{C_0 v} - \frac{1}{KC_0} ln\left(\frac{C_0}{C_x} - 1\right) \tag{7.4}$$

Both Eqs. (3) and (4) can be linearized as:

$$t = aZ - b \tag{7.5}$$

with slope = $a = \frac{N_0}{C_0 v}$ and intercept = $b = \frac{1}{KC_0} ln\left(\frac{C_0}{C_x} - 1\right)$

Now plotting t vs Z for a fixed flow rate, we get a straight line. From the slope and intercept of this straight line the adsorption capacity (N_0) and adsorption rate constant

[1] A breakthrough point is the time at which a packed bed is fully utilized and it has low adsorption capacity towards the influent wastewater and the effluent water has a sudden increase in concentration than the initial.

[2] A point on the breakthrough curve at which solute concentration in the outlet becomes almost equal to the influent concentration.

(*K*) are obtained respectively. Different flow rates give different straight lines with different values of N_0 and *K*. Effect of flow rates upon the performance of the column bed can thus be studied using BDST model. Validity of the linearized form of the BDST model for a particular dynamic system can be established by the higher values of regression coefficients (Kobya 2004). Utilising different values of N_0 and *K* (from graph), the theoretical values of service time (*t*) for a specific bed height (*Z*) can be obtained from Eq. (7.2) and these values can be fitted as predicted data along with the experimental data points over a series of flow rates.

A minimum bed depth that is required in a column filled with adsorbent for a specific breakthrough concentration (C_b) is known as the critical bed depth (Z_0) (Sankararamakrishnan et al. 2008). Z_0 is the theoretical bed depth of adsorbent column by which it can be confirmed that the solute concentration in the effluent does not surpass the breakthrough concentration (C_b) at time $t=0$. Hence Z_0 can be calculated by putting $t=0$ in Eq. (7.2) and solving for it in terms of Z_0, we get:

$$Z_0 = \frac{v}{KN_0} \ln\left(\frac{C_0}{C_b} - 1\right) \tag{7.6}$$

Another efficacy of the BDST model is that we can compute the minimum bed height essential for a specific influent concentration and a specific flow rate. However, critical bed depth varies with *K* (Vijayaraghavan et al. 2005). With a high value of *K*, a short bed can avoid breakthrough but as the value of *K* decreases gradually, longer bed is essential to eliminate breakthrough. At 50% of the breakthrough curve, the effluent solute concentration C_t is just half of the influent solute concentration C_0, i.e. $C_t = \frac{1}{2} C_0$, and Eq. (7.2) can be written as,

$$t_{50} = \frac{ZN_0}{vC_0} \tag{7.7}$$

where, t_{50} denotes the service time at 50% of the breakthrough curve (Netpradit et al. 2004). Eq. (7.7) expresses the straight line with no intercept. If the plot of t_{50} against Z is a straight line passing through the origin, an inference can be drawn that the adsorption data-set fits to the BDST model well.

An experiment with one flow rate can be consistently scaled up for the other flow rates without carrying out further experiments (Othman et al. 2001; Goel et al. 2005). From the known slope of a straight line already predicted, the slope of the straight line of t versus Z plot with a new flow rate can be obtained. If the previous flow rate is q with slope a, then the new slope a_1 with the new flow rate q_1 is obtained as follows,

$$a_1 = a\left(\frac{q}{q_1}\right) \tag{7.8}$$

In this case the intercept of the straight line (b) is not adjusted as this is dependent only on the influent solute concentration (C_0) but not affected by changes in flow rates.

Designing columns with other influent solute concentrations can be obtained by one influent solute concentration using the BDST model (Kumar and Chakraborty 2009). The slope and intercept of the known system are used to obtain the new values of the slope and the intercept with changes in influent concentrations. If a_1 and b_1 are the slope and intercept of a known system with the influent concentration C_1, then the new slope a_2 and new intercept b_2 for the influent concentration C_2 can be calculated by the following equations –

$$a_2 = a_1\left(\frac{C_1}{C_2}\right) \tag{7.9}$$

$$b_2 = b_1\left(\frac{C_1}{C_2}\right)\left[\frac{ln\left(\frac{C_2}{C_F}-1\right)}{ln\left(\frac{C_1}{C_B}-1\right)}\right] \tag{7.10}$$

where,

C_F = effluent concentration with influent concentration C_2

C_B = effluent concentration with influent concentration C_1

7.3.2 Thomas Model

Dynamics and performance of an adsorption column is also described by the Thomas model (Thomas 1944). This model has been derived from the second-order reaction kinetics (the rate determining step) and is followed in any adsorption process (Suksabye et al. 2008). This model assumes Langmuir's pseudo-kinetics of adsorption-desorption ignoring resistances from both intra-particle mass transfer and external fluid film and also assumes that there is no axial dispersion in the fixed bed (de Franco et al. 2017). Experimental values can be fitted to the Thomas Model to find the maximum adsorption capacity of the packed bed column and the kinetic rate constant (Fu and Viraraghavan 2004; Malkoc et al. 2006).

The Thomas model is expressed as:

$$\frac{C_t}{C_0} = \frac{1}{1+exp\left[\left(\frac{k_{Th}}{Q}\right)\left(Mq_0 - C_0V_{eff}\right)\right]} \tag{7.11}$$

where,

k_{Th} = Thomas rate constant (ml/min/gm)

Q = Flow rate (ml/min)

q_0 = Maximum adsorption capacity of the adsorbent bed (mg/g)

M = Mass of the adsorbent (g)

V_{eff} = Volume of the effluent (ml)

The linearized form of Eq. (11) is:

$$ln\left(\frac{C_0}{C_t}-1\right) = \frac{k_{Th}q_0M}{Q} - \frac{k_{Th}C_0V_{eff}}{Q} \quad (7.12)$$

As discussed before, the service time, $t=V_{eff}/Q$. So, Eq. (12) can be expressed as,

$$ln\left(\frac{C_0}{C_t}-1\right) = \frac{k_{Th}q_0M}{Q} - k_{Th}C_0t \quad (7.13)$$

By plotting $ln(C_0/C_t - 1)$ against t, a straight line is obtained. Thomas rate constant (k_{Th}) and the highest adsorption per gm of adsorbent (q_0) can be calculated from the intercept and slope of the straight line, respectively. Predicted results are compared with the experimental findings and the nature of breakthrough curves can be projected by the fitment of the curve. Primary disadvantage of this model is that it has been derived from second-order reversible reaction kinetics where physical adsorption does not follow chemical interactions always, rather controlled mainly by the inter phase mass transfer (Rao and Viraraghavan 2002). Therefore, when this model is applied for a process governed by physical adsorption, it generates some error. Instead, the Thomas Model may validate the cases well where chemisorption plays a significant role.

7.3.3 Yoon-Nelson Model

This model is usually expressed in the following linear form:

$$ln\left(\frac{C_0}{C}-1\right) = k_{YN}\,\tau - k_{YN}\,t \quad (7.14)$$

where, k_{YN} = Yoon-Nelson rate coefficient and τ = time required for 50% breakthrough. Eq. (7.14) has been derived by Yoon and Nelson (YOON and NELSON 1984) independently without claiming origins in the BDST model treatment. It is simple to illustrate that the Yoon-Nelson equation can be obtained from the simplified BDST model for $\exp^{KN_0Z/v} >> 1$, as given by the following equation:

$$ln\left(\frac{C_0}{C_t}-1\right) = \frac{KZN_0}{v} - KC_0\,t \tag{7.15}$$

At $t=\tau$ we have $C/C_0=0.5$, the simplified BDST model given by Eq.(7.15) may then be expressed as:

$$0 = \frac{KZN_0}{v} - KC_0\,\tau \tag{7.16}$$

Rearranging Eq. (7.16) we have,

$$\frac{ZN_0}{v} = C_0\,\tau \tag{7.17}$$

Substituting Eq. (7.17) in Eq. (7.15) we get:

$$ln\left(\frac{C_0}{C_t}-1\right) = KC_0\,\tau - KC_0\,t \tag{7.18}$$

If we consider, $KC_0 = k_{YN}$, then Eq. (7.18) becomes -

$$\ln\left(\frac{C_0}{C_t}-1\right) = k_{YN}\,\tau - k_{YN}\,t \tag{7.19}$$

Eq. (7.19) is the same as Eq. (7.14), the common expression of the Yoon-Nelson model. By plotting, $\ln\left(\frac{C_0}{C_t}-1\right)$ against time t, we get straight line with a negative slope. From the plots we can obtain k_{YN} and τ respectively.

7.4 Results and Discussion

During adsorption in a fixed bed, a concentration gradient between the adsorbate and the adsorbent is always available until the time the bed gets saturated since the adsorbate is in contact with fresh adsorbent at all times (Huang et al. 2002; Aksu et al. 2007). Fixed bed adsorption systems can be best designed by modelling the breakthrough curves for a given adsorbate-adsorbent system along with computation of breakthrough times and bed volumes for the same to understand the performance

of the designed column (Unuabonah et al. 2010). It has been observed experimentally that the shape of the breakthrough curve is heavily influenced by the design parameter: bed depth and the operating parameters: inflow rate and inlet concentration of adsorbate solution. Experimental data for studying the impact of the design and operating parameters on the adsorption performance of the bed are recorded until breakthrough time is reached.

7.4.1 Effect of bed height

The effect of bed depth on the shape of the breakthrough curve is studied at an inflow rate of adsorbate solution of 0.90 ml/min and inlet concentration of 100ppm modelled antibiotic solution at 3 different bed heights of 3cm, 5cm and 7cm. The breakthrough curve for each run is plotted using the values of the ratios of recorded effluent concentration to the influent concentration against service time of the bed $(C/C_0 \ vs \ t)$. From the obtained breakthrough curves for varying bed heights for both ciprofloxacin and ofloxacin as shown in Fig. 7.1, it can be observed that the shape and gradient of each curve changes with variation in bed depth. Although maximum adsorption of ciprofloxacin and ofloxacin is seen to occur at the beginning of the bed, the quantum of removal reduces with time. It can be concluded that the higher the bed depth, it will be saturated later since it has more adsorbent materials present. Thus, an adsorption column with greater height has more adsorption sites and a larger contact time between the adsorbate and the adsorbent, hence, more adsorption capacity with a greater breakthrough time.

7.4.2 Effect of inflow rate

The effect of inflow rate on the performance of the packed bed is studied at a bed height of 5cm and inlet concentration of the adsorbate solution of 100ppm for 3

different inflow rates: 2.14ml/min, 0.90ml/min and 0.67ml/min. It can be noted from Fig. 7.2, that as inflow rate decreases, the breakthrough curve becomes less steep and the breakthrough time increases. This is explained by the fact that at lesser flow rate, the residence time is higher, causing the removal efficiency of the packed bed to be on the higher side. A higher residence time ensures availability of sufficient time for the adsorbate to bond with the adsorbent, so a lesser flow rate is imperative to efficient removal of Ciprofloxacin and Ofloxacin. At higher flowrates, the mass transfer rate is high causing the bed to achieve breakthrough sooner.

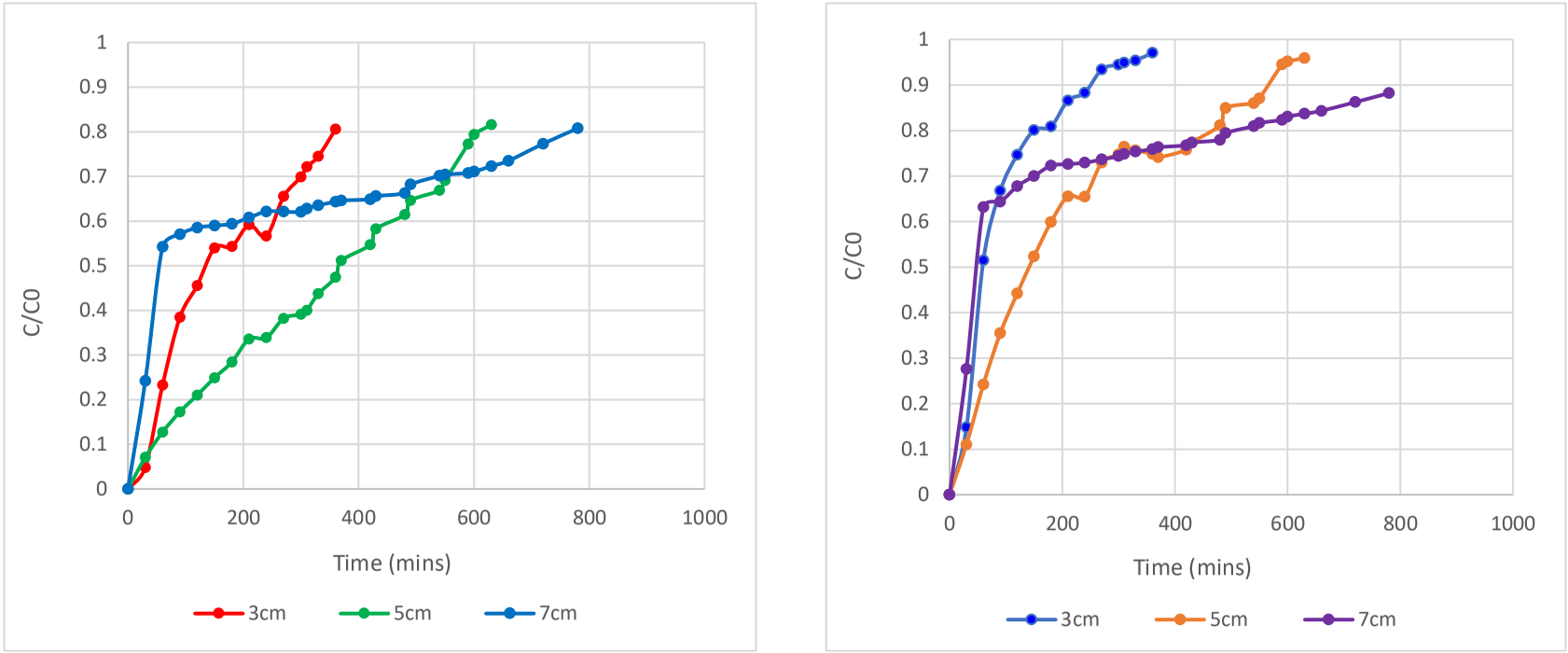

Fig. 7.1 C/C_0 values vs. time at varying bed heights [3 cm, 5 cm and 7 cm] with 0.90ml/min inflow rate and 100ppm inlet concentration for (a) Ciprofloxacin (b) Ofloxacin.

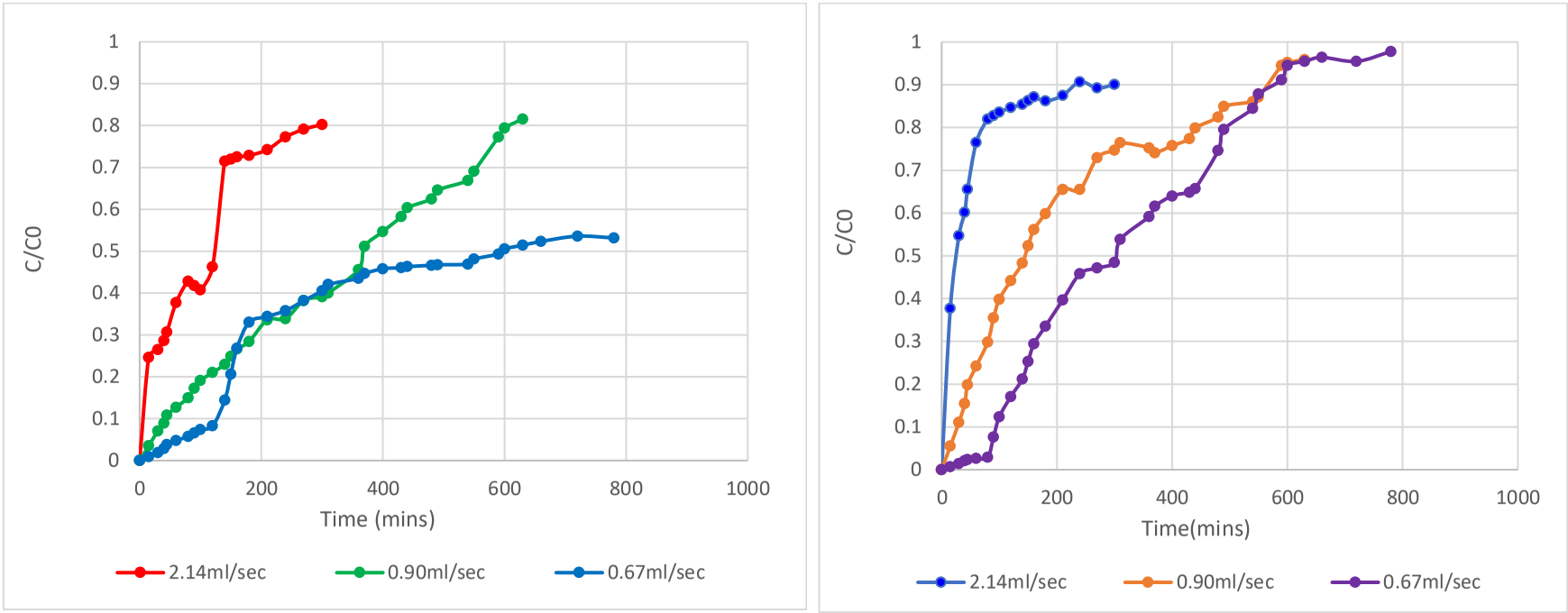

(a) (b)

Fig. 7.2 *C/C_0* values vs. time at varying inflow rates [2.14 ml/min, 0.9 ml/min and 0.67 ml/min] with 5cm bed height and 100ppm inlet concentration for (a) Ciprofloxacin (b) Ofloxacin.

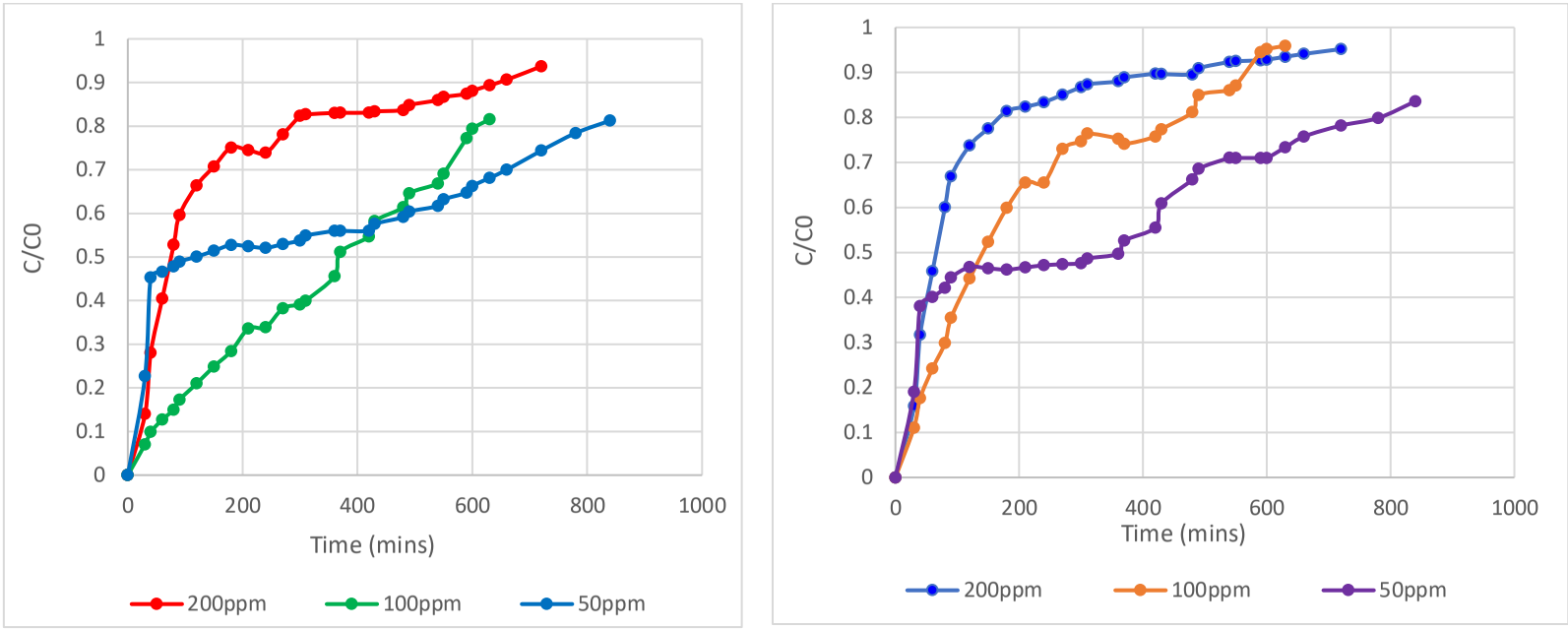

(a) (b)

Fig. 7.3 *C/C₀* values vs. time at varying inlet concentrations [200 ppm, 100 ppm, 50 ppm] with 5 cm bed height and 0.90ml/min flow rate for (a) Ciprofloxacin (b) Ofloxacin.

7.4.3 Effect of inlet concentration

The effect of inlet adsorbate solution concentration on the shape of the breakthrough curve is studied by taking a bed height of 5cm and keeping the inflow rate at 0.90ml/sec and varying the inlet concentrations at 200ppm, 100ppm and 50ppm. The modelled breakthrough curves from Fig. 7.3 indicate that breakthrough time increases with decreasing influent concentration as the same adsorbent bed is exposed to a lesser amount of adsorbate when exposed to the same amount of model antibiotic solution. From the iconic works of K. H. Chu (Chu 2020), it is observed that despite different assumptions for derivations of all the existing semi empirical models, such as the BDST model, the Thomas model and the Yoon–Nelson model, they all can be linearized into a simple format.

Linearized BDST Model Equation: $ln\left(\frac{C_0}{C}-1\right)=\frac{k_{BA}N_0L}{u}-k_{BA}C_0t$ (7.20)

Linearized Thomas Model: $ln\left(\frac{C_0}{C}-1\right)=\frac{k_Tq_0M}{Q}-k_TC_0t$ (7.21)

Linearized Yoon-Nelson Model: $ln\left(\frac{C_0}{C}-1\right)=k_{YN}\tau-k_{YN}t$ (7.22)

When $ln\left(\frac{C_0}{C}-1\right)$ vs t is plotted, we get the same value of slope and intercept for all the 3 cases since $ln\left(\frac{C_0}{C}-1\right)$ and t are independent of the models used. The slopes and intercepts obtained from the regression analysis helps to find very important details about the adsorption process from the following equations:

$$k_{BA}=k_T=\frac{slope}{C_0} \quad (7.23)$$

$$k_{YN}=slope \quad (7.24)$$

The values of q_0, N_0 and τ obtained from each of the 3 models can be estimated using the values of the intercept calculated.

For BDST model: $N_0 = \frac{intercept * u}{k_{BA} L}$ (7.25)

For the Thomas model: $q_0 = \frac{intercept * Q}{k_T M}$ (7.26)

For Yoon-Nelson model: $\tau = \frac{intercept}{k_{YN}}$ (7.27)

So, the sigmoidal curve for all the 3 semi-empirical models can be generalised as the following equation of breakthrough curve:

$$\frac{C}{C_0} = \frac{1}{1+\exp\left(intercept-(slope*t)\right)} \quad (7.28)$$

In this study, since it could be proved that all the well-known semi-empirical models that exist, can essentially be represented by one generalized equation, the breakthrough curves are generated by fitting the experimental data-sets into the Yoon-Nelson model. Estimated model parameters are compiled in Table 7.1 as given below.

Table 7.1 Estimated model parameters for BDST Model, Thomas Model and Yoon-Nelson Model for both Ciprofloxacin and Ofloxacin.

Fixed Parameters	Variable Parameters	BDST Model		Thomas Model		Yoon-Nelson Model		R^2	Breakthrough time	Bed Exhaustion time
		k_{BA}	N_0	k_T	q_0	k_{YN}	τ			
Ciprofloxacin										
Q=0.90ml/min c_{in} = 100ppm	Z=3cm	96.3	0.001185	96.3	0.00138	0.0096	193.946	0.9020	50.9091	338.1818
	Z=5cm	57.7	0.001366	57.7	0.00698	0.0058	372.4957	0.9766	133.6364	610.9091
	Z=7cm	19.8	0.000241	19.8	0.00838	0.0020	91.8737	0.7209	18	780
Z=5cm c_{in} = 100ppm	Q=2.14ml/min	98	0.000984	98	0.00604	0.0098	112.8571	0.8830	12.5	254.5455
	Q=0.90ml/min	57.7	0.001366	57.7	0.00838	0.0058	372.4957	0.9766	133.6364	610.9091
	Q=0.67ml/min	41	0.001562	41	0.00958	0.0041	572.0732	0.8107	236.3636	780
Z=5cm Q=0.90ml/min	c_{in} = 200ppm	19.2	0.000154	19.2	0.00094	0.0038	20.9375	0.6856	34.286	385.4545
	c_{in} = 100ppm	57.7	0.001366	57.7	0.00838	0.0058	372.4957	0.9766	133.6364	610.9091
	c_{in} = 50ppm	37.6	0.000337	37.6	0.00207	0.0019	183.5638	0.8149	26.0.87	840
Ofloxacin										
Q=0.90ml/min c_{in} = 100ppm	Z=3cm	127.9	0.000442	127.9	0.001031	0.0128	72.2596	0.8403	34	181
	Z=5cm	66.5	0.000675	66.5	0.0026	0.0067	184.1955	0.8630	57	394.5455
	Z=7cm	24.4	0.00018	24.4	0.00414	0.0024	68.7295	0.6065	21.4	496.3636
Z=5cm c_{in} = 100ppm	Q=2.14ml/min	75	0.00048	75	0.002923	0.0075	54.6400	0.5383	15.385	130.3030
	Q=0.90ml/min	66.5	0.000675	66.5	0.00414	0.0067	184.1955	0.8630	57	394.5455
	Q=0.67ml/min	94	0.00094	94	0.00577	0.0094	344.2660	0.9150	196.9697	488.4848
Z=5cm Q=0.90ml/min	c_{in} = 200ppm	20.8	0.00041	20.8	0.00253	0.0042	56.2260	0.5884	25.237	276.3636
	c_{in} = 100ppm	66.5	0.000675	66.5	0.00414	0.0067	184.1955	0.8630	57	394.5455
	c_{in} = 50ppm	52.4	0.00046	52.4	0.00282	0.0026	251.0305	0.8661	21.053	780.6061

It can be observed from Table 7.1, that most of the correlation coefficients for the plots are more than 0.81. The Yoon-Nelson constant, the Thomas constant and the Bohart-Adams constant can be seen to decrease with an increase in bed height. By calculating the parameters for the Thomas model, it may be noted that the maximum amount adsorbed increased from 0.00138g/g to 0.00838g/g for Ciprofloxacin while the same increased from 0.001031g/g to 0.0414g/g in case of Ofloxacin. The Yoon-Nelson model fits quite well for both of ciprofloxacin and ofloxacin with increasing bed height [refer Fig. 7.4]. The Yoon-Nelson Model gives an idea of the time where 50% breakthrough has taken place and it is seen to increase with increase in bed height.

For decreasing flow rates, the Yoon-Nelson constant, the Thomas constant and the Bohart-Adams constant decreased for Ciprofloxacin and increased for Ofloxacin. The calculations using Thomas model show that the maximum amount adsorbed increased with decrease in flow rate from 0.00604g/g to 0.00958g/g for Ciprofloxacin and 0.002923g/g to 0.00577g/g in case of Ofloxacin. The Yoon-Nelson model showed that the time when 50% breakthrough arrives increases with a decrease in flow rate for both Ciprofloxacin and Ofloxacin. The Yoon-Nelson model fits for Ciprofloxacin and Ofloxacin with decreasing inflow rate [refer Fig. 7.5].

For decreasing inlet concentration, the values of Yoon-Nelson constant, the Thomas constant and the Bohart-Adams constant decreased for both Ciprofloxacin and Ofloxacin. The Thomas model showed that the maximum amount adsorbed increased with decrease in flow rate from 0.00838g/g to 0.00207g/g for Ciprofloxacin and 0.00414g/g to 0.00282g/g in case of Ofloxacin when the inlet concentration was reduced from 100ppm to 50ppm. The Yoon-Nelson model showed that the time when 50% breakthrough takes place increases with a decrease in inlet concentration for both Ciprofloxacin and Ofloxacin. The Yoon-Nelson model fit for Ciprofloxacin and

Ofloxacin with decreasing inflow rate is shown in Fig. 7.6. The R^2 values for both Ciprofloxacin and Ofloxacin at very high concentration were <0.81 questioning the applicability of the semi empirical models at very high inlet concentrations.

It is observed, for most of the runs that at any point of time, concentration of Ciprofloxacin in the effluent solution is lower than Ofloxacin. Also, the breakthrough of Ofloxacin occurs earlier to that of Ciprofloxacin. All these indicate that Ciprofloxacin is adsorbed faster as compared to Ofloxacin. The maximum amount of Ciprofloxacin adsorbed is always greater than that of Ofloxacin adsorbed. Since the adsorption bed has fixed number of adsorption sites in a run, Ciprofloxacin wins the competition of adsorption and occupies most of the adsorption sites leaving fewer sited for adsorption of Ofloxacin to take place.

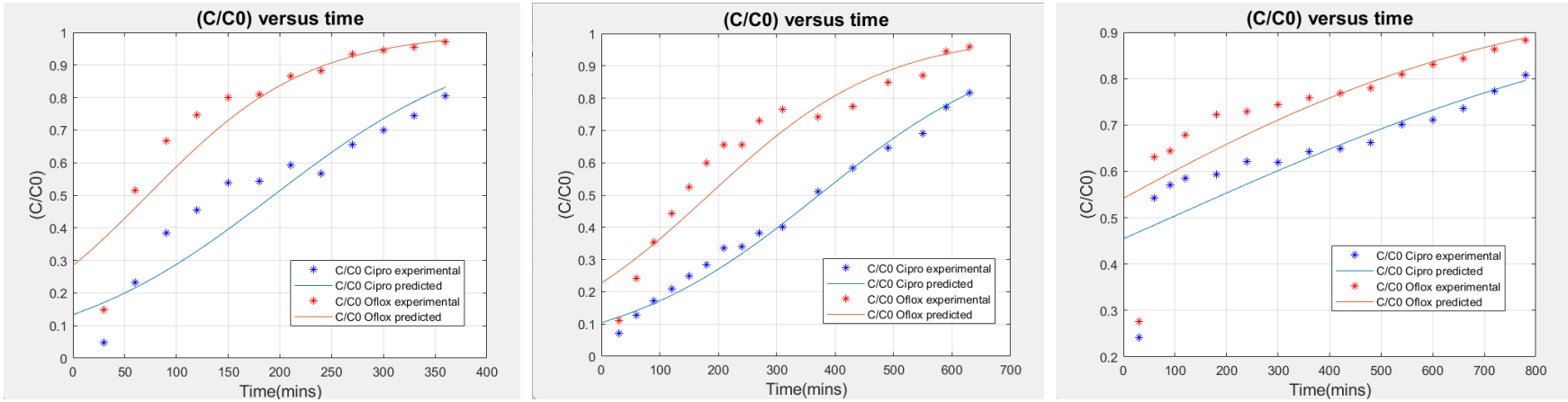

(a) (b) (c)

Fig. 7.4 Comparison of the experimental and predicted breakthrough curves for the adsorption of ciprofloxacin and ofloxacin by sewage sludge at inflow rate of 0.90ml/min and inlet concentration of 100ppm for different bed heights: (a) 3cm (b) 5cm (c) 7cm.

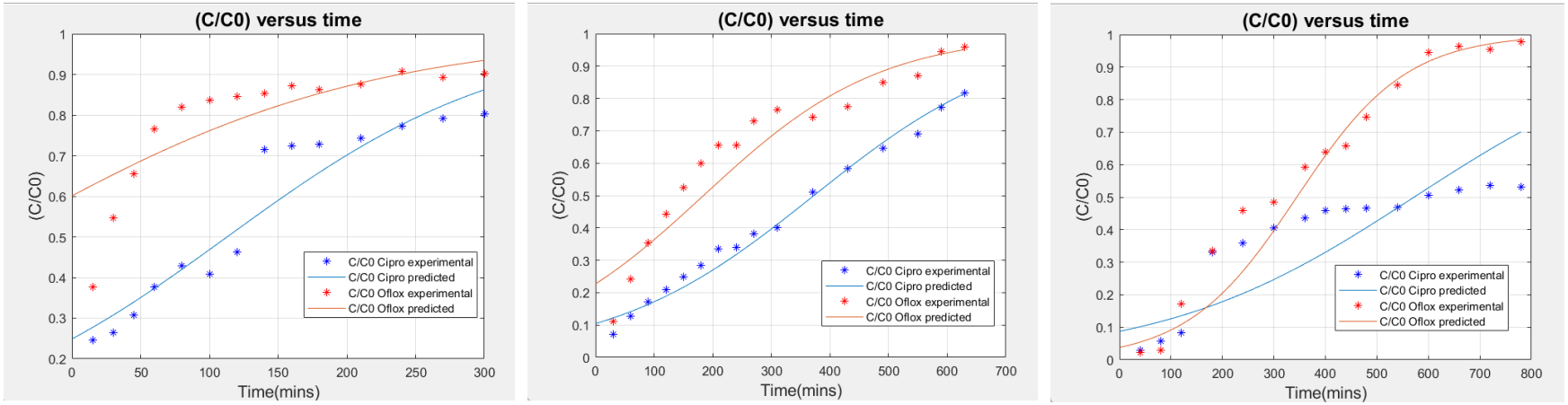

(a) (b) (c)

Fig. 7.5 Comparison of the experimental and predicted breakthrough curves for the adsorption of Ciprofloxacin and Ofloxacin by sewage sludge at 5cm bed height and 100ppm inlet concentration for different inflow rates: (a) 2.14ml/min (b) 0.90ml/min (c) 0.67ml/min.

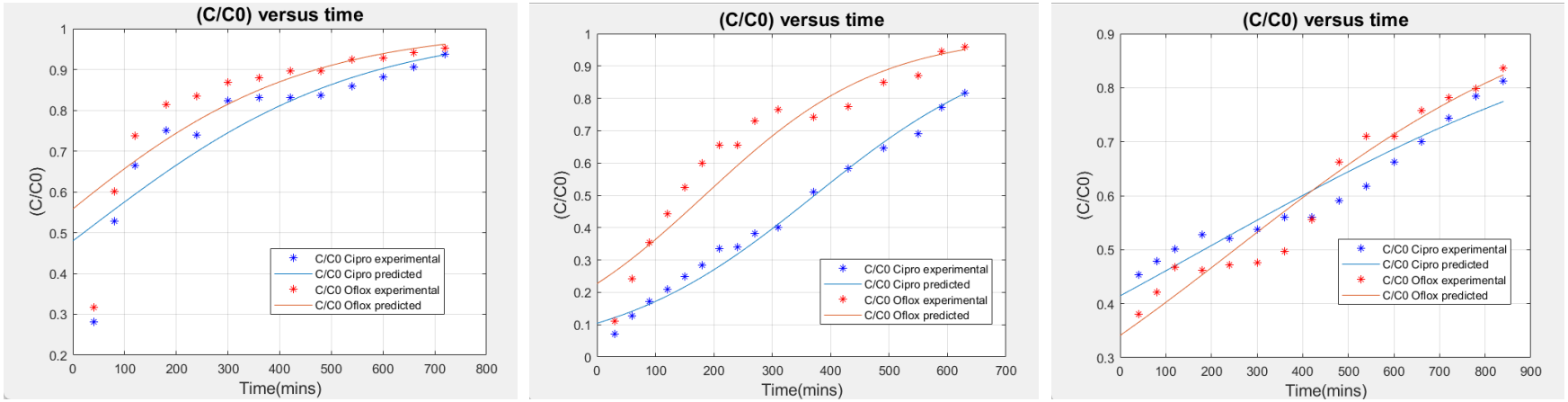

(a) (b) (c)

Fig. 7.6 Comparison of the experimental and predicted breakthrough curves for the adsorption of ciprofloxacin and ofloxacin by sewage sludge at 5cm bed height and 0.90ml/min of inflow rate for different inlet concentrations: (a) 200ppm (b) 100ppm (c) 50ppm.

Chapter 8

Novelty Elements, Concluding Remarks, and Recommendations for Future Work

8.1 Foreword

This chapter gives a brief summary of the complete research work, highlights the novelty elements and the specific conclusions with the important outcomes of each part of the research and provides recommendation for the future direction of research that should continue after this piece of research.

8.2 Novelty Elements

- ✓ Development of the modified competitive Langmuir-like model and the LeVan-Vermeulen model using fundamental hypotheses of statistical thermodynamics and application of these models for the multicomponent adsorption of ciprofloxacin and ofloxacin in combination.
- ✓ Model parameters are implicitly estimated using MATLAB and the *fsolve* MATLAB Library for each of CIP and OFLX with the fitted models indicating patterns of competitive adsorption dynamics and mechanism for each of ciprofloxacin and ofloxacin.

- ✓ Validation of the models on a relative scale, with the help of a robust scheme elucidating the probable mechanism behind the multicomponent adsorption scenarios (details are given in *section 5.7* Chapter 5 and Annex II). Adsorbent has been physically and chemically characterized using both destructive and non-destructive techniques involving FE-SEM, Zeta sizer, FT-IR, Goniometer, XPS instrument and elemental analysis using CHNS analyser.
- ✓ Development and validation of two transient forms of a convective-diffusion model, which include depletion terms (in liquid-phase), being represented by the first and second-order pseudo-kinetics. Starting with the species continuity equation, two convective-diffusion models are developed with ciprofloxacin [CIP] and ofloxacin [OFLX] being the target species, in combination
- ✓ Consideration of convective and diffusive terms of liquid phase mass transfer along with film diffusion, intra-pellet mass transfer, and *depletion of species governed by pseudo-kinetics of competitive adsorption under various dynamic conditions*. Parameters of the 1^{st} and 2^{nd} order pseudo-kinetic equations are estimated using experimental data collected under dynamic conditions and each of these convective-diffusion models is applied to carry out a thorough breakthrough analysis under varying dynamic conditions for both CIP and OFLX.
- ✓ Performance of the packed bed is analysed with respect to the effects of changes in bed height, flow rate, and initial concentration of both fluoroquinolones (CIP and OFLX), in combination, using *first-order and second-order convective diffusion models and estimated Damköhler numbers*.

- ✓ Validation of K. H. Chu's proposition: "Bohart-Adams model gives the same goodness of fit as compared to those of the Thomas and Yoon-Nelson models expectedly, as the three simplistic fixed bed models can be expressed in terms of mathematically equivalent logistic equations of population growth". [*Background story*: The century-old Bohart-Adams model is by far the best-known one which also serves as the foundation of the bed depth-service time (BDST) equation. The oversimplified Bohart-Adams equation is in effect an exponential function that predicts an exponentially increasing breakthrough value with time. As such, it is unable to fit typical breakthrough curves which are S-shaped or sigmoidal].

8.3 Concluding Remarks

8.3.1 Adsorption of Fluoroquinolones on a competitive scale: Batch equilibrium analysis

The results of this portion of the study reveal that:

- ➢ Raw sewage sludge can be utilized as a good adsorbent for the removal of pharmaceuticals from wastewater.
- ➢ Starting with the grand canonical partition function, for a system of non-interacting molecules adsorbed on a homogenous adsorbent, two important multicomponent adsorption models i.e. the modified competitive Langmuir-like model and the LeVan-Vermeulen model are developed using fundamental principles of statistical thermodynamics.
- ➢ Parameters are estimated using a routine *fsolve*, with the help of MATLAB library. The same is applied and validated for multicomponent adsorption of ciprofloxacin and ofloxacin onto sewage sludge.

- Pure components of CIP and OFLX follow the Langmuir adsorption isotherm and hence modified competitive Langmuir-like model exhibits quite good fits for both the adsorbates even though the adsorption capacities for the pure components differ from each other.

- The intra-particle diffusion model is not the rate-determining step for the adsorption of either ciprofloxacin or ofloxacin but only governs the initial mass transfer of the components onto the sludge.

- Film diffusion, assisted by the negative charge-assisted hydrogen bonding [see *'Probable Mechanism'* in *section 5.7* of Chapter 5] controls the adsorption mechanism for both ciprofloxacin and ofloxacin onto the semi-solid raw sewage sludge. The surface of RSS remains negative at the working pH of 7.8 during the entire process of adsorption, as indicated by the zeta potential. Zwitterionic forms of CIP and OFLX, at this pH, hardly aid the adsorption process through electrostatic interaction. RSS still exhibits a high adsorption capacity towards ciprofloxacin and ofloxacin in a weakly alkaline medium (pH at ~ 7.8) due to the negative charge-assisted hydrogen bonding. *Carboxylic acid groups of both FQs are hydrogen bonded to the basal oxygen atoms of the sludge layers*. The same is supplemented by the physical characterization of RSS using FT-IR and point of zero charges (see Chapter 3 and *Annex II*).

- Analyses using the intra-particle diffusion model, film diffusion model, and 2^{nd} order pseudo kinetic equation also validated the proposed mechanism of adsorption of ciprofloxacin and ofloxacin onto the RSS surface.

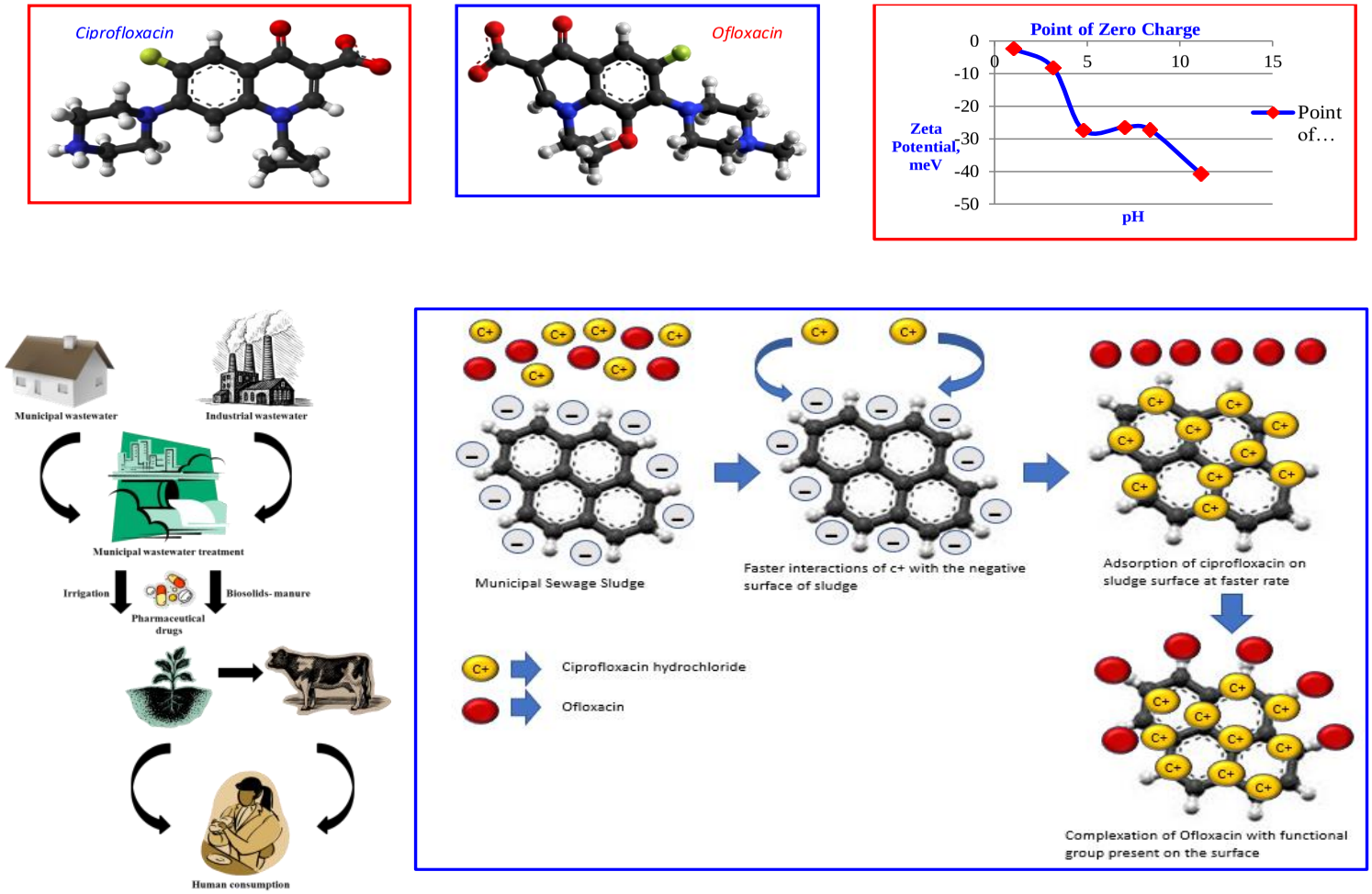

Fig. 8.1 Overview of the mechanism of competitive adsorption of ciprofloxacin and ofloxacin on the surface of RSS.

8.3.2 Transient behaviour of a packed column: Development and validation of convective diffusion models with due considerations for pseudo-kinetics driven depletion of species

The key highlights of this portion of the study are:

- The values of $n_{BT,max}$ for ciprofloxacin is always observed to be greater than the same for ofloxacin, indicating a greater amount of adsorption of ciprofloxacin from the same *n* number of bed volumes of solution passed.
- With reference to the values of SSQ shown in Table 6.1 [refer to Chapter 6], it may be inferred that multicomponent adsorption of ciprofloxacin and ofloxacin is better fitted by the convective-diffusion model including a second-order pseudo-reaction kinetics driven depletion term. The same implies chemisorption to be the primary mode of competitive adsorption for both the FQs.
- The values of Damköhler numbers (D_a*s*), evaluated from the first-order and second-order convective-diffusion models, used for both the FQs are much less than 1.
- The reaction rate is thus much less than the convective-diffusion rate and the entire adsorption process under dynamic conditions is reaction-limited[1]. This also supports chemisorption very strongly.
- D_a s increase with the increase in bed heights and decrease in flow rates, in general, irrespective of the order of the reaction and the component.

[1] *The reaction is slowest so reaction characteristics like pseudo-kinetic rate constants etc. dominate and the convective diffusion reaches equilibrium instantaneously.*

- The ratios of Damköhler numbers, for both ciprofloxacin and ofloxacin, do not change much with flow rate (refer to Table 6.3). It signifies that the pseudo-reaction rates of CIP and OFLX change in the same proportion as with the convective mass transfer.

- The ratio of the Damköhler numbers for the two FQs thus depends either on the ratio of the two pseudo rate constants (for both the components following 1^{st}-order pseudo-kinetics) or on the ratio of the product of pseudo-kinetic rate constant and maximum equilibrium adsorption (for both the FQs following pseudo-second-order kinetics).

- Under all the experimental conditions, the breakthrough time (BT) for ciprofloxacin is observed to be greater than the same for ofloxacin. It indicates that ofloxacin occupies the pores much faster than ciprofloxacin, on the basis of a competitive adsorption mechanism [refer to *section 5.7* of Chapter 5]. This is also validated by the values of the ratios of Damköhler numbers (see Table 6.3).

- Values of Damköhler numbers for both 1^{st}-order and 2^{nd}-order convective-diffusion models, in the case of adsorption of ofloxacin, are found greater than the same in the case of ciprofloxacin.

- Values of rate constants for both 1^{st}-order and 2^{nd}-order convective-diffusion models (see Table 6.1) for ofloxacin are found greater than the same for ciprofloxacin for both 1^{st}-order and 2^{nd}-order models.

- Breakthrough time (BT) increases with bed heights: BT-OFLX<BT-CIP for a particular bed height (refer to Table 6.2). This shows that OFLX wins in the competition and occupies the pores much faster than CIP.

- Experimental $\{\frac{\text{BT}-\text{CIP}}{\text{BT}-\text{OFLX}}\}\sim 1.58$, irrespective of flow rate and initial concentration, signifying that the pseudo-reaction rates of CIP and OFLX change in the same proportion with the convective mass transfer.
- Breakthrough time increases with a decrease in initial concentration (refer to Table 6.2).

8.3.3 Transient behaviour of a packed column: Scale-Up using Semi-Empirical Approach

The key findings of this portion of the study are:

- A couple of semi-empirical models are applied to analyse the transient behaviour of an adsorption column packed with raw sewage sludge in order to remove ciprofloxacin and ofloxacin from pharmaceutical wastewater.
- The three semi-empirical models from literature, the BDST model, the Thomas model and the Yoon-Nelson model are assessed and compared in order to arrive at a generalised equation representing the breakthrough curves.
- The experimental trends observed show that the breakthrough curve and hence the breakthrough times are affected by the design and the operating parameters of the setup.
- The breakthrough time increases with an increase in bed height while it decreases with an increase in inflow rate and inlet concentration of the model antibiotic solution.
- The semi-empirical models fit into the experimental data to generate the breakthrough curve for each run and ultimately help in validating the

generalised semi-empirical equation with the observed trends [*K. H. Chu's proposition*].

- The slope and intercept of the generalised equation help to calculate the maximum adsorption of adsorbate and time of 50% breakthrough based on the estimated model parameters. The R^2 values are >0.81 for most of the runs validating that the model fits with the recorded data well. The fit fails at very high values of inlet concentration of 200ppm.

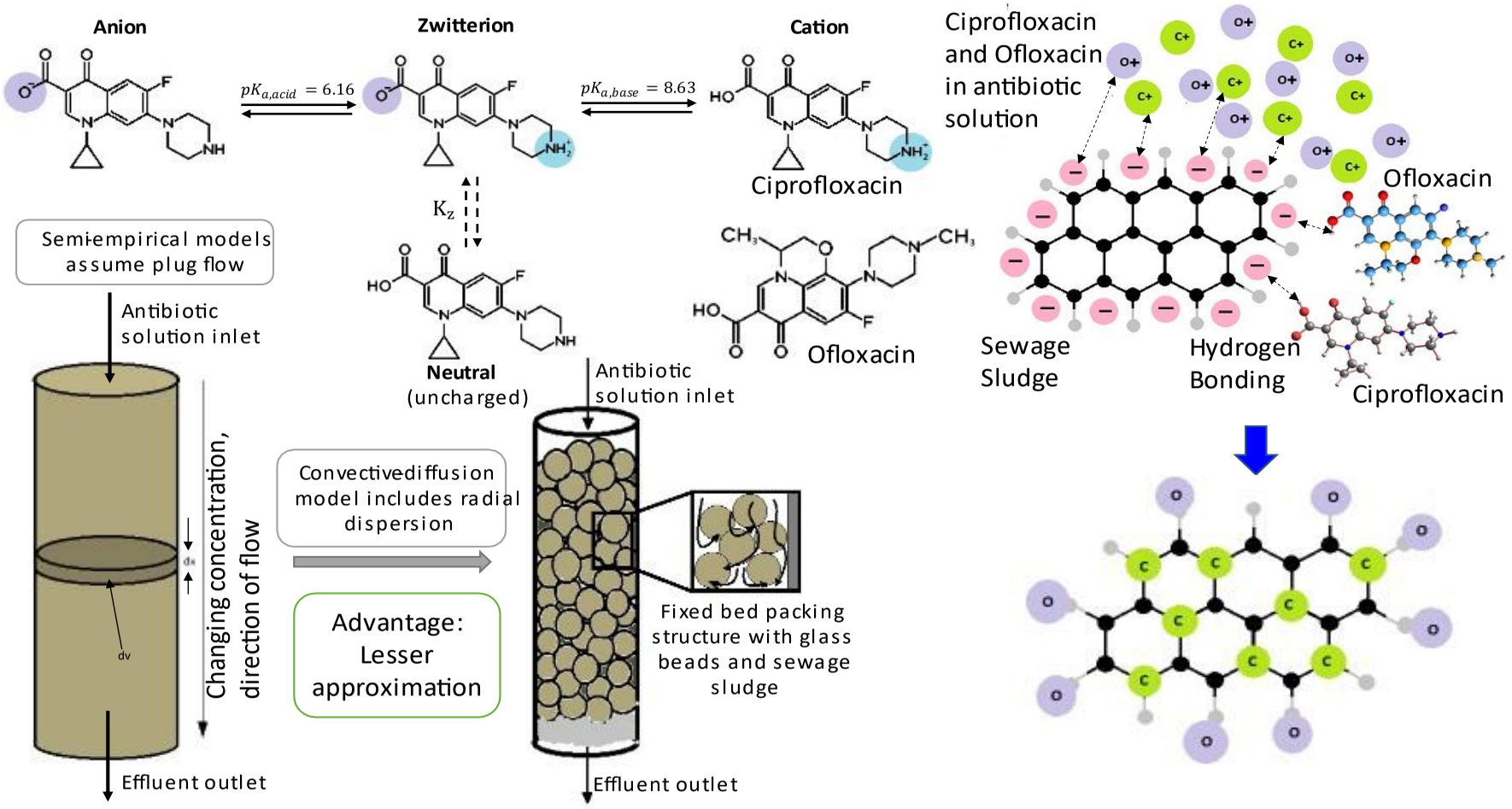

Fig. 8.2 Graphical representation of the aqueous phase adsorption of fluoroquinolones in a packed column filled with sewage-sludge under continuous mode.

- **Possible opportunities and challenges for using the studied method to remove target antibiotics from the wastewater matrix including possible interferences:**

To address the problem of water contamination by antibiotics the studied method renders a robust and effective treatment methodology. Removal of antibiotics using raw sewage sludge may be achieved in sewage treatment plants (STP), bulk drug manufacturing units, and formulation houses of pharmaceutical companies. Both batch and continuous processes may be applied for the removal of target antibiotics from wastewater matrix.

The possible major challenges encountered in using the studied methods include handling and disposal of a huge mass of sludge obtained after each treatment protocol since removal through adsorption using the sewage sludge as an adsorbent is proportional to excess sludge wastage (Andersen et al., 2005). The complete elimination of various antibiotics from the wastewater matrix becomes an intricate issue since the same appears in very low concentrations in municipal wastewater.

The surface of the raw sewage sludge remains negative at the working pH of ~ 7.8. The sewage sludge exhibits a relatively high adsorption capacity towards ciprofloxacin and ofloxacin in a weakly alkaline medium (pH at ~ 7.8) due to the negative charge-assisted hydrogen bonding. Carboxylic acid groups of both CIP and OFLX are hydrogen bonded to the basal oxygen atoms of the sludge layers. The presence of mono- or multivalent cations may affect the adsorption efficacy. The presence of heavy metals has varying effects on the adsorption of specific antibiotics onto the sewage sludge. Multivalent cations (Ca^{2+}, Mg^{2+}, Al^{3+}, Pb^{2+}, $Cd^{2+,}$ etc) suppress the adsorption process onto sewage sludge compared to the monovalent cations (Xiancai et al.,2017). Heavy metal cations interact with the negatively charged basal oxygen atoms of the sludge layers through strong electrostatic interaction. The same can reduce adsorption capacity of sewage sludge for removing the antibiotics by the formation of hydrogen bonds.

8.4 Recommendations for future work in the light of limitations of the study

8.4.1 Limitations

- The major limitation of both models is the adoption of a constant flow velocity throughout the packed bed. The velocity profile needs to be evaluated considering momentum transfer through packed-bed of specific voidage. This in turn will require a full-length solution of momentum transport equations under transient mode for the entire length of the bed considering advective diffusion of momentum and the same needs to be validated for various bed heights and flow rates.

- In the case of ofloxacin, observed breakthroughs come later than the predicted ones, while the same is not always true for ciprofloxacin.

- Pseudo-kinetics is not capable to substantiate either the complex hydrogen bonding or surface-complexation pathways efficiently, in this case.

8.4.2 Recommendations for future work

❖ Molecular modeling of each of CIP and OFLX, and in the presence of one another would be challenging work.

❖ If the effect of axial dispersion (at least in one dimension) could be studied, with respect to equation 6.1 of the convective diffusion model, a better scenario of the whole process of adsorption could be visualized.

❖ Effect of variation in bed diameter is another challenging objective that could be studied. Variations in bed diameter could be modeled by incorporating the convective and diffusive terms in the radial direction. This could be an

extremely demanding task, especially for multi-component systems with higher levels of non-linearities.

- ❖ Molecular modeling techniques are used in the fields of computational chemistry, drug design, computational biology, and material science for studying molecular systems ranging from small chemical systems to large biological molecules and material assemblies. Molecular modeling of each of the fluoroquinolones and in presence of one another would be a challenging work.

Annex I

Parameter Estimation using MATLAB and fsolve library function

The parameters of the Modified Competitive Langmuir-like model and the LeVan Vermeulen model i.e. A, $X_{m,1}$ and $X_{m,2}$ are estimated using **MATLAB** and the *fsolve Library function*. The *fsolve* library is devised to minimize a nonlinear sum of squares (**SSQ**) function. The problem is stated in the following way:

We have used non–linear least square regression. For this, we define a objective function as the sum of squares of errors.

Say X_1^m= value of X_1 by model; X_1^e= value of $X_1$by experiments

Then, the Sum of the Square of Error (SSE) function:

$(\psi) = (X_1^m - X_1^e)^2 + (X_2^m - X_2^e)^2$

We have to minimize the value of the least square error function.

Condition for minimisation of ψ is:

$\left(\frac{\partial\psi}{\partial A}\right)_B = 0; \left(\frac{\partial\psi}{\partial B}\right)_A = 0$

$$\left(\frac{\partial\psi}{\partial A}\right)_B = 0 : - \quad (X_1^m - X_1^e) * \left(\frac{\partial(X_1^m)}{\partial A}\right)_B + (X_2^m - X_2^e) * \left(\frac{d(X_2^m)}{\partial A}\right)_B = 0 \qquad \text{(I.1)}$$

$$\left(\frac{\partial\psi}{\partial B}\right)_A = 0 : - \quad (X_1^m - X_1^e) * \left(\frac{\partial(X_1^m)}{\partial B}\right)_A + (X_2^m - X_2^e) * \left(\frac{d(X_2^m)}{\partial B}\right)_A = 0. \qquad \text{(I.2)}$$

Hence, we have two non-linear equations with two unknowns. This can easily be solved by using "*fsolve"* command in MATLAB.

fsolve solves systems of non-linear equations of several variables by implementing 3 different algorithms. ¬ Trust region dogleg ¬ Trust region reflective ¬ Levenburg-Marquardt.

Annex II

Characterization of the post-treated sewage sludge

II.1 Elemental Analysis of Treated Sludge

The elemental analysis for estimating Carbon (C), Hydrogen (H), Nitrogen (N), and Sulphur (S) present in the post-treated sludge is carried out in a CHNS Analyzer (Make: ELEMENTAR, Germany; Model: VARIO MICRO CUBE). Temperatures of the combustion tube and the reduction tube are set at 1150^{o}C and 850^{o}C respectively. The pressure of the helium gas (carrier) is maintained at 1100 – 1200 millibar. The results are given in Table II.1.

Table II.1 Elemental analysis of raw and treated Sludge obtained from CHNS analyzer.

Sample	C % (wt % daf)	H% (wt % daf)	N% (wt % daf)	S% (wt % daf)
Treated Sludge	28.61	3.823	4.21	1.687

The carbon contents for pre (refer Table 3.1) and post-treated raw sludge are 19.97 ((wt % daf) and 28.61 ((wt % daf)) respectively. The hydrogen content of raw sludge is 2.847 (wt % daf) whereas for the treated sludge is 3.823 (wt % daf). Nitrogen content varies from 2.03 (wt % daf) to 4.21 (wt % daf) in the case of raw and post-adsorbed sludge. Increased values for carbon, nitrogen, and hydrogen contents of treated sludge (as compared to the raw sludge) clearly substantiate that the increased C%, H%, as well as N%, are due to the adsorption of ciprofloxacin and ofloxacin onto the sludge surface.

II.2 Scanning Electron Micrography (SEM) Images

The surface morphology of treated sludge is identified by a Field Emission Scanning Electron Micrograph (FE-SEM) with x6000 magnification [Make: HITACHI; Model: SU3800]. FE-SEM study for both raw and post-treated sludge is carried out in order to examine the change in the surface texture of raw sludge before and after adsorption.

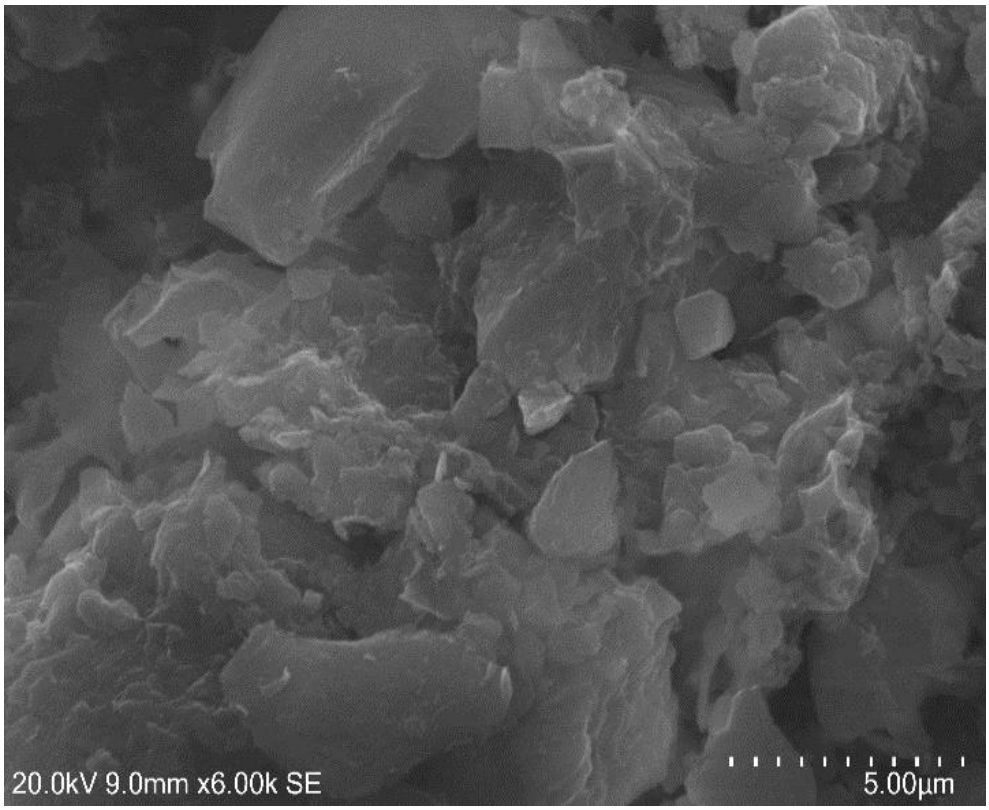

Fig. II.1 Scanning electron micrograph (SEM) images of treated sludge at ×6000 magnification.

Fig. II.1 represents the SEM images of post-treated sludge. Fig. 3.1 reveals a rough surface with a lot of cavities in the case of raw sludge. Fig. II.1 represents post-treated sludge with a comparatively smoother surface than the surface of raw sludge and it contains various cluster-like structures. Fig. II.1 of post-treated sludge contains a lesser number of cavities indicating pure physisorption of ciprofloxacin and ofloxacin

along with surface complexation through H-bonding, which is substantiated by the cluster-like structures present on the surface of the post-treated sludge.

II.3 FT-IR spectral analysis

Analysis of the functional groups, retained on the surface of the raw sewage sludge and sewage sludge after treatment are investigated by transmission infrared spectrum obtained using Fourier Transform Infrared Spectroscopy (FT-IR). An FT-IR spectrophotometer (Make: PerkinElmer; Model: FT-IR C120947) is used for this purpose. The entire IR spectrum is taken in the transmission range of 4000 cm^{-1} - 400 cm^{-1}. The FTIR spectrums are received at a resolution of 1 cm^{-1}. The spectrum of KBr which is set as background in the spectrometer is subtracted from the spectrum of each of the raw and post-treated sewage sludge samples.

The FT-IR spectra of raw sewage sludge are presented in Fig. 3.2 and corresponding spectra of the same after adsorption of ciprofloxacin and ofloxacin from wastewater are shown in Fig. II.2. The IR spectrum of the raw untreated sludge is described in detail in Chapter 3 *section 3.1.2*.

FT-IR spectrum of the post-treated sludge, after adsorption of ciprofloxacin and ofloxacin, is represented in Fig. II.2. The pattern of the FTIR spectrum of the treated sludge is quite similar to the same for raw sludge along with the inclusion of certain small bands in the region 2035 cm^{-1}, 1527 cm^{-1} - 1411 cm^{-1}, 1303 cm^{-1} - 1271 cm^{-1} and 670 cm^{-1}.

The band at 2035 cm^{-1} is attributed to -N-C=S stretch of iso-thiocyanate [57]. The band at 1527 cm^{-1} corresponds to aromatic carboxylic acid salt (Org-chem, IR Chart). The bands at 1484 cm^{-1} and 1458 cm^{-1} represent methylene C-H bend, C=C-

C aromatic ring stretch, and methyl C-H asymmetric or symmetric stretch respectively. The band at 1411 cm^{-1} represents carbonate ions. The band at 1303 cm^{-1} is probably due to skeletal C-C vibrations or due to the primary or secondary aromatic amines. The band at 1271 cm^{-1} is due to the aryl -O- stretch or could be due to the C-N stretch of aromatic primary amine. The peak at 1033 cm^{-1} is due to the strong C-O stretch of alkyl-substituted ether or primary alcohol. The band at 670 cm^{-1} is assigned to C-H out of plane bending corresponding to aromatics.

Comparison of both the spectra of raw and post-treated sludge reveals inclusions of certain new bands, particularly in the region of 1527 cm^{-1} – 1458 cm^{-1} indicating the presence of six-membered ring structures along with carboxylic and amine groups, resembling fluoroquinolones. Adsorption of ciprofloxacin and ofloxacin onto the sludge surface may be substantiated this way using FT-IR outputs.

II.4 Contact-angle based analysis

Contact angles are measured using a wettability analyzer [Make: KRÜSS Scientific, Germany; Model: DSA4; Drop shape: Sessile] in order to elucidate the hydrophobicity of sewage sludge surface after adsorption [refer Fig. II.3) of ciprofloxacin and ofloxacin in comparison to the precursor sludge surface [refer Fig. 3.4). The protocol of measurement of the hydrophobicity of raw and post-treated sewage sludge (RSS) is the same and the same is described in detail in Chapter 3 (refer *section 3.1.5*).

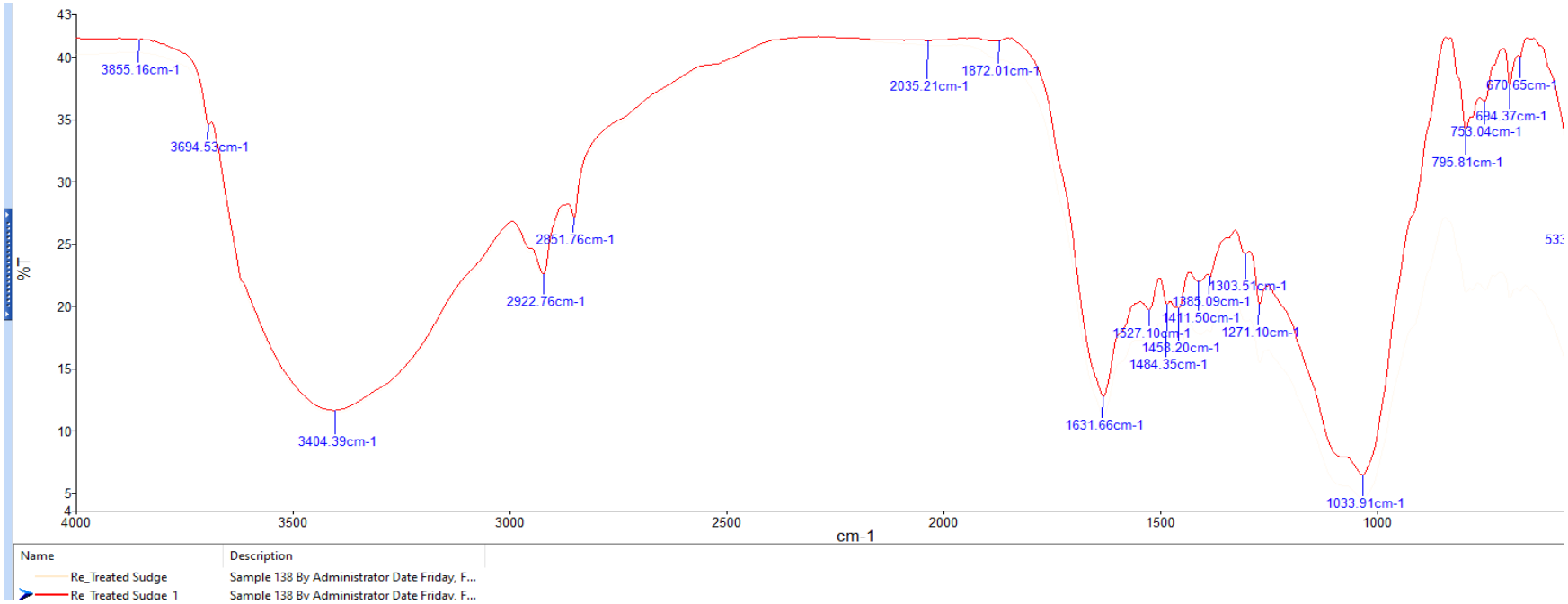

Fig. II.2 FT-IR spectra of treated sludge after adsorption.

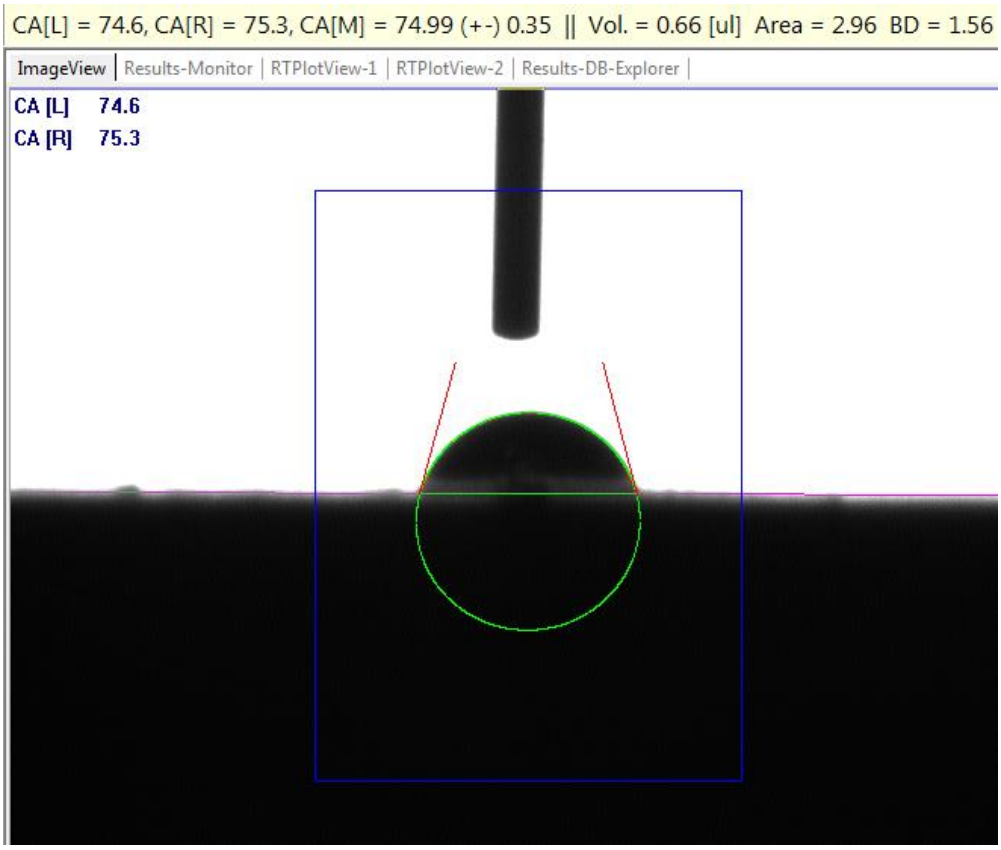

Fig. II.3 Contact angle measurement of treated sludge.

It is observed that the average θ_{H_2O} for raw sewage sludge surface is 76.6^o (± 0.98^o) and that for the treated sludge surface is 74.99^o (± 0.35^o) [see Fig. 3.4 and Fig. II.3] indicating both the surfaces are hydrophilic in nature. The decrease in contact angle value of the treated sludge (from 76.6^o to 74.99^o) affirms the inclusion of polar moieties i.e. ciprofloxacin and ofloxacin onto the surface of raw sewage sludge after adsorption and its hydrophilicity is also enhanced (R. Aslam, 2021b).

II.5 XPS analysis

The XPS study is carried out using an advanced electron spectroscopy system [Make: Omicron NanoTechnology GmbH, United Kingdom; Model: EIS-Sphera] meant for surface analysis. A monochromated Al Kα source [Model: XM 500; $h\nu$ = 1486.7 eV] is used for high-resolution X-rays. Various spectra are obtained by plotting intensity

versus binding energy curves for different elements. Results for the post-treated sludge are shown in Fig. II.4. The peaks in the full-scan spectrum of treated sludge are assigned to O 1s (531.8 eV), N 1s (399.7 eV), and C 1s (284.4 eV) (see Fig. II.4 B) along with the inclusion of a minor peak corresponding to elemental F 1s (687 eV). High-resolution spectra reveal the presence of various elements i.e Ca 2p, Si 2p, Fe 2p, P 2p both in raw sludge [refer *section 3.1.6*] and treated sludge. The high-resolution spectrum of C1s and O1s before and after adsorption reveals a band shift towards lower binding energy i.e red-shift occurs. The band of C1s of raw sludge and treated sludge are found to be 284.5 eV and 284.4 eV respectively. The band of O1s in raw sludge and treated sludge are found to be 532.2 eV and 531.8 eV respectively. The band of O 1s at 532.2 eV corresponds to either C-O or -C=O. The shift in the binding energy of O 1s from 532.2 to 531.8 eV might have been caused due to the existence of H-bonds between adsorbing molecules (ciprofloxacin and ofloxacin) and the adsorbent sewage sludge (Zhang *et al.* 2022). No obvious shift in the binding energies is observed in the N1s spectra. The band corresponding to F1s at 687eV has been detected in the spectrum of the treated sludge after the adsorption of ciprofloxacin and ofloxacin onto the sewage sludge surface.

Treated Sludge

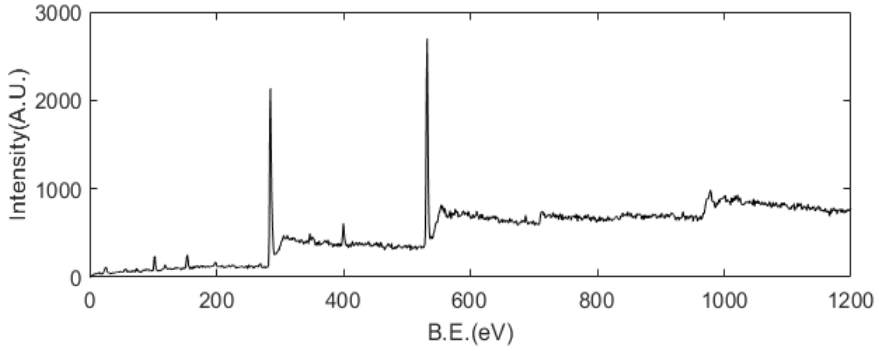

(B)

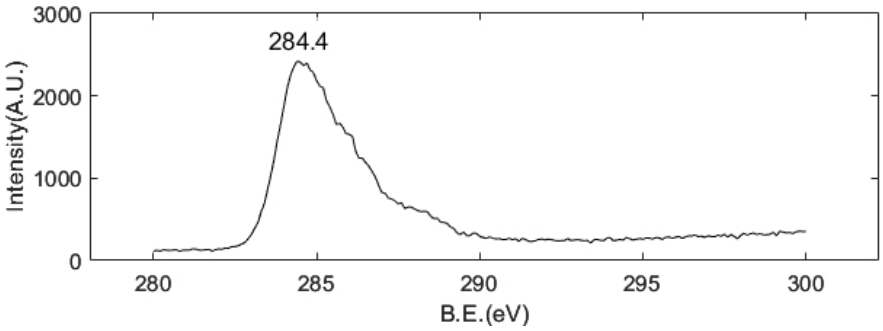

(B: C 1s)

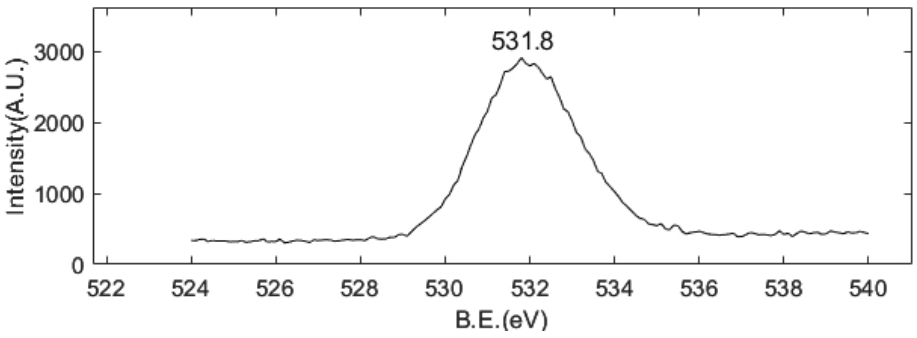

(B: O 1s)

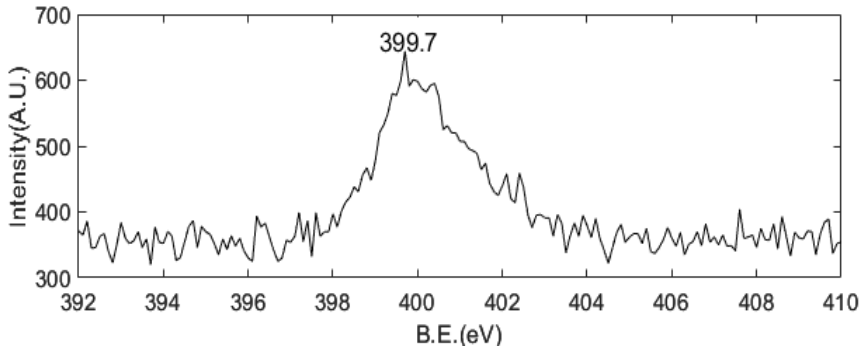

(B: N 1s)

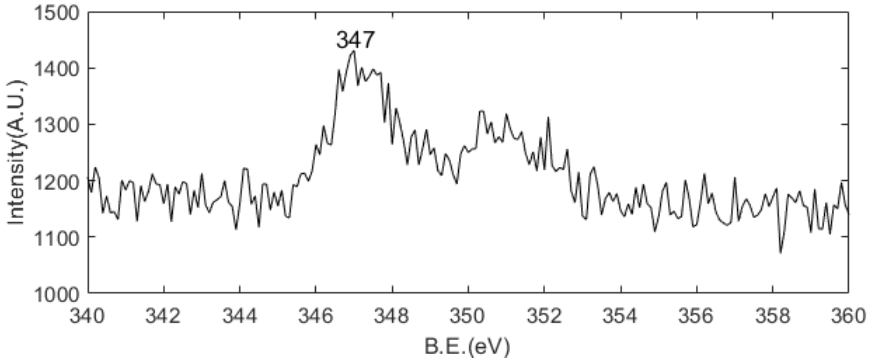

(B: Ca 2p)

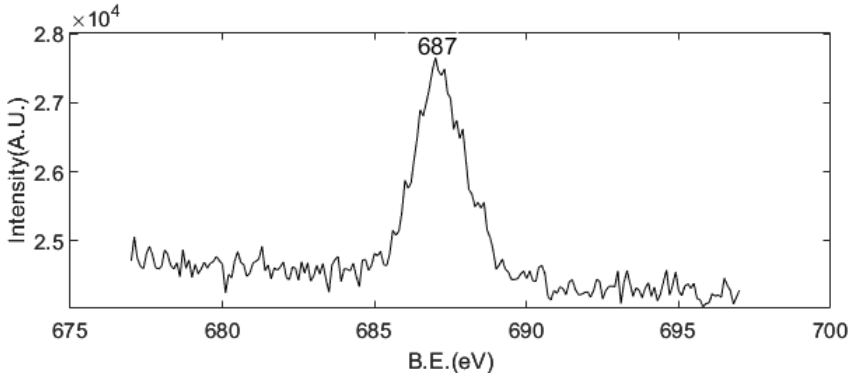

(B: F 1s)

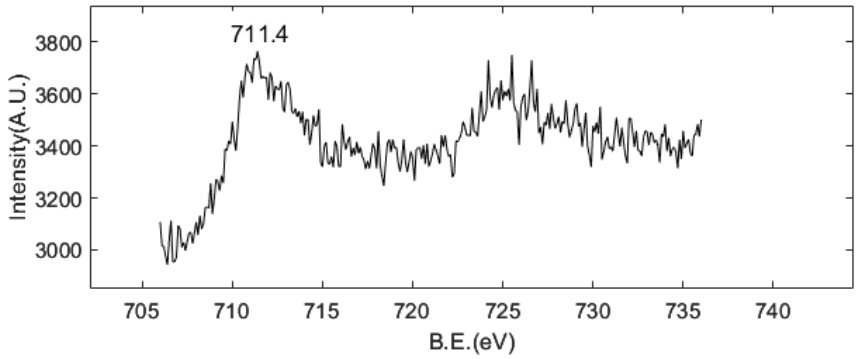

(B: Fe 2p)

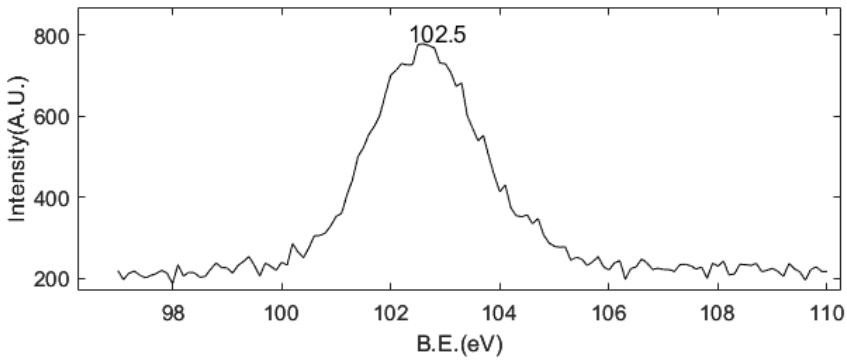

(B: Si 2p)

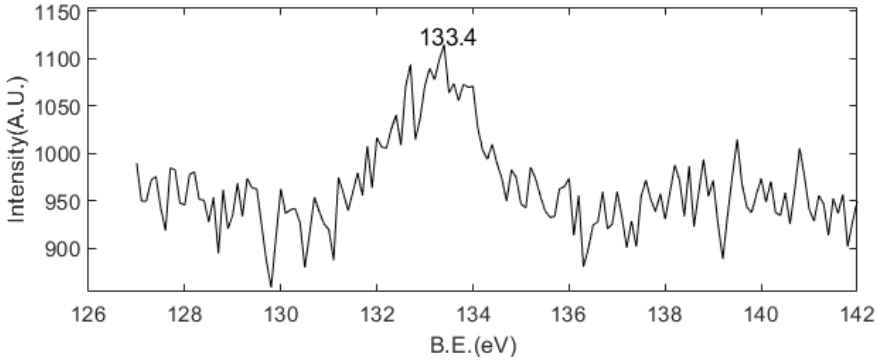

(B: P 2p)

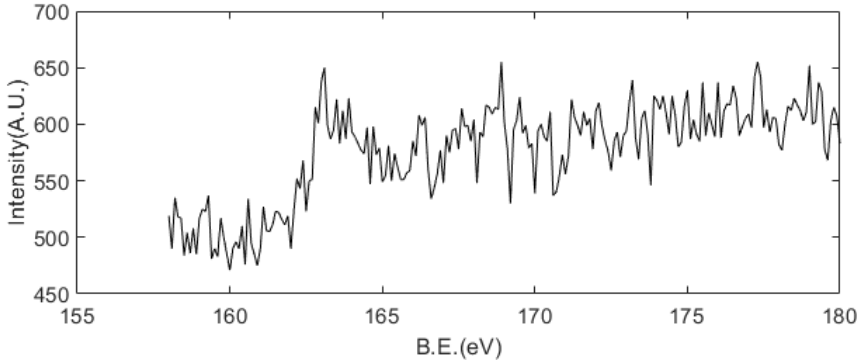

(B: S 2p)

Fig. II.4 XPS spectra of treated sludge at different levels.

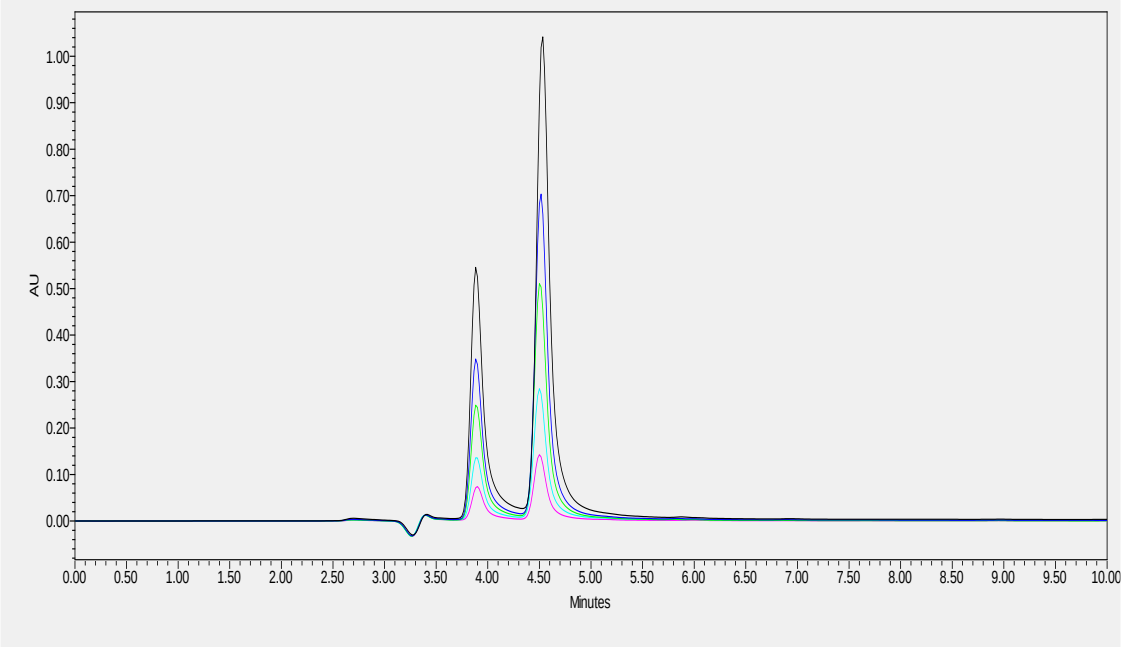

Fig. SI. Chromatograms generated from High Performance Liquid Chromatograph [HPLC] for Ciprofloxacin and Ofloxacin in combination.

Table SI Concentrations versus peak areas for the standard curve

Concentrations (ppm) Ciprofloxacin [CIP]	Peak areas (Volts-min) Ciprofloxacin [CIP]	Concentrations (ppm) Ofloxacin [OFLX]	Peak areas (Volts-min) Ofloxacin [OFLX]
100	6135554	100	11689514
75	4369980	75	8111124
50	3376774	50	6274043
25	2021399	25	3601883
10	1194951	10	1785143

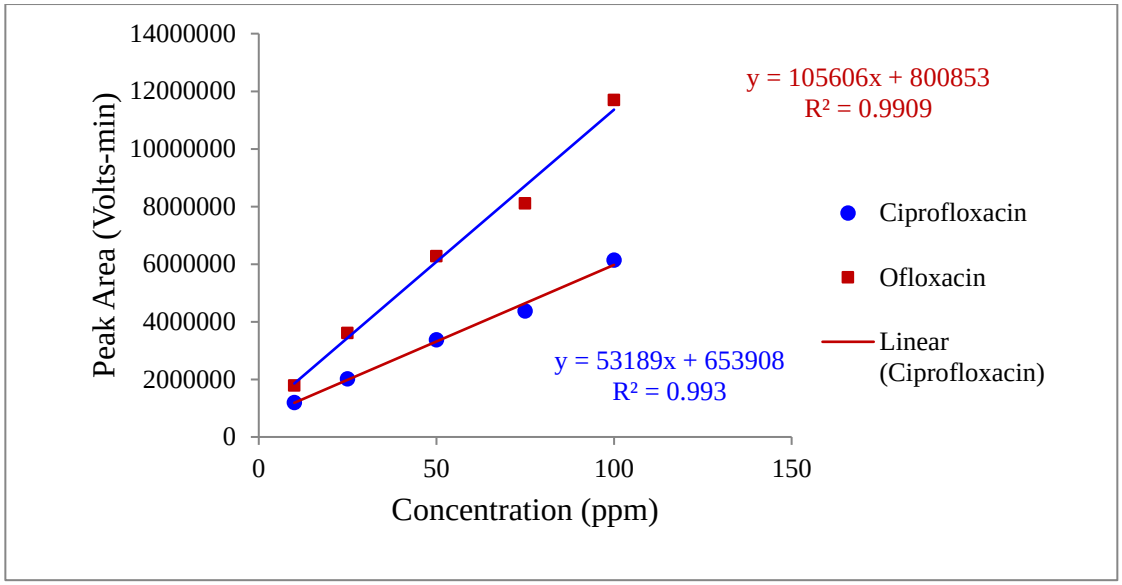

Fig. SII. Standard Curves for Ciprofloxacin and Ofloxacin in combination.

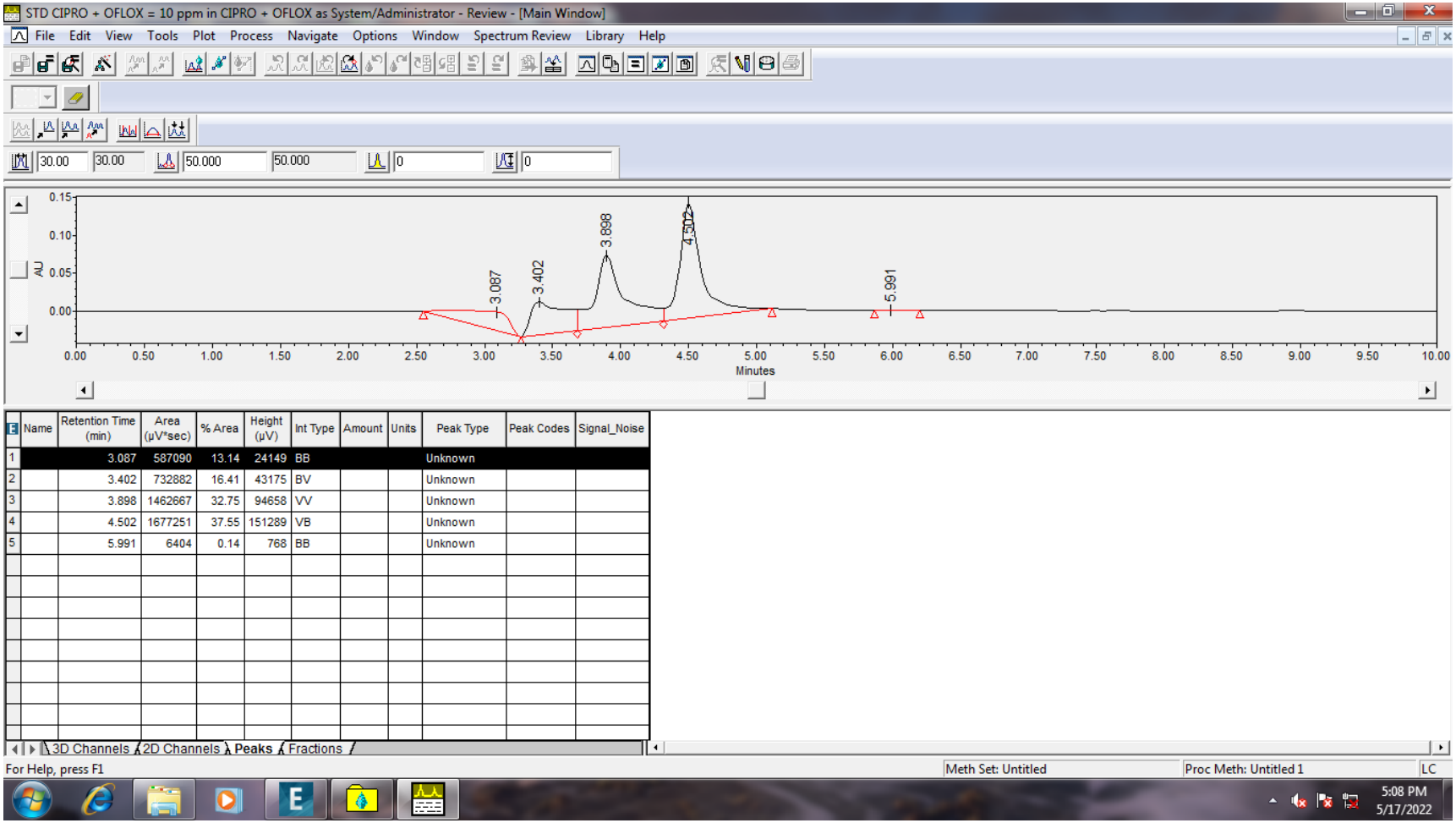

E	Name	Retention Time (min)	Area (µV*sec)	% Area	Height (µV)	Int Type	Amount	Units	Peak Type	Peak Codes	Signal_Noise
1		3.087	587090	13.14	24149	BB			Unknown		
2		3.402	732882	16.41	43175	BV			Unknown		
3		3.898	1462667	32.75	94658	VV			Unknown		
4		4.502	1677251	37.55	151289	VB			Unknown		
5		5.991	6404	0.14	768	BB			Unknown		

(i)

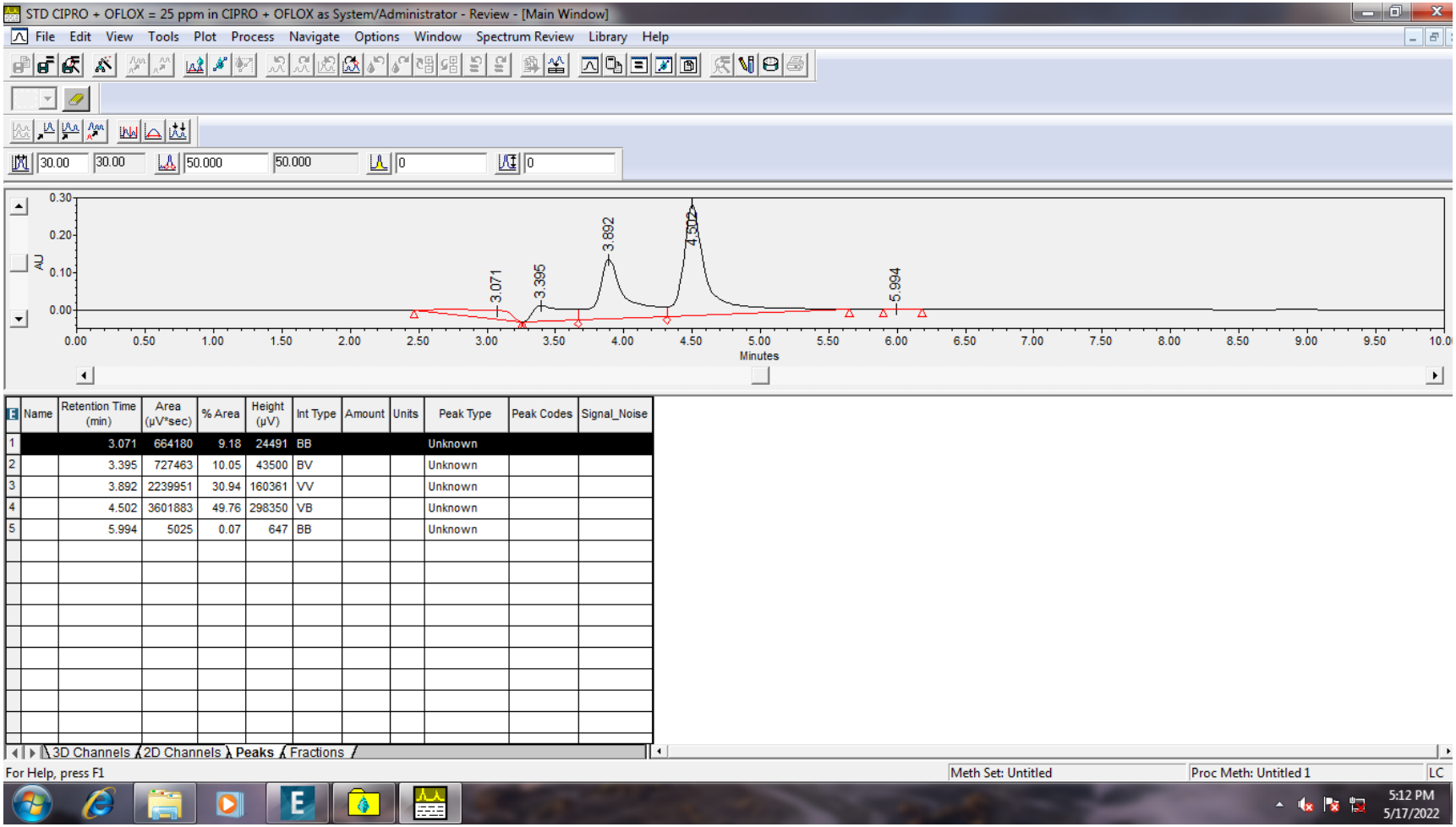

E	Name	Retention Time (min)	Area (µV*sec)	% Area	Height (µV)	Int Type	Amount	Units	Peak Type	Peak Codes	Signal_Noise
1		3.071	664180	9.18	24491	BB			Unknown		
2		3.395	727463	10.05	43500	BV			Unknown		
3		3.892	2239951	30.94	160361	VV			Unknown		
4		4.502	3601883	49.76	298350	VB			Unknown		
5		5.994	5025	0.07	647	BB			Unknown		

(ii)

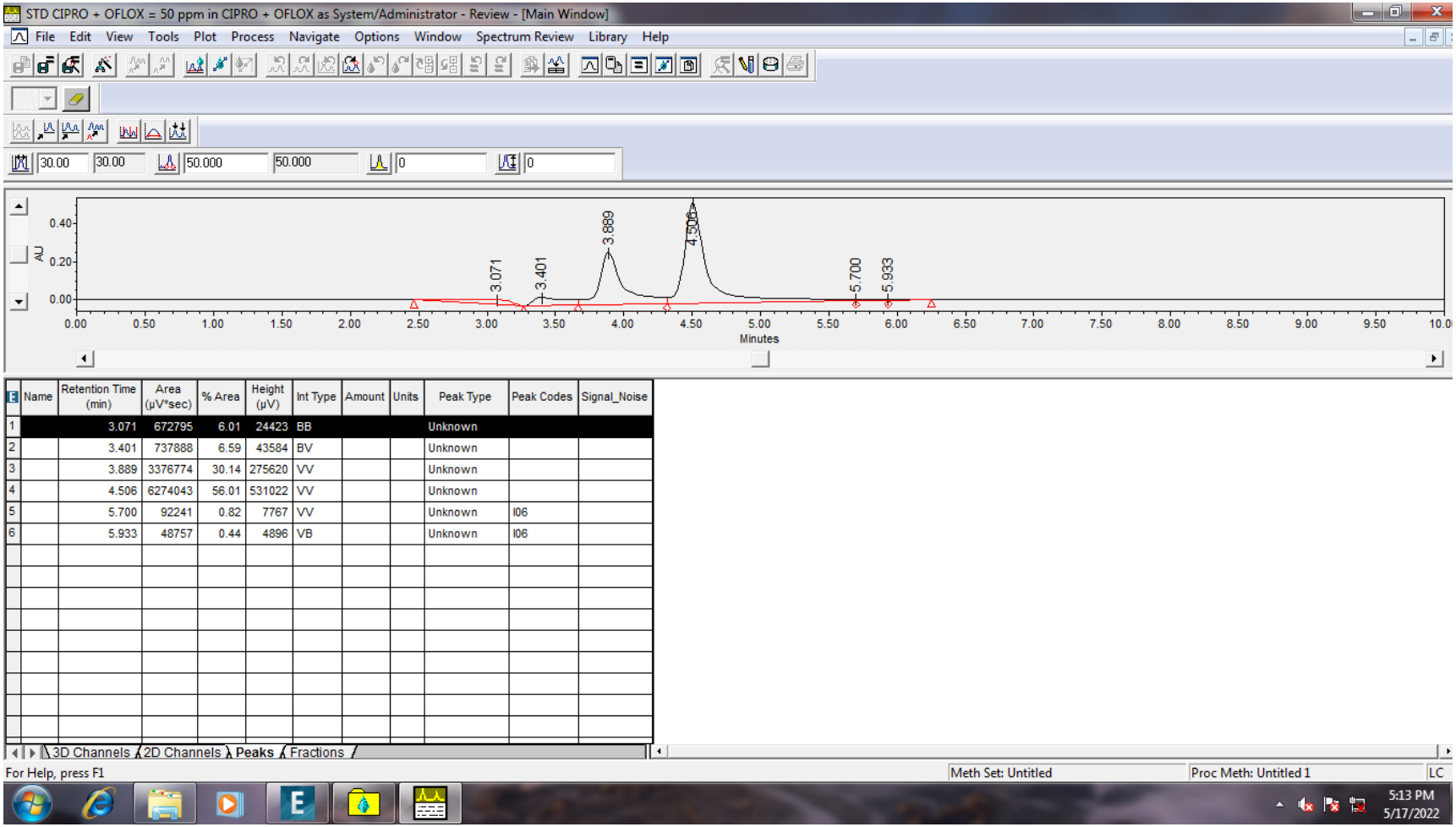

	Name	Retention Time (min)	Area (µV*sec)	% Area	Height (µV)	Int Type	Amount	Units	Peak Type	Peak Codes	Signal_Noise
1		3.071	672795	6.01	24423	BB			Unknown		
2		3.401	737888	6.59	43584	BV			Unknown		
3		3.889	3376774	30.14	275620	VV			Unknown		
4		4.506	6274043	56.01	531022	VV			Unknown		
5		5.700	92241	0.82	7767	VV			Unknown	I06	
6		5.933	48757	0.44	4896	VB			Unknown	I06	

(iii)

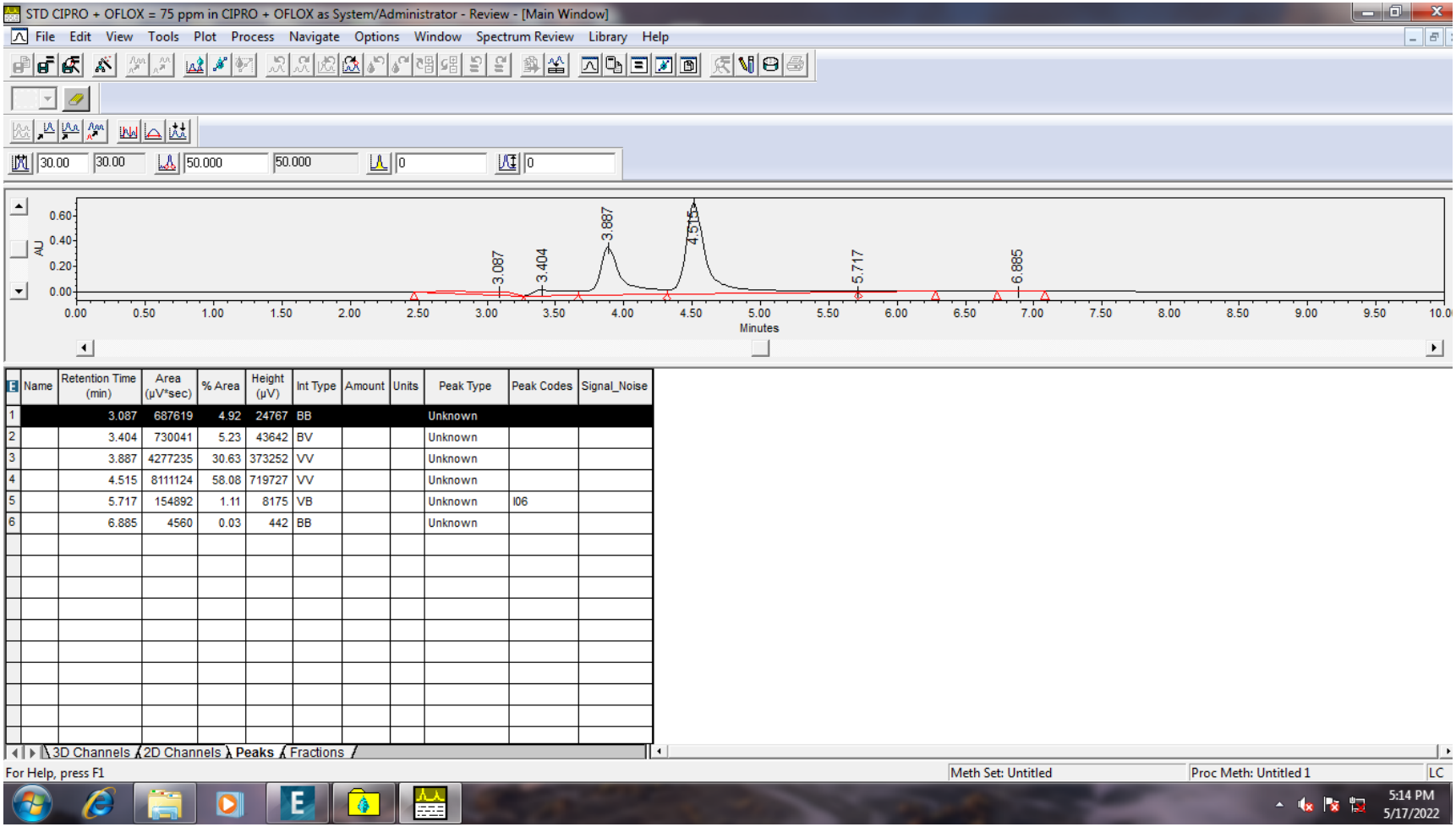

	Name	Retention Time (min)	Area (µV*sec)	% Area	Height (µV)	Int Type	Amount	Units	Peak Type	Peak Codes	Signal_Noise
1		3.087	687619	4.92	24767	BB			Unknown		
2		3.404	730041	5.23	43642	BV			Unknown		
3		3.887	4277235	30.63	373252	VV			Unknown		
4		4.515	8111124	58.08	719727	VV			Unknown		
5		5.717	154892	1.11	8175	VB			Unknown	I06	
6		6.885	4560	0.03	442	BB			Unknown		

(iv)

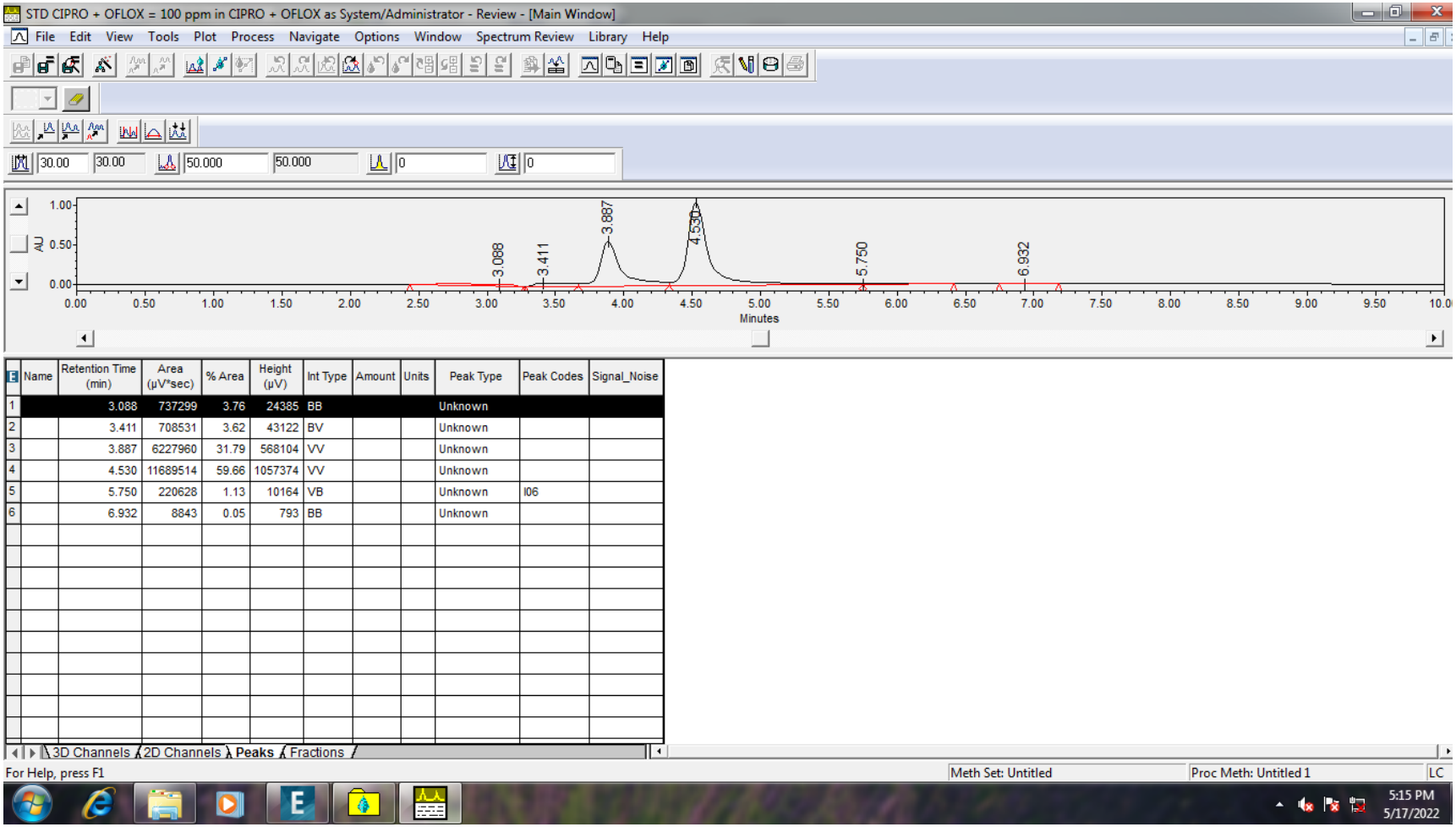

(v)

Fig. SIII. *Sample Chromatograms of analytical grade Ciprofloxacin and Ofloxacin [Machine generated through the software Empower 3 [Make: Waters, GMBH]; Strength (i) 10 ppm; (ii) 25 ppm; (iii) 50 ppm; (iv) 75 ppm; (v) 100 ppm.*

Empower™ 3 SOFTWARE

LC Calibration Report

Processing Method:	Rajib	System:	UV_VIS
Processing Method ID:	2027	Channel:	W2489 ChA
Calibration ID:	2032	Proc. Chnl. Descr.:	W2489 ChA 300nm
Date Calibrated:	5/17/2022 12:35:50 AM IST		

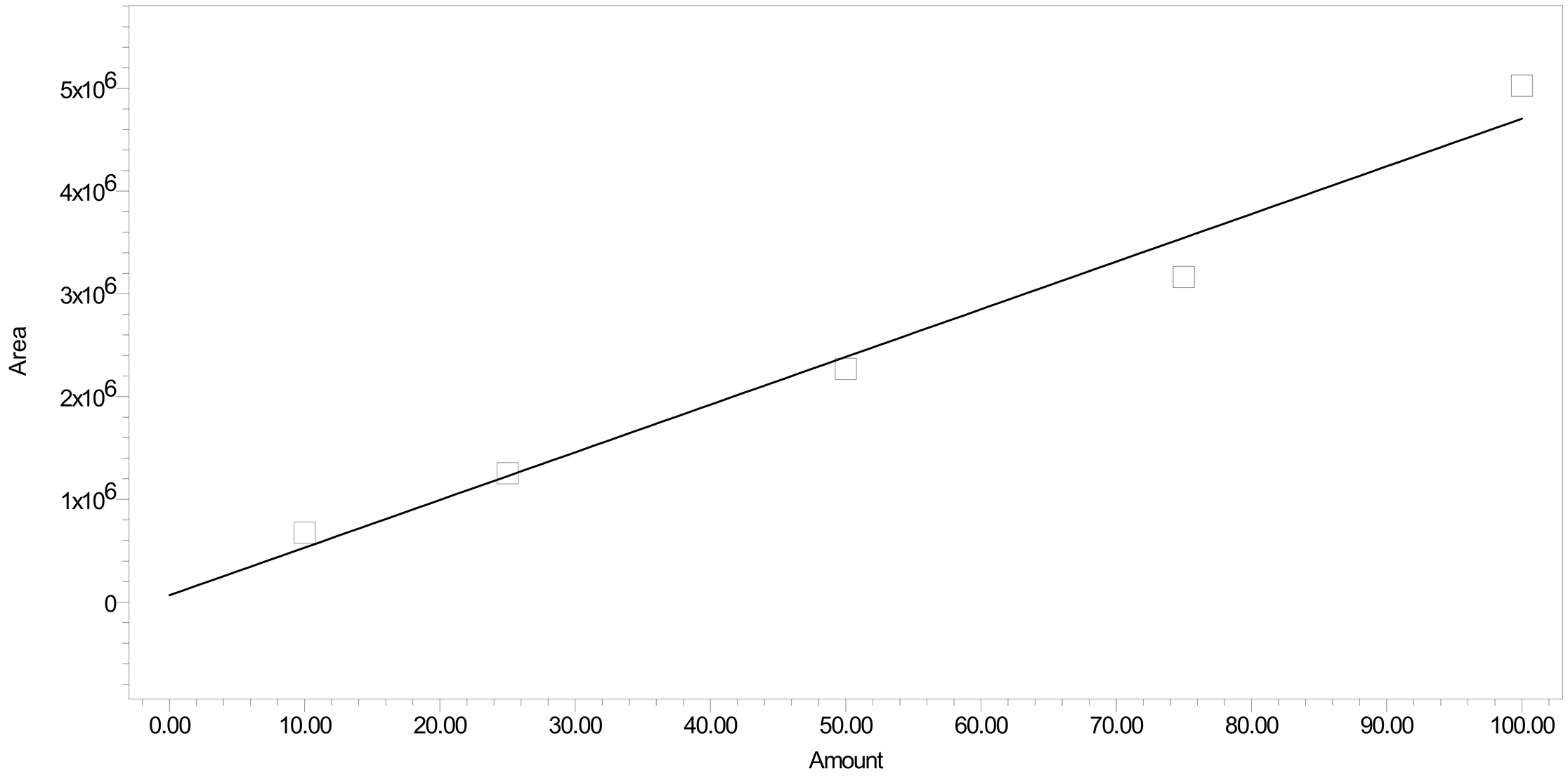

Peak Name: CIPRO; RT: 3.898; Fit Type: Linear (1st Order); Cal Curve Id: 2033; R: 0.987797; R^2: 0.975743; Weighting: None; Equation: Y = 4.64e+004 X + 6.67e+004; Normalized Intercept/Slope: 0.026146; RSD(E): 12.436589

Peak: CIPRO

	Sample Name	Result Id	Peak Name	Level	X Value	Response	Calc. Value
1	STD CIPRO + OFLOX = 10 ppm	2035	CIPRO		10.000	676595.763	13.150
2	STD CIPRO + OFLOX = 25 ppm	2036	CIPRO		25.000	1255158.297	25.624
3	STD CIPRO + OFLOX = 50 ppm	2037	CIPRO		50.000	2270211.893	47.509
4	STD CIPRO + OFLOX = 75 ppm	2038	CIPRO		75.000	3163547.797	66.770
5	STD CIPRO + OFLOX = 100 ppm	2039	CIPRO		100.000	5026970.241	106.947

Peak: CIPRO

	% Deviation	Manual	Ignore
1	31.50	No	No
2	2.50	No	No
3	-4.98	No	No
4	-10.97	No	No
5	6.95	No	No

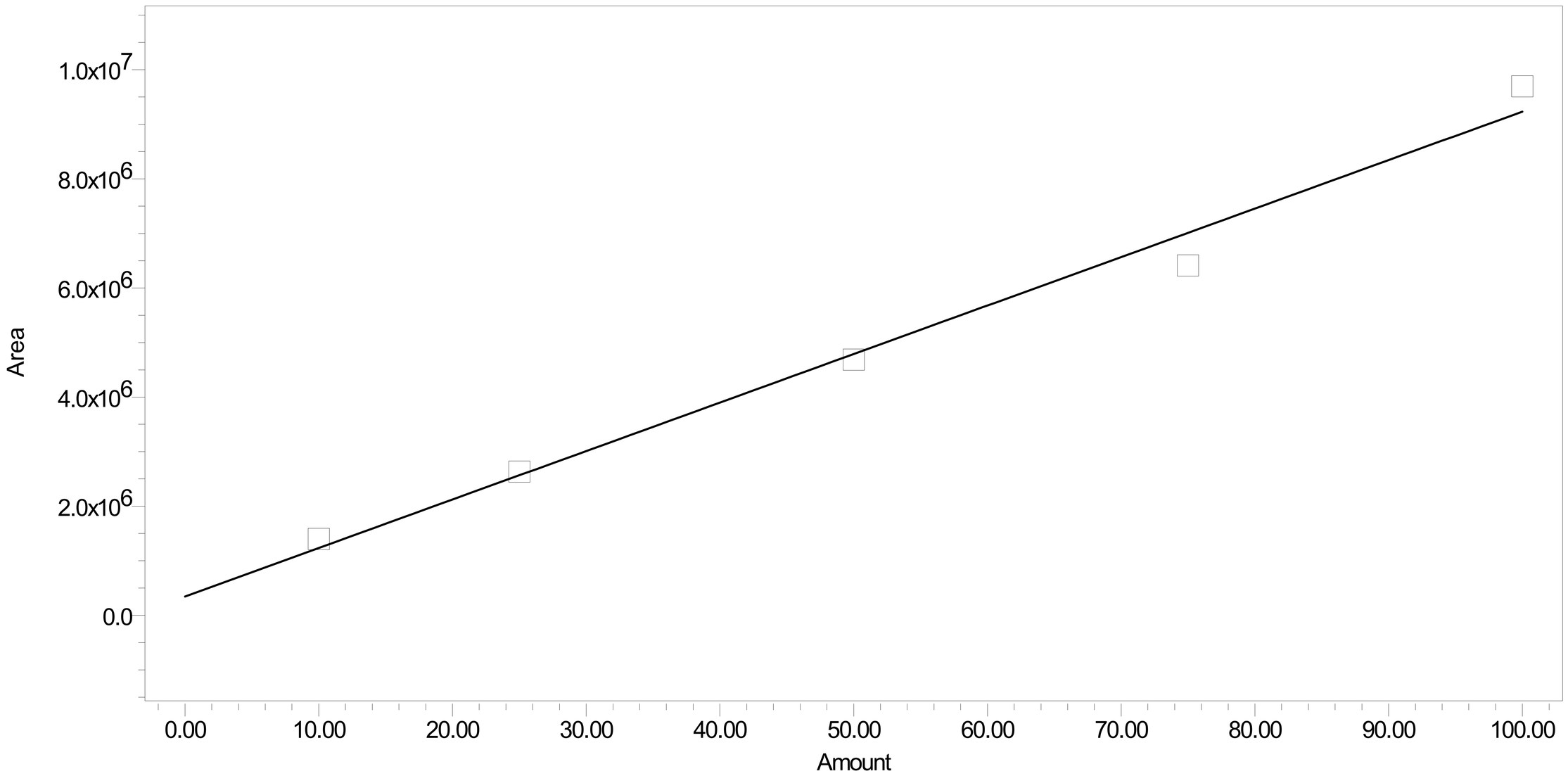

Peak Name: OFLOX; RT: 4.503; Fit Type: Linear (1st Order); Cal Curve Id: 2034; R: 0.992759; R^2: 0.985571; Weighting: None; Equation: Y = 8.89e+004 X + 3.46e+005; Normalized Intercept/Slope: 0.070739; RSD(E): 9.125028

Peak: OFLOX

	Sample Name	Result Id	Peak Name	Level	X Value	Response	Calc. Value
1	STD CIPRO + OFLOX = 10 ppm	2035	OFLOX		10.000	1400112.147	11.867
2	STD CIPRO + OFLOX = 25 ppm	2036	OFLOX		25.000	2635424.151	25.769
3	STD CIPRO + OFLOX = 50 ppm	2037	OFLOX		50.000	4686102.657	48.848
4	STD CIPRO + OFLOX = 75 ppm	2038	OFLOX		75.000	6412597.488	68.278
5	STD CIPRO + OFLOX = 100 ppm	2039	OFLOX		100.000	9696757.292	105.239

Peak: OFLOX

	% Deviation	Manual	Ignore
1	18.67	No	No
2	3.08	No	No
3	-2.30	No	No
4	-8.96	No	No
5	5.24	No	No

Supplementary Material C

- **Regeneration and Reusability of raw sewage sludge for the removal of ciprofloxacin and ofloxacin in combination in an aqueous phase using a packed bed filled with sewage sludge under dynamic condition:**

The dynamic study for the regeneration and reusability of the raw sewage sludge is selected with the following operational conditions:

1. Bed Length - 5 cm
2. Sludge taken 4.0 g.
3. In-flow rate 0.90 ml/sec
4. Concentration of antibiotics 100 ppm each

After the complete study, the bed is thoroughly washed with water until the pH of the outlet water becomes ~ 7.2 ensuring complete removal of excess adherence of CIP and OFLX onto the sludge bed. The fixed bed is then dried for several days under ambient conditions. A similar experiment maintaining the above-said operational condition is being conducted using this dried sludge in the packed bed to investigate the reusability of the dried raw sewage sludge. The results of the two studies are given below:

Table S-C. 1 Dynamic Study using raw sewage sludge.

Time (mins)	Ciprofloxacin (A1) in Volts-mins	Ofloxacin (A2) in Volts-mins	Ciprofloxacin (C1) in ppm	Ofloxacin (C2) in ppm
0	4011414	10001565	100	100
30	283125	1106285	7.05798504	11.06111893
60	510362	2422550	12.72274565	24.2217093
90	692596	3547251	17.26563252	35.46695942
120	842819	4421132	21.01052148	44.20440201
150	998823	5236514	24.89952421	52.35694614
180	1139897	5988887	28.41633898	59.87949886
210	1347255	6555277	33.58553867	65.5425126
240	1359194	6551290	33.88316439	65.50264884
270	1532240	7297564	38.19700485	72.9642211
310	1604238	7643548	39.9918333	76.42351972
370	2051292	7411291	51.13638233	74.10131314
430	2336239	7738416	58.23978777	77.37205127

490	2591479	8497343	64.60263139	84.96013374
550	2771561	8709296	69.09187135	87.07933208
590	3099212	9451654	77.25983905	94.50175048
630	3271561	9589412	81.55630409	95.87911492

Table S-C. 2 Dynamic Study using recycled sewage sludge.

Time (mins)	Ciprofloxacin (A1) in Volts-mins	Ofloxacin (A2) in Volts-mins	Ciprofloxacin (C1) in ppm	Ofloxacin (C2) in ppm
0	5068964	9387548	100	100
15	734615	2102709	14.49	22.39
30	1932932	4669226	38.13	49.73
90	3410824	7837776	67.3	83.49
210	4093874	9092132	80.76	96.85
270	4430663	9486838	87.4	101.05

The reusability study using raw sewage sludge and recycled raw sewage sludge has revealed the following:

From **Table S-C. 1**, the concentrations of ciprofloxacin and ofloxacin in outlet water are 7.05 and 11.06 ppm respectively after 30 mins. of interval from the study's starting point. That implies that the amount adsorbed by the packed bed filled with raw sewage sludge for ciprofloxacin and ofloxacin from the wastewater matrix is significantly high (93.0 and 89.0 ppm approx. for ciprofloxacin and ofloxacin respectively). Using recycled sewage sludge, the concentrations of ciprofloxacin and ofloxacin in outlet water become 38.1 and 49.7 ppm (**Table S-C. 2**) respectively which implies a drastic drop in the quantum of adsorption (61.9 and 50.3 ppm for ciprofloxacin and ofloxacin respectively) while reused sewage sludge is used.

The bed exhaustion time for raw sewage sludge is 630 minutes, whereas using reused sewage sludge the same is 270 mins.

Observing the above comparison study, it is evident that the reused sewage sludge exhibits less efficacy in terms of the adsorption capacity compared to the raw sewage sludge; hence, the reusability of recycled sludge is not a cost-effective option.

❖ **The study includes the use of raw sewage sludge without functionalization:**

In the case of IR spectrum of the raw sewage sludge [refer Fig. I.2 (a)] there is a significant peak at 3412 cm^{-1}, which is probably due to broad H bonded O-H stretching of alcohols. The bands at 2028 cm^{-1} and 1875 cm^{-1} indicate carbonyl compounds (>C=O group). The band at 1639 cm^{-1} is due to alkenyl -C=C- stretch or -N-H bending of primary amine (-NH_2 group). The band at 1548 cm^{-1} corresponds to mild >N-H bending of secondary amine (>NH group). The band at 1426 cm^{-1} is assigned to organic sulphates or carbonates (SO_4^{2-}, CO_3^{2-} groups). The bands at 1384 cm^{-1} and 1033 cm^{-1} are attributed to methyl C-H asymmetric stretch and primary alcohol C-O and P-O-C stretching of aliphatic phosphate respectively. The bands at 779 cm^{-1}, 759 cm^{-1}, and 730 cm^{-1} correspond to mild C-Cl stretch of aliphatic chloro-compounds. The bands at 694 cm^{-1} and 643 cm^{-1} are attributed to the C-Br stretch of aliphatic bromo compounds, the C-H stretch of thiols, and the alkyne C-H bend respectively. The band at 533 cm^{-1} is attributed to C-I stretch corresponding to aliphatic iodo compounds.

The FT-IR study of raw sewage sludge reveals the presence of several functional groups i.e. -OH, >C=O, -NH_2, >NH, SO_4^{2-}, CO_3^{2-}, PO_4^{3-}, -Cl, -Br and -I, onto the surface of the sewage sludge. Hence, the study is being conducted without functionalisation of the raw sewage sludge using NH_4OH, HCl, H_2SO_4, or H_3PO_4.

❖ **Data on Pure component and multi-component analysis:**

Batch Equilibrium analysis of pure component Ciprofloxacin

	C_{eq}				q_e		
No. of Expt.	C_{eq} Values	Mean Ceq	Std Dev.	No. of Expt.	q_e Values	Mean q_e	Std Dev.
1	0.00012	0.0001	0.00002	1	0.0019	0.0018	0.000265
2	0.0001			2	0.002		
3	0.00008			3	0.0015		
1	0.0002	0.0002	0.0001	1	0.005	0.0046	0.0004
2	0.0003			2	0.0042		
3	0.0001			3	0.0046		
1	0.0008	0.0005	0.0003	1	0.0091	0.009	0.0001
2	0.0002			2	0.009		
3	0.0005			3	0.0089		

1	0.0008	0.0009	0.000264575	1	0.0134	0.0132	0.0002
2	0.0007			2	0.0132		
3	0.0012			3	0.013		
1	0.002	0.0018	0.0002	1	0.014	0.014	0.0002
2	0.0016			2	0.0142		
3	0.0018			3	0.0138		
1	0.0028	0.0028	0.00010	1	0.0144	0.0144	0.0004
2	0.0027			2	0.014		
3	0.0029			3	0.0148		

Batch Equilibrium analysis of pure component Ofloxacin

	C_{eq}				q_e		
No. of Expt.	C_{eq} Values	Mean Ceq	Std Dev.	No. of Expt.	q_e Values	Mean q_e	Std Dev.
1	0.0002	0.0002267	0.000162	1	0.0016	0.0016	0.00010
2	0.0004			2	0.0017		
3	0.00008			3	0.0015		
1	0.0006	0.0005	0.000265	1	0.0037	0.004	0.00052
2	0.0007			2	0.0037		
3	0.0002			3	0.0046		
1	0.0014	0.0013	0.000173	1	0.0075	0.0074	0.00010
2	0.0014			2	0.0074		
3	0.0011			3	0.0073		
1	0.0024	0.0024	0.0001	1	0.0081	0.008	0.000265
2	0.0025			2	0.0082		
3	0.0023			3	0.0077		
1	0.003	0.0032	0.000346	1	0.0086	0.0086	0.0002
2	0.003			2	0.0088		
3	0.0036			3	0.0084		
1	0.0045	0.0044	0.00010	1	0.0112	0.0112	0.00010
2	0.0044			2	0.0111		
3	0.0043			3	0.0113		

Batch Equilibrium analysis of multi-component containing Ciprofloxacin and Ofloxacin

For Ciprofloxacin

X_1				C_{eq1}			
No.of Expt.	X_1 Values	Mean X_1	Std Dev.	No.of Expt.	C_{eq1} Values	Mean C_{eq1}	Std Dev.
1	0.0123	0.0125	0.00043589	1	0.1	0.1	0.02
2	0.0122			2	0.08		
3	0.013			3	0.12		
1	0.00966	0.00966	0.00002	1	0.075	0.075	0.001
2	0.00968			2	0.076		
3	0.00964			3	0.074		
No.of Expt.	X_1 Values	Mean X_1	Std Dev.	No.of Expt.	C_{eq1} Values	Mean C_{eq1}	Std Dev.
1	0.00681	0.00682	0.00002	1	0.05	0.05	0.005
2	0.00681			2	0.055		
3	0.00684			3	0.045		
1	0.00604	0.00604	0.00001	1	0.044	0.044	0.002
2	0.00603			2	0.046		
3	0.00605			3	0.042		
1	0.0048	0.0045	0.0003	1	0.0312	0.0312	0.0001
2	0.0045			2	0.0311		
3	0.0042			3	0.0313		
1	0.0037	0.0037	0.00020	1	0.026	0.025	0.001
2	0.0039			2	0.024		
3	0.0035			3	0.025		
1	0.00321	0.00323	0.00002	1	0.021	0.0213	0.0003
2	0.00325			2	0.0213		
3	0.00323			3	0.0216		
1	0.00222	0.00223	0.00001	1	0.0134	0.0134	0.0001
2	0.00223			2	0.0133		
3	0.00224			3	0.0135		
1	0.00174	0.00174	0.00004	1	0.01	0.01	0.001
2	0.0017			2	0.009		
3	0.00178			3	0.011		

1	0.0018	0.0014	0.0004	1	0.009	0.009	0.0002
2	0.001			2	0.0088		
3	0.0014			3	0.0092		
1	0.00104	0.00104	0.00002	1	0.0075	0.0075	0.00010
2	0.00102			2	0.0076		
3	0.00106			3	0.0074		
1	0.0009	0.0007	0.000264575	1	0.0062	0.0063	0.0001
2	0.0008			2	0.0063		
3	0.0004			3	0.0064		
1	0.00039	0.00036	0.00003	1	0.005	0.005	0.001
2	0.00034			2	0.006		
3	0.00035			3	0.004		

For Ofloxacin

	X_2				C_{eq2}		
No. of Expt.	X_2 Values	Mean X_2	Std Dev.	No.of Expt.	C_{eq2} Values	Mean C_{eq2}	Std Dev.
1	0.0125	0.0125333	0.00006	1	0.09	0.1033333	0.015275
2	0.0125			2	0.12		
3	0.0126			3	0.1		
1	0.0097	0.0097	0.0001	1	0.079	0.075	0.004
2	0.0098			2	0.071		
3	0.0096			3	0.075		
1	0.0067	0.0068	0.00010	1	0.06	0.0499667	0.01005
2	0.0069			2	0.05		
3	0.0068			3	0.0399		
1	0.0056	0.0056	0.0001	1	0.0408	0.0406	0.0002
2	0.0057			2	0.0406		
3	0.0055			3	0.0404		
1	0.005	0.0049667	0.00006	1	0.03437	0.0343667	0.00004
2	0.0049			2	0.0344		
3	0.005			3	0.03433		
1	0.0038	0.0037	0.0001414	1	0.026	0.025	0.001
2	0.0036			2	0.025		

3	0.037			3	0.024		
1	0.003	0.0029867	0.00002	1	0.019	0.0193	0.0003
2	0.00297			2	0.0196		
3	0.00299			3	0.0193		
1	0.0024	0.0025	0.0001	1	0.0156	0.0154	0.0002
2	0.0025			2	0.0154		
3	0.0026			3	0.0152		
1	0.00174	0.00174	0.00002	1	0.01	0.0116667	0.007638
2	0.00176			2	0.02		
3	0.00172			3	0.005		
1	0.0012	0.00122	0.00002	1	0.0081	0.00812	0.00002
2	0.00124			2	0.00814		
3	0.00122			3	0.00812		
1	0.00104	0.00104	0.00002	1	0.0074	0.0075	0.00010
2	0.00106			2	0.0075		
3	0.00102			3	0.0076		
No. of Expt.	X_2 Values	Mean X_2	Std Dev.	No.of Expt.	C_{eq2} Values	Mean C_{eq2}	Std Dev.
1	0.0009	0.0009	0.00001	1	0.0069	0.0069233	0.00007
2	0.00091			2	0.00687		
3	0.00089			3	0.007		
1	0.00039	0.00036	0.00003	1	0.005	0.0053333	0.000577
2	0.00036			2	0.006		
3	0.00033			3	0.005		

References

A. A. Ahmad, B. H. Hameed and N. Aziz, Adsorption of direct dyes on plant ash: kinetic and equilibrium modelling, J. Hazard. Mater. 141 (2007) 70 – 76.

A. A. Robinson, J. B. Belden, M. J. Lydy, Toxicity of fluoroquinolone antibiotics to aquatic organisms. Environ. Toxicol. Chem. 24 (2005) 423-430.

A. Bagreev, S. Bashkova, D.C. Locke, T.J. Bandosz, Sewage Sludge-Derived Materials as Efficient Adsorbents for Removal of Hydrogen Sulfide, Environ. Sci. Technol. 35 (2001) 1537-1543.

A. C. Lua and Q. Jia, Adsorption of phenol by oil-palm-shell activated carbons in a fixed bed, Chem. Eng. J. 150 (2009) 455-461.

A. Dabrowski, Adsorption: From Theory to Practice. Adv. Colloid Interface Sci.93 (2001) 135-224.

A. Dordio, S. Miranda, J. Ramalho, A. Carvalho, Mechanisms of removal of three widespread pharmaceuticals by two clay materials. J. Hazard. Mater. 323 (5) (2017) 575-583.

A. Erto, A. Lancia, D. Musmarra. A Real Adsorbed Solution Theory model for competitive multicomponent liquid adsorption onto granular activated carbon. Microporous and Mesoporous Mater. 154 (2012) 45-50.

A. Göbel, A. Thomsen, C.S. McArdell, A. Joss, W. Giger, Occurrence and sorption behavior of sulfonamides, macrolides, and trimethoprim in activated sludge treatment. Environ. Sci. Technol. 39 (2005) 3981-3989.

A. Gobel, C.S. McArdell, A. Joss, H. Siegrist, W. Giger, Fate of sulfonamides, macrolides, and trimethoprim in different wastewater treatment technologies, Sci. Total Environ. 372 (2007) 361-371.

A. Gulkowska, H.W. Leung, M.K. So, S. Taniyasu, N. Yamashita, L.W. Yeung, B.J. Richardson, A.P. Lei, J.P. Giesy, P.K. Lam, Removal of antibiotics from wastewater by sewage treatment facilities in Hong Kong and Shenzhen, China, Water Res. 42 (2008) 395-403.

A. Joss, E. Keller, A.C. Alder, A. Göbel, C.S. McArdell, T. Ternes et al. Removal of pharmaceuticals and fragrances in biological wastewater treatment, Water Res. 39 (2005) 3139–3152.

A. K. Mishra, Smart materials for waste water applications. John Wiley & Sons (2016).

A. M. Comerton, R. C. Andrews, D. M. Bagley, P. Yang, Membrane adsorption of endocrine disrupting compounds and pharmaceutically active compounds. J. Memb. Sci. 303 (1-2) (2007) 267-277.

A. Motiei, B. Brindefalk, M. Ogonowski, R. El-Shehawy, P. Pastuszek, K. Ek, B. Liewenborg, K. Udekwu, E. Gorokhova, Disparate effects of antibiotic-induced microbiome change and enhanced fitness in *Daphnia magna*. PloS One 15 (2020) e0214833.

A. O. Aderemi, S. C. Novais, M. F. L. Lemos, L. M. Alves, C. Hunter, O. Pahl, Oxidative stress responses and cellular energy allocation changes in microalgae following exposure to widely used human antibiotics. Aquat. Toxicol. 203 (2018) 130-139.

A. Prieto, M. Möder, R. Rodil, et al. Degradation of the antibiotics norfloxacin and ciprofloxacin by a white-rot fungus and identification of degradation products. Bioresour. Technol. 102 (2011) 10987–10995.

A. Ros, M.A. Montes-Moran, E. Fuente, D.M. Nevskaia, M.J. Martin, Dried Sludges and Sludge Based Chars for H2S Removal at Low Temperature: Influence of Sewage Sludge Characteristics, Environ. Sci. Technol. 40 (2006) 302-309.

A. Rusu, G .Hancu, V Uivaroşi, Fluoroquinolone pollution of food, water and soil, and bacterial resistance. Environ Chem Lett 13 (2014) 21–36.

A. S. Luna, A.L. Costa, A.C. da Costa, C.A. Henriques, Competitive biosorption of cadmium(II) and zinc(II) ions from binary systems by Sargassum filipendula. Bioresour. Technol. 101 (14) (2010), 5104–5111.

A. S. Maia, P. Paíga, C. Delerue-Matos, P.M.L. Castro, M.E. Tiritan, Quantification of fluoroquinolones in wastewaters by liquid chromatography-tandem mass spectrometry. Environ. Pollut. 259 (2020) 113927.

A. Tauxe-Wuersch, L.F. De Alencastro, D. Grandjean, J. Tarradellas, Occurrence 28 of several acidic drugs in sewage treatment plants in Switzerland and risk assessment, Water Res. 39 (2005) 1761-1772.

A. W. Adamson and A. P. Gast, Physical Chemistry of Surfaces, 6th Edition. Wiley-Interscience, New York (1997).

B. Bortone, C. Jackson, Y. Hsia, J. Bielicki, N. Magrini, M. Sharland, High global consumption of potentially inappropriate fixed dose combination antibiotics: analysis of data from 75 countries. PloS One 16 (2021) e0241899.

B. Halling-Sørensen, H. C. H. Lützhøft, H. R. Andersen, F.Ingerslev, Environmental risk assessment of antibiotics: comparison of mecillinam, trimethoprim and ciprofloxacin. J.Antimicrob.Chemother. 46 (2000) 53-58.

B. Kasprzyk-Hordern, R.M. Dinsdale, A.J. Guwy, The removal of pharmaceuticals, personal care products, endocrine disruptors and illicit drugs during wastewater treatment and its impact on the quality of receiving waters. Water Res. 43 (2009) 363–380.

B. Li and T. Zhang, Biodegradation and Adsorption of Antibiotics in the Sewage sludge Process. Environ. Sci. Technol. 44 (2010) 3468–3473.

B. Petrie, D. Camacho-Mu˜noz, Analysis, fate and toxicity of chiral non-steroidal anti-inflammatory drugs in wastewaters and the environment: a review. Environ. Chem. Lett. 19 (2021) 43–75.

B. Petrie, E.J. McAdam, M.D. Scrimshaw, J.N. Lester, E. Cartmell, Fate of drugs during wastewater treatment. TrAC Trends Anal. Chem. 49 (2013a) 145–159.

B. S. Rathi, P. S. Kumar, D. V. N. Vo, Critical review on hazardous pollutants in water environment: occurrence, monitoring, fate, removal technologies and risk assessment. Sci. Total Environ. 797 (2021) 149134.

B. Sizirici1, I. Yildiz, Organic matter removal via activated sludge immobilized gravel in fixed bed reactor. E3S Web of Conferences 191(2020) 03006.

B. Tang, Y. Lin, P. Yu and Y. Luo, Study of aniline/-caprolactam mixture adsorption from aqueous solution onto granular activated carbon: Kinetics and equilibrium, Chem. Eng. J. 187 (2012) 69–78.

B. Van Der Bruggen, J. Schaep, D. Wilms, C. Vandecasteele, Influence of molecular size, polarity and charge on the retention of organic molecules by nanofiltration. J. Memb. Sci. 156 (1) (1999) 29-41.

C. Afonso-Olivares, Z. Sosa-Ferrera, J.J. Santana-Rodríguez, Analysis of anti-inflammatory, analgesic, stimulant and antidepressant drugs in purified water from wastewater treatment plants using SPE-LC tandem mass spectrometry, J. Environ. Sci. Health A 47 (2012) 887–895.

C. F. Carolin, P. S. Kumar, G. J. Joshiba, V. V. Kumar, Analysis and removal of pharmaceutical residues from wastewater using membrane bioreactors: a review. Environ. Chem. Lett. 19 (2021) 329–343.

C. G. Daughton, T. A. Ternes, Pharmaceuticals and personal care products in the environment: Agents of subtle change?, Environ. Health Perspect. 107 (1999) 907-938.

C. Ort, M.G. Lawrence, J. Reungoat, G. Eaglesham, S. Carter, J. Keller, Determining the fraction of pharmaceutical residues in wastewater originating from a hospital, Water Res. 44 (2010) 605–615.

C. Sarangapani, D. Ziuzina, P. Behan, D. Boehm, B. F. Gilmore, P. J. Cullen, P. Bourke, Degradation kinetics of cold plasma-treated antibiotics and their antimicrobial activity. Sci. Rep. 9 (2019) 3955.

C. Tien, Adsorption calculations and modeling. Butterworth-Heinemann (1994).

C. Zhang, U. Tezel, K. Li, D. Liu, R. Ren, J. Du, S. G. Pavlostathis, Evaluation and modeling of benzalkonium chloride inhibition and biodegradation in activated sludge. Water Res. 45 (2011) 1238-1246.

Costa C. A. Rodrigues, Design of cyclic fixed-bed adsorption processes. Part I: phenol adsorption on polymeric adsorbents. AEChE J; (United States) 31 (11) (1985) 1645–1654.

Costa C. A. Rodrigues, S. Guan, H. Wu, L. Yang, Z. Wang, J. Wu, Use of a magnetic covalent organic framework material with a large specific surface area as an effective adsorbent for the extraction and determination of six fluoroquinolone antibiotics by HPLC in milk sample. J. Sep. Sci. 43 (2020) 3775–3784.

D. Akhil, D. Lakshmi, A. Kartik, D.V.N. Vo, J. Arun, K.P. Gopinath, Production, characterization, activation and environmental applications of engineered biochar: a review. Environ. Chem. Lett. 19 (2021a) 2261–2297.

D. Akhil, D. Lakshmi, P. Senthil Kumar, D. V. N. Vo, A. Kartik, Occurrence and removal of antibiotics from industrial wastewater. Environ. Chem. Lett. 19 (2021b) 1477–1507.

D. Banerjee, S. Basu, U. Sarkar, Removal of chlorhexidine gluconate in presence of a cationic surfactant using acid functionalized activated carbon: Validation of multicomponent models. J. Environ. Chem. Eng. 8 (5) (2020) 104154.

D. Banerjee, U. Sarkar, D. Roy, Multicomponent adsorption of chlorhexidine gluconate in presence of a cationic surfactant: Role of electrostatic interactions and surface complexation. J. Environ. Chem. Eng.1(3) (2013) 241-251.

D. Banerjee, U. Sarkar, D. Roy, Removal of a cationic bisbiguanide using Functionalized Activated Carbons (FACs). Process Saf. Environ. Prot. 92 (6) (2014) 957-972.

D. Bendz, N. A. Paxéus, T.R. Ginn, F.J. Loge, Occurrence and fate of pharmaceutically active compounds in the environment, a case study: Höje River in Sweden, J. Hazard. Mater. 122 (2005) 195-204.

D. C. da Silva, C.C. Oliveira, Development of micellar HPLC-UV method for determination of pharmaceuticals in water samples, J. Anal. Methods Chem. 2018 (2018) 1-12.

D. C. K. Ko, J. F. Porter, and G. Mckay, Fixed Bed Studies for the Sorption of Metal Ions onto Peat, Process Saf. Environ. Prot. 81 (2) (2003) 73–86.

D. C. Sharma & C. F. Forster, A comparison of the sorbtive characteristics of leaf mould and activated carbon columns for the removal of hexavalent chromium. Process Biochem. 31 (1996)213–218.

D. E. Wurster, K. A. Alkhamis and L. E. Matheson, Prediction of adsorption from multicomponent solutions by activated carbon using single-solute parameters. AAPS Pharm. Sci. Tech. 1(3) (2000), article 25.

D. G. Larsson, C.de Pedro, N. Paxeus, Effluent from drug manufactures contains extremely high levels of pharmaceuticals. J. Hazard Mater. 148 (2007) 751-755.

D. K. Mahmoud, M. A. M. Salleh, W. A. W. A. Karim, A. Idris, Z. Z. Abidina, Batch adsorption of basic dye using acid treated kenaf fibre char: Equilibrium, kinetic and thermodynamic studies. Chem. Eng. J. 181–182 (2012) 449–457.

D. Kratochvil and B. Volesky, Multicomponent biosorption in fixed beds, Water Res. 34 (12) (2000) 3186–3196.

D. Liu, Y. Tao, K. Li, J. Yu, Influence of the presence of three typical surfactants on the adsorption of nickel (II) to aerobic activated sludge. Bioresour.Technol. 126 (2012) 56-63.

D. M. Pavlovi´c, S. Babi´c, A.J.M. Horvat, M. Kaˇstelan-Macan, Sample preparation in analysis of pharmaceuticals, TrAC Trends Anal. Chem. 26 (2007) 1062–1075.

D. Reichenberg, Properties of ion-exchange resins in relation to their structure. III. Kinetics of exchange. J. Am. Chem. Soc. 75 (1953) 589-597.

D. Vishnu, B. Dhandapani, G. K. Panchamoorthy, D. V. N. Vo, S. R. Ramakrishnan, Comparison of surface-engineered superparamagnetic nano sorbents with low-cost adsorbents of cellulose, zeolites and biochar for the removal of organic and inorganic pollutants: a review. Environ. Chem. Lett. 19 (2021) 3181–3208.

D. W. Kolpin, E. T. Furlong, M. T. Meyer, E.M. Thurman, S. D. Zaugg, L. B. Barber, H. T. Buxton, Pharmaceuticals, hormones, and other organic

wastewater contaminants in US streams, 1999-2000: A national reconnaissance, Environ. Sci. Technol. 36 (2002) 1202-1211.

E. Awuah, R. Amankwaa-Kuffuor, "Characterisation of Wastewater, its sources and its Environmental Effects" I-Learning Seminar on Urban Wastewater Management (2002).

E. Gorokhova, C. Rivetti, S. Furuhagen, A. Edlund, K. Ek, M. Breitholtz, Bacteria-Mediated Effects of Antibiotics on Daphnia Nutrition, Environ. Sci. Technol. 49 (2015) 5779−5787.

E. I. Unuabonah, B. I. Olu-Owolabi, E. I. Fasuyi, K. O. Adebowale, Modelling of fixed-bed column studies for the adsorption of cadmium onto novel polymer-clay composite adsorbent. J. Hazard. Mater.179 (2010) 415–423.

E. J. McAdam, J. P. Bagnall, Y. K. K. Koh, et al. Removal of steroid estrogens in carbonaceous and nitrifying activated sludge processes. Chemosphere 81 ((2010)) 1–6.

E. M. Eckert, G. M. Quero, A. Di Cesare, G.Manfredini, F.Mapelli, S.Borin, D. Fontaneto, G. M. Luna, G.Corno, Antibiotic disturbance affects aquatic microbial community composition and food web interactions but not community resilience. Mol. Ecol. 28 (2019) 1170–1182.

E. Malkoc, Y. Nuhoglu, and Y. Abali, Cr(VI) adsorption by waste acorn of Quercus ithaburensis in fixed beds: Prediction of breakthrough curves, Chem. Eng. J. 119 (1) (2006) 61–68.

E. Malkoc, Y. Nuhoglu, Fixed bed studies for the sorption of chromium (VI) onto tea factory waste. Chem. Eng. Sci. 61 (2006) 4363–4372.

E. Smidt, P. Lechner, M. Schwanninger, G. Haberhauer, M.H. Gerzabek, Characterization of waste organic matter by FT-IR spectroscopy: application in waste science. Appl. Spectrosc. 56 (9) (2002) 1170 – 1175.

E. Tilley, L. Ulrich, C. Lüthi, Ph. Reymond, C. Zurbrügg, Compendium of Sanitation Systems and Technologies (2nd Revised ed.). Duebendorf, Swiss Federal Institute of Aquatic Science and Technology (Eawag) Switzerland

(2014). ISBN 978 – 3 – 906484 – 57 - 0. Archived from the original on 8April 2016.

E. Vazirinasab, R. Jafari, G. Momen, Application of superhydrophobic coatings as a corrosion barrier: a review. Surf. Coat. Technol. 341 (2018) 40–56.

E. Vulliet, C. Cren-Oliv´e, M. F. Grenier-Loustalot, Occurrence of pharmaceuticals and hormones in drinking water treated from surface waters. Environ. Chem. Lett. 9 (2011) 103–114.

E. Walters, K. McClellan, R.U. Halden, Occurrence and loss over three years of 72 pharmaceuticals and personal care products from biosolids–soil mixtures in outdoor mesocosms, Water Res. 44 (2010) 6011-6020.

E1-Hendawy ANA. Influence of HNO_3 oxidation on the structure and adsorptive properties of corncob-based activated carbon. Carbon 41 (2003) 713-722.

El-Khaiary, M.I., Malash, G.F., Common data analysis errors in batch adsorption studies. Hydrometallurgy 105 (2011) 314-320.

F. Rozada, L.F. Calvo, A.I. García, J. Martín-Villacorta, M. Otero, Dye adsorption by sewage sludge-based activated carbons in batch and fixed-bed systems, Bioresour. Technol. 87 (2003) 221-230.

Food and Agricultural Organisation Wastewater Treatment (2006) http://www.fao.org/docrep/t0551e/t0551e06.htm#TopOfPage.

Friedrich G. Helfferich (1995) Ion Exchange.

G. Gopal, C. Natarajan, A. Mukherjee, Adsorptive removal of fluoroquinolone antibiotics using greensynthesized and highly efficient Fe clay cellulose-acrylamideBeads. Environ. Technol. Innov. 28 (2022) 102783.

G. McKay and M. J. Bino, Fixed bed adsorption for the removal of pollutants from water, Environ.Pollut., 66 (1) (1990) 33–53.

G. S. Bohart, E. Q. Adams, Some aspects of the behavior of charcoal with respect to chlorine. J. Am. Chem. Soc. 42 (1920) 523–544.

G. Thirupathi, C. P. Krishnamoorthy, and S. Pushpavanam, Adsorption characteristics of inorganic salts and detergents on sand beds, Chem. Eng. J.125 (3) (2007) 177–186.

G. Xu, X. Yang, L. Spinosa, Development of sludge-based adsorbents: Preparation, characterization, utilization and its feasibility assessment, J. Environ. Manage.151 (2015) 221-232.

H. C. Thomas, Heterogeneous Ion Exchange in a Flowing System, J. Am. Chem. Soc. 66 (10) (1944)1664–1666.

H. D. S. S. Karunarathne, B. M. W. P. K. Amarasinghe. Fixed Bed Adsorption Column Studies for the Removal of Aqueous Phenol from Activated Carbon Prepared from Sugarcane Bagasse. Energy Procedia 34 (2013) 83 – 90.

H. R. Andersen, M. Hansen, J. Kjolholt, F. Stuer-Lauridsen, T. Ternes, B. Halling-Sorensen, Assessment of the importance of sorption for steroid estrogens removal during activated sludge treatment, Chemosphere 61 (2005) 139 – 146.

H. R. Rogers, Sources, behaviour and fate of organic contaminants during sewage treatment and in sewage sludges. Sci. Total Environ. 185 (1996) 3-26.

H. Tian, T. Liu, G. Mu, F. Chen, M. He, S. You, M. Yang, Y. Li, F. Zhang, Rapid and sensitive determination of trace fluoroquinolone antibiotics in milk by molecularly imprinted polymer-coated stainless-steel sheet electrospray ionization mass spectrometry. Talanta. 219 (2020) 121282.

H. Yao, J. Lu, J. Wu, Z. Lu, P. Wilson, Y. Shen, Adsorption of fluoroquinolone antibiotics by wastewater sludge biochar: role of the sludge source. Water, Air, Soil Pollut. 224 (2013) 1370.
https://water.unl.edu/article/wastewater/wastewater-what-it

I. Karampela, M. Dalamaga, Could Respiratory Fluoroquinolones, Levofloxacin and Moxifloxacin, Prove to be Beneficial as an Adjunct Treatment in COVID-19? Arch Med Res 51 (2020) 741–742.

I. Michael, L. Rizzo, C.S. McArdell, C.M. Manaia, C. Merlin, T. Schwartz, C. Dagot, D. Fatta-Kassinos, Urban wastewater treatment plants as hotspots for the release of antibiotics in the 2 environment: A review, Water Res. 47 (2013) 957-995.

I. T. Carvalho, L. Santos,Antibiotics in the aquatic environments: a review of the European scenario, Environ. Int.94 (2016) 736-757.

I. Villaescusa, N. Fiol, J. Poch, A. Bianchi, C. Bazzicalupi, Mechanism of paracetamol removal by vegetable wastes: the contribution of Π–Π interactions, hydrogen bonding and hydrophobic effect. Desalination 270 (2011) 135-142.

J. C. Crittenden, W.J. Weber, Predictive Model for Design of Fixed-Bed Adsorbers: Single-Component Model Verification. Journal of the Environmental Engineering Division 104 (1978) 433–443.

J. Coates, Interpretation of Infrared Spectra, A Practical Approach, in Encyclopedia of Analytical Chemistry, Chichester, UK: John Wiley & Sons, Ltd, 2006.

J. Crittenden, J. Berrigan, and D. Hand, Design of rapid small-scale adsorption tests for a constant diffusivity, J. Water Pollut. Control Fed. 1986.

J. D. Maul, L.J.Schuler, J.B.Belden, M.R.Whiles, M.J.Lydy, Effects of the antibiotic ciprofloxacin on stream microbial communities and detritivorous macroinvertebrates. Environmental Toxicology and Chemistry: An International Journal 25 (2006) 1598-1606.

J. E. Drewes, T. Heberer, K. Reddersen, Fate of Pharmaceuticals DuringIndirect Potable Reuse, Water Sci. Technol. 46 (3) (2002) 73-80.

J. F. Ericson, Evaluation of the OECD 314B activated sludge die-away test for assessing the biodegradation of pharmaceuticals, Environ. Sci. Technol. 44 (2010) 375-381.

J. Goel, K. Kadirvelu, C. Rajagopal, V. K. Garg, Removal of lead(II) by adsorption using treated granular activated carbon: Batch and column studies. J. Hazard. Mater. 125 (2005) 211–220.

J. H. Tay, P. Yang, W. Q. Zhuang, S. T. L. Tay, Z.H.Pan, Reactor performance and membrane filtration in aerobic granular sludge MBR. J. Membr. Sci. 304 (2007) 24-32.

J. Ho Yun, H. Chul Park, H. Moon, Multicomponent adsorption calculations based on adsorbed solution theory. Korean J. Chem. Eng**.** 13 (1996) 246–254.

J. L. Sotelo, A. Rodríguez, S. Álvarez, J. García. Removal of caffeine and diclofenac on activated carbon in fixed bed column: Chem. Eng. Res. Des. 90 (7) (2012) 967-974.

J. R. Rao and T. Viraraghavan, Biosorption of phenol from an aqueous solution by Aspergillus niger biomass, Bioresour. Technol. 85 (2)(2002) 165–171.

J. Radjenović, M. Petrović, D. Barceló, Fate and distribution of pharmaceuticals in wastewater and sewage sludge of the conventional activated sludge (CAS) and advanced membrane bioreactor (MBR) treatment. Water Res 43 (2009) 831–841.

J. Rivera-Utrilla, M. Sánchez-Polo, M.Á. Ferro-García, G. Prados-Joya, R.Ocampo-Pérez, Pharmaceuticals as emerging contaminants and their removal from water: A review, Chemosphere. 93 (2013) 1268-1287.

J. S. Jain, V. L. Snoeyink, Adsorption from bisolute systems on active carbon. Journal (Water Pollution Control Federation). (1973) 2463-2479.

J. Wang, S. Wang, Removal of pharmaceuticals and personal care products (PPCPs) from wastewater: a review. J. Environ. Manage. 182 (2016) 620-640.

K. Alkhamis, M. Salem, M. Khanfar, The sorption of ketotifen fumarate bychitosan. AAPS Pharm. Sci. Tech. 9 (2008) 866–869.

K. H. Chu, Breakthrough curve analysis by simplistic models of fixed bed adsorption: In defense of the century-old Bohart-Adams model. Chem. Eng. J.380 (2020) 122513.

K. Kümmerer, A. Al-Ahmad, V. Mersch-Sundermann, Biodegradability of some antibiotics, elimination of the genotoxicity and affection of wastewater bacteria in a simple test. Chemosphere 40 (2000) 701-710.

K. Kümmerer.,Antibiotics in the aquatic environment - a review - part I, Chemosphere (2009).

K. M. Onesios, J. T. Yu, E. J. Bouwer, Biodegradation and removal of pharmaceuticals and personal care products in treatment systems: A review, Biodegradation. 20 (2009) 441-466.

K. Vijayaraghavan, D. Prabu, Potential of Sargassum wightii biomass for copper(II) removal from aqueous solutions: Application of different mathematical models to batch and continuous biosorption data. J. Hazard. Mater. 137 (2006) 558–564.

K. Vijayaraghavan, J. Jegan, K. Palanivelu, M. Velan, Batch and column removal of copper from aqueous solution using a brown marine alga Turbinaria ornata. Chemical Engineering Journal 106 (2005) 177–184.

K. Y. Foo, B. H. Hameed, Insights into the modeling of adsorption isotherm systems. Chem. Eng. J.156 (2010) 2-10.

L. Bing, T. Zhang, Biodegradation and adsorption of antibiotics in the activated sludge process. Environ. Sci. Technol. 44 (2010) 3468-3473.

L. Fournel, P. Mocho, R. Brown, P. le Cloirec, Modeling breakthrough curves of volatile organic compounds on activated carbon fibers. Adsorption 16 (2010) 147–153.

L. Lapidus and N. R. Amundson, Mathematics of Adsorption in Beds. VI. The Effect of Longitudinal Diffusion in Ion Exchange and Chromatographic Columns, J. Phys. Chem. 56 (8) (1952) 984–988.

L. Leng, X. Yuan, H. Huang, J. Shao, H. Wang, X. Chen, G. Zeng, Bio-char derived from sewage sludge by liquefaction: Characterization and application for dyeadsorption, Appl. Surf. Sci. 346 (2015) 223-231.

L. Madhura, S. Singh, S.Kanchi, M.Sabela, K.Bisetty, Inamuddin, Nanotechnology-based water quality management for wastewater treatment. Environ. Chem. Lett. 17 (2019) 65–121.

L. R. Marcelo, J. S. de Gois, A. A. da Silva, D. V. Cesar, Synthesis of iron-based magnetic nanocomposites and applications in adsorption processes for water treatment: a review. Environ. Chem. Lett. 19 (2021) 1229-1274.

L. Wang, Z. Qiang, Y. Li, Weiwei Ben. An insight into the removal of fluoroquinolones in sewage sludge process: Sorption and biodegradation characteristics. J. Environ. Sci. 56 (2017) 263-271.

L. Yu, M.E. Yue, J. Xu, T.F. Jiang, Determination of fluoroquinolones in milk, honey and water samples by salting out-assisted dispersive liquid-liquid microextraction based on deep eutectic solvent combined with MECC. Food Chem. 332 (2020) 127371.

M. A. E. de Franco, C. B. de Carvalho, M. M. Bonetto, R. de P. Soares, and L. A. Féris, Removal of amoxicillin from water by adsorption onto activated carbon in batch process and fixed bed column: Kinetics, isotherms, experimental design and breakthrough curves modelling, J. Clean. Prod. 161 (2017) 947–956.

M. Abhinaya, R. Parthiban, P. S. Kumar, D. V. N. Vo, A review on cleaner strategies for extraction of chitosan and its application in toxic pollutant removal. Environ. Res. 196 (2021) 110996.

M. Amarasiri, D. Sano, S. Suzuki, Understanding human health risks caused by antibiotic resistant bacteria (ARB) and antibiotic resistance genes (ARG) in water environments: current knowledge and questions to be answered. Crit. Rev. Environ. Sci. Technol. 50 (2020) 2016–2059.

M. Ashfaq, K. N .Khan, S. Rasool, G. Mustafa, M. Saif-Ur-Rehman, et al., Occurrence and ecological risk assessment of fluoroquinolone antibiotics in hospital waste of Lahore. Pak., Environ. Toxicol. Pharm. 42 (2016) 16–22.

M. Caban, P. Stepnowski, How to decrease pharmaceuticals in the environment? A review, Environ. Chem. Lett. 19 (2021) 3115–3138.

M. Clara, N. Kreuzinger, B. Strenn, O. Gans, H. Kroiss, The solids retention time - a suitable design parameter to evaluate the capacity of wastewater treatment plants to remove 36 micropollutants, Water Res. 39 (2005) 97-106.

M. D. Hernando, M. Mezcua, A.R. Fernandez-Alba, D. Barcelo, Environmentalrisk assessment of pharmaceutical residues in wastewater effluents, surface waters and sediments, Talanta. 69 (2006) 334-342.

M. D. LeVan, T. Vermeulen, Binary Langmuir and Freundlich isotherms for ideal adsorbed solutions. J. Phys. Chem. 85 (1981) 3247-3250.

M. Farr´e, M. Petrovic, D. Barcel´o, Recently developed GC/MS and LC/MS methods for determining NSAIDs in water samples, Anal. Bioanal. Chem. 387 (4) (2007) 1203–1214.

M. González-Pleiter, S. Gonzalo, I. Rodea-Palomares, et al. Toxicity of five antibiotics and their mixtures towards photosynthetic aquatic organisms: Implications for environmental risk assessment. Water Res 47 (2013) 2050–2064.

M. Grassi, L. Rizzo, A. Farina, Endocrine disruptors compounds, pharmaceuticals and personal care products in urban wastewater: Implications for agricultural reuse and their removal by adsorption process. Environ. Sci. Pollut. Res. 20 (6) (2013) 3616-3628.

M. Hu, X.H. Wang, X.H. Wen, Y. Xia, Microbial community structures in different wastewater treatment plants as revealed by 454-pyrosequencing analysis. Bioresour. Technol. 117 (2014) 72-79.

M. I. El-Khaiary, G. F. Malash, Common data analysis errors in batch adsorption studies. Hydrometallurgy 105 (2011) 314-320.

M. J. Ahmed, B. H. Hameed, Removal of Emerging Pharmaceutical Contaminants by Adsorption in a Fixed-Bed Column: A Review. Ecotoxicol. Environ. Saf. 149 (2018) 257−266.

M. J. Bueno, M. J. Gomez, S. Herrera, M.D. Hernando, A. Aguera, A.R. Fernandez-Alba, Occurrence and persistence of organic emerging contaminants and priority pollutants in five sewage treatment plants of Spain: Two years pilot survey monitoring, Environ Pollut. 164 (2012) 267-273.

M. Kah, G. Sigmund, F. Xiao, T. Hofmann, Sorption of ionizable and ionic organic compounds to biochar, activated carbon and other carbonaceous materials. Water Res. 124 (2017) 673–692.

M. Kobya, Removal of Cr(VI) from aqueous solutions by adsorption onto hazelnut shell activated carbon: kinetic and equilibrium studies. Bioresour. Technol. 91 (2004) 317–321.

M. Lehmann, A. I. Zouboulis, and K. A. Matis, Modelling the sorption of metals from aqueous solutions on goethite fixed-beds, Environ. Pollut. 113 (2) (2001) 121–128.

M. Low, Kinetics of chemisorption of gases on solids. Chem. Rev. 60 (1960) 267-312.

M. M. Bello, A. A. A. Raman, Synergy of adsorption and advanced oxidation processes in recalcitrant wastewater treatment. Environ. Chem. Lett. 17 (2019) 1125–1142.

M. Mobin, Huda, M. Shoeb, R. Aslam, and P. Banerjee, Synthesis, characterisation and corrosion inhibition assessment of a novel ionic liquid-graphene oxide nanohybrid. J. Mol. Struct. 1262 (2022) 133027.

M. P. Schlüsener, K. Bester, Persistence of antibiotics such as macrolides, tiamulin and salinomycin in soil. Environ. Pollut. 143 (2006) 565-571.

M. U. Dural, L. Cavas, S. K. Papageorgiou, F. K. Katsaros, Methylene blue adsorption on activated carbon prepared from Posidoniaoceanica (L.) dead leaves: Kinetics and equilibrium studies. Chem. Eng. J.168 (2011) 77-85.

M.Z. Othman, F. A. Roddick, R. Snow, Removal of dissolved organic compounds in fixed-bed columns: Evaluation of low-rank coal adsorbents. Water Res 35 (2001) 2943–2949.

M-C. Huang, C-H. Chou, H. Teng, Pore-size effects on activated-carbon capacities for volatile organic compound adsorption. AIChE Journal 48 (2002) 1804–1810.

Metcalf and Eddy, Inc.. “Wastewater Engineering”: Treatment Disposal and Reuse, third edition. New York: McGraw-Hill (1991).

N. A. Séveno, D. Kallifidas, K. Smalla, J.D. van Elsas, J. M. Collard,, A. D. Karagouni, E. M. Wellington, Occurrence and reservoirs of antibiotic resistance genes in the environment. Rev. Med. Microbiol. 13 (2002) 15-27.

N. Janecko, L. Pokludova, J. Blahova, Z. Svobodova, I. Literak, Implications of fluoroquinolone contamination for the aquatic environment–A review. Environ. Toxicol. Chem. 35 (2016) 2647–2656.

N. Jiao, Y.L. Shen, X.K. Song, The efficiency and membrane fouling characteristics of MBR for removing PPCPs in the micro-polluted water, Technol. Water Treat. 38 (2012) 90-98.

N. Kreuzinger, M. Clara, B. Strenn, H. Kroiss, Relevance of the sludge retention time 32 (SRT) as design criteria for wastewater treatment plants for the removal of endocrine 33 disruptors and pharmaceuticals from wastewater, Water Sci. Technol. 50 (2004) 149-156.

N. Le-Minch, S. J. Khan, J. E. Drewes, R.M. Stuetz, Fate of antibiotics during municipal water recycling treatment processes. Water Res. 44 (15) (2010) 4295-4323.

N. Sankararamakrishnan, P. Kumar, V Chauhan, Modeling fixed bed column for cadmium removal from electroplating wastewater. Sep. Purif. Technol. 63 (2008) 213–219.

N. Selvaraju, S. Pushpavanam, Adsorption characteristics on sand and brick beds. Chemical Engineering Journal 147 (2009) 130–138.

N. Zhang, Y. Gao, K. Sheng, W. Jing, X. Xu, T. Bao, S. Wang. Effective extraction of fluoroquinolones from water using facile-modified plant fibers. J. Pharm. Anal. 12 (2022) 791-800.

O. Altin, H. O. Ozbelge, T. Dogu, Use of General Purpose Adsorption Isotherms for Heavy Metal–Clay Mineral Interactions. J. Colloid and Interface Sci. 198 (1998) 130-140.

O. Hamdaouia and E. Naffrechoux, Modeling of adsorption isotherms of phenol and chlorophenols onto granular activated carbon Part I. Two-parameter models and equations allowing determination of thermodynamic parameters. J. Hazard. Mater. 147 (2007) 381-394.

O. Moradi, A. Fakhri and S. Adami, Isotherm, thermodynamic, kinetics, and adsorption mechanism studies of Ethidium bromide by single-walled carbon nanotube and carboxylate group functionalized single-walled carbon nanotube. J. Colloid Interface Sci. 395 (2013) 224-229.

P. A. Kumar, S. Chakraborty, Fixed-bed column study for hexavalent chromium removal and recovery by short-chain polyaniline synthesized on jute fiber. J Hazard Mater 162 (2009) 1086–1098.

P. Gao, D. Mao, Y. Luo, L. Wang, B. Xu, L. Xu, Occurrence of sulfonamide and tetracycline-resistant bacteria and resistance genes in aquaculture environment. Water Res. 46 (2012a) 2355-2364.

P. Gao, M. Munir, I. Xagoraraki, Correlation of tetracycline and sulfonamide antibiotics with corresponding resistance genes and resistant bacteria in a conventional municipal wastewater treatment plant. Sci. Total Environ. 421 (2012b) 173-183.

P. N. Christman, Industrial Odour Technology Assessment. Ann Arbor Science Publishers, Michigan (2012).

P. Suksabye, P. Thiravetyan, and W. Nakbanpote, Column study of chromium(VI) adsorption from electroplating industry by coconut coir pith, J. Hazard. Mater. 160 (1) (2008) 56–62.

P. Sukul, M. Spiteller, Fluoroquinolone antibiotics in the environment. Reviews of environmental contamination and toxicology (2007) 131-162.

P. Verlicchi, A. Galletti, M. Petrovic, D. BarcelO´, Hospital effluents as a source of emerging pollutants: an overview of micropollutants and sustainable treatment options. J. Hydrol. 389 (3-4) (2010) 416-428.

P. Westerhoff, Y. Yoon, S. Snyder, E. Wert, Fate of endocrine disruptor, pharmaceutical and personal care product chemicals during simulated drinking water treatment processes, Sci. Technol. 39 (2005) 6649 – 6663.

Q. Zhao, X.J. He, Z.P. Tang, X.D. Li, J.P. Qiu, Research Progress on Treatment Processes of Pharmaceuticals and Personal Care (PPCPs). Water Purification Technol. 29 (2010) 5-10.

R. A. Hutchins, New method simplifies design of activated-carbon systems. Chem. Eng. J. 80 (1973) 133–138.

R. Alaaeldin, M. Mustafa, Abuo-Rahma GEDA, M. Fathy, In vitro inhibition and molecular docking of a new ciprofloxacin-chalcone against SARS-CoV-2 main protease. Fundam. Clin. Pharmacol. 36 (2022) 160–170.

R. Andreozzi, V. Caprio, A. Insola, R. Marotta, Advanced oxidation processes(AOP) for water purification and recovery. Catal. Today 53 (1999) 51-59.

R. Aslam, M. Mobin, Huda, M. Murmu, P. Banerjee, and J. Aslam, L-Alanine methyl ester nitrate ionic liquid: synthesis, characterization and anti-corrosive application. J. Mol. Liq. 334 (2021) 116469.

R. Aslam, M. Mobin, Huda, M. Shoeb, M. Murmu, and P. Banerjee, Proline nitrate ionic liquid as high temperature acid corrosion inhibitor for mild steel: Experimental and molecular-level insights, J. Ind. Eng. Chem. 100 (2021) 333–350.

R. Baccar, M. Sarr`a, J. Bouzid, M. Feki, P. Bl´anquez, Removal of pharmaceutical compounds by activated carbon prepared from agricultural by-product. Chem. Eng. J. 211-212 (2012) 310-317.

R. Ding, P. Zhang, M. Seredych, T. J. Bandosz, Removal of antibiotics from water using sewage sludge- and waste oil sludge-derived adsorbents. Water Res. 46 (2012) 4081-4090.

R. Gothwal, T. Shashidhar, Antibiotic pollution in the environment: a review. Clean–Soil, Air, Water 43 (2015) 479-489.

R. Gothwal, T. Shashidhar, Occurrence of high levels of fluoroquinolones in aquatic environment due to effluent discharges from bulk drug manufacturers. J. Hazard. Toxic Radioact. Waste 21 (2017) 05016003.

R. L. Oulton, T. Kohn, D. M. Cwiertny, Pharmaceuticals and personal care products in effluent matrices: a survey of transformation and removal during wastewater treatment and implications for wastewater management. J. Environ. Monit. 12 (11) (2010) 1956-1978.

R. Petrus and J. Warchoł, Ion exchange equilibria between clinoptilolite and aqueous solutions of Na+/Cu2+, Na+/Cd2+ and Na+/Pb2+, Microporous and Mesoporous Mater. 61 (1–3) (2003) 137–146.

R. Portinho, O. Zanella, L.A. F´eris, Grape stalk application for caffeine removal through adsorption. J. Environ. Manage. 202 (2017) 178–187.

R. Rojas, E. Vanderlinden, J. Morillo, J. Usero, H. El Bakouri, Characterization of sorption processes for the development of low-cost pesticide decontamination techniques, Sci. Total Environ. 488– 489 (2014) 124-135.

R. Salgado, J.P. Noronha, A. Oehmen, G. Carvalho, M.A.M. Reis,Analysis of 65 pharmaceuticals and personal care products in 5 wastewater treatment plants in Portugal using a simplified analytical methodology, Water Sci. Technol. 62 (2010) 2862–2871.

R. Srinivasan, Advances in application of natural clay and its composites in removal of biological, organic, and inorganic contaminants from drinking water. Adv. Mater. Sci. Eng. (2011) 872531.

S. Ayoob, A. K. Gupta, and P. B. Bhakat, Analysis of breakthrough developments and modeling of fixed bed adsorption system for As(V) removal from water by modified calcined bauxite (MCB), Sep. Purif. Technol. 52 (3) (2007) 430–438.

S. Cairoli, R. Simeoli, M. Tarchi, M. Dionisi, A. Vitale, L. Perioli, C. Dionisi-Vici, B.M. Goffredo, A new HPLC–DAD method for contemporary quantification of 10 antibiotics for therapeutic drug monitoring of critically ill pediatric patients. Biomed. Chromatogr. 34 (2020) e4880.

S. D. Manjare and A. K. Ghoshal, Studies on dynamic adsorption behaviour of ethyl acetate from air on 5A and 13X molecular sieves, Canadian J. Chem. Eng. 83 (2005) 232-241.

S. D. W. Comber, M. Upton, S. Lewin, et al, COVID-19, antibiotics and One Health: a UK environmental risk assessment. Journal of Antimicrobial Chemotherapy 75 (2020) 3411.

S. Hussain, M. Naeem, M. N. Chaudhry, Estimation of residual antibiotics in pharmaceutical effluents and their fate in affected areas. Pol. J. Environ. Stud. 25 (2016) 607–614.

S. I. Polianciuc, A. E. Gurzˇau, B. Kiss, M. G. Stefan, F. Loghin, Antibiotics in the environment: causes and consequences. Med. Pharm. Rep. 93 (2020) 231–240.

S. Kim, P. Eichhorn, J. N. Jensen, A. S. Weber, D. S. Aga, Removal of antibiotics in wastewater: Effect of hydraulic and solid retention times on the fate of tetracycline in the activated sludge process. Environ. Sci. Technol. 39 (15) (2005) 5816–5823.

S. Lagergren, Zurtheorie der sogenannten adsorption gelosterstoffe, K. Sven. Vetenskapsakad. Handl. 24 (1898) 1 - 39.

S. M. Derayea, M. A. Omar, M. A. Hammad, Y. F. Hassan, K. M. Badr El-Din, Augmented spectrofluorimetric determination of certain fluoroquinolones via micellar—Metal complex connection: Application to pharmaceuticals and biological fluids. Microchem. J. 160 (2021) 105717.

S. Mondal, K. Aikat, G. Halder, Ranitidine hydrochloride sorption onto superheated steam activated biochar derived from mung bean husk in fixed bed column. J. Environ. Chem. Eng. 4 (2016) 488-497.

S. Netpradit, P. Thiravetyan, S. Towprayoon, Evaluation of metal hydroxide sludge for reactive dye adsorption in a fixed-bed column system. Water Res 38 (2004) 71–78.

S. Pe´rez, P. Eichhorn, D. S. Aga, Evaluating the biodegradability of sulfamethazine, sulfamethoxazole, sulfathiazole, and trimethoprim at different stages of sewage treatment. Environ. Toxicol. Chem. 24 (6) (2005) 1361–1367.

S. Rio, C. Faur-Brasquet, L. le Coq, P. le Cloirec, Structure Characterization and Adsorption Properties of Pyrolyzed Sewage Sludge. Environ. Sci. Technol. 39 (2005) 4249–4257.

S. Sadhukhan, S. Singha, U. Sarkar, Adsorption of para chloro meta xylenol (PCMX) in composite adsorbent beds: parameter estimation using nonlinear least square technique. Chem. Eng. J. 152 (2009) 361-366.

S. Saha, U. Sarkar, and S. Mondal., Modelling the transient behaviour of a fixed bed considering both intra and inter-pellet diffusion for adsorption of parachloro-meta-xylenol (PCMX), Desalination Water Treat. 37 (1–3) (2012) 277–287.

S. Singha, U. Sarkar, Analysis of the dynamics of a packed column using semi-empirical models: Case studies with the removal of hexavalent chromium from effluent wastewater. Korean J. Chem. Eng. 32 (2015) 20–29.

S. Singha, U. Sarkar, S. Mondal, and S. Saha, Transient behavior of a packed column of Eichhorniacrassipes stem for the removal of hexavalent chromium, Desalination. 297 (2012) 48–58.

S. Ufnalska, E. Lichtfouse, Unanswered issues related to the COVID-19 pandemic. Environ. Chem. Lett. 19 (2021) 3523–3524.

S. Weiss, T. Reemtsma, Membrane bioreactors for municipal wastewater treatment - a viable option to reduce the amount of polar pollutants discharged into surface waters. Water Res. 42 (2008) 3837-3847.

S. Xiancai, L. Dongfang, Z. Lejun, Adsorption mechanisms and impact factors of oxytetracycline on activated sludge. IOP Conference Series: Earth Environ. Sci. IOP Publishing, 59 (2017) 012068.

S. Yıldırım, H.N. Karakoç, A. Yaşar, İ. Köksal, Determination of levofloxacin, ciprofloxacin, moxifloxacin and gemifloxacin in urine and plasma by HPLC–FLD–DAD using pentafluorophenyl core–shell column: Application to drug monitoring. Biomed. Chromatogr. 34 (2020) e4925.

T. D. Nguyen, V. H. Nguyen, S. Nanda, D. V. N. Vo, V. H. Nguyen, T. Van Tran, L. N. Xuan, T. T. Nguyen, L. G. Bach, B. Abdullah, S. S. Hong, T. V. Nguyen, BiVO4 photocatalysis design and applications to oxygen production and degradationof organic compounds: a review. Environ. Chem. Lett. 18 (2020) 1779–1801.

T. L. Hill, 1986. An introduction to statistical thermodynamics. Courier Corporation.

T. Lu, Y. Zhu, M. Ke, W.J.G.M. Peijnenburg, M. Zhang, T. Wang, J. Chen, H. Qian, Evaluation of the taxonomic and functional variation of freshwater plankton

communities induced by trace amounts of the antibiotic ciprofloxacin. Environ. Int. 126 (2019) 268–278.

T. M. Darweesh, M. J. Ahmed, Adsorption of ciprofloxacin and norfloxacin from aqueous solution onto granular activated carbon in fixed bed column. Ecotoxicol. Environ. Saf.138 (2017) 139-145.

T. R. Muraleedharan, L. Philip, L. Iyengar, C. Venkobachar, Application studies of biosorption for monazite processing industry effluents. Bioresour Technol 49 (1994) 179–186.

T. Vieira Madureira, M.J. Rocha, Q. Bezerra Cass, M.E. Tiritan,Development and optimization of a HPLC-DAD method for the determination of diverse pharmaceuticals in estuarine surface waters, J. Chromatogr. Sci. 48 (2010) 176–182.

T. W. Weber and R. K. Chakravorti, Pore and solid diffusion models for fixed-bed adsorbers, AiChE J. 20 (2) (1974) 228–238.

V. K. C. Lee, J. F. Porter and G. McKay, Development of Fixed-Bed Adsorber Correlation Models, Ind. Eng. Chem. Res. 39 (2000) 2427-2433.

V. K. Gupta, P. J. M. Carrott, M. M. L. Ribeiro-Carrott, Suhas, Low-cost adsorbents: growing approach towards wastewater treatment-a review. Crit. Rev. Environ. Sci. Technol. 39 (10) (2009) 783-842.

V. Reveille, L. Mansuy, E. Jarde, E. Garnier-Sillam, Characterization of sewage sludge-derived organic matter: lipids and humic acids. Org. Geochem. 34 (4) (2003) 615 – 627.

V. Sarin, T. S. Singh, and K. K. Pant, Thermodynamic and Breakthrough Column Studies for the Selective Sorption of Chromium From Industrial Effluent on Activated Eucalyptus Bark, Bioresour. Technol. 97 (16) (2006) 1986–1993.

V. Vinayagam, S. Murugan, R. Kumaresan, M. Narayanan, M. Sillanp¨a¨a , D. V. N. Vo, O. S. Kushwaha, P. Jenis, P. Potdar, S. Gadiya. Sustainable adsorbents for the removal of pharmaceuticals from wastewater: A review. Chemosphere 300 (2022) 134597.

V.K. Sharma, N. Johnson, L. Cizmas, T. J. McDonald, H. Kim, A review of theinfluence of treatment strategies on antibiotic resistant bacteria and antibiotic resistance genes, Chemosphere. 150 (2016) 702-714.

W. H. Glaze, J. W. Kang, D. H. Chapin, The chemistry of water treatment processes involving ozone, hydrogen peroxide and ultraviolet radiation. Ozone: Sci. Eng. 9 (9) (1987) 335-352.

W. J. Weber Jr., J. C. Morris, Kinetics of adsorption on carbon from solution. Journal of the sanitary engineering division 89 (1963) 31-59.

W. N. Wan Ismail, M. I. Arif Irwan Syah, N. H. Abd Muhet, et al. Adsorption Behavior of Heavy Metal Ions by Hybrid Inulin-TEOS for Water Treatment. Civil Engineering Journal 8 (2022) 1787–1798.

W. Sheen, Z. Li and Y. Liu, Surface chemical functional groups modification of porous carbon. Recent Pat. Chem. Eng. 1 (2008) 27-40.

W. T. Vieira, M. B. de Farias, M. P. Spaolonzi, M. G. C. da Silva, M. G. A. Vieira, Removal of endocrine disruptors in waters by adsorption, membrane filtration and biodegradation. A review. Environ. Chem. Lett. 18 (2020) 1113– 1143.

W. Xu, G. Zhang, X. Li, S. Zou, P. Li, Z. Hu, J. Li, Occurrence and elimination of antibiotics at four sewage treatment plants in the Pearl River Delta (PRD), South China, Water Res. 41 (2007) 4526-4534.

W. Yang, H. Zhou, N. Cicek, Treatment of organic micropollutants in waterand wastewater by UV-based processes: a literature review. Crit. Rev. Environ. Sci. Technol. 44 (13) (2014) 1443-1476.

W. Zhu, W. Yao, Y. Zhan, Y. Gu, Phenol removal from aqueous solution by adsorption onto solidified landfilled sewage sludge and its modified sludges, J. Mater. Cycles Waste Manag. (2014) 1-10.

Wastewater engineering: treatment and reuse. George Tchobanoglous, Franklin L. Burton, H. David Stensel, Metcalf & Eddy (4th ed.). Boston: McGraw-Hill. 2003. ISBN 0-07-041878-0. OCLC 48053912.

X. Chen, S. Jeyaseelan, N. Graham, Physical and chemical properties study of the activated carbon made from sewage sludge, Waste Manage. 22 (2002) 755-760.

X. Li, M. Ji, L. D. Nghiem, Y. Zhao, D. Liu, Y. Yang, Q. Wang, Q. T. Trinh, D. V. N. Vo, V. Q. Pham, N. H. Tran, A novel red mud adsorbent for phosphorus and diclofenac removal from wastewater. J. Mol. Liq. 303 (2020) 112286.

X. S. Miao, F. Bishay, M. Chen, C.D. Metcalfe, Occurrence of antimicrobials in the final effluents of wastewater treatment plants in Canada. Environ. Sci. Technol. 38 (2004) 3533-3541.

X. Tan, Y. Liu, G. Zeng, X. Wang, X. Hu, Y. Gu, Z. Yang, Application of biochar for the removal of pollutants from aqueous solutions. Chemosphere 125 (2015) 70–85.

X. Van Doorslaer, J. Dewulf, H. Van Langenhove, K. Demeestere, Fluoroquinolone antibiotics: an emerging class of environmental micropollutants. Sci. Total Environ. 500–501 (2014) 250–269.

X. Xu, X. Cao, and L. Zhao, Comparison of rice husk- and dairy manure-derived biochars for simultaneously removing heavy metals from aqueous solutions: Role of mineral components in biochars, Chemosphere. 92 (8) (2013) 955–961.

Y. A. Alhamed, Adsorption kinetics performance of packed bed adsorber for phenol removing using activated carbon from dates stones, J. Hazard. Mater. 170 (2009) 763-770.

Y. Fu and T. Viraraghavan, Column studies for biosorption of dyes from aqueous solutions on immobilised Aspergillus niger fungal biomass, Water SA, 29 (4) (2004).

Y. H. Yoon, J. H. Nelson, Application of Gas Adsorption Kinetics I. A Theoretical Model for Respirator Cartridge Service Life. Am. Ind. Hyg. Assoc. J. 45 (1984) 509−516.

Y. H. Yoon, J. H. Nelson, Application of Gas Adsorption Kinetics I. A Theoretical Model for Respirator Cartridge Service Life. Am. Ind. Hyg. Assoc. J.45 (1984) 509–516.

Y. Hsia, B.R. Lee, A. Versporten, Y. Yang, J. Bielicki, C. Jackson, J. Newland, H. Goossens, N. Magrini, M. Sharland, GARPEC, Global-PPS networks, Use of the WHO Access, Watch, and Reserve classification to define patterns of hospital antibiotic use (AWaRe): an analysis of paediatric survey data from 56 countries. Lancet Glob. Health 7 (2019) e861–e871.

Y. K. K. Koh, T. Y. Chiu, A. R. Boobis, et al, Influence of operating parameters on the biodegradation of steroid estrogens and nonylphenolic compounds during biological wastewater treatment processes. Environ. Sci. Technol. 43 (2009) 6646–6654.

Y. S. Ho and G. McKay, Pseudo-second order model for sorption processes, Process Biochem. 34 (5) (1999) 451–465.

Y. S. Ho, Review of second order models for adsorption systems, J. Hazard. Mater. 136 (2006) 681 – 689.

Y. Su, X. Sun, X. Zhou, C. Dai, Y. Zhang, Zero-valent iron doped carbons readily developed from sewage sludge for lead removal from aqueous solution, J. Environ. Sci. 36 (2015) 1-8.

Y. Suyadal, M. Erol, H. Oguz, Deactivation model for adsorption of TCE vapour on an activated carbon bed. Ind. Eng. Chem. Res. 39 (2000) 724-730.

Y. Talero-P´erez, O. Medina, W. RozoNu˜nez.,T´ecnicasanalíticascontempor´aneas para la identificaci´on de residuos de sulfonamidas, quinolonas y cloranfenicol, Univ. Sci. 19 (2014) 11–28.

Y. Yoon, P. Westerhoff, S. A. Snyder, E. C. Wert, J. Yoon, Removal of endocrine disrupting compounds and pharmaceuticals by nanofiltration and ultrafiltration membranes. Desalination 202 (1-3) (2007) 16-23.

Z. Aksu, Biosorption of reactive dyes by dried activated sludge: equilibrium and kinetic modelling, Biochem. Eng. J. 7 (2001) 79-84.

Z. Aksu, Ş. Ş. Çağatay, F. Gönen, Continuous fixed bed biosorption of reactive dyes by dried Rhizopus arrhizus: Determination of column capacity. J. Hazard. Mater. 143 (2007) 362–371.

Z. Wang, X.Y. Wang, H. Tian, Q.H. Wei, B.S. Liu, G.M. Bao, M.L. Liao, J.L. Peng, X.Q. Huang, L.Q. Wang, High through-put determination of 28 veterinary antibiotic residues in swine wastewater by one-step dispersive solid phase extraction sample clean up coupled with ultra-performance liquid chromatography-tandem mass spectrometry. Chemosphere. 230 (2019) 337–346.

Z. Zulfadhly, M. D. Mashitah, and S. Bhatia, Heavy metals removal in fixed-bed column by the macro fungus Pycnoporussanguineus, Environ. Pollut. 112 (3) (2001) 463–470.

Journal of Environmental Chemical Engineering 11 (2023) 109896

Contents lists available at ScienceDirect

Journal of Environmental Chemical Engineering

journal homepage: www.elsevier.com/locate/jece

Efficacy of convective-diffusion models to study the transient behaviour of a sewage-sludge-filled packed column for aqueous phase adsorption of fluoroquinolones: Consideration of pseudo-kinetics driven depletion of species

Rajib Kumar Das, Debamita Pal, Ujjaini Sarkar *

Department of Chemical Engineering, Jadavpur University, Kolkata 700032, West Bengal, India

ARTICLE INFO

Editor: Despo Fatta-Kassinos

Keywords:
SARS-CoV-2
Fluoroquinolones
Convective diffusion models
Pseudo-kinetics
Transient behaviour of packed bed
Damköhler number

ABSTRACT

Ciprofloxacin and ofloxacin belong to a class of antibiotics called Fluoroquinolones (FQs), which have a wide anti-bacterial activity against Gram-positive and Gram-negative bacteria. Since the recent Covid-19 pandemic witnessed a magnanimous rise in the use of antibiotics to prevent secondary bacterial infections, it led to vast production and use of such antibiotics. Ultimately the antibiotics get discharged into the municipal sewer pipes, thereby killing the useful microbial colony. In order to prevent environmental degradation a commercial scale-up of the adsorption of these antibiotics using raw sewage sludge is an absolute necessity.

In this study, a continuous adsorption operation is conducted in a packed bed of semi-dried raw sewage sludge to remove the FQs from wastewater. Two transient convective-diffusion models are developed including pseudo-first and second-order kinetics driven depletion terms. The models are optimised using the data collected under various dynamic conditions in order to analyse the performance of the packed bed in terms of bed height, flow rate and initial concentration of the FQs. Damköhler numbers of the FQs are estimated to predict the break-through times of both the FQs. The ratios of Damköhler numbers of ciprofloxacin and ofloxacin do not change much with flow rate. In all the experiments, $D_a s << 1$ for both the FQs, indicating a faster diffusion process with respect to the rate of pseudo-reaction. Diffusion reaches an 'equilibrium' well before the reaction achieves pseudo-chemical equilibrium. Ratios of the Damköhler numbers, meant to represent the first-order and second-order convective-diffusion models for ciprofloxacin to ofloxacin is < 1.

1. Introduction

In the recent past an outbreak of a pandemic triggered by SARS-CoV-2 [Severe Acute Respiratory Syndrome Corona Virus 2], also known as the Coronavirus Disease of 2019 (Covid-19) [1,2], has brought large-scale turbulence all over the globe. Health systems of almost every country have faced an acute and critical challenge during the pandemic. Most Covid-19 patients have the symptoms of fever, cough, tiredness, loss of taste and smell, and shortness of breath that resemble symptoms of a bacterial infection. Various therapeutic agents have been prescribed for effective use in the medical treatment of coronavirus related diseases [3–6]. Bacteria led secondary infections are very common features in patients suffering from Covid-19 related diseases [7]. Efficacy of specific antibiotics reported in the treatment of secondary infections includes fluoroquinolones, tetracycline, and macrolides [8]. Fluoroquinolones (FQs) are known to be a group of synthetic antibiotics that have broad-spectrum anti-bacterial effects against both gram-positive and gram-negative bacteria [9]. A variety of fluoroquinolones have been tested in vitro against SARS-CoV-2. Molecular docking studies suggested ciprofloxacin, enoxacin and moxifloxacin as possible inhibitors of SARS-CoV-2 [10]. Furthermore, some of the fluoroquinolone (FQ) derivatives have exhibited antiproliferative activity [11,12], like ciprofloxacin (CIP) on prostate and bladder cancer cells [13,14]. Other FQs such as ofloxacin, fleroxacin and levofloxacin have proven records of inhibition of growth of transitional cell bladder carcinoma cell lines [15].

Large-scale use of the FQs during and after Covid-19 pandemic has increased the quantum of FQs being discharged into inland surface

* Correspondence to: Department of Chemical Engineering, Jadavpur University, Jadavpur, Kolkata 700032, India.
E-mail address: ujjaini.sarkar@jadavpuruniversity.in (U. Sarkar).

https://doi.org/10.1016/j.jece.2023.109896
Received 3 January 2023; Received in revised form 21 March 2023; Accepted 11 April 2023
Available online 14 April 2023

waterbodies with an enhancement of risks [16]. The FQs exist in the range of ng/L to μg/L in aqueous matrices and ng/Kg to mg/Kg in solid matrices resulting in acute and chronic toxicity as well as the emergence of antibiotic-resistant bacteria [7]. Ciprofloxacin (CIP) and ofloxacin (OFLX) are broad spectrum antibiotics belonging to this class. The amount of ciprofloxacin (CIP) and ofloxacin (OFLX) found in aqueous matrices are approximately 44.0 μg/L and 35.5 μg/L respectively [17–19].

Various techniques like catalytic and photo catalytic degradation, ozonation, biodegradation, advanced oxidation, biological filtration and ion exchange processes have been applied to remove antibiotics from waste water [20–23]. Majority of these methods produces huge amount of sludge and other degraded products (mostly non-elucidated), thereby limiting effectiveness [24–26]. Accumulation of antibiotics in aquatic environments has been affecting humans through the consumption of water. Adsorption is a widely used separation process, simple as well as environment-friendly, possessing relatively higher capability of removal of contaminants when compared to other available techniques [27–29].

A huge quantity of pharmaceutical wastewater containing CIP and OFLX can be treated using a packed column with suitable adsorbent. Activated sludge is a widely used environment-friendly adsorbent for its proven ability to remove various micropollutants from waste water [30–35]. Activated sludge, composed of carbonaceous matter along with other chemical and biological constituents, is an effective adsorbent due to the presence of high degree of porosity and internal surface area [36]. Efficiency of the adsorber depends on a proper design, which in turn requires prediction of effluent concentration-time profile. Effects of several parameters i.e. height and diameter of packing, influent concentration and flow rate are examined in order to find out the breakthrough curves for a fixed bed column. In most of the semi-empirical models, including Thomas model and BDST model, cross sections of the functional adsorbent bed are considered homogeneous, thereby neglecting the radial movements. This causes significant error in the analysis because these models are developed on the basis of a strictly plug flow behaviour [37]. Thomas model assumes Langmuir equilibrium relationship to hold good for the specific adsorbent, but are mostly used extensively disregarding the sorbate-adsorbent adsorption equilibrium. Also, the original Thomas model was found computationally complex as it uses first order Bessel function [38]. The simplified Bohart-Adams model is generally unable to accurately predict the nature of the breakthrough curve beyond the breakthrough concentration of 30 % [39]. Even though the semi-empirical models are derived independently, a critical analysis performed by Khim Hoong Chu [40] shows the mathematical equivalence of simplified Bohart-Adams, simplified Thomas, and Yoon-Nelson models.

Determination of the breakthrough curve for adsorption in a packed bed is a very important concern because it provides basic but very important information in the design of a packed column. The experimental method is usually a time-consuming and un-economical process, particularly for trace contaminants with long residence times [41]. In order to overcome the stringent assumptions of these semi-empirical models, both in their primary and linearized forms, in this piece of research, a robust and novel convective-diffusion model is proposed with generation/depletion terms being governed by pseudo kinetics of adsorption under dynamic condition. A pore and solid diffusion model is developed for a fixed bed column considering irreversible adsorption isotherms and neglecting outside film resistance [42]. Lapidus and Amundson applied a convective-diffusion model to analyze the transport mechanism of solute in an unsteady one-dimensional saturated flow, neglecting intra-pellet mass transfer [43]. Similarly, a number of research groups analysed packed-bed adsorption using the convective-diffusion model with due consideration for inter-pellet diffusion [44–47].

A fixed bed packed with sewage sludge (adsorbent) and inert granular glass materials (packing material) is used in this study. The novelty of this piece of research involves: a) development and validation of two transient forms of a convective-diffusion model, which include depletion terms (in liquid-phase), being represented by the first and second-order pseudo-kinetics, b) consideration of convective and diffusive terms of liquid phase mass transfer along with film diffusion, intra-pellet mass transfer, and depletion of species governed by pseudo-kinetics of competitive adsorption under various dynamic conditions. Starting with the species continuity equation, two convective-diffusion models are developed with ciprofloxacin [CIP] and ofloxacin [OFLX] being the target species, in combination. c) Parameters of the 1st and 2nd order pseudo-kinetic equations are estimated using experimental data collected under dynamic conditions. d) Each of these convective-diffusion models is applied to carry out a thorough breakthrough analysis under varying dynamic conditions for both CIP and OFLX. e) Performance of the packed bed is analysed with respect to the effects of changes in bed height, flow rate, and initial concentration of both fluoroquinolones (CIP and OFLX), in combination, using first-order and second-order convective diffusion models and estimated Damköhler numbers.

2. Materials and methods

2.1. Sampling and processing of raw sewage sludge

Raw sewage sludge [RSS] is collected from the Sewage Treatment Plant (STP), managed by Kamarhati Municipality, North 24 Parganas, West Bengal, India. The sludge is dried in ambient air under natural convective mode for a duration of 5–6 days. The dried semi-solid sludge is then used as the adsorbent to serve as the primary component of packing for the fixed bed used during the dynamic study afterward.

2.2. Chemicals

CIFRAN-500 (Make: Ranbaxy Laboratories Ltd., India) and OFLOMAC-200 (Make: Macleods Pharmaceuticals Ltd., India) are used as the representative sources for CIP and OFLX respectively for the dynamic study. In order to generate the standard curves for pure component CIP and OFLX, standard analytical grade Ciprofloxacin [Make: Sigma–Aldrich, India; CAS No: 86483-48-9; Grade: Analytical] and standard analytical grade ofloxacin [Make: Sigma-Aldrich, India; CAS No: 82419-36-1; Grade: Analytical] are used respectively. The mobile phase used during HPLC-based analysis consists of acetonitrile [Make: Sigma-Aldrich, India; CAS No.: 75-05-8; Grade: HPLC grade], ultra-pure water [Make: Sigma-Aldrich, India; CAS No.: 7732-18-5; Grade: HPLC grade], tri-ethylamine [Make: Sigma-Aldrich, India; CAS No.: 121-44-8; Grade: HPLC grade] and phosphoric acid [Make: Sigma-Aldrich, India; CAS No.: 7664-38-2; Grade: HPLC grade].

2.3. Analytical technique

Analysis of ciprofloxacin and ofloxacin (in solution) is carried out using a High-Performance Liquid Chromatography (HPLC) based system (Make: Waters, Germany; Model: 515) equipped with a 190–400 nm wavelength UV detector, a quaternary gradient system pump with working pressure in between 0 and 4000 psi and a column oven with an operating temperature ranging in between 25 °C to 100 °C. In this study, temperature of the column is maintained at 25 °C. Identification of compounds is carried out with a UV detector (Make: Waters, Germany; Model: 2489), and the wavelength is set at 300 nm. In order to carry out simultaneous detection of ciprofloxacin and ofloxacin in the influent and effluent wastewater, a reverse phase column (Make: Waters, Germany; Model: Sunfire C18) having dimensions 150 mm × 4.6 mm and a particle size limitation of 5 μm is employed. pH of the mobile phase is maintained within a range of 2–7. The mobile phase is a combination of HPLC grade acetonitrile (Make: Sigma-Aldrich, India) and a buffer solution in the ratio of 20:80 (v/v). The buffer solution is prepared by adding 2 ml tri-ethylamine in 200 ml HPLC grade ultrapure water.

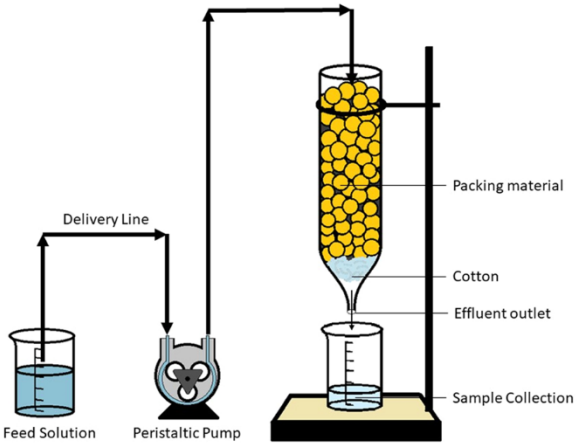

Fig. 1. Experimental setup consisting of a packed bed column made by a combination of sewage sludge and glass beads in a ratio of 1:2 for the removal of ciprofloxacin and ofloxacin.

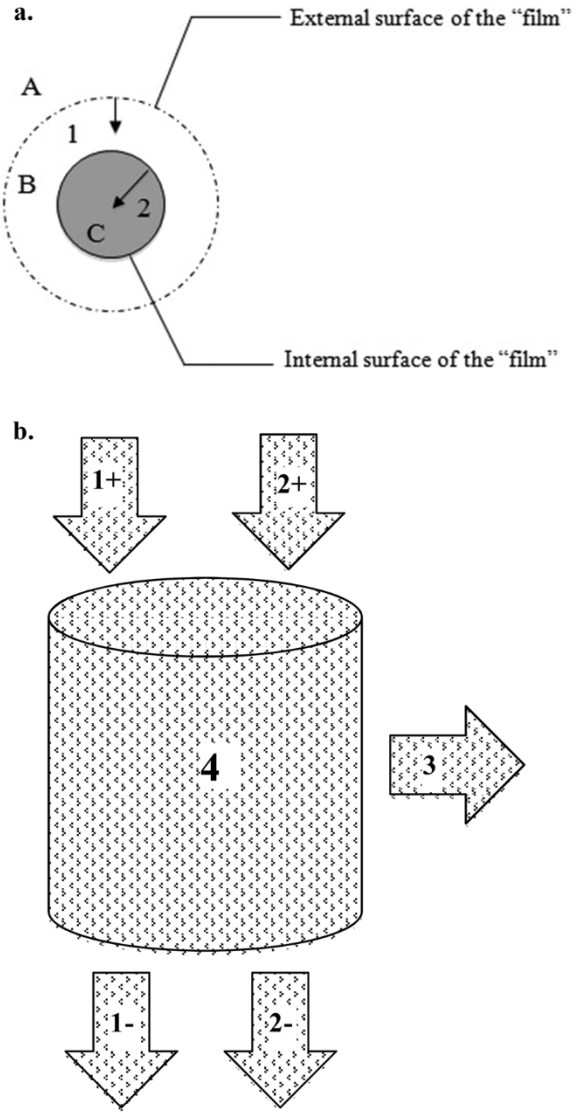

Fig. 2. Fig. 2a. Adsorption process of an adsorbent pellet, represented on a macroscopic scale.
Fig. 2b. Schematic diagram of the species conservation around a differential control volume.

Following this, the pH is adjusted to 6 by adding ortho-phosphoric acid dropwise and the volume is made up to 250 ml. The buffer solution is then filtered through a cellulose acetate membrane filter (pore size: 0.2 μm). The flow rate (mobile phase) is maintained at 1.0 ml/min. Peak areas are plotted against concentrations of known amounts of ciprofloxacin and ofloxacin in order to generate the standard curves of respective antibiotics. Standard curves, thus prepared, are further used to obtain the unknown concentrations of each of the antibiotics, before and after the adsorption. Standard curves of CIP and OFLX in combination, along with relevant chromatograms, are provided within Supplementary Material A [*refer* Fig. SI, Table SI, Fig. SII, and Fig. SIII]. The LC calibration report of the standard curves, as generated using Empower 3 Software, a chromatography data system (CDS) [Make: Waters, Germany] is shown in Supplementary Material B.

2.4. Operational conditions

Various factors considered during the breakthrough analysis are bed depths (3, 5, and 7 cm), influent concentrations (50, 100, and 200 ppm), and flow rates (0.67, 0.90, and 2.14 ml/min). The wastewater is fed and treated till the ratio C_t/C_0 becomes equal to 0.85. The experiments are conducted at different bed heights, flow rates, and feed concentrations without changing the pattern of packing of the column with the adsorbent and inert glass beads. Treated wastewater emerging out of the bottom of the column is collected at specific intervals of time and then the same is analyzed for the unknown concentrations of ciprofloxacin and ofloxacin simultaneously using respective standard curves.

3. Theory

In order to model a solid-liquid column adsorption system, it is necessary to describe the adsorption process into four basic steps (refer Fig. 2a) [48]:

(1) liquid phase mass transfer includes convective mass transfer and molecular diffusion.
(2) film diffusion is defined as the interfacial diffusion between the liquid phase and the exterior surface of the adsorbent.
(3) intra-pellet mass transfer concerning pore diffusion and surface diffusion and
(4) the adsorption-desorption reaction governed by 1st and 2nd order pseudo-kinetics [49–51].

3.1. Liquid phase mass transfer

Specific pharmaceutical species (in the forms of molecules and ions) present in the column, can transport both in the axial and radial directions under convective as well as diffusive modes. In order to simplify the model, it is usually assumed that all cross-sections are homogeneous and the radial transports (both convective and diffusive) are neglected [41]. Considering the axial dispersion to be present, a mass conservation equation is developed, on a macroscopic scale, to relate different process variables in the column, like concentration of the adsorbed adsorbate (q), concentration of the bulk solution (C), distance to the inlet (z), superficial velocity (u_s) and axial dispersion coefficient (D_z). Starting with a differential control volume [refer Fig. 2b] within the packed column [52–54], a convective-diffusion based species transport equation is developed [Eq. (1)] considering a depletion term, consisting of the removal of primary species [adsorbate] by virtue of adsorption.

$$\varepsilon_b \frac{\partial C}{\partial t} + u_s \frac{\partial C}{\partial z} + (1-\varepsilon_b)\rho_a \frac{\partial q}{\partial t} = D_z \frac{\partial^2 C}{\partial z^2} \quad (1)$$

where, the initial and boundary conditions are:

$t = 0 \rightarrow C(z,t) = 0,$

$t = 0 \rightarrow q(z,t) = 0,$

$z = 0 \rightarrow C(0, t = 0) = 0, C(0,\ t > 0) = C_0,$

$z = H \rightarrow \frac{\partial C}{\partial z} = 0$

When the axial dispersion is neglected, Eq. (1) becomes

$$\varepsilon_b \frac{\partial C}{\partial t} + u_s \frac{\partial C}{\partial z} + (1 - \varepsilon_b)\rho_a \frac{\partial q}{\partial t} = 0 \tag{2}$$

The initial and boundary conditions also change to the following:

$t = 0 \rightarrow C(z,t) = 0,$

$t = 0,\ for\ z \geq 0 \rightarrow C = 0,\ q = 0$

$z = 0 \rightarrow C = C_0\ for\ t > 0,$

$z = H \rightarrow \frac{\partial C}{\partial z} = 0$

where, ε_b is the bed porosity, t is the time, ρ_a is the adsorbent density, C_0 is the initial concentration of the influent, and H is the bed height.

In Fig. 2a, A = bulk fluid, B = interface region, C = adsorbent pellet, 1 ≡ film diffusion 2 ≡ intra-pellet diffusion.

In Fig. 2 b, 1 = convective mass transfer, 2 = axial dispersion, 3 = adsorbed by adsorbent, 4 = accumulation of adsorbate. In Fig. 2b

$(1+) - (1-) \rightarrow -u_s \frac{\partial C}{\partial z}$

$(2+) - (2-) \rightarrow -D_z \frac{\partial^2 C}{\partial^2 z}$

$(3-) \rightarrow (1 - \varepsilon_b)\rho_a \frac{\partial q}{\partial t}$

$(4) \rightarrow \varepsilon_b \frac{\partial C}{\partial t}$

Eqn 1 are based on the following assumptions [41]:

(1) the entire process is isothermal;
(2) no chemical reaction occurs in the column;
(3) the packed bed is made of porous spherical adsorbent particles, uniform in size;
(4) the bed is homogeneous and the concentration gradient in the radial direction of the bed is negligible;
(5) the flow rate is constant and invariant with the column position [55]; and,
(6) the activity coefficient of each species is unity.

Now, we can write the bulk density of the bed as: $\rho_b = (1 - \varepsilon_b)\rho_a$. So, Eq. (2) can be written as,

$$\varepsilon_b \frac{\partial C}{\partial t} + u_s \frac{\partial C}{\partial z} + \rho_b \frac{\partial q}{\partial t} = 0 \tag{3}$$

Integrating Eq. (3) over the bed from z = 0 (where $C = C_0$) to z = H (where, $C = C_t$), and noting that $\rho_b q >> \varepsilon_b C$ we obtain

$$\frac{C_t}{C_0} = 1 - \frac{\rho_b H}{u_s C_0} \frac{d\overline{q}}{dt} \tag{4}$$

where, $\overline{q}$ is the average solid-phase adsorbate concentration in the bed, given by

$$\overline{q} = \frac{1}{H} \int_0^H q dx \tag{5}$$

However, $\overline{q}$ is also a function of time t, since the mass transfer zone shifts from the beginning of the bed to the end with time, thus increasing the adsorbent uptake of the bed with time.

$$\overline{q_t} = \frac{Total\ mass\ of\ adsorbate\ adsorbed\ in\ the\ bed\ upto\ time\ t}{Mass\ of\ adsorbate\ in\ the\ bed} = \frac{m_t^a}{m_A} \tag{6}$$

m_A attributes to the weight of sludge taken in the bed. Mass adsorbed by the differential control element of the bed $dm(t)$, at any time is given by the difference of inlet concentration and the outlet concentration at that time i.e.

$$dm(t) = (C_0 - C_t)Qdt \tag{7}$$

Where Q = volumetric flow rate of the solution through the bed.

$$\therefore m_t^a = \int_{t=0}^{t} dm(t) = \int_{t=0}^{t} (C_0 - C_t)Qdt \tag{8}$$

Thus,

$$\overline{q_t} = \frac{\int_{t=0}^{t} (C_0 - C_t)Qdt}{m_A} \tag{9}$$

Also, q_{eq} signifying the maximum amount of adsorbate that can be adsorbed by the bed, that is, the adsorbent loading at time $t = t_{eq}$ (a time when the entire bed is saturated), is given by:

$$q_{eq} = \frac{\int_{t=0}^{t=t_{eq}} (C_0 - C_t)Qdt}{m_A} \tag{10}$$

3.2. First order model

The pseudo first-order kinetic model is given by the equation

$$\frac{d\overline{q}}{dt} = k_1 \left(q_{eq} - \overline{q}\right) \tag{11}$$

The solution of Eq. (11), subject to the initial condition $\overline{q} = 0$ at t = 0, is

$$\overline{q} = q_{eq}(1 - \exp(-k_1 t)) \tag{12}$$

Using Eq. (12) in Eq. (4), we find

$$\frac{C_t}{C_0} = 1 - \frac{\rho_b H k_1 q_{eq}}{u_s C_0} \exp(-k_1 t) \tag{13}$$

Let n be the number of bed volumes of fluid that have passed through the bed since $t = 0$, that is,

$$n = \frac{u_s(t - H\varepsilon_b/u_s)}{H} = \frac{Qt}{V_{bed}} - \varepsilon_b \approx \frac{Qt}{V_{bed}} \tag{14}$$

Where, Q and V_{bed} are the volumetric flow rate of the fluid though the adsorbent bed and the volume of the bed respectively. The expression for the breakthrough curve, given by Eq. (13), can be written as:

$$\frac{C_t}{C_0} = 1 - D_{a_1} n_{stoic} \exp(-nD_{a_1}) \tag{15a}$$

Or,

$$\frac{C_t}{C_0} = 1 - \exp(-D_{a_1}(n - n_{BT})) \tag{15b}$$

Where, n_{BT} is the number of bed volumes at breakthrough (i.e. when $C_t \cong 0$). The dimensionless parameters D_{a1} and n_{stoic} are given by

$$D_{a_1} = \frac{k_1 H}{u_s} = \frac{k_1 V_{bed}}{Q} \tag{16}$$

$$n_{stoic} = \frac{\rho_b q_e}{C_0} \tag{17}$$

Thus, the two parameters governing the breakthrough curve equation are D_{a1} and n_{stoic} [from Eq. (15a)], or D_{a1} and n_{BT} [from Eq. (15b)].

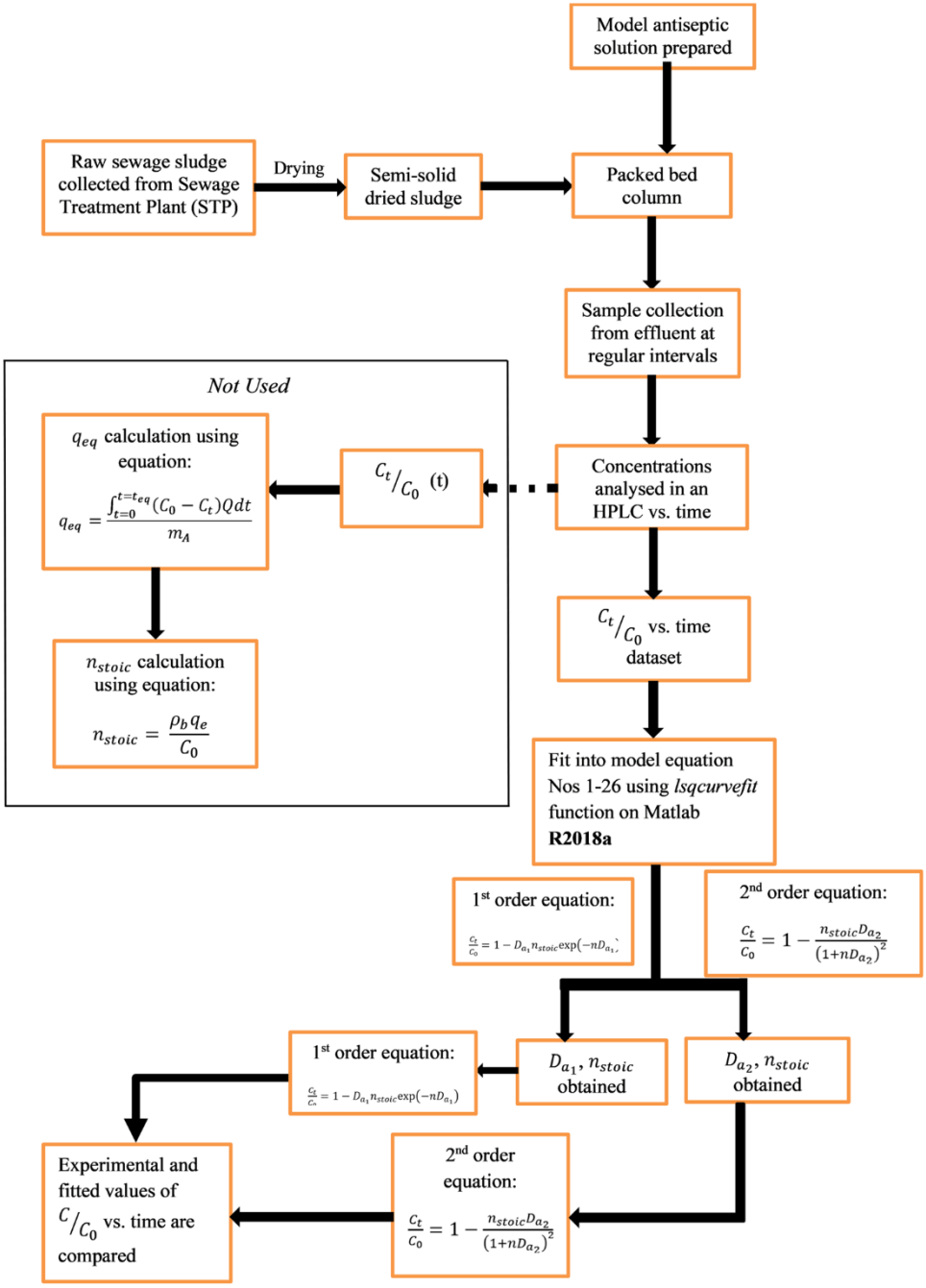

Fig. 3. Flowchart representing the sequence of solution.

Equating Eqs. (15a) and (15b), one can obtain,

$$n_{BT} = \frac{\ln(D_{a_1} n_{stoic})}{D_{a_1}} \tag{18}$$

Assuming n_{stoic} to be constant, differentiating Eq. (18) with respect to D_{a1} and setting the derivative equal to zero, the maximum number of bed volumes at breakthrough is obtained, as given below,

$$n_{BT,\max} = \frac{n_{stoic}}{e} = 0.368 n_{stoic} = 0.368 \frac{\rho_b q_{eq}}{C_0} \tag{19}$$

3.3. Second-order model

The second-order kinetic model [56], is given by

$$\frac{d\bar{q}}{dt} = k_2 (q_{eq} - \bar{q})^2 \tag{20}$$

Integrating Eq. (20), subject to the initial condition: $\bar{q} = 0$ at $t = 0$, is given by

$$\bar{q} = \frac{q_{eq}^2 k_2 t}{1 + q_{eq} k_2 t} \tag{21}$$

Using Eq. (21) in Eq. (4), gives

$$\frac{C_t}{C_0} = 1 - \frac{\rho_b H k_2 q_{eq}^2}{u_s C_0 (1 + k_2 q_{eq} t)^2} \tag{22}$$

Eq. (22) can also be expressed equivalently as

Table 1
Breakthrough times in minutes, for the dynamic study of removal of (a) ciprofloxacin and (b) ofloxacin by raw sewage sludge at various flow rates, bed height and initial concentrations.

Parameters	Ciprofloxacin			Ofloxacin		
	Experimental datapoint closest to breakthrough	1st order model prediction	2nd order model prediction	Experimental datapoint closest to breakthrough	1st order model prediction	2nd order model prediction
Bed Height↓						
7 cm	780	845	898	540	456	393
5 cm	630	669	785	430	309	321
3 cm	360	323	357	150	132	133
Flow Rate↓						
2.14 ml/min	300	251	286	80	81	84
0.90 ml/min	630	669	785	430	309	321
0.67 ml/min	Didn't reach breakthrough	1305	1616	540	556	648
Initial Concentration↓						
200 ppm	300	269	268	180	178	193
100 ppm	630	669	785	430	309	321
50 ppm	840	900	981	780	797	878

$$\frac{C_t}{C_0} = 1 - \frac{n_{stoic} D_{a_2}}{(1 + nD_{a_2})^2} \tag{23a}$$

Or

$$\frac{C_t}{C_0} = 1 - \left(\frac{1 + n_{BT} D_{a_2}}{1 + nD_{a_2}}\right)^2 \tag{23b}$$

Where,

$$D_{a_2} = \frac{q_{eq} k_2 H}{u_s} = \frac{q_{eq} k_2 V_{bed}}{Q} \tag{24}$$

Thus, from the pseudo second-order kinetic reaction, the two parameters governing breakthrough are D_{a2} and n_{stoic} [from equation (23 a)], or D_{a2} and n_{BT} [from Eq. (23b)]. Equating Eqs. (23a) and (23b), we obtain

$$n_{BT} = \frac{\sqrt{n_{stoic} D_{a_2}} - 1}{D_{a_2}} \tag{25}$$

Differentiating Eqn 25 with respect to D_{a2} and equating to zero, $n_{BT,\max}$ is obtained as:

$$n_{BT,\max} = \frac{n_{stoic}}{4} = 0.25 n_{stoic} = 0.25 \frac{\rho_b q_{eq}}{C_0} \tag{26}$$

4. Method of solution

The equation of the breakthrough curve given by pseudo 1st order model [Eq.(15a)] and pseudo 2nd order model [Eqn 23a] have two unknown constants, D_{a_1} and n_{stoic_1} and D_{a_2} and n_{stoic_2} respectively. Once estimated, these can help predict the outlet concentration at any time t for $t < t_{eq}$.

From Eq. (17) n_{stoic} can be calculated directly when q_e is known. In order to calculate q_{eq} from *equation* (10), it is necessary to know the outlet concentration C_t as a function of time, which is exactly what we are trying to find out by modelling.

So, the experimental values of outlet concentration C_t versus time t along with the inlet concentration (C_0), for every run, are used to form the model dataset C_t/C_0 vs t. This data set and the model equation are fed into the *lsqcurvefit* function on **Matlab R2018a** in order to optimize the model parameters to find the best fit curve of input dataset for every run for both FQs for pseudo-first and pseudo-second-order models using a *non-linear least square method*. The model parameters for each of the experiments, are estimated by minimizing the SSQ values (Sum of Squares of Residuals),

$$SSQ = \sum_{i=1}^{n} \frac{(Predicted - Observed)^2}{N - k - 1} \tag{27}$$

The parameters, so estimated, are finally used to formulate the model equations. Corresponding SSQ values (refer Eqn 27) indicate the accuracy of prediction. For sufficiently low SSQ values, it can be concluded that the fit is a 'good fit'. Hence the rate constants (k_1 and q_{eq}) and (k_2 and q_{eq}) can be calculated from the model parameters of both the models using Eqns 16, 17 and 24. Estimated parameters of the first-order and second-order models are given in Table SII [*see* Supplementary Material A]. A flowchart representing the sequential methods of solution is given in Fig. 3.

Considering pseudo-kinetics to be valid, D_{a1} and D_{a2} can be considered as equivalent Damköhler numbers (Da).[1] Damköhler number (D_a) is a useful ratio for determining whether diffusion rates or reaction rates are 'important' on a relative scale, for defining a steady-state distribution of a chemically reactive species over the length and time scales of interest. For $D_a >> 1$ the reaction rate is much greater than the diffusion rate. Corresponding concentration distribution is said to be diffusion limited (diffusion is slower, so diffusion characteristics dominate and the reaction is assumed to be instantaneously in equilibrium). For $D_a << 1$ diffusion occurs much faster than the reaction, thus diffusion reaches an 'equilibrium' well before the reaction achieves equilibrium.

5. Results and discussion

5.1. Effect of bed height

For both first-order and second-order models, the effective maximum breakthrough times, for both FQs increase with an increase in bed depth [refer to Table 1 and Fig. 4] while maintaining flow rate and inlet concentration constant. The experimental breakthroughs come much earlier for ofloxacin as compared to the same for ciprofloxacin. This outcome is in line with the fact that OFLX occupies the pores much faster than CIP. The existing functional groups of the sewage sludge start playing a major role as both the FQs interact with the functional groups

[1] **Damköhler numbers (Da)** are, in general, are dimensionless numbers used in chemical engineering to relate the chemical reaction timescale (reaction rate) to the transport phenomena rate occurring in a system. It is named after German chemist **Gerhard Damköhler**. In its most commonly used form, the Damköhler number relates the reaction timescale to the convection times scale, flow rate, though the packed bed reactor for a continuous processes: $Da = \frac{reaction\ \ rate}{convective\ mass\ transport\ rate}$

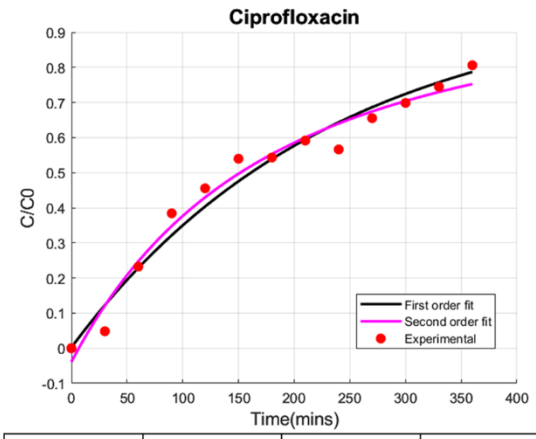

	D_a	n_{stoic}	B.T. Time
1st order	0.0701	14.2259	323
2nd order	0.0476	21.8030	357

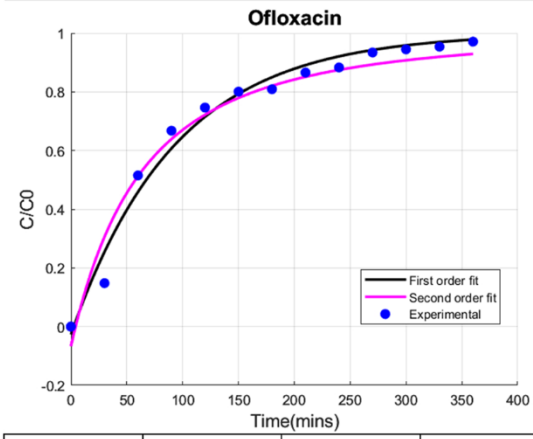

	D_a	n_{stoic}	B.T. Time
1st order	0.1748	5.8781	132
2nd order	0.1307	8.1611	133

3 cm

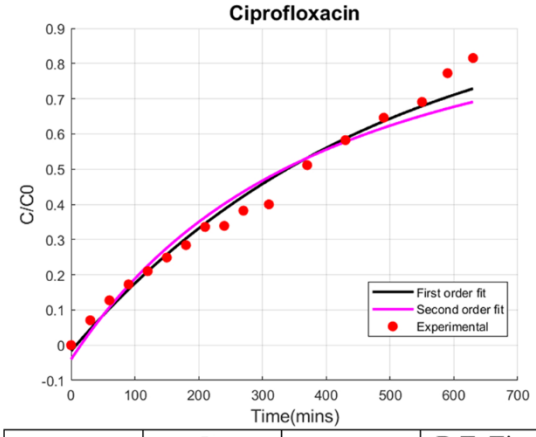

	D_a	n_{stoic}	B.T. Time
1st order	0.057	17.7816	669
2nd order	0.036	28.7899	785

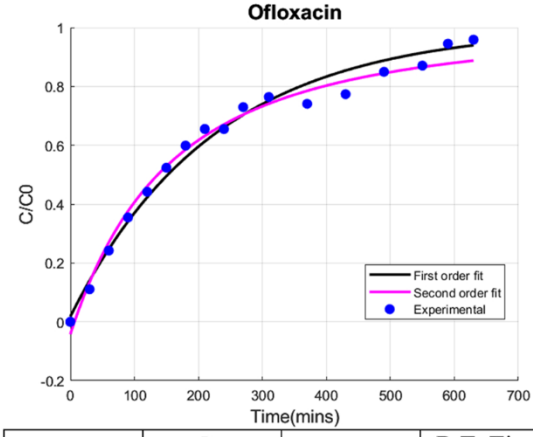

	D_a	n_{stoic}	B.T. Time
1st order	0.1209	8.1234	309
2nd order	0.0885	11.7689	321

5 cm

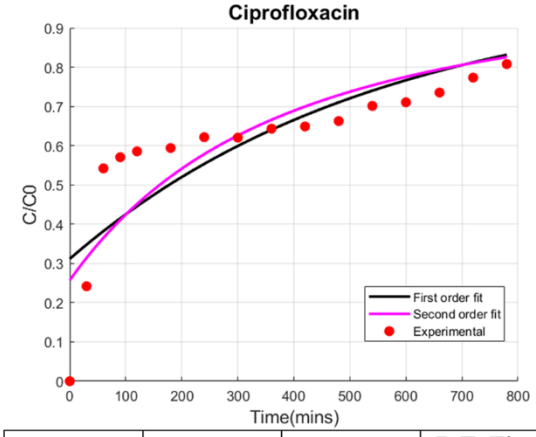

	D_a	n_{stoic}	B.T. Time
1st order	0.069	9.999	845
2nd order	0.052	14.267	898

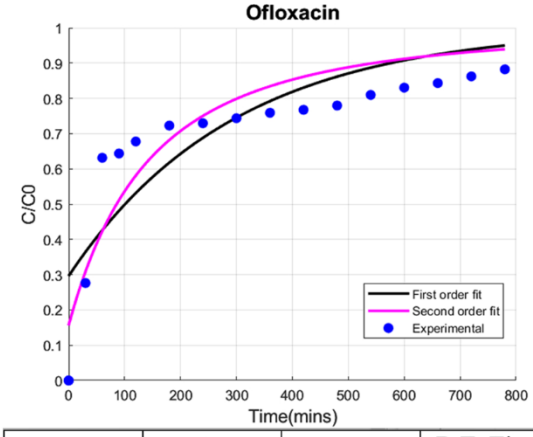

	D_a	n_{stoic}	B.T. Time
1st order	0.129	5.44	456
2nd order	0.133	6.329	393

7 cm

Fig. 4. Predicted breakthrough curves using first-order and second-order kinetic models with respect to experimental data collected for increasing bed heights [a) 3 cm, b) 5 cm, c) 7 cm] at an inflow rate = 0.9 ml/min and inlet concentration = 100 ppm.

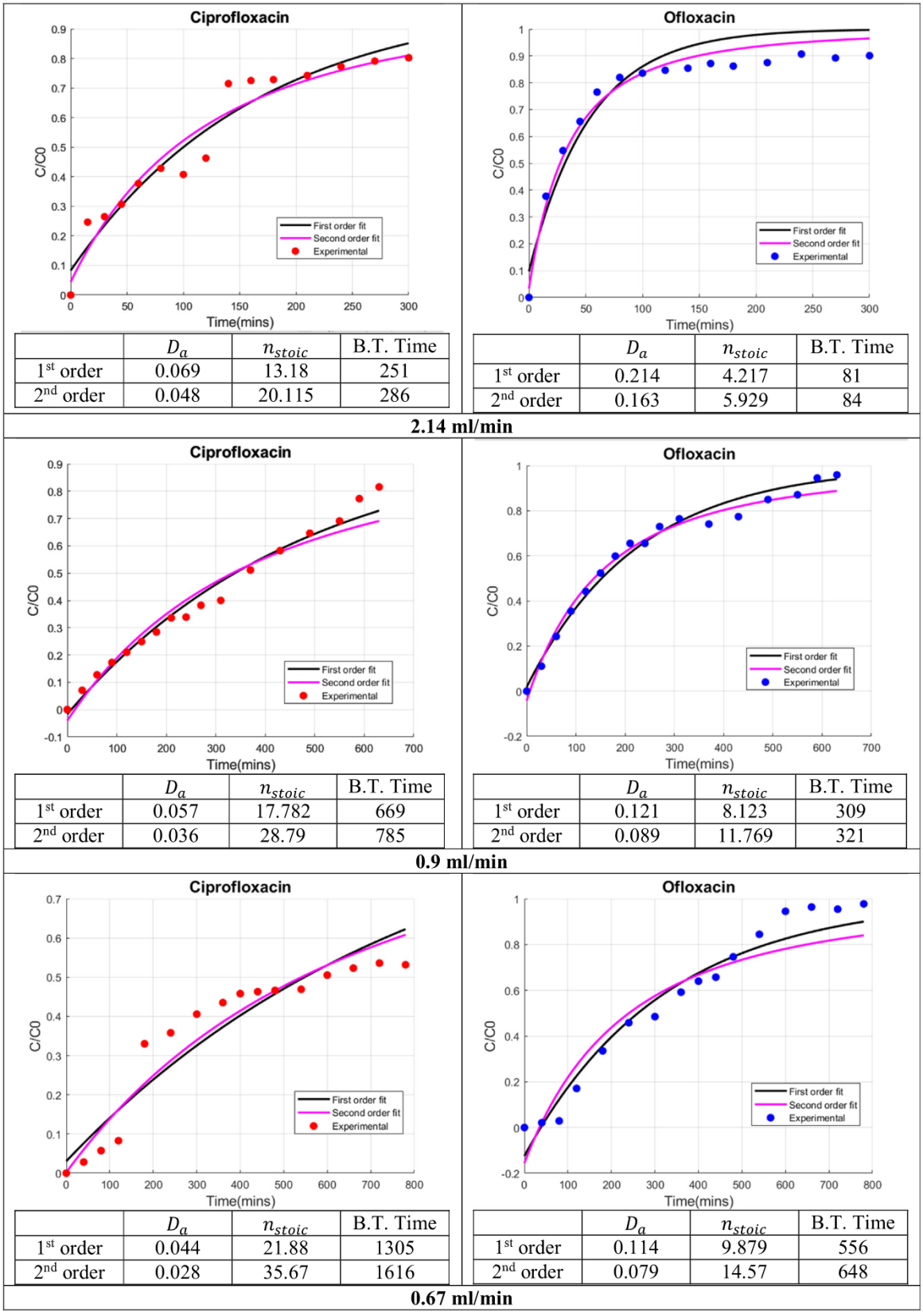

	D_a	n_{stoic}	B.T. Time
1st order	0.069	13.18	251
2nd order	0.048	20.115	286

	D_a	n_{stoic}	B.T. Time
1st order	0.214	4.217	81
2nd order	0.163	5.929	84

2.14 ml/min

	D_a	n_{stoic}	B.T. Time
1st order	0.057	17.782	669
2nd order	0.036	28.79	785

	D_a	n_{stoic}	B.T. Time
1st order	0.121	8.123	309
2nd order	0.089	11.769	321

0.9 ml/min

	D_a	n_{stoic}	B.T. Time
1st order	0.044	21.88	1305
2nd order	0.028	35.67	1616

	D_a	n_{stoic}	B.T. Time
1st order	0.114	9.879	556
2nd order	0.079	14.57	648

0.67 ml/min

Fig. 5. Predicted breakthrough curves using first-order and second-order kinetic models with respect to experimental data collected with decreasing flow rates [(a) 2.14 ml/min, (b) 0.90 ml/min, (c) 0.67 ml/min] using a bed height = 5 cm and inlet concentration = 100 ppm.

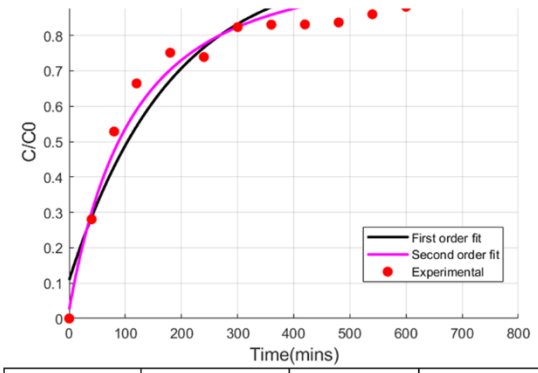

	D_a	n_{stoic}	B.T. Time
1st order	0.152	5.87	269
2nd order	0.123	7.937	268

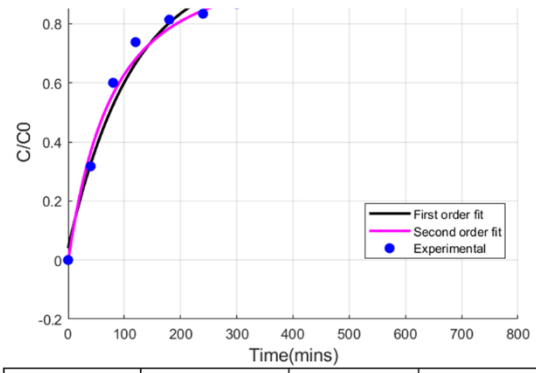

	D_a	n_{stoic}	B.T. Time
1st order	0.24	4.004	178
2nd order	0.175	5.721	193

200 ppm

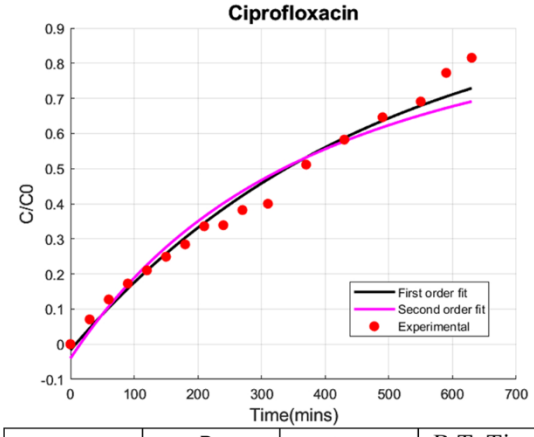

	D_a	n_{stoic}	B.T. Time
1st order	0.057	17.782	669
2nd order	0.036	28.79	785

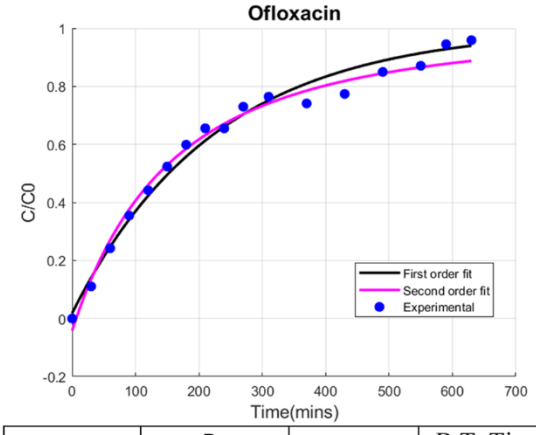

	D_a	n_{stoic}	B.T. Time
1st order	0.121	8.123	309
2nd order	0.089	11.769	321

100 ppm

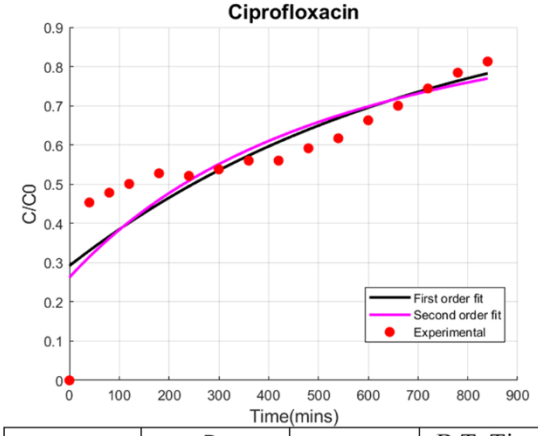

	D_a	n_{stoic}	B.T. Time
1st order	0.0383	18.483	900
2nd order	0.026	28.835	981

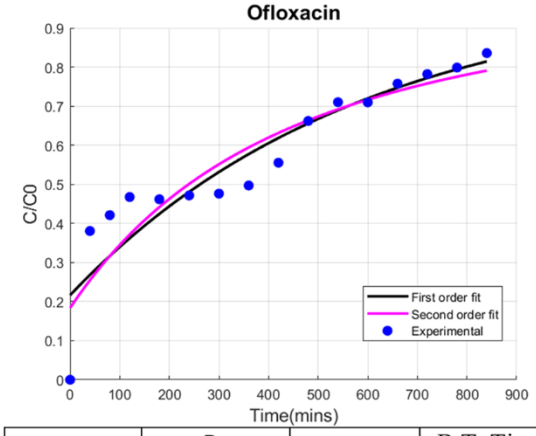

	D_a	n_{stoic}	B.T. Time
1st order	0.047	16.767	797
2nd order	0.0327	25.766	878

50 ppm

Fig. 6. Predicted breakthrough curves using first-order and second-order kinetic models with respect to experimental data collected with decreasing inlet concentrations: (a) 200 ppm, (b) 100 ppm, (c) 50 ppm at a bed height = 5 cm and inflow rate = 0.90 ml/min.

of the sludge, primarily due to hydrogen bonding [refer to Section 6]. In case of ofloxacin, it is observed that the experimental breakthroughs come later than the predicted ones, while the same for ciprofloxacin is not always so. Pseudo-kinetics is not taking care of the complex surface-coordination pathways. This is the probable reason for the mismatch. The first-order and second-order Damköhler numbers initially decreases with an increase in bed height but increases afterward for both the antibiotics, under constant flow rate and inlet concentration, probably due

Table 2
Variations in the ratio of first-order and second-order Damköhler numbers of ciprofloxacin to ofloxacin with changes in flow rate and inlet concentration.

Parameter	$D_{a_{1_{Cipro}}} : D_{a_{1_{Oflox}}}$	$D_{a_{2_{Cipro}}} : D_{a_{2_{Oflox}}}$
Flow Rate↓		
2.14	1:3.076	1:3.434
0.9	1:2.114	1:2.452
0.67	1:2.569	1:2.511
Initial Concentration↓		
200	1:1.578	1:1.429
100	1:2.114	1:2.452
50	1:1.219	1:1.238

to the competitive adsorption of CIP and OFLX onto the functionalized surface sites.

5.2. Effect of flow rate

When bed height and concentration are kept constant, the values of $n_{BT,max}$ for both ciprofloxacin and ofloxacin are seen to increase almost uniformly while D_{a_1} and D_{a_2} decrease with a decrease in flow rate from 2.14 ml/min to 0.67 ml/min for both first and second- order models [refer to Table 1 and Fig. 5].

5.3. Effect of inlet concentration

With a constant bed height and flow rate, $n_{BT,max}$ decreases with an increase in the inlet concentration. The rate of increase of $n_{BT,max}$ is found to be much more with inlet concentration varying from 100 ppm to 200 ppm as compared to the rate of increase of $n_{BT,max}$ with variation of inlet concentration in between 50 ppm and 100 ppm [refer to Table 1 and Fig. 6]. At very high concentrations, there is so much of adsorbate available that the rate of adsorption is very high causing faster saturation of bed and this explains much less value of $n_{BT,max}$.

Also, for both the compounds, values of D_{a_1} and D_{a_2} increase subtly when inlet concentration is changed from 50 ppm to 100 ppm while the corresponding values increase significantly when the inlet concentration increases from 100 ppm to 200 ppm, keeping the bed height and flow

Table A1
Elemental analysis of raw and treated Sludge obtained from CHNS analyzer.

Sample	C % (wt% daf)	H % (wt% daf)	N % (wt% daf)	S % (wt% daf)
Raw Sludge	19.97	2.847	2.03	0.455
Treated Sludge	28.61	3.823	4.21	1.687

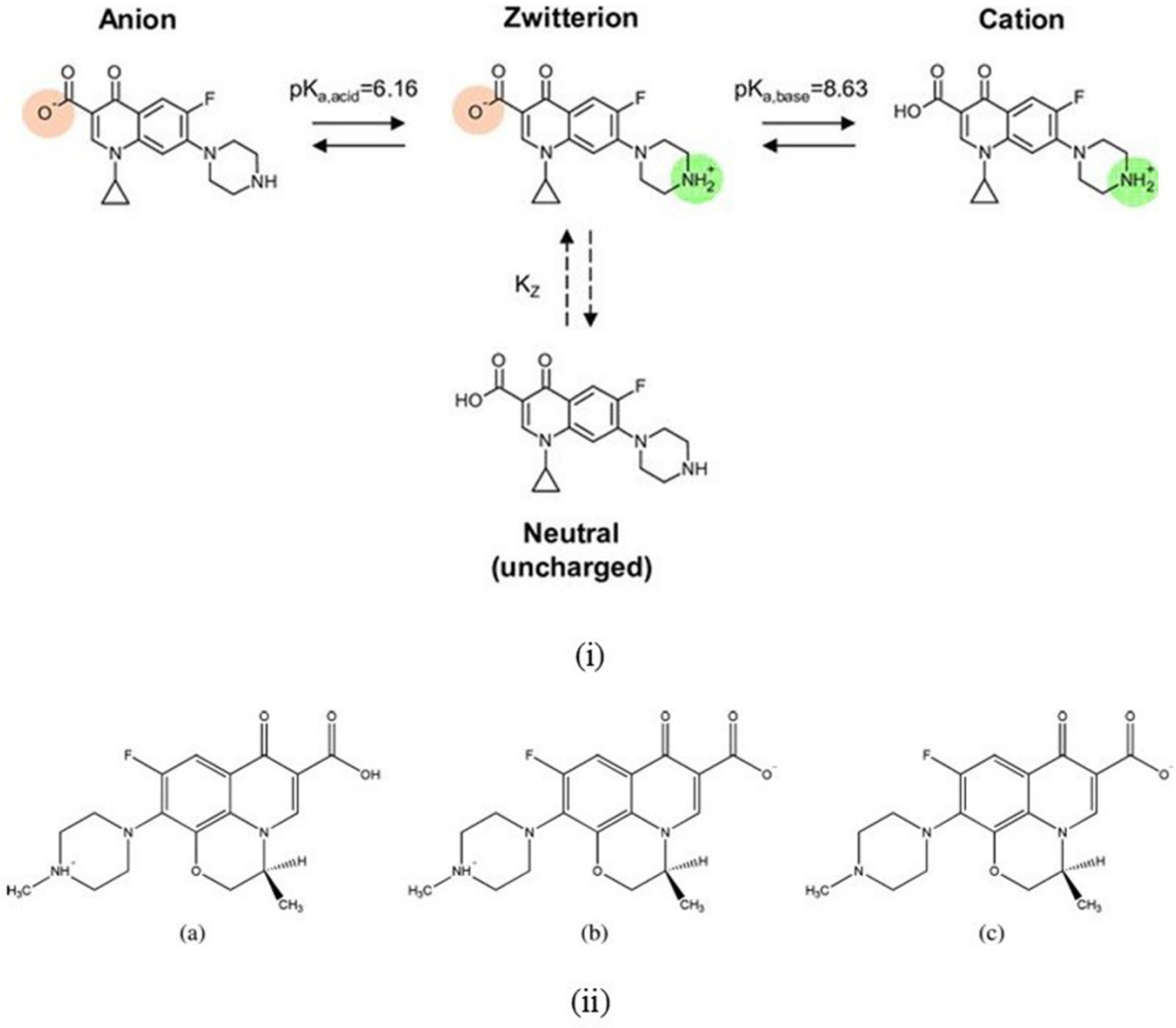

Fig. 7. Different ionic states of (i) Ciprofloxacin in different ranges of pH and (ii) Ofloxacin existing at various ranges of pH; (a) Cationic (at pH ~ 4), (b) Neutral or Zwitterionic (at pH ~ 7) and (c) Anionic (at pH ~ 9).

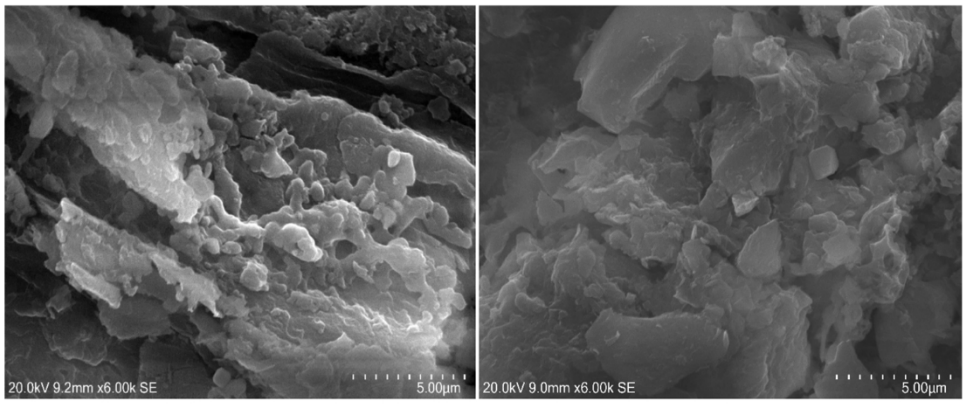

Fig. A1. Scanning electron micrograph (SEM) images of (a) Raw Sludge and (b) Treated Sludge at × 6000 magnification.

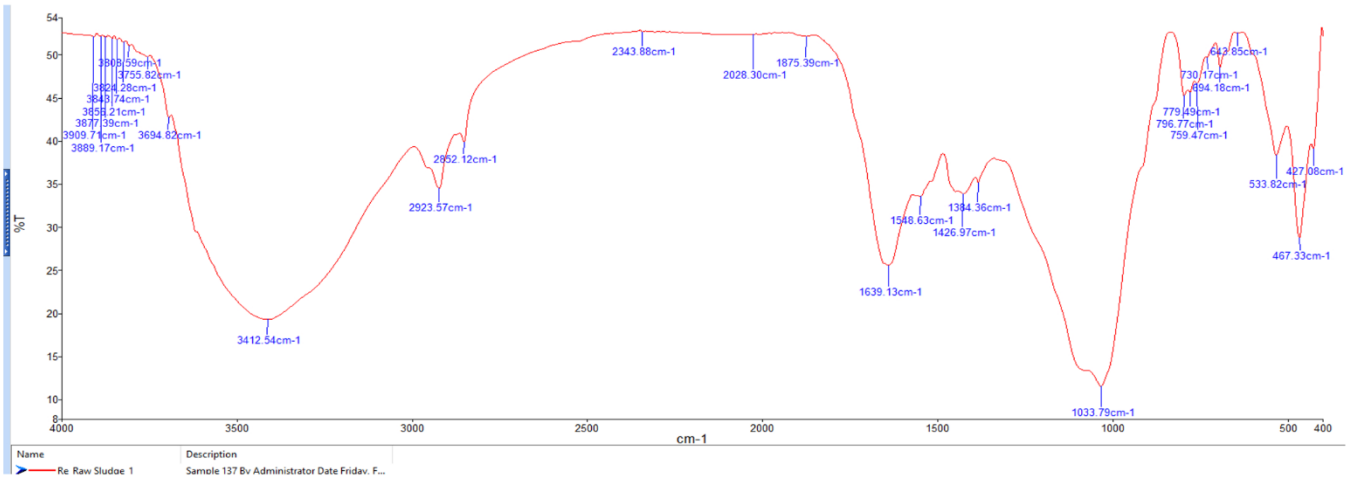

(a)

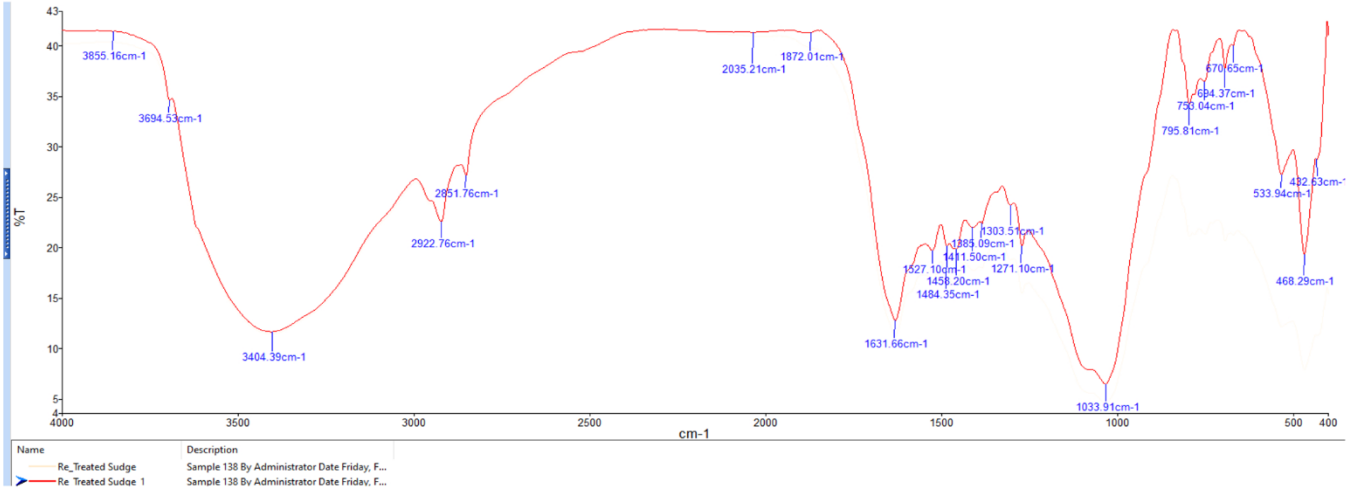

(b)

Fig. A2. (a) FT-IR spectra of untreated sludge before adsorption; (b) FT-IR spectra of treated sludge after adsorption.

rate constant. The increase in values of Damköhler number also validates the increase in reaction rate with increase in inlet concentration. With the values of Damköhler numbers being $<<1$, adsorption remains the rate determining step.

The accuracy of curve-fitting using non-linear regression analysis is effectively quantified by the SSQ values calculated for both the models with every dataset. From Table SII [see Supplementary Material A], it is observed that the SSQ values are predominantly less than 0.02 and even

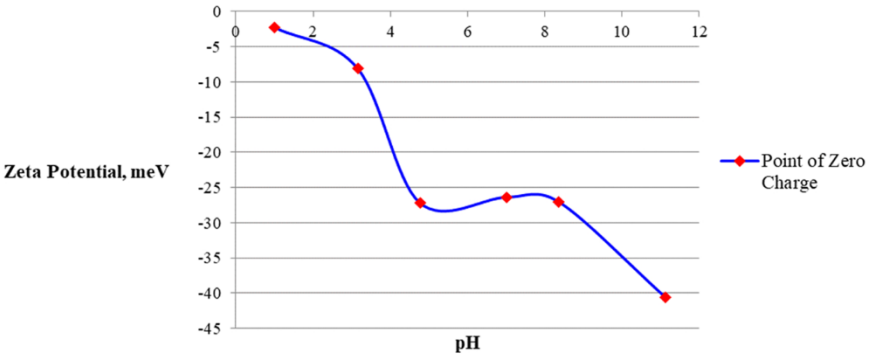

Fig. A3. Zeta potential versus pH of untreated sewage sludge.

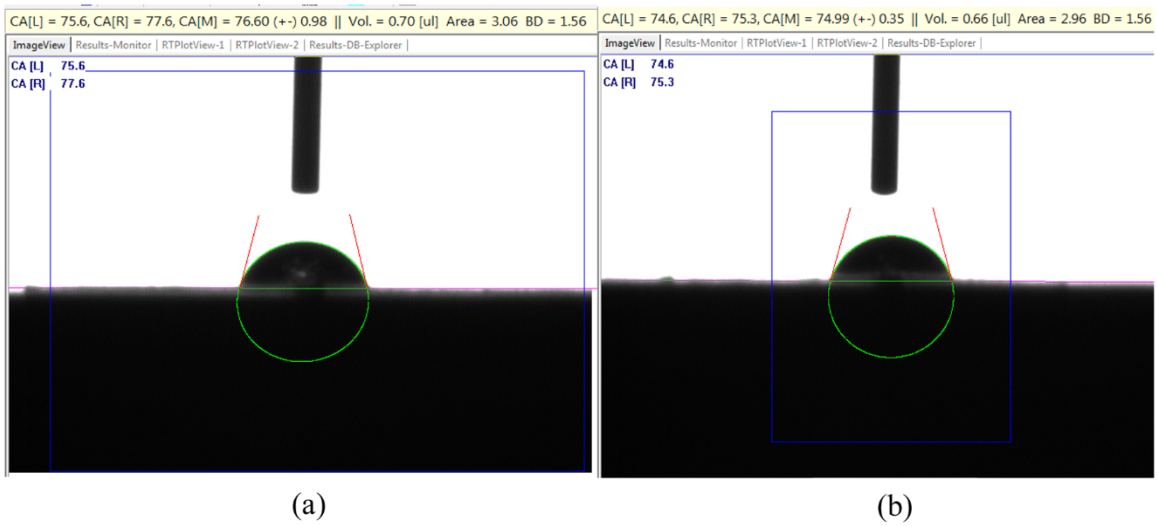

Fig. A4. Contact angle measurement of (a) Raw Sludge and (b) Treated Sludge.

less than 0.01 in quite a number of cases, ensuring a very good fit of the data. Overall, the second order model gives a better fit for ciprofloxacin in 5 out of 7 cases and for ofloxacin in 6 out of 7 cases. So, it can be concluded that both the FQs are chemisorbed onto the sludge. The same is substantiated through a probable mechanism of adsorption of CIP and OFLX, described in Section 6 (refer to Annex I for specific figures that supplement the mechanism). The values of q_{eq} are estimated for both CIP and OFLX for each of the models (see Supplementary Material A: Table SII) using Eqns. 19 and 26. It is observed that the estimated values of q_{eq} are close to one another for both models for a particular bed height, flow rate and initial concentration. Minor differences are attributed to the differences in the rates of depletion for 1st and 2nd order pseudo-kinetics.

In general, the breakthrough time (BT) increases with an increase in bed height, a decrease in flow rate and a decrease in inlet concentration. Also, the breakthrough time for ciprofloxacin is higher than the same for ofloxacin indicating a slower adsorption of ciprofloxacin as compared to adsorption of ofloxacin. On a competitive time-scale, ofloxacin occupies the pores faster and ciprofloxacin largely forms surface complexes through hydrogen bonding. In most of the cases the predicted breakthrough times using first-order and second-order convective-diffusion models are quite close to the observed breakthrough times (refer Table 1), thereby validating the effectiveness of the adopted method. Minor differences are primarily due to the differences in the rates of depletion for 1st and 2nd order pseudo-kinetics.

In cases, where there is insufficiency of data points, that is, in cases where data is recorded to time lesser than or just up to the breakthrough time, there are deviations from the actual experimental breakthrough times (observed). Best predictions are achieved when there are a few more data points recorded even after the bed has achieved breakthrough. Additionally, the models are still capable of predicting breakthrough times even if the bed did not actually reach breakthrough during the total span of experimentation.

In all the experiments, $D_a s << 1$ for both CIP and OFLX. It indicates a faster diffusion process with respect to the rate of pseudo-reaction. Diffusion thus reaches an 'equilibrium' well before the reaction achieves pseudo chemical equilibrium. Ratios of the Damköhler numbers, meant to represent the first-order and second-order convective-diffusion models for ciprofloxacin to ofloxacin is < 1 (refer to Table 2). It indicates a faster rate of pseudo-reaction for ofloxacin as compared to ciprofloxacin. Additionally, the values of pseudo rate constants for ofloxacin are observed to be greater than the same for ciprofloxacin in case of both the models (see Supplementary Material A: Table SII).

6. Probable mechanism of adsorption of ciprofloxacin and ofloxacin onto the raw sewage sludge [refer Annex I] [57–62]

Generally, organic adsorbents containing various oxygenated functional groups and phenolic groups make interactions with FQs through electrostatic attraction, hydrogen bonding, π–π interaction, and hydrophobic interactions. These interactions are possible because of the presence of functional groups like -COOH, -NH_2, and -OH in ciprofloxacin and ofloxacin and a variety of functional groups present on the sludge surface (refer to Annex A: Fig. A2). The possibility of π–π interaction between the semi-dried raw sewage sludge and the adsorbates [CIP and OFLX] leading to the observed adsorption of ciprofloxacin and

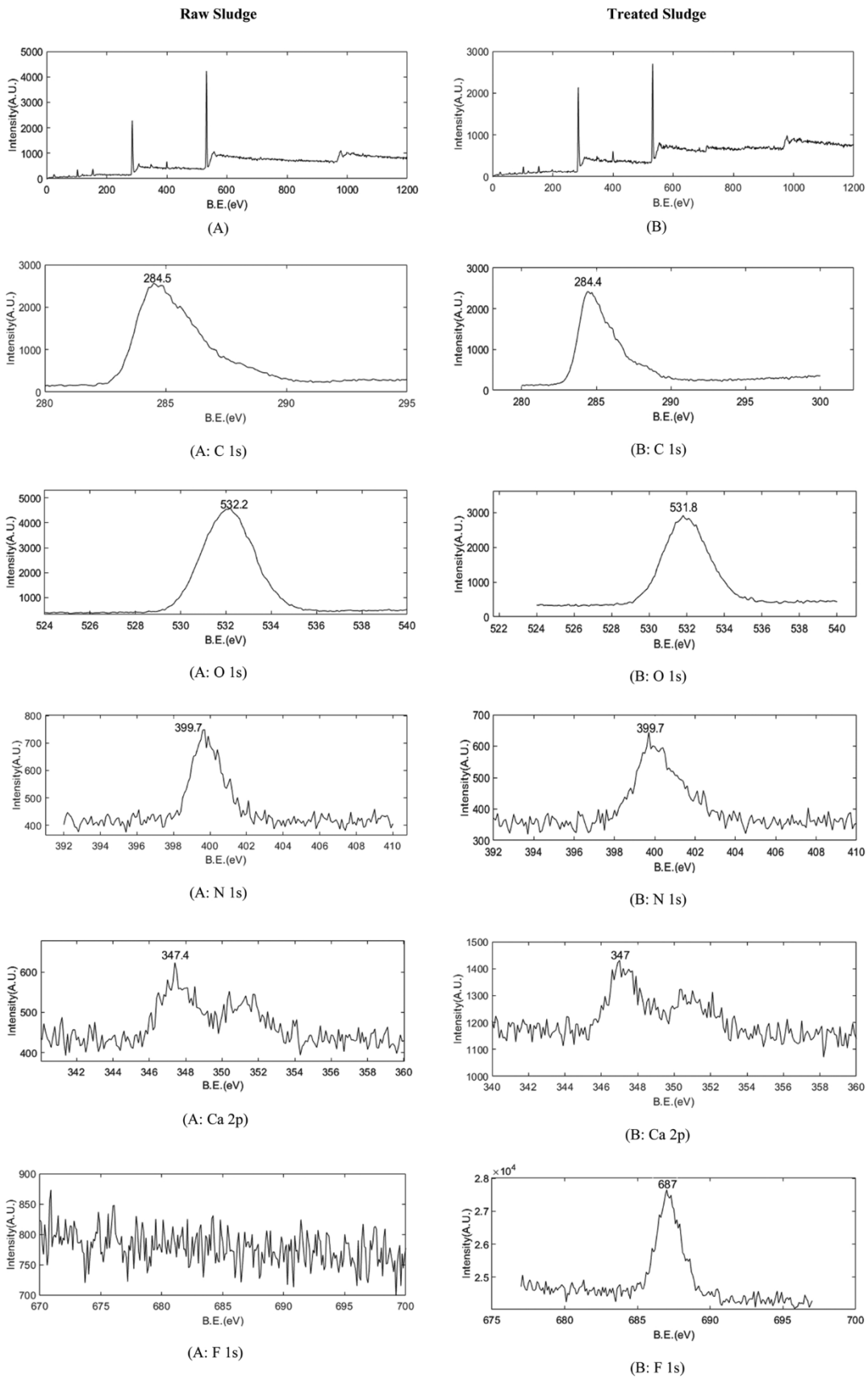

Fig. A5. XPS spectrum of (A) raw sludge and (B) treated sludge.

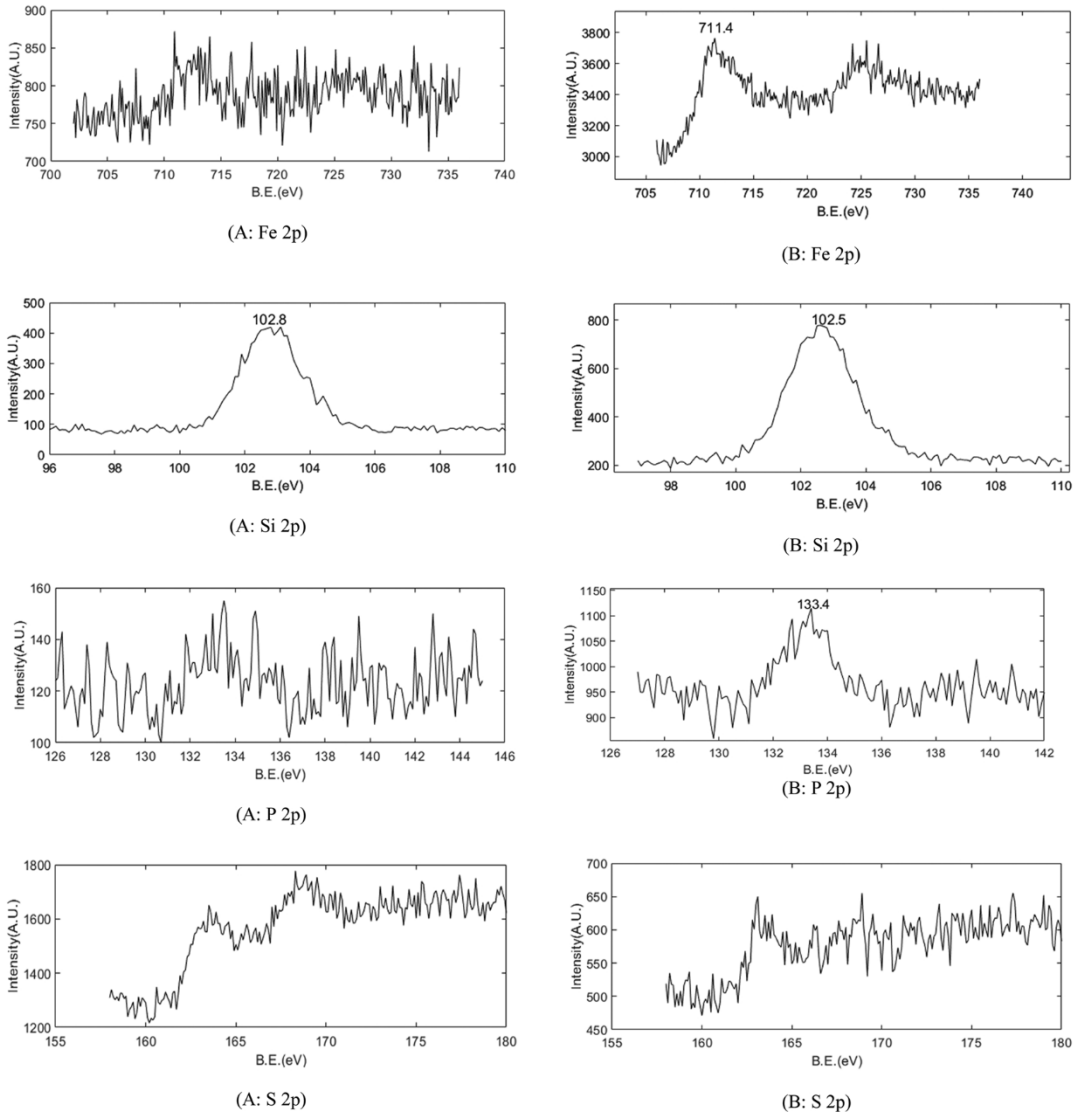

(A: Fe 2p) (B: Fe 2p)

(A: Si 2p) (B: Si 2p)

(A: P 2p) (B: P 2p)

(A: S 2p) (B: S 2p)

Fig. A5. (*continued*).

ofloxacin is much less as abundant ionic groups are present in the sludge surface, as substantiated by the FTIR spectrum of the raw sludge [see Fig. A2(a)] and point of zero charge of the adsorbent that refers the surface to be negatively charged at a working pH of ~7.8 [refer Fig. A3] [58,59,61].

In an acidic solution with pH below 6.1, CIP and OFLX molecules exist in a cationic form mainly due to the protonation of the amine group in the piperazine moiety [refer to Fig. 7.]. When its pH is higher than 8.7, it exists as an anion due to the loss of a proton from the carboxylic group. With 6.1 <pH< 8.7, CIP exists in a zwitterionic form. In the working pH of 7.8, CIP and OFLX exist primarily in zwitterionic or neutral forms. Also, the semi-dried sludge surface is negative at pH= 7.8 [refer to Fig. A3]. FT-IR results further suggested that the protonated amine group of ciprofloxacin and ofloxacin, in its zwitterionic form, was not electrostatically attracted to a large extent to the negatively charged sites of the sludge surfaces. Thus, the net ionic attraction between zwitterionic CIP and negative sludge surface is not appreciably effective.

The hydrophobic interaction is also negligible because both the adsorbent and adsorbates are hydrophilic in nature as substantiated by a contact angle measurement study [refer Fig. A4 (a) and (b)] that indicates the contact angles of both the raw sludge and the treated sludge are less than 90°. Apart from these theoretical speculations, a modified competitive Langmuir-like model fitted well for ciprofloxacin. The modified competitive Langmuir-like model mainly follows the monolayer adsorption [63] of adsorbates onto the semi-dried sludge surface. The weak hydrophobic interactions, that results from multilayer adsorptions, have very little contribution to the process.

The sewage sludge still exhibits a relatively high adsorption capacity towards ciprofloxacin and ofloxacin in weakly alkaline medium (pH at ~ 7.8) due to the negative charge assisted hydrogen bonding, on the basis of the following equations [see Eqns 27a, 27b, 28, 29 and 30]. Carboxylic acid groups of both CIP and OFLX are hydrogen bonded to the basal oxygen atoms of the sludge layers.

$$\text{CIP-COO}^- + \text{H}_2\text{O} \rightarrow \text{CIP-COOH} + \text{OH}^- \quad (27a)$$

$$\text{OFLX-COO}^- + \text{H}_2\text{O} \rightarrow \text{OFLX-COOH} + \text{OH}^- \quad (27b)$$

$$\text{RSS-O}^- + \text{HOOC-FQs} \rightarrow \text{RSS} - [\ \text{O}\ldots\text{H} - \text{OOC}]^- \text{- FQs} \quad (28)$$

Or.

$$\text{RSS-COOO}^{2-} + \text{HOOC-FQs} \rightarrow \text{RSS} - [\ \text{COOO}\ldots\text{H} - \text{OOC}]^- \text{- FQs} \quad (29)$$

Or.

$$(\text{RSS-O})_3\text{–P=O} + \text{HOOC-FQs} \rightarrow (\text{RSS-O})_3 - [\text{P=O}\ldots\text{H-OOC}]\text{-FQs} \quad (30)$$

The neutral forms of the two FQs probably react with the raw sewage

sludge [RSS] as shown in Eqns 28 and 29. The XPS study [refer Fig. A5 (A O 1s) and (B O 1s)] mentions a shift in the binding energy of O 1s from 532.2 eV to 531.8 eV substantiating the existence of H-bonding between the negatively charged surface of raw sewage sludge and specific functional groups on the surface of two FQs resulting due to lesser electron density on base O element after the formation of H bonds with the FQs.

Outcomes of both pseudo-second-order kinetic model and Boyd's film diffusion model supplement the probable surface-complex interactions of CIP and OFLX with the sludge surface. The same supports that the interactions are chemical in nature and chemisorption is taking place on the surface of the sludge.

A significant change in the sludge surface, after the adsorption of ciprofloxacin and ofloxacin, is observed in the FTIR spectrum of post-treated sludge [refer to Fig. A2 (b) of Annex I]. Certain new bands in the region 1527 cm^{-1} – 1548 cm^{-1} indicate the presence of aromatic ring systems along with amine and carboxylic acid groups. This indicates that both of the FQ molecules interact with the functional groups of the sludge, primarily due to hydrogen bonding. The adsorption process is also evaluated in terms of the XPS study [refer Fig. A5 (B F 1s)] which indicates that presence of an F atom in the treated sludge originates after the adsorption of the two FQs onto the raw sludge surface.

7. Conclusion

7.1. Concluding remarks highlighting key findings

The values of $n_{BT,\max}$ for ciprofloxacin is always observed to be greater than the same for ofloxacin, indicating a greater amount of adsorption of ciprofloxacin from the same n number of bed volumes of solution passed. With reference to the values of SSQ shown in Table SII [refer Supplementary Material A], it may be inferred that multicomponent adsorption of ciprofloxacin and ofloxacin is better fitted by the convective-diffusion model including a second-order pseudo-reaction kinetics driven depletion term. The same implies chemisorption to be the primary mode of competitive adsorption for both the FQs.

The values of Damköhler numbers (D_as), evaluated from the first-order and second-order convective-diffusion models, used for both the FQs are much less than 1. Thus, it may be concluded that the reaction rate is much less than the convective-diffusion rate and the entire adsorption process under dynamic conditions is reaction-limited (reaction is slowest so reaction characteristics like pseudo-kinetic rate constants etc. dominate and the convective diffusion reaches equilibrium instantaneously). This also supports chemisorption very strongly.

D_a s increase with the increase in bed heights and decrease in flow rates, in general, irrespective of the order of the reaction and the component. The ratios of Damköhler numbers, for both ciprofloxacin and ofloxacin, do not change much with flow rate (refer Table 2). It signifies that the pseudo-reaction rates of CIP and OFLX change in the same proportion as with the convective mass transfer. The ratio of the Damköhler numbers for the two FQs thus depends either on the ratio of the two pseudo rate constants (for both the components following 1st-order pseudo-kinetics) or on the ratio of the product of pseudo-kinetic rate constant and maximum equilibrium adsorption (for both the FQs following pseudo-second-order kinetics).

Under all the experimental conditions, the breakthrough time (BT) for ciprofloxacin is observed to be greater than the same for ofloxacin. It indicates that ofloxacin occupies the pores much faster than ciprofloxacin, on the basis of a competitive adsorption mechanism [refer to Section 6]. This is also validated by the values of the ratios of Damköhler numbers (see Table 2) where values of Damköhler numbers for both 1st-order and 2nd-order convective-diffusion models, in case of adsorption of ofloxacin, are found greater than the same in case of ciprofloxacin and values of rate constants for both 1st-order and 2nd-order convective-diffusion models (see Supplementary Material A: Table SII) for ofloxacin are found greater than the same for ciprofloxacin for both 1st-order and 2nd-order models.

- Breakthrough time (BT) increases with bed heights: BT-OFLX<BT-CIP for a particular bed height. This shows that OFLX wins in the competition and occupies the pores much faster than CIP.
- Experimental $\{\frac{BT-CIP}{BT-OFLX}\} \sim 1.58$, irrespective of flow rate and initial *concentration*. It signifies that the pseudo-reaction rates of CIP and OFLX change in the same proportion with the convective mass transfer.
- Breakthrough time increases with a decrease in initial concentration.

7.2. Limitations

Major limitation of both models is the adoption of a constant flow velocity throughout the packed bed. The velocity profile needs to be evaluated considering momentum transfer through packed-bed of specific voidage. This in turn will require a full-length solution of momentum transport equations under transient mode for the entire length of the bed considering advective diffusion of momentum and the same needs to be validated for various bed heights and flow rates.

In case of ofloxacin, observed breakthroughs come later than the predicted ones, while the same is not always true for ciprofloxacin. Pseudo-kinetics is not capable to substantiate the complex surface-complexation pathways efficiently, in this case.

7.3. Recommendations for future work

- Molecular modeling of each of CIP and OFLX, and in presence of one another would be challenging work.
- If the effect of axial dispersion (at least in one dimension) could be studied, with respect to Eq. 1 of the convective diffusion model, a better scenario of the whole process of adsorption could be visualized.
- Effect of variation in bed diameter is another challenging objective that could be studied. Variations in bed diameter could be modeled by incorporating the convective and diffusive terms in the radial direction. This could be an extremely demanding task, especially for multicomponent systems with higher levels of non-linearities.

Ethical Approval

All authors approve that:

- the work described has not been published before;
- that it is not under consideration for publication anywhere else;
- that its publication has been approved by all co-authors, as well as by the responsible authorities – tacitly or explicitly – at Jadavpur University where the work has been carried out.
- The publisher will not be held legally responsible should there be any claims for compensation.

Funding

The authors did not receive support from any organization for the submitted work.

Declaration of Competing Interest

The authors declare that they have no known competing financial interests or personal relationships that could have appeared to influence the work reported in this paper.

Data Availability

Data will be made available on request.

Acknowledgements

The authors are grateful to Prof (Dr.) Asim Bhaumik [School of Materials Sciences] and Dr. Subhadeep Datta [School of Physical Sciences], Indian Association for the Cultivation of Science, 2A and 2B, Raja S. C. Mullick Road, Kolkata 700032, for extending help in carrying out XPS and FT-IR based analyses respectively. The authors are grateful to Shri Swachchha Majumdar, Chief Scientist and Head, Membrane and Separation Technology Division, CSIR-Central Glass & Ceramic Research Institute, 196, Raja S.C. Mullick Road, Kolkata 700 032, West Bengal, India, for extending help in carrying out contact angle based analysis. The authors are thankful to Mr. Jatish Das, Bioprocess Laboratory, Chemical Engineering Department, Jadavpur University, Kolkata 700032, for extending help during elemental analysis for C, H, N, and S. The authors would also like to thank Mr. Rakesh Dey, Technical Assistant, for helping in the dynamic study. The authors acknowledge Metallurgy & Material Engineering Department, Jadavpur University, Kolkata 700032, for helping in carrying out morphological characterization using FE-SEM.

Declarations

All authors agreed with the content and that all gave explicit consent to submit and that they obtained consent from the responsible authorities at Jadavpur University where the work has been carried out, before the work is submitted.

Consent to Publish

All authors agreed with the content and that all gave explicit consent to publish the piece of research.

Authors contributions

All authors whose names appear on the submission:

1) made substantial contributions to the conception or design of the work **[Prof Ujjaini Sarkar]**; or the acquisition, analysis, or interpretation of data **[Mr Rajib Kumar Das]**; or the acquisition, analysis, creation of new software used in the work **[Ms Debamita Pal]**;
2) drafted the work **[Mr Rajib Kumar Das & Ms Debamita Pal]** or revised it critically for important intellectual content **[Prof Ujjaini Sarkar]**;
3) approved the version to be published **[Prof Ujjaini Sarkar]**; and
4) agree to be accountable for all aspects of the work in ensuring that questions related to the accuracy or integrity of any part of the work are appropriately investigated and resolved **[Prof Ujjaini Sarkar]**.

Annex A

Characterization of the raw sewage sludge

Elemental analysis of raw sludge and treated sludge

The elemental analysis for estimating Carbon (C), Hydrogen (H), Nitrogen (N), and Sulphur (S) present in the raw and post-treated sludge is carried out in a CHNS Analyzer (Make: ELEMENTAR, Germany; Model: VARIO MICRO CUBE). Temperatures of the combustion tube and the reduction tube are set at 1150 °C and 850 °C respectively. The pressure of the helium gas (carrier) is maintained at 1100–1200 millibar. The results are given in Table A1.

The carbon contents for pre and post-treated raw sludge are 19.97 ((wt% daf) and 28.61 ((wt% daf)) respectively. The hydrogen content of raw sludge is 2.847 (wt% daf) whereas for the treated sludge is 3.823 (wt % daf). Nitrogen content varies from 2.03 (wt% daf) to 4.21 (wt% daf) in the case of raw and post-adsorbed sludge. Increased values for carbon, nitrogen and hydrogen contents of treated sludge (as compared to the raw sludge) clearly substantiate that the increased C %, H %, as well as N %, are due to the adsorption of ciprofloxacin and ofloxacin onto the sludge surface.

Scanning electron micrography (SEM) images

The surface morphology of raw sludge and treated sludge is identified by a Field Emission Scanning Electron Micrograph (FE-SEM) with x6000 magnification [Make: HITACHI; Model: SU3800]. FE-SEM study for both raw and post-treated sludge is carried out in order to examine the change in the surface texture of raw sludge before and after adsorption.

The Fig. A1 (a) and (b) represent the SEM images of raw and post-treated sludge respectively. Fig. A1 (a) reveals a rough surface with a lot of cavities. Fig. A1 (b) represents post-treated sludge with a comparatively smoother surface than the surface of raw sludge and it contains various cluster-like structures. Fig. A1 (b) of post-treated sludge contains a lesser number of cavities indicating pure physisorption of ciprofloxacin and ofloxacin along with surface complexation through H-bonding, which is substantiated by the cluster-like structures present on the surface of the post-treated sludge.

FT-IR spectral analysis

Analysis of the functional groups, retained on the surface of the raw sewage sludge and sewage sludge after treatment are investigated by transmission infrared spectrum obtained using Fourier Transform Infrared Spectroscopy (FT-IR). An FT-IR spectrophotometer (Make: PerkinElmer; Model: FT-IR C120947) is used for this purpose. The entire IR spectrum is taken in the transmission range of 4000–400 cm^{-1}. The FTIR spectrums are received at a resolution of 1 cm^{-1}. The spectrum of KBr which is set as background in the spectrometer is subtracted from the spectrum of each of the raw and post-treated sewage sludge samples.

The FT-IR spectra of raw sewage sludge are presented in Fig. A2 (a) and corresponding spectra of the same after adsorption of ciprofloxacin and ofloxacin from wastewater are shown in Fig. A2 (b).

In the case of IR spectrum of the raw untreated sludge [refer Fig. A2 (a)] there is a significant peak at 3412 cm^{-1}, which is probably due to broad H bonded O-H stretching of alcohols [57]. The bands at 2923 cm^{-1} and 2852 cm^{-1} correspond to methylene C-H asymmetric or symmetric stretch of alkanes. No characteristic functional group is found corresponding to the band at 2343 cm^{-1}. The bands at 2028 cm^{-1} and 1875 cm^{-1} indicate carbonyl compounds. The band at 1639 cm^{-1} is due to alkenyl -C═C- stretch or -N-H bending of primary amine. The band at 1548 cm^{-1} corresponds to mild >N-H bending of secondary amine. The band at 1426 cm^{-1} is assigned to organic sulphates or carbonates. The bands at 1384 cm^{-1} and 1033 cm^{-1} are attributed to methyl C-H asymmetric stretch and primary alcohol C-O and P-O-C stretching of aliphatic phosphate respectively. The peak at 796 cm^{-1} is due to the mild =C-H bending of alkenes. The bands at 779 cm^{-1}, 759 cm^{-1} and 730 cm^{-1} correspond to mild C-Cl stretch of aliphatic chloro compounds. The band at 730 cm^{-1} is due to the presence of weak $-(CH_2)_n$ bend of alkanes and alkyls. The bands at 694 cm^{-1} and 643 cm^{-1} are attributed to C-Br stretch of aliphatic bromo compounds, C-H stretch of thiols and alkyne C-H bend respectively. The band at 533 cm^{-1} is attributed to C-I stretch corresponding to aliphatic iodo-compounds. The band at 467 cm^{-1} may be due to S-S polysulphides.

FT-IR spectrum of the post-treated sludge, after adsorption of ciprofloxacin and ofloxacin, is represented in Fig. A2 (b). The pattern of FTIR spectrum of the treated sludge is quite similar to the same for raw sludge along with the inclusion of certain small bands in the region 2035 cm^{-1}, 1527 cm^{-1} - 1411 cm^{-1}, 1303 cm^{-1} - 1271 cm^{-1} and 670 cm^{-1}.

The band at 2035 cm^{-1} is attributed to -N-C═S stretch of isothiocyanate [57]. The band at 1527 cm^{-1} corresponds to aromatic carboxylic acid salt (Org-chem, IR Chart). The bands at 1484 cm^{-1} and 1458 cm^{-1} represent methylene C-H bend, C═C-C aromatic ring stretch,

and methyl C-H asymmetric or symmetric stretch respectively. The band at 1411 cm^{-1} represents carbonate ions. The band at 1303 cm^{-1} is probably due to skeletal C-C vibrations or due to the primary or secondary aromatic amines. The band at 1271 cm^{-1} is due to the aryl -O- stretch or could be due to the C-N stretch of aromatic primary amine. The peak at 1033 cm^{-1} is due to the strong C-O stretch of alkyl-substituted ether or primary alcohol. The band at 670 cm^{-1} is assigned to C-H out of plane bending corresponding to aromatics.

Comparison of both the spectra of raw and post-treated sludge reveals inclusions of certain new bands, particularly in the region of 1527–1458 cm^{-1} indicating the presence of six-membered ring structures along with carboxylic and amine groups, resembling fluoroquinolones. Adsorption of ciprofloxacin and ofloxacin onto the sludge surface may be substantiated this way using FT-IR outputs.

Point of zero charge

Nature of the surface charge of the raw sewage sludge is determined by measuring the zeta potential range using a zeta sizer [Make: Malvern Inc., USA; Series: Nano-Z; Model No: ZEN 2600]. pH values of the sludge solutions are adjusted to approximately 1.0, 3.0, 5.0, 7.0, 8.0, 10.0, and 12.0 by adding 0.1 (M) HCl and 0.1 (M) NaOH to the primary raw sludge sample at 25°C. The average zeta potential for each of the pH-adjusted samples is estimated using the zeta-sizer. After estimating the zeta potential as a function of pH, a curve is regressed using the pH-zeta potential scattered dataset. Afterward, the nature of the surface charge is ascertained effectively. It is explicit that solution pH affects the surface charge of raw sewage sludge. At a working solution pH of 7.8, maintained constant for all the experiments of batch adsorption, the surface of sewage sludge remains negative all along [refer Fig. A3].

Contact-angle based analysis

Contact angles are measured using a wettability analyzer [Make: KRÜSS Scientific, Germany; Model: DSA4; Drop shape: Sessile] in order to elucidate the hydrophobicity of sewage sludge surface after adsorption of ciprofloxacin and ofloxacin in comparison to the precursor sludge surface. In this case, millipore ultra-pure water (1 μL) is dropped over the solid surface, and the contact angle is measured using a goniometer.

The contact angle (θ) and hence the degree of wettability changes when solid and liquid surfaces interact with each other [58,59]. Quantification of contact angle allows assessment of hydrophobicity of liquid film on solid surface. According to the theory of wetting, a solid surface, in contact with water, is considered to be hydrophobic in nature, distinctively, if the contact angle of the surface area of the material with water (θ_{H2O}) $> 90°$. On the other hand, if $\theta_{H2O} < 90°$, the surface is considered susceptible to wetting [61].

It is observed that the average θ_{H2O} for raw sewage sludge surface is 76.6° (± 0.98°) and that for the treated sludge surface is 74.99° (± 0.35°) [see Fig. A4 (a) and (b)] indicating both the surfaces are hydrophilic in nature. The decrease in contact angle value of the treated sludge (from 76.6° to 74.99°) affirms the inclusion of polar moieties i.e. ciprofloxacin and ofloxacin onto the surface of raw sewage sludge after adsorption and its hydrophilicity is also enhanced [60].

XPS analysis

The XPS study is carried out using an advanced electron spectroscopy system [Make: Omicron NanoTechnology GmbH, United Kingdom; Model: EIS-Sphera] meant for surface analysis. A monochromated Al Kα source [Model: XM 500; $h\nu = 1486.7$ eV] is used for high-resolution X-rays. Various spectra are obtained by plotting intensity versus binding energy curves for different elements. XPS-based analysis is conducted in order to obtain the elemental composition and chemical states of the raw sludge surface and the treated sludge surface [62]. Results are shown in Fig. A5. The peaks in the full-scan spectrum of raw sludge are assigned to O 1s (532.2 eV), N 1s (399.7 eV) and C 1s (284.5 eV) (see Fig. A5 A) and the peaks in the full-scan spectrum of treated sludge are assigned to O 1s (531.8 eV), N 1s (399.7 eV), and C 1s (284.4 eV) (see Fig. A5 B) along with the inclusion of a minor peak corresponding to elemental F 1s (687 eV). High-resolution spectra reveal the presence of various elements i.e Ca 2p, Si 2p, Fe 2p, P 2p both in raw sludge and treated sludge. The high-resolution spectrum of C1s and O1s before and after adsorption reveal a band shift towards lower binding energy i.e red shift occurs. The band of C1s of raw sludge and treated sludge are found to be 284.5 eV and 284.4 eV respectively. The band of O1s in raw sludge and treated sludge are found to be 532.2 eV and 531.8 eV respectively. The band of O 1s at 532.2 eV corresponding to either C-O or -C═O. The shift in binding energy of O 1s from 532.2 to 531.8 eV might have been caused due to the existence of H-bonds between adsorbing molecules (ciprofloxacin and ofloxacin) and the adsorbent sewage sludge [62]. No obvious shift in the binding energies was observed in the N1s spectra. The band corresponding to F1s at 687 eV has been detected in the spectrum of the treated sludge after the adsorption of ciprofloxacin and ofloxacin onto the sewage sludge surface.

Appendix A. Supporting information

Supplementary data associated with this article can be found in the online version at doi:10.1016/j.jece.2023.109896.

References

[1] Z. Wang, B. Yang, Q. Li, L. Wen, R. Zhang, Clinical features of 69 cases with coronavirus disease 2019 in Wuhan, China, Clin. Infect. Dis. 71 (15) (2020) 769–777, https://doi.org/10.1093/CID/CIAA272.

[2] A.L. Phelan, R. Katz, L.O. Gostin, The novel coronavirus originating in Wuhan, China: challenges for global health governance, JAMA 323 (8) (2020) 709–710, https://doi.org/10.1001/JAMA.2020.1097.

[3] S.A. Meo, D.C. Klonoff, J. Akram, Efficacy of chloroquine and hydroxychloroquine in the treatment of COVID-19, Eur. Rev. Med. Pharmacol. Sci. 24 (8) (2020) 4539–4547.

[4] P. Gautret, et al., Hydroxychloroquine and azithromycin as a treatment of COVID-19: results of an open-label non-randomized clinical trial, Int. J. Antimicrob. Agents 56 (1) (2020), 105949, https://doi.org/10.1016/j.ijantimicag.2020.105949.

[5] J. Grein, et al., Compassionate use of remdesivir for patients with severe Covid-19, N. Engl. J. Med. 382 (24) (2020) 2327–2336, https://doi.org/10.1056/NEJMoa2007016.

[6] Q. Zhou, et al., Interferon-α2b treatment for COVID-19, Front. Immunol. 11 (2020), https://doi.org/10.3389/FIMMU.2020.01061.

[7] X. van Doorslaer, J. Dewulf, H. van Langenhove, K. Demeestere, Fluoroquinolone antibiotics: an emerging class of environmental micropollutants, Sci. Total Environ. 500–501 (2014) 250–269, https://doi.org/10.1016/J.SCITOTENV.2014.08.075.

[8] Z.A. Damanhouri, H.M. Alkreathy, A.S. Ali, S. Karim, The potential role of Fluoroquinolones in the management of Covid-19 a rapid review, J. Adv. Pharm. Educ. Res. 11 (1) (2021) 125–134, https://doi.org/10.51847/FE1IOIPTWD.

[9] A. Rusu, G. Hancu, V. Uivaroşi, Fluoroquinolone pollution of food, water and soil, and bacterial resistance, Environ. Chem. Lett. 13 (1) (2015) 21–36, https://doi.org/10.1007/s10311-014-0481-3.

[10] R. Alaaeldin, M. Mustafa, G.E.A. Abuo-Rahma, M. Fathy, In vitro inhibition and molecular docking of a new ciprofloxacin-chalcone against SARS-CoV-2 main protease, Fundam. Clin. Pharm. 36 (1) (2022) 160–170, https://doi.org/10.1111/fcp.12708.

[11] K. Dileep, S. Polepalli, N. Jain, S.K. Buddana, R.S. Prakasham, M.S.R. Murty, Synthesis of novel tetrazole containing hybrid ciprofloxacin and pipemidic acid analogues and preliminary biological evaluation of their antibacterial and antiproliferative activity, Mol. Divers 22 (1) (2018) 83–93, https://doi.org/10.1007/S11030-017-9795-Y.

[12] F. Gao, J. Xiao, G. Huang, Current scenario of tetrazole hybrids for antibacterial activity, Eur. J. Med. Chem. 184 (2019), https://doi.org/10.1016/J.EJMECH.2019.111744.

[13] O. Aranha, D.P. Wood, F.H. Sarkar, U. D. P W, Ciprofloxacin Mediated Cell Growth Inhibition, S/G 2-M Cell Cycle Arrest, and Apoptosis in a Human Transitional Cell Carcinoma of the Bladder Cell Line. [Online]. Available: ⟨http://aacrjournals.org/clincancerres/article-pdf/6/3/891/2074201/df030000891.pdf⟩ (Accessed: 28 December 2022).

[14] B.F. El-Rayes, R. Grignon, N. Aslam, O. Aranha, F.H. Sarkar, Ciprofloxacin inhibits cell growth and synergises the effect of etoposide in hormone resistant prostate cancer cells, Int. J. Oncol. 21 (1) (2002) 207–211, https://doi.org/10.3892/IJO.21.1.207/HTML.

[15] V. Yadav, P. Talwar, Repositioning of fluoroquinolones from antibiotic to anticancer agents: an underestimated truth, Biomed. Pharmacother. 111 (2019) 934–946, https://doi.org/10.1016/J.BIOPHA.2018.12.119.

[16] S.D.W. Comber, M. Upton, S. Lewin, N. Powell, T.H. Hutchinson, COVID-19, antibiotics and One Health: a UK environmental risk assessment, J. Antimicrob. Chemother. 75 (11) (2020) 3411, https://doi.org/10.1093/JAC/DKAA338.

[17] M.P. Schlüsener, K. Bester, Persistence of antibiotics such as macrolides, tiamulin and salinomycin in soil, Environ. Pollut. 143 (3) (2006) 565–571, https://doi.org/10.1016/J.ENVPOL.2005.10.049.

[18] A. Prieto, M. Möder, R. Rodil, L. Adrian, E. Marco-Urrea, Degradation of the antibiotics norfloxacin and ciprofloxacin by a white-rot fungus and identification of degradation products, Bioresour. Technol. 102 (23) (2011) 10987–10995, https://doi.org/10.1016/j.biortech.2011.08.055.

[19] M. González-Pleiter, et al., Toxicity of five antibiotics and their mixtures towards photosynthetic aquatic organisms: implications for environmental risk assessment, Water Res. 47 (6) (2013) 2050–2064, https://doi.org/10.1016/J.WATRES.2013.01.020.

[20] J. Gao, J.A. Pedersen, Adsorption of sulfonamide antimicrobial agents to clay minerals, Environ. Sci. Technol. 39 (24) (2005) 9509–9516, https://doi.org/10.1021/es050644c.

[21] J.W. Peterson, L.J. Petrasky, M.D. Seymour, R.S. Burkhart, A.B. Schuiling, Adsorption and breakdown of penicillin antibiotic in the presence of titanium oxide nanoparticles in water, Chemosphere 87 (8) (2012) 911–917, https://doi.org/10.1016/J.CHEMOSPHERE.2012.01.044.

[22] E.A. Serna-Galvis, J. Silva-Agredo, A.L. Giraldo-Aguirre, O.A. Flórez-Acosta, R. A. Torres-Palma, High frequency ultrasound as a selective advanced oxidation process to remove penicillinic antibiotics and eliminate its antimicrobial activity from water, Ultrason. Sonochem. 31 (2016) 276–283, https://doi.org/10.1016/j.ultsonch.2016.01.007.

[23] Y. Liu, X. He, Y. Fu, D.D. Dionysiou, Degradation kinetics and mechanism of oxytetracycline by hydroxyl radical-based advanced oxidation processes, Chem. Eng. J. 284 (2016) 1317–1327, https://doi.org/10.1016/j.cej.2015.09.034.

[24] D. Balarak, F. Mostafapour, Batch equilibrium, kinetics and thermodynamics study of sulfamethoxazole antibiotics onto Azolla filiculoides as a Novel Biosorbent, Br. J. Pharm. Res. 13 (2) (2016) 1–14, https://doi.org/10.9734/BJPR/2016/28521.

[25] W. Zhang, G. He, P. Gao, G. Chen, Development and characterization of composite nanofiltration membranes and their application in concentration of antibiotics, Sep Purif. Technol. 30 (1) (2003) 27–35, https://doi.org/10.1016/S1383-5866(02)00095-3.

[26] X.-D. Zhu, Y.-J. Wang, R.-J. Sun, D.-M. Zhou, Photocatalytic degradation of tetracycline in aqueous solution by nanosized TiO2, Chemosphere 92 (8) (2013) 925–932, https://doi.org/10.1016/j.chemosphere.2013.02.066.

[27] D. Balarak, H. Azarpira, Rice husk as a biosorbent for antibiotic Metronidazole removal: Isotherm studies and model validation, Int. J. Chemtech Res. 9 (7) (2016) 566–573. Accessed: Dec. 29, 2022. [Online]. Available, (https://sciexplore.ir/Documents/Details/181-702-967-731).

[28] R. Ocampo-Pérez, J. Rivera-Utrilla, C. Gómez-Pacheco, M. Sánchez-Polo, J. J. López-Peñalver, Kinetic study of tetracycline adsorption on sludge-derived adsorbents in aqueous phase, Chem. Eng. J. 213 (2012) 88–96. Accessed: 29 December 2022. [Online]. Available: (https://www.academia.edu/25419199/Kinetic_study_of_tetracycline_adsorption_on_sludge_derived_adsorbents_in_aqueous_phase).

[29] A.R. Araujo Scharnberg, A. Carvalho de Loreto, A. Kopp Alves, Optical and structural characterization of Bi2FexNbO7 nanoparticles for environmental applications, Emerg. Sci. J. 4 (1) (2020) 11–17, https://doi.org/10.28991/esj-2020-01205.

[30] M. Clara, N. Kreuzinger, B. Strenn, O. Gans, H. Kroiss, The solids retention time - a suitable design parameter to evaluate the capacity of wastewater treatment plants to remove micropollutants, Water Res. 39 (1) (2005) 97–106, https://doi.org/10.1016/J.WATRES.2004.08.036.

[31] Y.K.K. Koh, et al., Influence of operating parameters on the biodegradation of steroid estrogens and nonylphenolic compounds during biological wastewater treatment processes, Environ. Sci. Technol. 43 (17) (2009) 6646–6654, https://doi.org/10.1021/ES901612V.

[32] J. Radjenović, M. Petrović, D. Barceló, Fate and distribution of pharmaceuticals in wastewater and sewage sludge of the conventional activated sludge (CAS) and advanced membrane bioreactor (MBR) treatment, Water Res. 43 (3) (2009) 831–841, https://doi.org/10.1016/J.WATRES.2008.11.043.

[33] E.J. McAdam, et al., Removal of steroid estrogens in carbonaceous and nitrifying activated sludge processes, Chemosphere 81 (1) (2010) 1–6, https://doi.org/10.1016/j.chemosphere.2010.07.057.

[34] B. Petrie, E.J. McAdam, M.D. Scrimshaw, J.N. Lester, E. Cartmell, Fate of drugs during wastewater treatment, Trends Anal. Chem. 49 (2013) 145–159, doi: 10.1016/J.TRAC.2013.05.007.

[35] W.N. Wan Ismail, M.I. Arif Irwan Syah, N.H. Abd Muhet, N.H. Abu Bakar, H. Mohd Yusop, N. Abu Samah, Adsorption behavior of heavy metal ions by hybrid inulin-TEOS for water treatment, Civ. Eng. J. 8 (9) (2022) 1787–1798, https://doi.org/10.28991/CEJ-2022-08-09-03.

[36] S. Rio, C. Faur-Brasquet, L. le Coq, P. le Cloirec, Structure characterization and adsorption properties of pyrolyzed sewage sludge, Environ. Sci. Technol. 39 (11) (2005) 4249–4257, https://doi.org/10.1021/es0497532.

[37] J.C. Knox, A.D. Ebner, M.D. Levan, R.F. Coker, J.A. Ritter, Limitations of breakthrough curve analysis in fixed-bed adsorption, Ind. Eng. Chem. Res 55 (16) (2016) 4734–4748, https://doi.org/10.1021/ACS.IECR.6B00516/ASSET/IMAGES/LARGE/IE-2016-00516N_0011.JPEG.

[38] H.C. Thomas, Heterogeneous ion exchange in a flowing system, J. Am. Chem. Soc. 66 (10) (. 1944) 1664–1666, https://doi.org/10.1021/JA01238A017.

[39] Z. Aksu, Application of biosorption for the removal of organic pollutants: a review, Process Biochem. 40 (3–4) (2005) 997–1026, https://doi.org/10.1016/J.PROCBIO.2004.04.008.

[40] K.H. Chu, Breakthrough curve analysis by simplistic models of fixed bed adsorption: In defense of the century-old Bohart-Adams model, Chem. Eng. J. 380 (2020), 122513, https://doi.org/10.1016/j.cej.2019.122513.

[41] X. Xu, X. Cao, L. Zhao, Comparison of rice husk- and dairy manure-derived biochars for simultaneously removing heavy metals from aqueous solutions: Role of mineral components in biochars, Chemosphere 92 (8) (2013) 955–961, https://doi.org/10.1016/J.CHEMOSPHERE.2013.03.009.

[42] T.W. Weber, R.K. Chakravorti, Pore and solid diffusion models for fixed-bed adsorbers, Aiche J. 20 (2) (1974) 228–238, https://doi.org/10.1002/AIC.690200204.

[43] L. Lapidus, N.R. Amundson, Mathematics of adsorption in beds. VI. The effect of longitudinal diffusion in ion exchange and chromatographic columns, J. Phys. Chem. 56 (8) (1952) 984–988, https://doi.org/10.1021/J150500A014.

[44] S. Singha, U. Sarkar, S. Mondal, S. Saha, Transient behavior of a packed column of Eichhornia crassipes stem for the removal of hexavalent chromium, Desalination 297 (2012) 48–58, https://doi.org/10.1016/J.DESAL.2012.04.016.

[45] S. Saha, U. Sarkar, S. Mondal, Modelling the transient behaviour of a fixed bed considering both intra and inter-pellet diffusion for adsorption of parachloro-meta-xylenol (PCMX), Desalin. Water Treat. 37 (1–3) (2012) 277–287, https://doi.org/10.1080/19443994.2012.661299.

[46] N. Selvaraju, S. Pushpavanam, Adsorption characteristics on sand and brick beds, Chem. Eng. J. 147 (2–3) (2009) 130–138, https://doi.org/10.1016/J.CEJ.2008.06.040.

[47] G. Thirupathi, C.P. Krishnamoorthy, S. Pushpavanam, Adsorption characteristics of inorganic salts and detergents on sand beds, Chem. Eng. J. 125 (3) (2007) 177–186, https://doi.org/10.1016/J.CEJ.2006.08.023.

[48] E. Worch, Adsorption Technology in Water Treatment Fundamentals, Processes, and Modeling, 92, DE GRUYTER, Berlin, 2012, https://doi.org/10.1515/9783110240238.

[49] J.C. Crittenden, W.J. Weber, Predictive model for design of fixed-bed adsorbers: single-component model verification, J. Environ. Eng. Div. 104 (3) (1978) 433–443, https://doi.org/10.1061/JEEGAV.0000768.

[50] J. Crittenden, J. Berrigan, and D. Hand, Design of rapid small-scale adsorption tests for a constant diffusivity Journal of Water Pollution Control Federation, 1986.

[51] Friedrich G. Helfferich, Ion Exchange. 1995. [Online]. Available: (https://www.goodreads.com/book/show/3415261-ion-exchange) (Accessed: 29 December 2022.).

[52] C. Costa, A. Rodrigues, Design of cyclic fixed-bed adsorption processes. Part I: phenol adsorption on polymeric adsorbents, A. E. Ch. E. J. 31:11 (10) (1985) 1645–1654, https://doi.org/10.1002/AIC.690311008.

[53] C. Tien. Adsorption Calculations and Modeling, 1st ed., Butterworth-Heinemann, Boston, 1994.

[54] L. Fournel, P. Mocho, R. Brown, P. le Cloirec, Modeling breakthrough curves of volatile organic compounds on activated carbon fibers, Adsorption 16 (3) (2010) 147–153, https://doi.org/10.1007/S10450-010-9207-4.

[55] R. Petrus, J. Warchoł, Ion exchange equilibria between clinoptilolite and aqueous solutions of Na+/Cu2+, Na+/Cd2+ and Na+/Pb2+, Microporous Mesoporous Mater. 61 (1–3) (2003) 137–146, https://doi.org/10.1016/S1387-1811(03)00361-5.

[56] Y.S. Ho, G. McKay, Pseudo-second order model for sorption processes, Process Biochem. 34 (5) (1999) 451–465, https://doi.org/10.1016/S0032-9592(98)00112-5.

[57] J. Coates, Interpretation of Infrared Spectra, A Practical Approach in Encyclopedia of Analytical Chemistry, John Wiley & Sons, Ltd, Chichester, UK, 2006, https://doi.org/10.1002/9780470027318.a5606.

[58] M. Mobin, Huda, M. Shoeb, R. Aslam, P. Banerjee, Synthesis, characterisation and corrosion inhibition assessment of a novel ionic liquid-graphene oxide nanohybrid, J. Mol. Struct. 1262 (2022), 133027, https://doi.org/10.1016/j.molstruc.2022.133027.

[59] R. Aslam, M. Mobin, Huda, M. Shoeb, M. Murmu, P. Banerjee, Proline nitrate ionic liquid as high temperature acid corrosion inhibitor for mild steel: experimental and molecular-level insights, J. Ind. Eng. Chem. 100 (2021) 333–350, https://doi.org/10.1016/j.jiec.2021.05.005.

[60] E. Vazirinasab, R. Jafari, G. Momen, Application of superhydrophobic coatings as a corrosion barrier: a review, Surf. Coat. Technol. 341 (2018) 40–56, https://doi.org/10.1016/j.surfcoat.2017.11.053.

[61] R. Aslam, M. Mobin, Huda, M. Murmu, P. Banerjee, J. Aslam, L-Alanine methyl ester nitrate ionic liquid: synthesis, characterization and anti-corrosive application, J. Mol. Liq. 334 (2021), 116469, https://doi.org/10.1016/j.molliq.2021.116469.

[62] N. Zhang, et al., Effective extraction of fluoroquinolones from water using facile modified plant fibers, J. Pharm. Anal. 12 (5) (2022) 791–800, https://doi.org/10.1016/j.jpha.2022.06.004.

[63] A.S. Luna, A.L.H. Costa, A.C.A. da Costa, C.A. Henriques, Competitive biosorption of cadmium(II) and zinc(II) ions from binary systems by Sargassum filipendula, Bioresour. Technol. 101 (14) (2010) 5104–5111, https://doi.org/10.1016/j.biortech.2010.01.138.

Rajib Kumar Das
10/05/2023